

Timarete posteria, a new cirratulid species from Korea (Annelida, Polychaeta, Cirratulidae)

Hyun Ki Choi¹, Hana Kim¹, Seong Myeong Yoon²

1 National Marine Biodiversity Institute of Korea, Seocheon, Chungcheongnam-do 33662, Korea **2** Department of Biology, College of Natural Sciences, Chosun University, Gwangju 61452, Korea

Corresponding author: Seong Myeong Yoon (smyun@chosun.ac.kr)

Academic editor: G. Rouse | Received 14 June 2018 | Accepted 28 October 2018 | Published 13 December 2018

<http://zoobank.org/C2B05C47-2CE5-4F8F-9462-2C7C1E61D3E1>

Citation: Choi HK, Kim H, Yoon SM (2018) *Timarete posteria*, a new cirratulid species from Korea (Annelida, Polychaeta, Cirratulidae). ZooKeys 806: 1–15. <https://doi.org/10.3897/zookeys.806.27436>

Abstract

A new cirratulid species, *Timarete posteria* **sp. n.**, is described from the intertidal habitats of the eastern coast of South Korea. The new species is closely related to *Timarete luxuriosa* (Moore, 1904) from southern California based on morphological similarity of the branchial and tentacular filaments and the noto- and neuropodial spines. However, *T. posteria* **sp. n.** differs from the latter based on the following characteristics: 1) evenly divided peristomium into three annulations; 2) 2–4 neuropodial spines originating in the posterior chaetigers alternated by a few capillaries; and 3) complete shift in branchial filaments located about one-third between the notopodium and the dorsal midline. The new species has a methyl green staining pattern (MGSP) distinct from other *Timarete* species. Detailed description and illustrations of the new species are provided with molecular information based on the partial sequences of the mitochondrial cytochrome c oxidase subunit I (COI) and 16S ribosomal RNA (16S). This study also includes a key and discussion of known *Timarete* species from East Asia.

Keywords

Korean waters, polychaete, taxonomy, *Timarete*, COI, 16S

Introduction

The genus *Timarete* Kinberg, 1866 is a typical multi-tentaculate genus assigned to the cirratulid polychaetes (Blake 1996). *Timarete* species are clearly distinguished from other multi-tentaculate species by having chaetae including capillaries and acicular

spines, tentacular filaments forming a transverse series arising from two or more chaetigers, and branchiae originating in the segment anterior to tentacular filaments and shifted toward the mid-dorsum of the body in middle and posterior chaetigers (Fauchoald 1977, Blake 1996).

Recently, several species belonging to *Timarete* have been taxonomically re-evaluated (Blake 1996, Çinar 2007, Magalhães and Bailey-Brock 2010, Magalhães et al. 2014). Blake (1996) redescribed *Timarete perbranchiata* (Chamberlin, 1918) from California and confirmed the taxonomic state of *T. convergens* (Chamberlin, 1918) as a junior synonym of it. Blake (1996) also determined that *Cirriformia luxuriosa* (Moore, 1904), which had been misconstrued and redescribed it as a species of *Timarete*. Çinar (2007) redescribed *Timarete punctata* (Grube, 1859) and designated a lectotype and paralectotypes based on syntypes from the U. S. Virgin Islands (Caribbean Sea) deposited in the Zoological Museum of Copenhagen, and he also examined materials from the Mediterranean Sea and South Africa. Magalhães and Bailey-Brock (2010) redescribed an endemic Hawaiian species, previously been known as *Cirriformia hawaiiensis* Hartman, 1956, as a species of *Timarete* species, *T. hawaiiensis* (Hartman, 1956). Magalhães et al. (2014) re-examined several multi-tentaculate cirratulid species collected from the Brazilian coast including four *Timarete* species: *T. caribous* (Grube & Ørsted in Grube, 1859), *T. ceciliae* Magalhães, Seixas, Paiva, & Elias, 2014, *T. oculata* (Treadwell, 1932), and *T. punctata* species complex. Seixas et al. (2017) find out that the presence of two cryptic species within *T. punctata* species complex, one species widely distributed from Atlantic and Pacific Oceans and another species from Bahia, South Atlantic Ocean, using the genetic data of COI and 16S sequences.

Within Korean waters, *Timarete antarctica* (Monro, 1930) is the only recorded species of *Timarete* known in this region (Paik 1989). However, Paik (1989)'s description was very brief and lacked a review of the specific characters. While studying the polychaetes from Korean waters, a new species belonging to the genus *Timarete* was discovered. Here, we conducted a detailed examination of this species using methyl green staining pattern (MGSP) and several ontogenetic characters including the segmental origins of tentacular filaments, distributions of the neuroacicular and notoacicular spines, and dorsal shift of branchial filaments as used by previous investigators (Çinar 2007, Magalhães and Bailey-Brock 2010, Magalhães et al. 2014). In this study, the description and illustrations of the new species are provided together with molecular data pertaining to the barcoded regions of the mitochondrial cytochrome c oxidase subunit I (COI) and 16S ribosomal RNA (16S). Additionally, we reviewed and discussed *Timarete* species recorded from East Asia.

Materials and methods

Sampling and morphological observations

Samples were collected from the intertidal rocky bottoms. Specimens were sorted using sieves with a pore size of 0.5 mm, fixed initially with a 5% formaldehyde-seawater solu-

tion, and transferred to 85% ethyl alcohol. The characteristics of the whole body were observed with appendages dissected in a petri-dish using a pair of dissection forceps, or surgical knives and needles under a stereomicroscope (SMZ1500; Olympus, Tokyo, Japan). Dissected specimens were mounted onto temporary slides using glycerol or permanent slides using polyvinyl lactophenol solution. Drawings were based on stereomicroscopy and light microscopy (LABOPHOT-2; Nikon, Tokyo, Japan) aided by drawing tubes. Photographs were captured using an image system (LAS V4.7, Leica Microsystems, Heerbrugg, Switzerland). Specimens for scanning electron microscopy (SEM) were dehydrated with a *t*-BuOH freeze dryer (VFD-21S; Vacuum Device, Ibaraki, Japan). They were mounted on stubs and coated with gold-palladium. SEM observations were conducted using a scanning electron microscope (SU3500; Hitachi, Tokyo, Japan). Type material and additional material examined were deposited at the National Institute of Biological Resources (NIBR) in Incheon, Korea and the National Marine Biodiversity Institute of Korea (MABIK) in Seocheon, Chungcheongnam-do, Korea, respectively.

Molecular analysis

Genomic DNA was extracted from the posterior segments of three specimens selected from the additional material using a DNeasy Blood and Tissue Kit (Qiagen, Hilden, Germany) according to the manufacturer's protocol. The partial sequences of the mitochondrial cytochrome *c* oxidase subunit I (COI) and 16S ribosomal RNA (16S) from gDNA were amplified using polymerase chain reaction (PCR) with the following primers: LCO 1490 5'-GGTCAACAAATCATAAAGATATTGG-3' and HCO 2198 5'-TAAACTTCAGGGTGACCAAAAAATCA-3' in COI amplification (Folmer et al. 1994) and 16SarL 5'-CGCCTGTTTATCAAAAACAT-3' and 16SANR 5'-GCTTACGCCGGTCTAACTCAG-3' in 16S amplification (Palumbi 1996; Zanol et al. 2010). PCR amplification was conducted in a total volume of 20 μ L: 10 μ L of 2x DyeMIX-Tenuto (Enzynomics), 0.5 μ L of each primer, 1 μ L of gDNA, and 8 μ L of sterile water. Touchdown-PCR was carried out according to the following cycling program: 94 °C for 5 min, 94 °C for 1 min, 50 °C for 1 min and 72 °C for 1 min, followed by 20 cycles at decreasing annealing temperatures in decrements of 0.5 °C per cycle, followed by 1 min at 94 °C, 15 cycles of 1 min at 40 °C, 1 min at 72 °C, and final extension at 72 °C for 7 min. PCR products were purified with a QIAquick PCR Purification Kit (Qiagen, Chatsworth, CA, USA). Sequences of the new species were obtained using an Applied Biosystems 3730 DNA sequencer. These sequences were aligned with those of other *Timarete* species using Clustal W (Thompson et al. 1994, Larkin et al. 2007) in Geneious Pro v.9.1.8 (Biomatters, Auckland, New Zealand). The genetic distances of the new species from other species and the Maximum likelihood (ML) tree were determined by MEGA v.6.06 (Tamura et al. 2013).

Systematic accounts

Family Cirratulidae Ryckholt, 1851

Genus *Timarete* Kinberg, 1866

Timarete posteria sp. n.

<http://zoobank.org/E13A2164-7182-4D18-ACD1-80C4F4C1A9B1>

Figs 1–4

Material examined. *Type locality:* South Korea, Gyeongsangbuk-do Province: Pohang-si County, Heunghae-eup, Odo-ri, 36°09'17"N, 129°24'02"E, 13 July 2017, intertidal rocky bottom. *Holotype:* complete specimen (NIBRIV0000829700). *Paratypes:* one complete specimen (MABIKNA00146231); one complete specimen (MABIKNA00146236); one complete specimen (MABIKNA00146238); one complete specimen (MABIKNA00146239); one complete specimen (MABIKNA00146245). *Non-type material:* 16 specimens (13 complete and 3 incomplete specimens), collection details same as type materials; 11 specimens (all complete), South Korea, Gangwon-do Province: Goseong-gun County, Jugwang-myeon, Munamjin-ri, 35°18'41"N, 129°32'33"E, 10 April 2017, intertidal rocky bottom.

Diagnosis. Body with deep ventral groove and distinct segments. Prostomium triangular, without eyespots. Peristomium evenly divided into three annulations. Branchial filaments one pair per segment, beginning from third peristomial annulus, and gradually shifting to mid-dorsum between chaetigers 30–78; completely shifted branchiae at about one-third distance between notopodium and dorsal midline. Grooved tentacular filaments arising from chaetigers 5–6 and occasionally 6–7 or 7–8. Chaetae including capillaries and acicular spines; notopodial spines 1–4, pale brown in color, from chaetigers 16–45; neuropodial spines 2–4, curved distally, thicker than notoacicular spines, dark brown in color, from chaetiger 24–69.

Description. Holotype: complete, 5.5 cm in length (4.8–13.2 cm in paratypes) and 5.7 mm in maximum width (4.0–6.0 mm in paratypes), with approximately 261 segments.

Body elongated, rounded dorsally, flattened ventrally, with distinct ventral groove throughout and tapering posterior end. All segments distinct, narrow, crowded throughout body with distinct lateral shoulders. Body color in alcohol pale grey to dark grey, branchiae and tentacular filaments yellowish grey; live specimens with body dark red and branchiae and tentacular filaments light orange. No separate pigmentation on body (Fig. 1).

Prostomium short, triangular, blunt distally, and as long as three anterior chaetigers. Nuchal organs round, present on posterior-lateral prostomial region. Eyespots absent (Figs 2A, B, 3A).

Peristomium with three annulations nearly equal in length, longer than prostomium and as long as four anterior chaetigers; second and third annulations with 2–3 lateral wrinkles (Figs 2A, B, 3A).

Branchial filaments one pair per segment, from posterior margin of third peristomial annulus, continuing on most segments except about last ten segments; branchial



Figure 1. *Timarete posteria* sp. n., paratype (MABIKNA00146236), lateral view. Scale bar: 1.0 mm.

filaments located just above notopodial ridges in anterior 42 chaetigers (29–77 chaetigers in all specimens examined); then shifting gradually to mid-dorsum forming lateral bulge over notopodia from chaetiger 43 (30–78 in all specimens examined) to near posterior end; fully shifted branchiae located about one-third distance between notopodium and dorsal midline. (Figs 2A–C, 3B).

Tentacular filaments formed two transverse groups separated by median gap and arising on dorsum of chaetigers 5–6 (6–7 or 7–8 in some specimens examined); each group with about 18–21 filaments arranged in 2–3 transverse rows (Figs 2A, B, 3A).

Parapodia, notopodia forming lateral shoulders dorsally; noto- and neuropodium widely separated throughout (Figs 2A–C, 3A, B).

Chaetae including capillaries with serrated edge observed under light microscopy (400x) and SEM observation and acicular spines. Capillary chaetae about 8–10 capillaries arranged in two longitudinal rows in anterior parapodia. Notopodial spines nearly straight, pale brown in color, present from chaetiger 40 (16–45 in all specimens examined); 1–3 spines per segment accompanied by 1–3 companion capillaries from chaetiger 40 to posterior end. Neuropodial spines curved distally, slightly thicker than notopodial spines, dark brown in color, from chaetiger 30 (24–69 in all specimens examined); 2–3 spines per segment with 1–2 companion capillaries from chaetiger 30 to very posterior end (Figs 3C, D, 4A–C).

Pygidium with terminal anus (Fig. 4D).

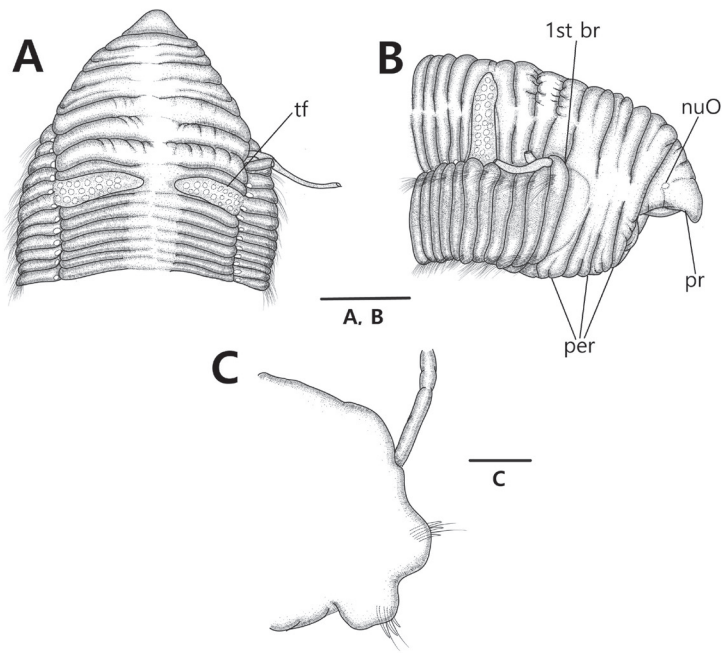


Figure 2. *Timarete posteria* sp. n., **A–B** holotype (NIBRIV0000829700) **C** paratype (MABIK-NA00146239) **A** anterior end, dorsal view **B** anterior end, lateral view **C** parapodium of mid-body. Scale bars: 1.0 mm (**A**, **B**), 0.5 mm (**C**). Abbreviations: branchia (br), chaetiger (ch), nuchal organ (nuO), peristomium (per), prostomium (pr), tentacular filaments (tf).

Methyl green staining pattern (MGSP). Body stained with transverse bands on posterior half of each segment forming complete rings. Branchial and tentacular filaments not stained. Prostomium, peristomium, and dorsum of first 3 or 4 chaetigers intensely stained with dark green. Noto- and neuropodial ridges not stained (Fig. 3A, B).

Variations. Several morphological characters in cirratulids are highly variable ontogenetically and a few of them are clearly considered size-dependent in *Timarete* species (Blake 1996, Magalhães and Bailey-Brock 2010, Magalhães et al. 2014). We examined the relationships between the ontogenetic characteristics including the segmental origin of noto- and neuropodial spines and the shift of branchial filaments, and the total number of chaetigers in the new species according to the correlation analyses based on 31 complete specimens (Fig. 5). In *Timarete posteria* sp. n., the segmental origin of neuropodial spines ranged from chaetigers 16 to 45, strongly size-dependent ($N = 31$, $r = 0.81$). The segmental origin of notopodial spines varied from chaetigers 24 to 69, with weak size-dependent characteristics if compared with those of neuropodial spines ($N = 31$, $r = 0.67$). The dorsal shift of branchial filaments occurred between chaetigers 30 and 78 regardless of the total number of chaetigers in the new species ($N = 31$, $r = 0.40$) (Fig. 5). It is known that the appearance of tentacular filaments is generally variable in a few *Timarete* species (Magalhães et al. 2014). In *T. posteria* sp. n., the tentacular fila-

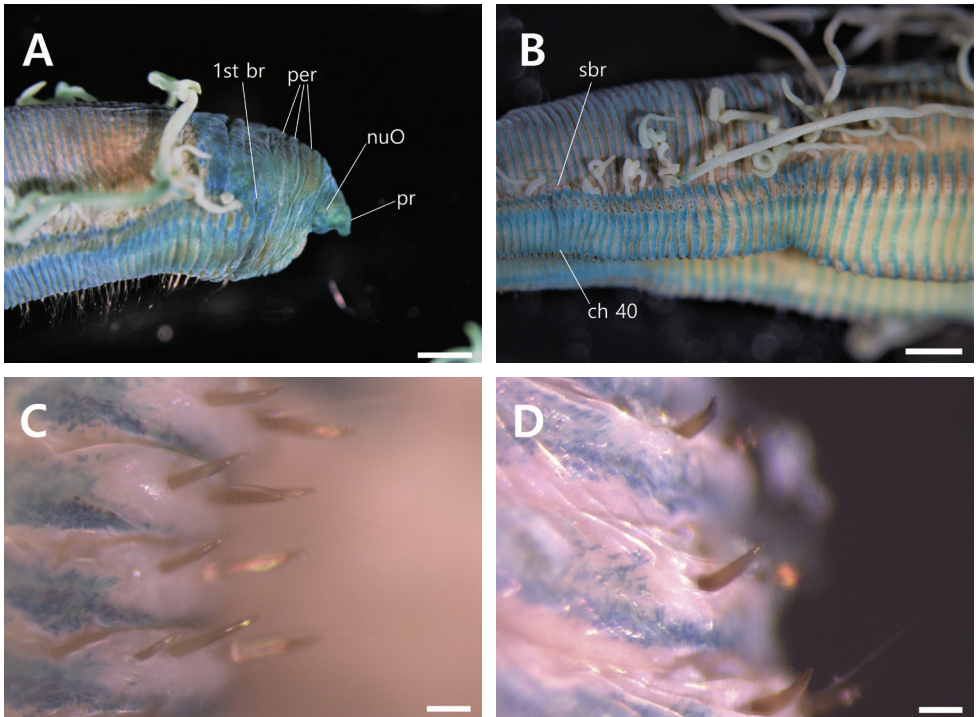


Figure 3. *Timarete posteria* sp. n., **A–D** holotype (NIBRIV0000829700) **A** anterior end, lateral view with MGSP **B** mid-body segments, lateral view with MGSP **C** notopodial spines of mid-body segments **D** neuro-podial spines of mid-body segments. Scale bars: 1.0 mm (**A, B**), 0.1 mm (**C, D**). Abbreviations: branchia (br), chaetiger (ch), nuchal organ (nuO), peristomium (per), prostomium (pr), shift of branchial filament (sbr).

ments always originated in the dorsum of two consecutive chaetigers although their locations were variable: usually on chaetigers 5–6 (in 28 specimens) and occasionally 6–7 (in two specimens) or 7–8 (in four specimens) in all the 34 specimens examined. This variation appears to be somewhat related to body size because the tentacular filaments on chaetigers 7–8 occur in specimens containing more than 300 segments (almost similar to specimens with less than 300 segments on chaetigers 5–6). Further studies with a larger population and more temporal samples are needed to determine a more accurate relationship between the segmental origin of the tentacular filaments and the body size.

Etymology. The epithet of the specific name, *posteria*, is derived from the Latin *posterior*, meaning ‘hind’. This name refers to the shift in the appearance of the branchial filaments from relatively posterior chaetigers. The gender of the genus name, *Timarete*, is feminine and the specific name of this new species is designated as feminine.

Habitat and distribution. This species is a common inhabitant of seagrass beds in the intertidal rocky bottoms and distributed in the East Sea (or the Sea of Japan) of South Korea.

Molecular information. In the present study, partial COI sequences each measuring 658 bp in size from five specimens and partial 16S sequence of 519 bp in size

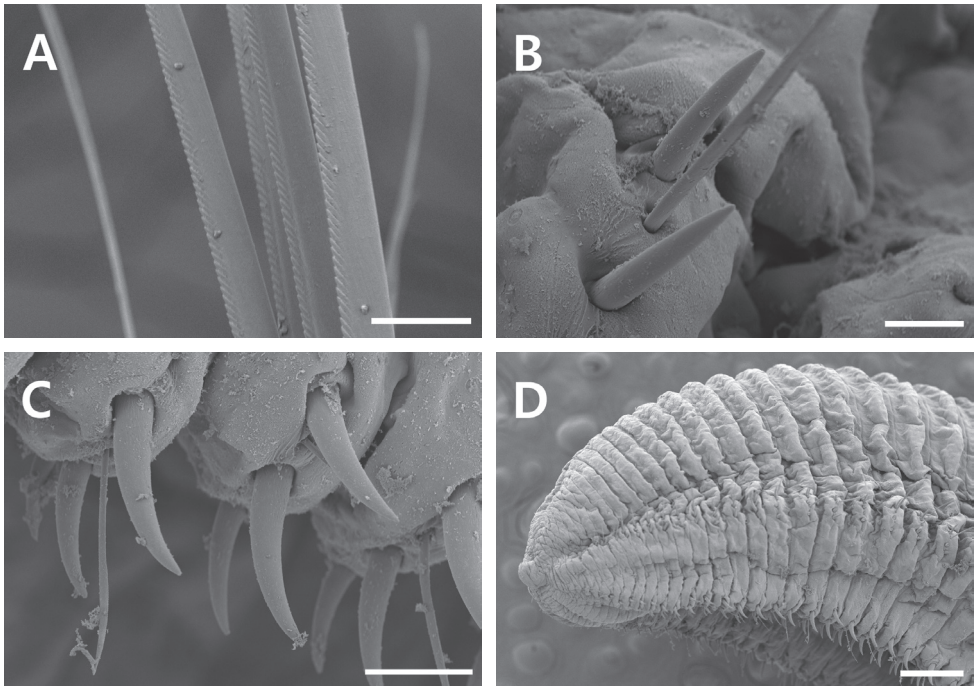


Figure 4. SEM observation of *Timarete posteria* sp. n., **A–D** paratype (MABIKNA00146238) **A** capillary chaetae of anterior chaetiger **B** notopodial spines of posterior chaetiger **C** neuropodial spines of posterior chaetiger **D** pygidium, lateral view. Scale bars: 0.02 mm (**A**), 0.025 mm (**B**), 0.05 mm (**C**), 0.25 mm (**D**).

from a single specimen were obtained for the genetic analysis of *Timarete posteria* sp. n. They were deposited in GenBank under the accession number MH708229–MH708233 (COI) and MH822840 (16S). The intra-specific genetic distance between five COI sequences was measured according to the Kimura-2-parameter (K2P) model and ranged from 0 to 0.4 %. We carried out the genetic comparison of the new species with three *Timarete* species available, including *T. caribous* (Grube and Ørsted in Grube, 1859), *T. ceciliae* Magalhães, Seixas, Paiva, and Elias, 2014, and *T. punctata* (Grube, 1859) from the Brazilian coast, with COI and 16S sequences previously announced from GenBank (Magalhães et al. 2014). Based on entire genetic data uploaded in GenBank, the inter-specific genetic distances of COI and 16S sequences between the new species and other *Timarete* species were 23.7–26.2 % and 22.2–26.5 %, respectively (K2P distance). We examined the molecular phylogenetic relationship based on the Maximum likelihood (ML) tree using the genetic data available from GenBank on several cirratulids belonging to the multi-tentaculate genera, *Cirriformia*, *Cirratulus*, and *Timarete*, with the new species (Rousset et al. 2007, Hardy et al. 2011, Magalhães et al. 2014, Weidhase et al. 2014, Lado et al. 2016, Weidhase et al. 2016). The GenBank accession numbers of them are represented on Table 1. In ML tree (Fig. 6), all cirratulid species showed the specific validity by the molecular data of the present study. In generic level, the *Timarete* species including *T. posteria* sp.

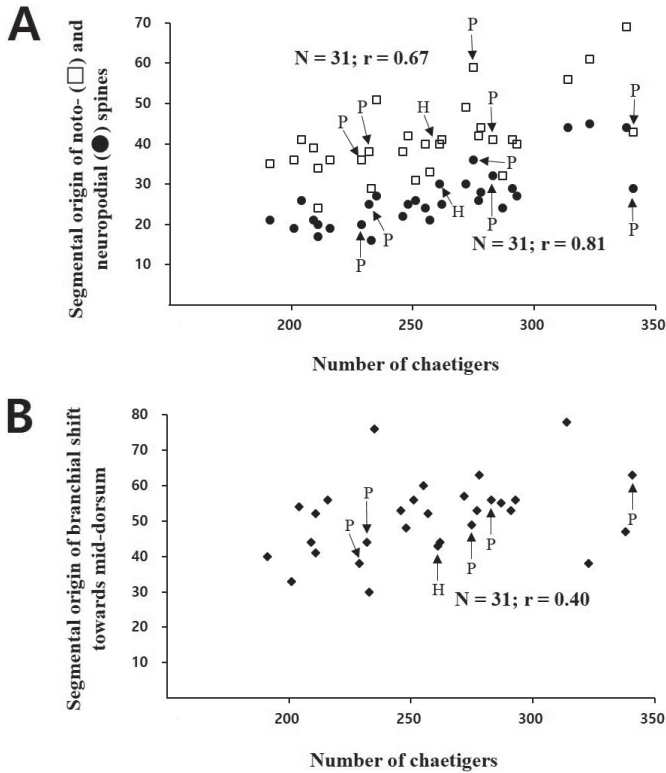


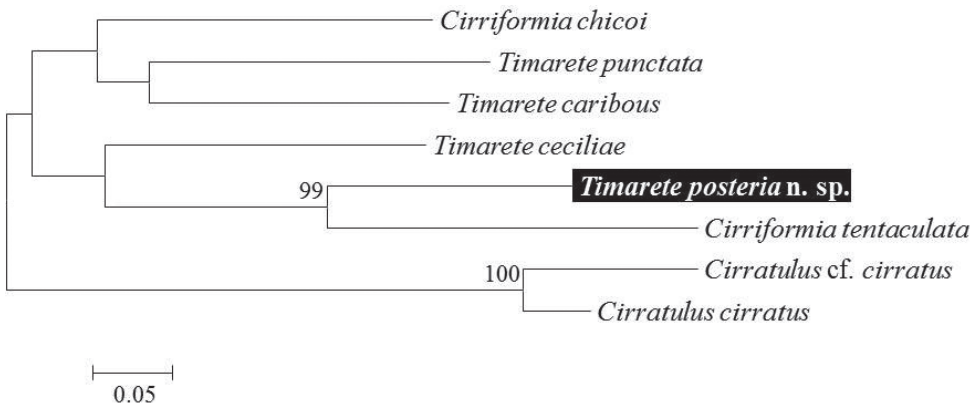
Figure 5. Variation of ontogenetic characters in *Timarete posteria* sp. n. **A** relationship between total number of chaetigers and segmental origin of noto- and neuropodial spines **B** relationship between total number of chaetigers and segmental origin of branchial shift toward mid-dorsum. Abbreviations: holotype (H), paratypes (P).

n. formed a clade with two *Cirriformia* species, *C. chicoi* Magalhães, Seixas, Paiva, & Elias, 2014 and *C. tentaculata* (Montagu, 1808), showing a similar result to the phylogenetic tree of Magalhães et al. (2017). This result suggests that both of the genera *Timarete* and *Cirriformia* are not monophyletic and they are closely related to each other. However, the reality of phylogenetic relationship between *Timarete* and *Cirriformia* still merits further study with more morphological and molecular information of the multi-tentaculate genera.

Remarks. The major characteristics of *Timarete posteria* sp. n. are mostly similar to those of *Timarete luxuriosa* (Moore, 1904), originally described from Southern California (Blake 1996). Both species share the following morphological features: 1) branchial filaments a single pair per segment, gradually shifting toward mid-dorsum from relatively posterior chaetigers compared to its congeners (the dorsal shift of branchial filaments occurred at about chaetiger 35 when the body with 350 segments in *T. luxuriosa* and occurred at chaetigers 38–78 with more than 300 segments and at chaetigers 30–76 with less than 300 segments in the new species, while that occurred at chaetigers 7–26 in other *Timarete* species); 2) tentacular filaments arising from the

Table 1. GenBank accession numbers for sequences obtained in the present study.

Species	GenBank accession number		Data source
	COI	16S	
<i>Timarete posteria</i> sp. n.	MH708229	MH822840	Present study
<i>Timarete caribous</i>	KM192177	KM192193	Magalhães et al. 2014
<i>Timarete ceciliae</i>	KM192179	KM192195	Magalhães et al. 2014
<i>Timarete punctata</i>	KM192188	KM192205	Magalhães et al. 2014
<i>Cirriiformia tentaculata</i>	KR916808	KT033725	Lado et al. 2016 (COI) Weidhase et al. 2016 (16S)
<i>Cirriiformia chicoi</i>	KM192165	KM192189	Magalhães et al. 2014
<i>Cirratulus cirratus</i>	HM417794	DQ779609	Rousset et al. 2007 (16S) Hardy et al. 2011 (COI)
<i>Cirratulus</i> cf. <i>cirratus</i>	KM083601	KT033724	Weidhase et al. 2014 (COI) Weidhase et al. 2016 (16S)

**Figure 6.** Maximum likelihood (ML) tree for four species of *Timarete* with four other related species in the multi-tentaculate cirratulid genera, *Cirriiformia* and *Cirratulus*, inferred from combined dataset with COI and 16S. Numbers above the branch indicate ML bootstrap values from 1000 replication.

dorsum of chaetigers 5–6 (usually 5–6 and sometimes 6–7 or 7–8 in the new species); 3) notopodial spines originating from chaetiger 50 (24–69 in the new species) and pale brown in color; and 4) neuropodial spines originating from chaetiger 31 (16–45 in the new species) and dark brown in color (Blake 1996). However, *T. posteria* sp. n. clearly differs from *T. luxuriosa* in peristomium, notopodial spines, and shifting branchial filaments as follows: 1) the peristomium is evenly divided into three annulations in *T. posteria* sp. n., while that of *T. luxuriosa* comprises one large and three smaller annulations; 2) *T. posteria* sp. n. bears 2–4 neuropodial spines accompanied by a few capillaries in the posterior chaetigers, however, *T. luxuriosa* contains a single neuropodial spine without capillaries in the posterior chaetigers after around chaetiger 90; 3) completely shifted branchial filaments are located at about one-third distance between notopodium and dorsal midline in *T. posteria* sp. n., whereas those of *T. luxuriosa* are positioned at about two-thirds distance (Blake 1996).

The methyl green staining pattern (MGSP), which may be of diagnostic value, is unavailable for many *Timarete* species except for a few species recently described (Imajima and Hartman 1964, Blake 1996, Çinar 2007, Magalhães and Bailey-Brock 2010, Magalhães et al. 2014). Nevertheless, the MGSP of the new species is distinct from the previously described patterns from five *Timarete* species, including *T. caribous* (Grube, 1859), *T. ceciliae* Magalhães, Seixas, Paiva & Elias, 2014, *T. hawaiiensis* (Hartman, 1956), *T. oculata* (Treadwell, 1932), and *T. punctata* (Grube, 1859), by a combination of the following features: 1) intense staining of the prostomium, peristomium, and dorsum of the first three chaetigers; 2) the presence of transverse bands forming complete rings in the posterior half of each segment (Magalhães and Bailey-Brock 2010, Magalhães et al. 2014). MGSP is a useful diagnostic feature in *Timarete* species, and additional MGSP information for several *Timarete* species is still required.

Discussion

Timarete antarctica (Monro, 1930) was originally reported from South Georgia in the Antarctic region (Monro 1930, Hartman 1966). It also has been widely reported from Korean and Japanese waters (Imajima and Hartman 1964, Paik 1989). However, this species is clearly distinguished from other *Timarete* species including *Timarete posteria* sp. n. based on having single capillary chaetae and longitudinal rows of tentacular filaments, while other *Timarete* species contain both capillary chaetae and acicular spines, and tentacular filaments arranged in transverse rows (Monro 1930, Imajima and Hartman 1964, Hartman 1966, Paik 1989, Blake 1996, Magalhães et al. 2014). Therefore, generically *T. antarctica* should be referred to the genus *Protocirrinieris* Czerniavsky, 1881 based on the chaetal composition and arrangement of tentacular filaments (Blake 1996).

Blake (1996) suggested that the shift of the branchial filaments toward the mid-dorsum in middle and posterior chaetigers is a significant generic diagnostic feature of *Timarete*. However, some *Timarete* species, including *T. japonica* Zachs, 1933, *T. dasylophius* (Marenzeller, 1879), and *T. gibbosa* (Moore, 1903) from East Asia, have been recorded or combined without considering the shift in branchial filaments (Zachs 1933, Imajima and Hartman 1964). Zachs (1933) defined *T. japonica* from the Sea of Japan based on a very brief record without description and illustration. Although the detailed diagnostic features of the species were inadequately dealt with, *T. japonica* is distinctly different to *Timarete* species in the diagnostic features suggested by Blake (1996). Zachs (1933) suggested that the lateral branchial filaments attached almost at the bases of notopodia are a diagnostic feature of *T. japonica*. We think that *T. japonica* may be a species of *Cirriformia* Hartman, 1936, because of the absence of shifting branchial filaments.

Imajima and Hartman (1964) redefined two cirratulid species originally recorded from Japanese waters, which were described as species of the genus *Cirratulus* Lamarck, 1818, as *Timarete* species, *T. dasylophius* and *T. gibbosa*. The single diagnostic feature of *Timarete* species included the tentacular filaments present on the dorsum of two or

more chaetigers, which determined the taxonomic status of these two species (Imajima and Hartman 1964). Among these two species, *T. gibbosa* has the shift of branchial filaments, which indicates that a pair of branchiae per segment are located at about midway between the parapodium and the dorsal mid-line except those on anterior segments (Moore 1903). Despite of having shifted branchial filaments, *T. gibbosa* is suspected to be a species of *Cirratulus* based on Imajima and Hartman's (1964) description indicating that this species has the transverse series of eyespots on the prostomium and the neuropodial spines from chaetiger 1. These characteristic features are commonly observed in *Cirratulus* (Blake 1996, Bottero et al. 2017). Moreover, the shift of branchial filaments, which is one of the representative characteristic features of this species, is also found from *Cirratulus* as well as *Timarete* (Blake 1996, Bottero et al. 2017). The affiliation of *C. dasylophius* to *Timarete* is also questionable because of the lack of reference to the shift of branchial filaments in the original description as well as Imajima and Hartman's study (Marenzeller 1879, Imajima and Hartman 1964). Furthermore, *T. dasylophius* has the branchial filaments from chaetiger 2 (Imajima and Hartman 1964) while *Timarete* species generally bear those from the last peristomial annulation or chaetiger 1 (Blake 1996, Magalhães et al. 2014). We suppose that Imajima and Hartman (1964) may have overlooked the presence of the scars of branchial filaments present on the peristomium or chaetiger 1.

Consequently, we suggest that three *Timarete* species previously recorded from East Asia, *T. japonica*, *T. dasylophius*, and *T. gibbosa*, are not valid species within the genus yet. Further study with the type materials is needed to verify their generic affiliation. Under a modern view of cirratulid taxonomy, meanwhile, three species among presently known *Timarete* species, *T. anchylochaeta* (Schmarda, 1861), *T. norvegica* (Quatrefages, 1865), and *T. polytricha* (Schmarda, 1861), are still remaining to be designated as valid members of *Timarete* because previous records of them have only poor information with brief descriptions and simple drawings (Schmarda 1861, Quatrefages 1865, Blake 1996, Magalhães et al. 2014). We herein provide a key to the species regarded as valid members of *Timarete*.

Key to valid species of the genus *Timarete*

- 1 Dorsal branchiae abruptly shifted 2
- Dorsal branchiae gradually shifted 4
- 2 Neuropodial spine on posterior segments single.....
..... ***T. caribous* (Grube & Ørsted in Grube, 1859)**
- Neuropodial spine on posterior segments more than two 3
- 3 Number of tentacular filaments 7–9 ***T. hawaiiensis* (Hartman, 1956)**
- Number of tentacular filaments 15–20 ***T. filigera* (Delle Chiaje, 1828)**
- 4 Branchial filaments one pair per segment 5
- Branchiae filaments 2–5 pair per segment.....
..... ***T. perbranchiata* (Chamberlin, 1918)**

5	Branchiae and tentacular filaments with black lateral stripes	<i>T. punctata</i> (Grube, 1859)
–	Branchiae and tentacular filaments without pigmentation patterns	6
6	Lateral bulge over notopodia formed in shift of branchiae	7
–	Lateral bulge over notopodia not formed in shift of branchiae	9
7	Shift of branchiae arising beyond chaetiger 30	8
–	Shift of branchiae arising in chaetigers 12–14	<i>T. nasuta</i> Ehlers, 1897
8	Posterior chaetigers with 2–4 neuropodial spines	<i>T. posteria</i> sp. n.
–	Posterior chaetigers with single neuropodial spine.....	<i>T. luxuriosa</i> (Moore, 1904)
9	Notopodial spines originated from chaetigers 11–23	<i>T. ceciliae</i> Magalhães, Seixas, Paiva & Elias, 2014
–	Notopodial spines originated from chaetigers 57–58	<i>T. oculata</i> (Treadwell, 1932)

Acknowledgments

This study was supported by the National Institute of Biological Resources (NIBR), funded by the Ministry of Environment (MOE) of the Republic of Korea (NIBR201401201), and partly supported by the National Marine Biodiversity Institute of Korea as a part of the ‘Securement, Discovery, and Basic Survey of Marine Bio-resources (2018M00100)’. We are grateful to editor, Dr. Greg Rouse and two reviewers, Drs. James A. Blake and Wagner F. Magalhães, for providing valuable suggestions.

References

- Blake JA (1996) 8. Family Cirratulidae Ryckholdt, 1851. Including a revision of the genera and species from the eastern North Pacific. In: Blake JA, Hilbig B, Scott PH (Eds) Taxonomic Atlas of the Benthic Fauna of the Santa Maria Basin and the Western Santa Barbara Channel. Volume 6 – The Annelida Part 3, Polychaeta: Orbiniidae to Cossuridae. Santa Barbara Museum of Natural History Press, Santa Barbara, California, 263–384.
- Bottero MAS, Elias R, Magalhães WF (2017) Taxonomic revision of *Cirratulus* (Polychaeta: Cirratulidae) from the coasts of Argentina, with description of a new species. Journal of the Marine Biological Association of the United Kingdom 97: 889–896. <https://doi.org/10.1017/S0025315417000807>
- Çinar ME (2007) Re-description of *Timarete punctata* (Polychaeta: Cirratulidae) and its occurrence in the Mediterranean Sea. Scientia Marina 71: 755–764. <https://doi.org/10.3989/scimar.2007.71n4755>
- Fauchald K (1977) The Polychaete Worms. Definitions and keys to the orders, families and genera. Natural History Museum of Los Angeles County. Science Series 28: 1–190.

- Folmer O, Black M, Hoeh W, Lutz R, Vrijenhoek R (1994) DNA primers for amplification of mitochondrial cytochrome c oxidase subunit I from diverse metazoan invertebrates. *Molecular Marine Biology and Biotechnology* 3: 294–299.
- Hardy SM, Carr CM, Hardman M, Steinke D, Corstorphine E, Mah C (2011) Biodiversity and phylogeography of Arctic marine fauna: insights from molecular tools. *Marine Biodiversity* 41: 195–210. <https://doi.org/10.1007/s12526-010-0056-x>
- Hartman O (1966) Polychaeta Myzostomidae and Sedentaria of Antarctica. *Antarctic Research Series* 7: 1–158. <https://doi.org/10.1029/AR007>
- Imajima M, Hartman O (1964) The polychaetous annelids of Japan. Allan Hancock Foundation Publications. Occasional Papers 26: 1–452.
- Larkin MA, Blackshields G, Brown NP, Chenna R, McGettigan PA, McWilliam H, Valentin F, Wallance IM, Wilm A, Lopez R, Thopson JD, Gibson TJ, Higgins DG (2007) Clustal W and Clustal X version 2.0. *Bioinformatics* 23: 2947–2948. <https://doi.org/10.1093/bioinformatics/btm404>
- Lobo J, Teixeira MA, Borges LM, Ferreira MS, Hollatz C, Gomes PA, Sousa R, Ravara A, Costa MH, Costa FO (2016) Starting a DNA barcode reference library for shallow water polychaetes from the southern European Atlantic coast. *Molecular Ecology Resources* 16(1): 298–313. <https://doi.org/10.1111/1755-0998.12441>
- Magalhães WF, Bailey-Brock JH (2010) Redescription of *Cirriformia crassicollis* (Kinberg, 1866) and *Timarete hawaiiensis* (Hartman, 1956) new combination, (Polychaeta: Cirratulidae), endemic polychaetes to the Hawaiian Islands. *Zootaxa* 2625: 53–62.
- Magalhães WF, Seixas VC, Paiva PC, Elias R (2014) The Multitentaculate Cirratulidae of the Genera *Cirriformia* and *Timarete* (Annelida: Polychaeta) from Shallow Waters of Brazil. *PLoS ONE* 9(11): e112727. <https://doi.org/10.1371/journal.pone.0112727>
- Magalhães WF, Linse K, Wiklund H (2017) A new species of *Raricirrus* (Annelida: Cirratuliformia) from deep-water sunken wood off California. *Zootaxa* 4353: 51–68. <https://doi.org/10.11646/zootaxa.4353.1.3>
- Marenzeller E (1879) Südjapanische Anneliden. *Denkschriften der Kaiserlichen Akademie der Wissenschaften, Mathematisch-naturwissenschaftliche Classe, Wien* 41: 109–154.
- Monro CCA (1930) Polychaete worms. *Discovery Reports, Cambridge* 2: 1–222.
- Moore JP (1903) Polychaeta from the coastal slope of Japan and from Kamchatka and Bering Sea. *Proceedings of the Academy of Natural Sciences of Philadelphia* 55: 401–490.
- Paik EI (1989) Illustrated encyclopedia of fauna and flora of Korea, Vol. 31. Polychaeta. Ministry of Education, Seoul, 764 pp.
- Palumbi SR (1996) Nucleic acid II: the polymerase chain reaction. In: Hillis DM, Moritz C, Mable BK (Eds) *Molecular Systematics*. Sinauer Associates, Sunderland, MA, 205–247.
- Quatrefages A (1865) Histoire naturelle des Annelés marins et d'eau douce. *Annélides et Géphyriens*. Volume 1. Librairie Encyclopédique de Roret, Paris, 588 pp. <https://doi.org/10.5962/bhl.title.122818>
- Rousset V, Pleijel F, Rouse GW, Erséus C, Siddall ME (2007) A molecular phylogeny of annelids. *Cladistics* 23(1): 41–63. <https://doi.org/10.1111/j.1096-0031.2006.00128.x>
- Seixas VC, Zanol J, Magalhães WF, Paiva PC (2017) Genetic diversity of *Timarete punctata* (Annelida: Cirratulidae): Detection of pseudo-cryptic species and a potential biological

- invader. *Estuarine, Coastal and Shelf Science* 197: 214–220. <https://doi.org/10.1016/j.ecss.2017.08.039>
- Schmarda LK (1861) Neue wirbellose Thiere beobachtet und gesammelt auf einer Reise um die Erdr 1853 bis 1857. Turbellarien, Rotatorien und Anneliden. Zweite Hälfte. Wilhelm Engelmann, Leipzig, 164 pp.
- Tamura K, Stecher G, Peterson D, Filipski A, Kumar S (2013) MEGA6: molecular evolutionary genetics analysis version 6.0. *Molecular Biology and Evolution* 30: 2725–2729. <https://doi.org/10.1093/molbev/mst197>
- Thompson JD, Higgins DG, Gibson TJ (1994) CLUSTAL W: improving the sensitivity of progressive multiple sequence alignment through sequence weighting, position-specific gap penalties and weight matrix choice. *Nucleic Acids Research* 22(22): 4673–4680. <https://doi.org/10.1093/nar/22.22.4673>
- Weidhase M, Bleidorn C, Helm C (2014) Structure and anterior regeneration of musculature and nervous system in *Cirratulus cf. cirratus* (Cirratulidae, Annelida). *Journal of Morphology* 275: 1418–1430. <https://doi.org/10.1002/jmor.20316>
- Weidhase M, Bleidorn C, Simon CA (2016) On the taxonomy and phylogeny of *Ctenodrilus* (Annelida: Cirratulidae) with a first report from South Africa. *Marine Biodiversity* 46(1): 243–252. <https://doi.org/10.1007/s12526-015-0355-3>
- Zachs I (1933) K. faune kol'chatykh chervi Severo-Yaponskogo morya (Polychaeta). Gosudarstvennyi Gidrologicheskii Institut, Issledovaniia Morei SSSR. Leningrad 14: 125–137.
- Zanol J, Halanych K, Struck T, Fauchald K (2010) Phylogeny of the bristle worm family Eunicidae (Eunicida, Annelida) and the phylogenetic utility of noncongruent 16S, COI and 18S in combined analyses. *Molecular Phylogenetics and Evolution* 55: 660–676. <https://doi.org/10.1016/j.ympev.2009.12.024>

A survey of basal insects (Microcoryphia and Zygentoma) from subterranean environments of Iran, with description of three new species

Rafael Molero¹, Mohadeseh Sadat Tahami², Miquel Gaju¹, Saber Sadeghi²

1 Departamento de Zoología, C-1 Campus de Rabanales, University of Córdoba, 14071 – Córdoba, Spain

2 Entomology Research Lab, Faculty of Science, Biology Department, Shiraz University, Shiraz, Iran

Corresponding authors: *Rafael Molero* (ba1mobar@uco.es); *Saber Sadeghi* (ssadeghi@shirazu.ac.ir)

Academic editor: *Pavel Stoev* | Received 11 June 2018 | Accepted 24 October 2018 | Published 13 December 2018

<http://zoobank.org/A312BA39-89FF-4D43-B6E2-06F880B956E6>

Citation: Molero R, Tahami MS, Gaju M, Sadeghi S (2018) A survey of basal insects (Microcoryphia and Zygentoma) from subterranean environments of Iran, with description of three new species. *ZooKeys* 806: 17–46. <https://doi.org/10.3897/zookeys.806.27320>

Abstract

A survey of wingless insects belonging to the orders Microcoryphia (=Archaeognatha) and Zygentoma (=Thysanura s. str.) has been performed in subterranean habitats of central Iran. As a result, several new species have been discovered. In this work, three new species are described: a new species of bristletail of the family Machilidae, *Haslundiella iranica* **sp. n.**, a new silverfish of the family Lepismatidae, *Ctenolepisma subterraneum* **sp. n.**, and a new Nicoletiidae, *Lepidospora (Brinckina) montaziana* **sp. n.** These new taxa are compared with related species in their respective genera and keys for their identification are provided: one for all known species of *Haslundiella* and one for all basal insects of subterranean environments of Iran which includes those previously reported. Moreover, the previously published keys of Iranian *Ctenolepisma* and the subgenus *Brinckina* are modified to include the new species. Three additional species of Lepismatidae are reported in this work: *Neoasterolepisma palmonii* and *Ctenolepisma targionii* are newly recorded from Iran and both species, together with *Acrotelsa collaris*, are cited for the first time in the subterranean habitats. This survey progresses the knowledge on the biodiversity of these insects in Iran.

Keywords

Archaeognatha, cave fauna, *Ctenolepisma*, *Haslundiella*, *Lepidospora*, Lepismatidae, Machilidae, Nicoletiidae, taxonomy, Thysanura

Introduction

The subterranean fauna of basal insects is poorly studied in most parts of the world. We consider here as basal insects the orders Microcoryphia (=Archaeognatha) and Zygentoma (=Thysanura s.str.), which both belong to class Insecta. They are primitively wingless and have been included traditionally in the group Apterygota together with Collembola, Protura and Diplura, groups of the superclass Hexapoda that are nowadays excluded from Insecta.

Recently, Iranian caves have been the subject of an extensive faunal study and as a result numerous new invertebrate species, subspecies and even higher taxa are described, most of them known to be highly endemic to only one cave (Christophoryová et al. 2013, Kashani et al. 2013, Malek-Hosseini et al. 2015a, 2015b, 2016a, 2016b, Tahami et al. 2016, 2017a, 2017b, 2017c, 2017d, 2018).

A basal insects survey has been performed in subterranean environments of the Zagros Mountain ranges and the central zone of Iran, covering a vast area of the center of the country. Fars province (Fig. 1) presented the greatest diversity of species and higher taxa. This is in part due to a higher abundance of caves, favorable climate (such as suitable annual humidity and temperature, sufficient precipitation and soil fertility) and, compared to other provinces, high diversity of all insect groups on the surface.

As a result of this study, eight species belonging to two orders (Microcoryphia and Zygentoma) and three families (Machilidae, Lepismatidae and Nicoletiidae) have been found. Of these eight species, five of them are new; two belong to new supraspecific taxa of the family Nicoletiidae and were described previously (Tahami et al. 2018). The remaining three new species are described in this work – one Machilidae belonging to the genus *Haslundiella* Janetschek, 1954, one Lepismatidae to the genus *Ctenolepisma* Escherich, 1905 and a third species of Nicoletiidae belonging to the genus *Lepidospora* Escherich, 1905 – together with comments on other three species of Lepismatidae that have been found in subterranean habitats, two of them reported for the first time for Iran.

Keys for identifying these eight species of subterranean basal insects in Iran are presented, together with a key to the genus *Haslundiella* (Microcoryphia, Machilidae) and annotations to include the new species of Zygentoma in previously published keys: Kahrarian et al. (2014) for Iranian *Ctenolepisma* and Mendes (2002) for *Lepidospora*.

Material and methods

Collecting methods

Specimens were collected during a faunal survey of the caves of Zagros and the Central zone of Iran. Locations where basal insects were collected are shown in Fig. 1. Accord-

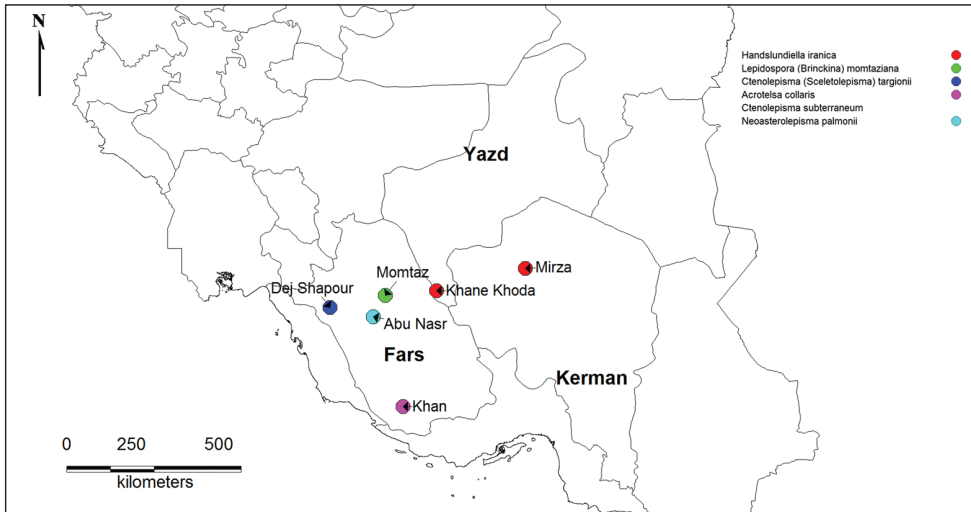


Figure 1. Distribution map of cave localities, Iran.

ing to the policy of the Iranian Speleological Society, cave coordinates could not be published, for the sake of caves' safety and conservation. The collection was carried out through a meticulous investigation of all zones of the caves, generally referred to as the endogean (entrance), parahypogean (twilight) and hypogean (dark) zones. Specimens were found mainly in the soil or under stones and collected with a fine brush. After their capture, they were preserved in labeled vials with ethanol 75% and transported to the laboratory for further studies.

Laboratory material and methods

When dissected, specimens were mounted on a slide using Tendeiro medium (Molero-Baltanás et al. 2000). Identifications were made using a Nikon Labophot light microscope, and for new species, drawings were made using a camera lucida attached to the microscope. Some micrographs were taken using a Nikon DS-Fi1 digital camera on the aforementioned microscope.

Abbreviations for the descriptions of *Microcoryphia* are explained in the legend of Tables 1 and 2.

The types of the new species are deposited in the collection of the Museo Nacional de Ciencias Naturales in Madrid (MNCN, Spain). The remaining material is deposited in the scientific collection of the Department of Zoology of Córdoba University, Spain (UCO) and in the Zoological Museum and Biological Collection of Shiraz University, Iran (ZM-CBSU).

Taxonomy

Order Microcoryphia (=Archaeognatha)

Family Machilidae

Haslundiella iranica Gaju, Molero, Tahami & Sadeghi, sp. n.

<http://zoobank.org/DF55D262-64C2-47CE-8ED9-0A8834DA25DD>

Figs 2–6; Tables 1, 2

Type material. **Holotype** (MNCN): male, body length = 8.5 mm, preserved in alcohol and partially mounted on slide, both vial and slide labelled “Mirza Cave, Rafsanjan, Kerman Province, Iran. 20.VI.2015. Cat. Types N. 2834”; “HOLOTYPE ♂ *Haslundiella iranica* sp. n., des. Gaju, Molero, Tahami & Sadeghi, 2018”. **Paratypes** (3 ex.): 1 male (UCO): same data as holotype, preserved in alcohol and partially mounted on slide, Ref. M1655a. 1 female juvenile, preserved in alcohol (Fig. 2): same locality and date, Ref. M1655b. 1 female (ZM-CBSU): from Khane Khoda cave, Heart, Yazd Province, Iran. 30.IX.2015, preserved in alcohol and partially mounted on slide (#C2636).

Diagnosis. Machilidae of medium size, about 8–9 mm. Body unpigmented. Compound eyes wider than long ($l/w = 0.65$), lateral ocelli in sublateral position. Antennae shorter than body length, distal chains with a lower number of annuli compared with the remaining species of the genus. Coxal styli on middle and hind legs. Urosternites with 1+1 eversible vesicles; sternites with their posterior angle slightly obtuse, about 95° . Male without special chaetotaxy on maxillary palps and legs. Proximal part of the penis less than 1.3 times longer than the distal part. Female ovipositor with 1+58 divisions.

Description. *Habitus of the new species.* All specimens, although coming from two different locations (about 300 km apart from each other), are very similar because their whitish, unpigmented bodies (Fig. 2). Body length of male 8.5 mm, female 9 mm. Body and appendages covered with scales and completely devoid of pigment. Paracercus and cerci broken. Dorsal scales pattern unknown. Meso and metathorax as usual in the order, not especially humped. Antennae shorter than the body, the specimen with longest antennae, a subadult female 7.5 mm long, with antennae of 3.9 mm (Fig. 2). Compound eyes black (Fig. 3, from adult female, those of males not clearly visible), wider than long ($l/w: 0.65$ and $cl/l: 0.53$). Frons not especially protruded between paired ocelli, which are brownish, sublateral, transversally ovoid: $w/l: 2.29$; not especially small ($w.ocellus/w.eye: 0.55$).

Description of males. Head: Antennae broken in the holotype (preserved length: 3.6 mm), scapus (Fig. 4A) not especially long ($l/w: 1.52$); distal chains with 10, 11 annuli (Fig. 4B); each annulus with one circle of bristles, slightly longer than the diameter of the annuli (Fig. 4C), some of them straight and strong others thinner and curled; the penultimate annuli of each chain with two specialized basiconic sensilla. Male maxillary palp not modified and without special chaetotaxy (Fig. 4D, E), all articles of similar length, only the third article slightly shorter ($l\ 3^{rd}/l\ 7^{th} = 0.88$). Hyaline spines in articles 5, 6 and 7 typical, low in number (2, 6 and 7 respectively); article ratios shown in Table 1. Labial palp typical, third article not specially enlarged (Fig. 4F);



Figure 2. *Haslundiella iranica* sp. n., habitus (female specimen from Mirza cave).

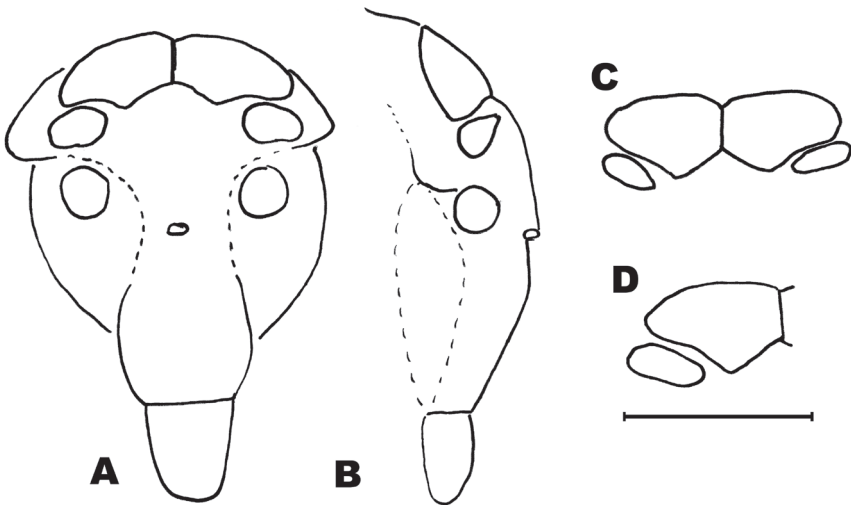


Figure 3. *Haslundiella iranica* sp. n., female from Khane Khoda cave. **A** head frontal view **B** head, lateral view **C** frontal view of compound eyes **D** frontal view of right eye and lateral ocellus. Scale bar: 1 mm.

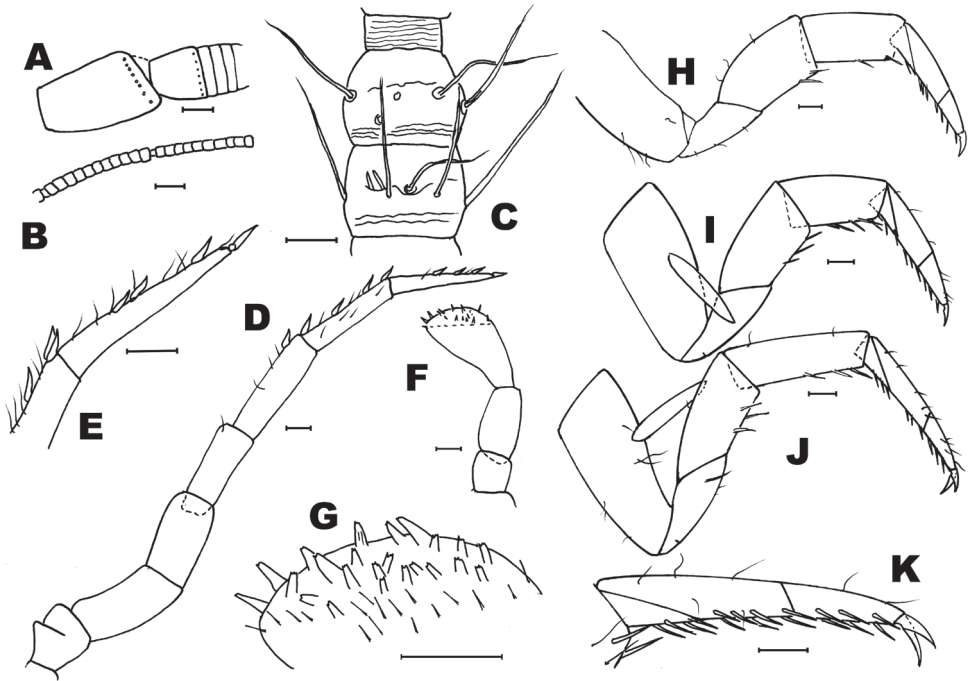


Figure 4. *Haslundiella iranica* sp. n., male holotype (Mirza cave). **A** antennal scapus, pedicellus and basal annuli of flagellum **B** antennal distal chains **C** chaetotaxy of apical annuli of antennal distal chain **D** maxillary palp **E** seventh article of maxillary palp **F** labial palp **G** field of sensorial cones of third article of labial palp **H** fore leg **I** mid leg **J** hind leg **K** tarsus of hind leg. Scale bars: 0.1 mm (**A, B, D–K**); 50 μ m (**C**).

sensorial cones typical, not very numerous (Fig. 4G), surrounded by strong bristles slightly longer than these cones (in the female this character is clearer).

Thorax: Second and third pair of legs with a stylus on the coxa, their length about 2/3 of the coxa (0.63). Fore femur not especially enlarged (Fig. 4H); hind tibiae longer than fore and mid tibiae (Figs. 4H–J); all legs without special chaetotaxy, only with spines inserted ventrally on femora, tibiae and tarsi (Fig. 4K and Table 2); these spines have their distal part dark.

Abdomen: urosternites with medial sternite (Fig. 5A), slightly obtusangle (95°); with one pair of eversible vesicles on urocoxites I–VII; styli present on segments II–IX, the terminal spine of each stylus not so long; styli with strong subterminal spiniform setae (Fig. 5B); stylus/coxite and spine/stylus ratios shown in Table 1. Coxites VII–IX with hyaline spines (Fig. 5C, F and Table 1). Male genitalia without parameres VIII; penis and parameres IX completely covered by coxites IX, surpassing slightly half the coxite (Fig. 5E); parameres with 1+6–7 divisions (Fig. 5G), not surpassing the tip of penis; proximal part of penis longer than distal part, ratio pp/pd: 1.26. Penis opening subterminal (Fig. 5H).

Description of females. The only adult female has most of its appendages broken and some of them are lost, specifically right antennae, left maxillary palp, fore legs and left middle leg.

Table 1. Comparison of several morphometric parameters of *Haslundiella iranica* sp. n. with the remaining species of the genus. **Length:** body length from frons until the end of tenth tergite; **eyes cl/l:** eye contact line/eye length; **eye l/w:** length/width of eye; **paired ocelli w/l:** width/length; **w ocelli/w eye:** width ocelli/width eye; **l ant:** length antennae; **scapus l/w:** scapus length/width; **ant d.c.:** number of annuli of antennal distal chains; **l cerci:** length cercus; **l p.cercus:** length paracercus; **mx-p7-p6-p5-p4-p3-p2/mx-p7:** length of maxillary palp articles 7–6–5–4–3–2/length of maxillary palp 7; **sp mx-p 7** and **sp mx-p 6:** spines on the dorsal side of maxillary palp articles 7th and 6th; **l Ti1:** length of fore tibia; **Fe1 (l/w):** length/width of fore femur; **l st-cx-L2-L3:** length of coxal stylus from second and third legs respectively; **l st/l cx-L2-L3:** length of coxal stylus/ length of coxa for second and third legs respectively; **angle of st abd V:** angle of urosternite V; **st/cx abd V, VIII, IX:** length stylus without spine/length coxite of urosternites V, VIII and IX; **sp/st abd V, VIII, IX:** length terminal spine/length of stylus without spine V, VIII and IX; **pp/pd penis:** length proximal /length distal part of penis; **parameres:** number of divisions of parameres; **g-VIII, IX:** number of divisions of gonapophysis VIII and IX. Data from *H. steinitzi* and *H. nisensis* obtained from text or drawings of original descriptions (those calculated from drawings are marked with bold).

	Males			Females		
	<i>H. steinitzi</i>	<i>H. nisensis</i>	<i>H. iranica</i> n. sp.	<i>H. steinitzi</i>	<i>H. nisensis</i>	<i>H. iranica</i> n. sp.
length (mm)	9.5	8.3–10	8.5		11–12	9
eyes cl/l	0.5	0.54–0.58			0.5	0.53
eyes l/w	0.7	0.74–0.77			0.73	0.65
paired ocelli w/l	2.33	2			2.25	2.29
w ocelli/w eye	0.5	0.57–0.59			0.54	0.55
l ant (mm)	> 9.5	> 8.3/10				3.6
scapus (l/w)			1.7			1.98
ant d.c.	18	13 (12–17)	10–11			
l cerci (mm)					4.9	
l p-cercus (mm)		>8.3–10				
mx-p 6/7	1.54	1	1	1.29		
mx-p 5/7	2	1.42	1.05	1.71		
mx-p 4/7	2.23	1.46	0.98	1.64		
mx-p 3/7	0.77	0.88	0.88	1		
mx-p 2/7	1.31	0.88	0.93	1.43		
sp mx-p 7		6–7	7		8–10	
sp mx-p 6		6–7	6		8–10	
l Ti1 (mm)			0.6			
Fe1 (l/w)	2.17	2.26	1.89			
l st-cx-L2-L3 (mm)		0.6–0.65	0.5			
l st/l cx-L2-L3		0.52–0.56	0.52			
angle st abd V	> 90°	95°	95°			95°
st/cx abd V	0.4–0.45	0.55–0.65	0.43	0.4–0.45	0.55–0.65	0.45
sp/st abd V			0.32		0.21	0.32
st/cx abd VIII	0.9	1	0.7	0.9	1	0.87
sp/st abd VIII			0.27			0.27
st/cx abd IX	1	1.4	0.77	0.75	1	0.74
sp/st abd IX	0.11		0.21		0.09	0.15
pp/pd penis	ca 1.87	1.6	1.26			
parameres	1+(7–8)	1+7	1+(6–7)			
g-VIII				1+(45–50)		1+58
g-IX					1+65	1+58

Table 2. Comparison of the numbers of spines in different articles of legs of *Haslundiella iranica* sp. n. with the remaining species of the genus. **sp Fe1, 2, 3:** number of spines on fore, mid and hind femur; **sp Ti1, 2, 3:** number of spines on fore, mid and hind tibia; **sp Ta1–1, 2, 3:** number of spines on the three articles of fore tarsus (the same for mid tarsus –**sp-Ta2**– and hind tarsus –**sp-Ta3**).

	Males			Females		
	<i>H. steinitzi</i>	<i>H. nisensis</i>	<i>H. iranica</i> n. sp.	<i>H. steinitzi</i>	<i>H. nisensis</i>	<i>H. iranica</i> n. sp.
sp Fe1	1	1	1			
sp Ti1	2	3–6	2–4			
sp Ta1–1		3–6	2–3			
sp Ta1–2		8–12	6–7			
sp Ta1–3		6–8	6			
sp Fe2	1		1–2			
sp Ti2	2		3–6			6
sp Ta2–1			2–4			3–4
sp Ta2–2			5–6			8
sp Ta2–3			6			6
sp Fe3	1		0–1			0–2
sp Ti3	5		3–4			7
sp Ta3–1			4			6
sp Ta3–2			7			8–9
sp Ta3–3			6			5–6

Head: As described in habitus section. Antennae broken, only the basal part of the left one is preserved; scapus similar to that of the male (Fig. 5I). Maxillary palp broken, the three basal articles preserved shown in Fig. 5L. Labial palp (Fig. 5J) as in male, but the strong setae surrounding the sensorial cones of the third article seem stronger (Fig. 5K).

Thorax: Middle and hind legs (Fig. 6A, B) similar to that of male, but slightly bigger; without special chaetotaxy, only ventral spines on femora, tibiae and tarsi (Table 2).

Abdomen: sternites typical of the genus, slightly obtusangle (95°), slightly bigger than those of male (Fig. 6C); styli of coxite similar to those of males (Fig. 6D). Coxite VII modified, with a terminal inner projection (Fig. 6E); one spine in its outer side. Coxites VIII and IX typical, with one spine in the outer side of the former (Fig. 6F) and two spines in the inner part of the later (Fig. 6G). Ovipositor of tertiary type, with 1 + 58 divisions, not attaining the apex of styli IX (Fig. 6G); gonapophysis VIII (Fig. 6H, I) with conspicuous chaetotaxy in the 22 distal divisions (36–58) and gonapophysis IX (Fig. 6J, K) in the 19 distal divisions (39–58), in the remaining divisions the chaetotaxy consists of very small bristles (if they are present).

Discussion. The first species described of the genus *Haslundiella* Janetschek, 1954 was found in Palestine and was named as *Praemachilis steinitzi* (Wygodzinsky, 1942). In their description Wygodzinsky (1942) suggested that “*The remarkable formation of maxillary palp and the genitalia of the male might, in the future, lead to establish a new genus within the Praemachilinae*”. Janetschek (1954) erected the genus *Haslundiella*, including in it only *H. steinitzi*. Kaplin (1982) described the second species of this genus (*H. nisensis* Kaplin, 1982) from Turkmenistan. Now, *Haslundiella iranica* sp. n. is described from Iran, geographically placed between the two former species.

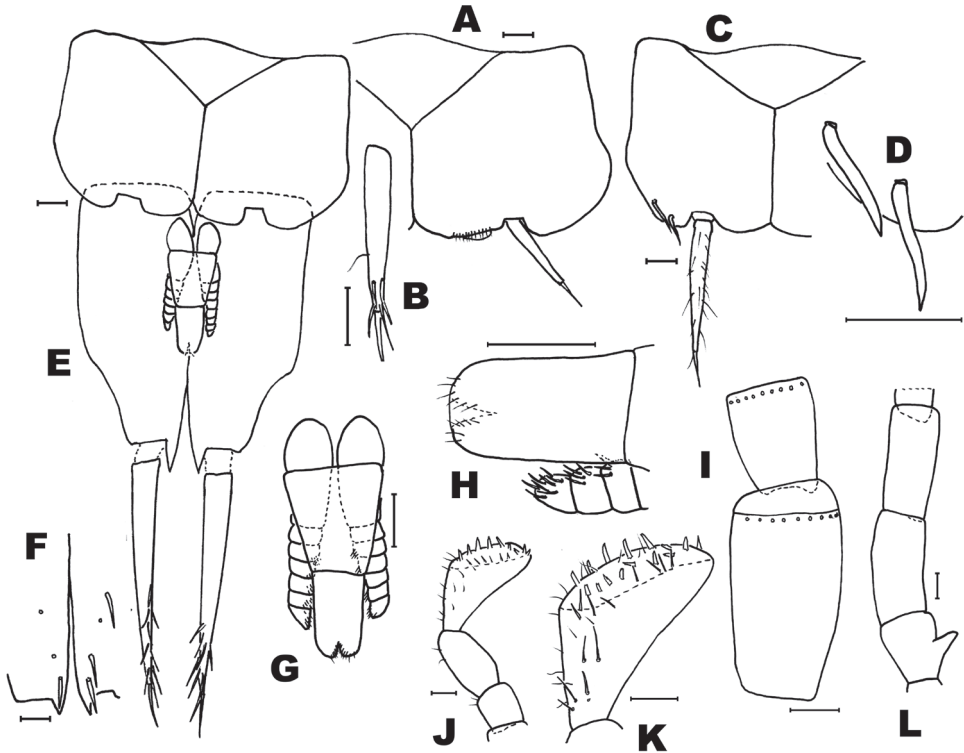


Figure 5. *Haslundiella iranica* sp. n.: male holotype (A, B, E, G, H), male paratype from Mirza cave (C, D, F) and female paratype (I–L). A fifth urosternite B fifth abdominal stylus C eighth urosternite D detail of lateral spines of eighth coxite E eighth and ninth urosternites with male genitalia F detail of spines in coxite IX G penis and nine parameres H penis opening I antennal scapus and pedicellus J labial palp K third labial palp article L preserved part of maxillary palp. Scale bar: 0.1 mm.

Haslundiella iranica sp. n., can be distinguished from the other species by several characters, with the most remarkable being the significant absence of special chaetotaxy on the maxillary palps and the legs of males. Moreover, some other characters can be mentioned: Antennae are shorter than body length; the shape of the maxillary palp is different because all articles are similar in length, showing clear differences with *H. steinitzi* and *H. nisensis* (Table 1); and legs are similar in shape but with very different chaetotaxy. The male genitalia of *H. iranica* is clearly different from that of *H. steinitzi* and similar to *H. nisensis*, although penis ratios are different to those of both previously described species. The female ovipositor does not surpass the styli IX, as in *H. nisensis*, although with lower number of divisions, meanwhile that of *H. steinitzi* has a low number of divisions but surpasses the styli IX.

Distribution. Only known from the two localities in Kerman and Yazd provinces in Iran (see Fig. 1).

Etymology. The name *iranica* is a genitive case of the name Iran, the country where the new species is found.

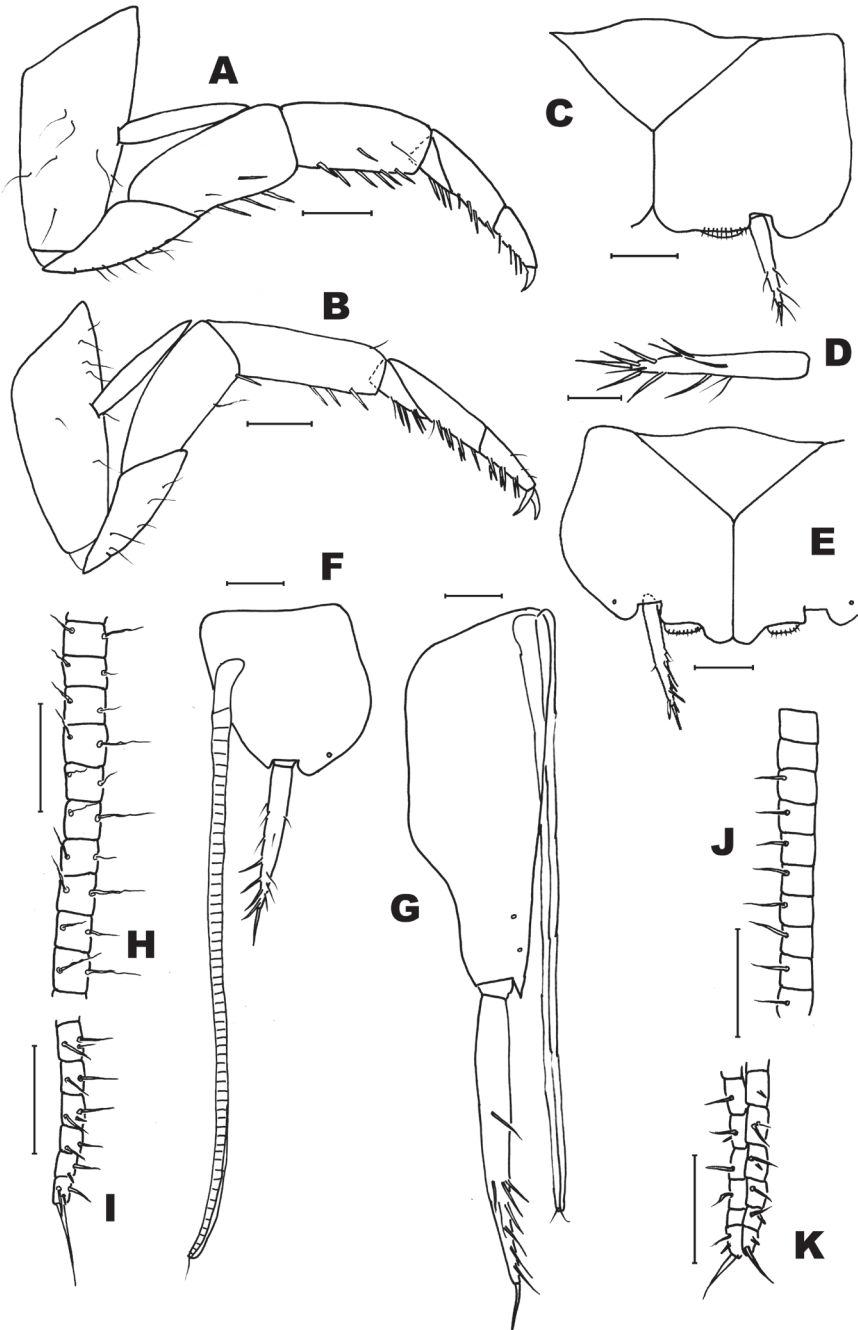


Figure 6. *Haslundiella iranica* sp. n.: female paratype. **A** mid leg **B** hind leg **C** fifth urosternite **D** fifth abdominal stylus **E** seventh urosternite **F** eighth urocoxite and gonapophysis **G** ninth urocoxite and gonapophysis **H** medial part of eighth gonapophysis (divisions 36–45) **I** distal part of eighth gonapophysis (divisions 53–58) **J** medial part of ninth gonapophysis (divisions 37–46) **K** distal part of ninth gonapophysis (divisions 53–58). Scale bars: 0.25 mm (**A–C, E**); 0.2 mm (**F, G**); 0.1 mm (**D, H–K**).

Habitat. The specimens were found and collected close to the entrance of the cave where it was still darker and more humid than the outside (somewhere between the endogean and parahypogean zones) and couldn't be found deeper in as the cave is a complex of horizontal (about 50 m from the entrance) and then vertical (a 50 m of a vertical pit) passages reaching a big hall at the end.

Key to *Haslundiella* species

- | | | |
|---|--|--------------------------|
| 1 | Males..... | 2 |
| – | Females..... | 4 |
| 2 | Maxillary palp with especial chaetotaxy..... | 3 |
| – | Maxillary palp without especial chaetotaxy | <i>H. iranica</i> sp. n. |
| 3 | Fore femur and tibia with short delicate setae; tibia with a dorsal field of long bristles | <i>H. steinitzi</i> |
| – | Fore femur without especial chaetotaxy..... | <i>H. nisensis</i> |
| 4 | Ovipositor projecting beyond styli IX for one third (with 45–50 divisions); ratio stylus/coxite IX: 0.75 | <i>H. steinitzi</i> |
| – | Ovipositor not surpassing the IX styli | 5 |
| 5 | Ovipositor with 65 divisions; ratio stylus/coxite IX: 1..... | <i>H. nisensis</i> |
| – | Ovipositor with 58 divisions; ratio stylus/coxite IX: 0.74... .. | <i>H. iranica</i> sp. n. |

Order Zygentoma

Family Lepismatidae

Ctenolepisma subterraneum Molero, Tahami, Sadeghi & Gaju, sp. n.

<http://zoobank.org/08CC79A7-2E2C-4330-A6C8-4028B5503B47>

Figs 7, 8

Type material. Holotype (MNCN): female, body length = 7 mm, mounted on slide, labelled “Abu Nasr cave, Shiraz, Fars Province, Iran. 12.XI.2015. Cat. Types N. 2835”; “HOLOTYPE ♀ *Ctenolepisma subterraneum* sp. n., des. Molero, Tahami, Sadeghi & Gaju, 2018”.

Diagnosis. Very faintly pigmented and medium-sized lepismatid. Distribution of scales and trichobothrial areas as in *C. ciliatum*. Apical article of the labial palp with almost parallel sides and three sensory papillae arranged in a single row. Pronotum with 9–10 combs of macrosetae, mesonotum with 14 pairs and metanotum with 11 pairs of combs. Prosternum with 2+2 bristle-combs, mesosternum with 1–2 pairs of combs and metasternum with 1+1 combs. Macrosetae of thoracic sternites arranged in one row. Urosternites III–VIII with 1+1 lateral combs. All urosternites without median combs (subgenus *Ctenolepisma* s. str. sensu Irish, 1987). Urotergite I with 1+1 combs, II–VI with 3+3 combs and VII–VIII with 2+2 combs (*ciliatum*-group sensu Mendes, 1982). Urotergite X trapezoidal. Two pairs of styli. Ovipositor with 40 divisions. Male sex unknown.

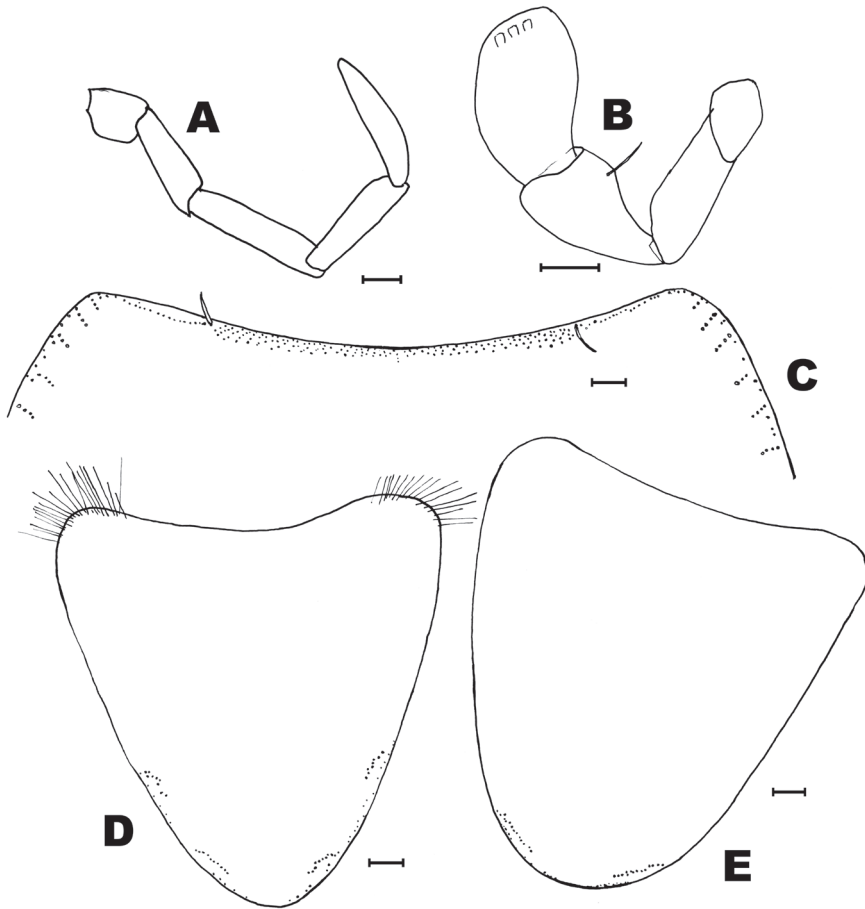


Figure 7. *Ctenolepisma subterraneum* sp. n. holotype, head and thorax. **A** maxillary palp **B** labial palp **C** anterior part of the pronotum, showing insertions of macrosetae **D** prosternum **E** mesosternum. Scale bar: 0.1 mm.

Description. Body length: 7 mm. Body fusiform, with the thorax slightly wider than the abdomen, maximum thorax width 1.75 mm. Epidermal pigment very faint, yellowish-brown in alcohol. Scales with brownish pigment (perhaps greyish in live specimens). Most macrosetae are lost, they can be detected by their insertions, when preserved they are almost hyaline to brown-yellowish. Setation of the head with the pattern typical of the genus. Eyes with 12 ommatidia. Antennae broken (maximum length preserved: 2.2 mm). Maxillary palp (Fig. 7A) with the apical article about 5.5 times longer than wide and as long as the penultimate. Apical article of the labial palp about 1.4 times longer than wide, without any expansion in the inner side, with three sensory papillae arranged in a single row (Fig. 7B). Pronotum with a brush of macrosetae in the central part of the anterior margin, with 2–4 rows of macrosetae. A row of 20–24 short

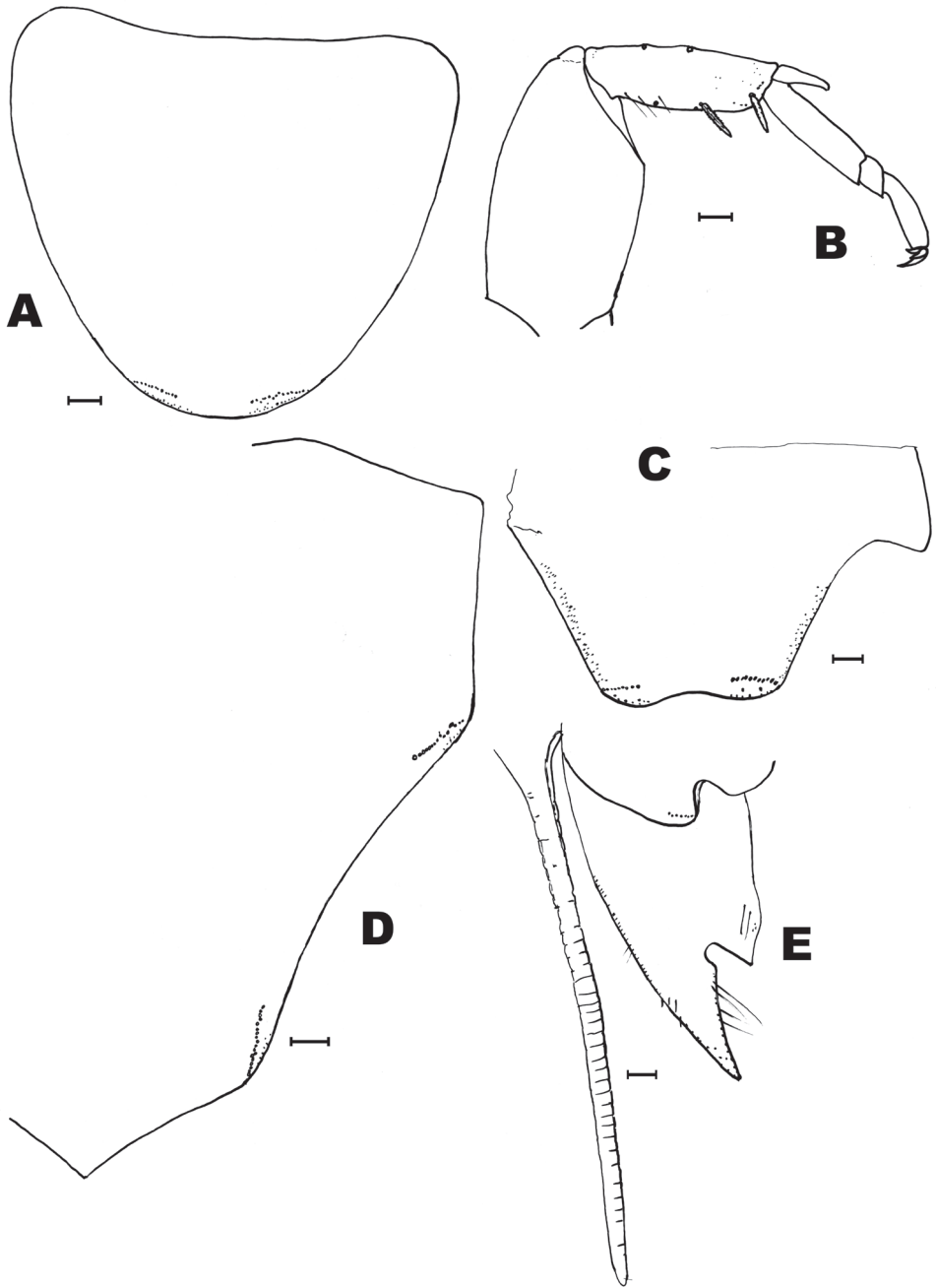


Figure 8. *Ctenolepisma subterraneum* sp. n. holotype, thorax and abdomen. **A** metasternum **B** last articles of middle leg, showing macrochaetae and their insertion on the tibia **C** urotergite X **D** urosternite VII **E** hind margin of coxite VIII, coxite IX and ovipositor (styli VIII and IX lost). Scale bar: 0.1 mm.

smooth setae extends from the median brush to the anterolateral corner of the pronotum (Fig. 7C). The lateral margins of this notum show 9+10 lateral combs with 2–5 macrosetae each. Mesonotum with 14+14 lateral combs with 1–5 macrosetae (the two anterior “combs” are composed only by one macroseta). Metanotum with 11+11 lateral combs with 1–4 macrosetae (the first composed also by one macroseta). Additionally, the three nota have 1+1 posterolateral combs with 6–8 macrosetae. Anterior trichobothrial areas of the thoracic nota not well visible, but apparently following the same arrangement than in *Ctenolepisma ciliatum*, i.e., those of the pronotum situated on lateral comb N-3; those of the mesonotum associated with the antepenultimate (N-2) lateral comb and those of the metanotum associated with the penultimate (N-1) lateral comb. All posterior trichobothria associated with the last lateral comb (N) on the three nota.

Prosternum heart shaped, as long as wide at its base and with the hind margin rounded but slightly truncated at the apex (Fig. 7D). It bears 1+1 brushes of thin and long setae in the anterolateral corners and 2+2 oblique combs in the antedistal region; each comb with 11–12 macrosetae arranged in a single row, although the anterior ones are more irregular. Mesosternum slightly longer than wide at its base, with only 1+1 oblique antedistal combs of 11–14 macrosetae arranged in a single row (Fig. 7E), although the comb of the left side is irregular, apparently broken in two close smaller combs (could be interpreted as 1+2 combs). Metasternum wider than long (ratio length/width about 0.85) with only one pair of combs of 13–14 macrosetae arranged in one row (Fig. 8A). Hind margins of meso- and metasternum slightly truncated. Distance between the combs 1.4–1.5 times the width of a comb. Protibiae 2.9–3.0 times longer than wide; mesotibiae 3.2 times longer than wide and about 1.15 times longer than the protibiae; metatibiae lost. All preserved tibiae with 2 dorsal and 4 ventral macrosetae shorter than diameter of the article (Fig. 8B). Tibiae without scales. Scales of femora rounded.

Urotergite I with 1+1 bristle-combs; urotergites II–VI with 3+3 combs; urotergites VII and VIII with 2+2 combs. Submedian bristle-combs with 6 macrosetae, lateral combs with 6–7, and sublateral combs with 7–10. Urotergite X trapezoidal, somewhat long (its apical part about 0.46 longer than wide at its base), with slightly concave posterior margin and 1+1 combs of 10–11 macrosetae (Fig. 8C). Urosternites I and II without setae, III–VIII with 1+1 lateral bristle-combs with 11–15 macrosetae. Distance between lateral combs of urosternites 4.8–5.6 times wider than the width of a comb (Fig. 8D).

Male sex unknown. In female, two pairs of abdominal styli (they are lost, but their insertions are clearly visible). Inner process of coxite IX about 1.8 times longer than wide at its base and 3.1 times longer than the outer process (Fig. 8E). Ovipositor with 40 divisions, its apex surpassing the tip of the inner process of the coxite IX approximately by its length (Fig. 8E). Apices of gonapophyses unsclerotized. Caudal filaments broken; maximum length preserved 1.3 mm (in a cercus).

Discussion. The new species is related to *C. ciliatum* (Dufour, 1831), *C. longicaudatum* Escherich, 1905 and *C. armeniacum* Molero, Gaju, Bach & Mendes, 2010, sharing with them the following characteristics: abdominal setation (absence of median combs on urosternites, 3+3 combs of macrosetae on urotergites II–VI), the trapezoidal shape of the tenth urotergite, the distribution of scales on legs (rounded on femora and absent on tibiae and tarsi), the distribution of trichobothria of the nota, and the

smooth setae of the anterolateral row of the pronotum. However, all of these species show 5 papillae in the apical article of the labial palp, whilst *Ctenolepisma subterraneum* sp. n. has 3 papillae. There is only one species of the genus *Ctenolepisma* that shares this particular characteristic in the labial palp and the aforementioned abdominal characters: *C. barchanicum* Kaplin, 1985, from the Karakum region in Turkmenistan, but this species is clearly a different taxon because several differences can be detected:

- Number of pairs of styli: *C. barchanicum* has only one pair of styli, and *C. subterraneum* sp. n. has two pairs (at least, females);
- Shape and setation of thoracic sternites: Kaplin's drawings of *C. barchanicum* reveal that these sternites are clearly rounded at their apex, while in the new species their hind margins are slightly truncated. Moreover, the number of combs in the Turkmenian species is higher (5–8 pairs in the prosternum, 3–4 pairs in the mesosternum and 2 pairs in the metasternum, versus 2, 1–2 and 1 pairs of combs respectively in the Iranian species);
- Shape of the apex of the labial palp: Following Kaplin (1985), the inner side of the apical article of the labial palp is strongly widened in *C. barchanicum*, while in *C. subterraneum* sp. n. the labial palp has subparallel sides;
- Number of lateral combs in nota: According Kaplin's description (in Russian), the Turkmenian species has a lower number of combs in the pronotum (5 pairs), in the mesonotum (8–10 pairs) and in the metanotum (7–9 pairs), while the new species from Iran has respectively 9+10 combs, 14 pairs and 11 pairs of combs;
- Shape of the hind margin of the urotergite X: Kaplin's drawing of the urotergite X of *C. barchanicum* shows a convex hind margin, while this is concave in *C. subterraneum* sp. n.;
- Length and number of divisions of the ovipositor. *C. barchanicum* has only 12–13 division and the new species has 40 divisions. In spite of this, the length of the ovipositor of *C. subterraneum* sp. n. is only slightly higher relative to coxites IX.

The genus *Ctenolepisma* was revised recently in Iran by Kahrarian et al. (2016); then, seven species were considered to occur in this country, if *C. mauritanicum* (Lucas, 1846), with doubtful status, is included. *Ctenolepisma subterraneum* sp. n. fits at step 5 of the key of Kahrarian et al. (op. cit.) with the following modifications:

- 5 Macrosetae in meso and metasternum arranged in combs of 2 or 3 irregular rows **6**
- Macrosetae in meso and metasternum arranged in combs of 1 row **5'**
- 5' Apical article of the labial palp with 5 papillae. Prosternum with acute apex and usually with 3 or more pairs of bristle-combs. Combs of urotergites with more than 8 macrosetae ***C. ciliatum* (Dufour, 1831)**
- Apical article of the labial palp with 3 papillae. Prosternum with rounded and slightly truncated apex and with only 2 pairs of bristle-combs. Number of macrosetae of the submedian and lateral combs of urotergites lower than 8 ..
..... ***C. subterraneum* sp. n.**

Distribution. Known only from the type locality, Abu Nasr cave, in Fars province, Iran.

Etymology. The specific name of the new species refers to its habitat, not common within species of the genus (see next section). Subterraneum is an adjective in the nominative case.

Habitat. This new species has been found near the cave's entrance (endogean). This habitat is unusual within members of the genus *Ctenolepisma*, since most of them are associated to more superficial (epigean) habitats: under stones or vegetal debris, in trunks of trees, etc.

Acrotelsa collaris (Fabricius, 1793)

Studied material. Two young specimens from Khan cave, Khon, Fars province, Iran. 10.IX.2015, one deposited in UCO, Ref. Z2517, and the other in ZM-CBSU #C2637.

Distribution and habitat. This pantropical species has been previously reported from Iran (Irish 1995, Kahrarian et al. 2014), but never in a subterranean habitat. The two specimens were collected in the dark zone of the cave (hypogean), where humidity is greater than 90% and the soil was wet, mixed with piles of guano.

Neoasterolepisma palmonii (Wygodzinsky, 1942)

Studied material. One male, mounted in a slide. Abu Nasr cave, Shiraz Province, Iran. 12.XI.2015. Deposited in UCO, Ref. Z2515.

Distribution and habitat. This species is new for Iran. It was previously known from Turkey and Israel (Mendes 1988), so this record represents a significant extension of its geographic distribution. The only specimen available has been collected from the endogean zone of the cave. The only species of this genus recorded previously from a cave is *N. caeca* Molero-Baltanás, Bach de Roca & Gaju-Ricart, 1999, collected inside a lava cave (Molero et al. 1999) in La Palma (Canary Islands).

Ctenolepisma (*Sceletolepisma*) *targionii* (Grassi & Rovelli, 1889)

Studied material. One male, mounted in a slide, two females and one juvenile in alcohol. Endogean zone in Dej Shapour cave, Kazerun, Fars Province, Iran. 21.X.2015. Deposited in UCO, Ref. Z2516.

Distribution and habitat. This species is widespread in the southern Palaearctic, but it is new for Iran. It is the first time that it has been recorded in the subterranean environment. *Ctenolepisma targionii* is found as a domestic form in the Western Palaearctic, but it lives in natural habitats in southwestern Asia, suggesting that it is native from the latter area.

Discussion. Together with the above-described *Ctenolepisma subterraneum*, the number of species of this genus in Iran increases to nine; *C. targionii* represents the third species known for Iran of the subgenus *Sceletolepisma*.

Family Nicoletiidae

***Lepidospora (Brinckina) momtaziana* Molero, Tahami, Sadeghi & Gaju, sp. n.**

<http://zoobank.org/2E74DC29-44F0-4DDB-9C28-B833420D9F89>

Figs 9–14, Table 3

Type material. Holotype (MNCN): male, body length = 7 mm, mounted on slide, labelled “Momtaz cave, Marvdahst, Fars Province, Iran. 11-XI-2016, Cat. Types N. 2836”; “HOLOTYPE ♂ *Lepidospora (Brinckina) momtaziana* sp. n., des. Molero, Tahami, Sadeghi & Gaju, 2018”. **Paratypes** (2 ex.): One female, collected in the same locality and date (preserved in alcohol and deposited in ZM-CBSU #C2638). One female from the same locality, 18-II-2015, mounted in slide and reported as *Lepidospora (Brinckina)* sp. in Tahami et al. (2018), deposited in UCO (Ref. Z2513).

Diagnosis. Light yellowish nicoletiid; adults about 7 mm long, antennae slightly longer. Body covered with scales except on head (typical in the subgenus *Brinckina*). Pedicel of male antennae with slightly asymmetrical apophyses; this asymmetry involves shape and chaetotaxy. Dorsally with few setae, those inserted on the disc of nota very small and sparse, their length about 1/20 of the respective notum. Male urotergite X with 7+7 pegs, 3+3 of them inserted on the posterolateral projections. Subgenital plate of female widely triangular. Male cerci with 6 pegs arranged in a single row, the basal division with 1–2 pegs.

Description. Body length of the male (holotype): 6.8 mm. Length of the female (paratype): 7.7 mm.

Thorax length: 2.5–2.6 mm. Thorax width: 1.4–1.7 mm. Shape of the body sub-cylindrical, the thorax nearly as wide as the abdomen. Epidermal pigment light yellowish, slightly darkened in the abdomen; gut contents are visible because transparency of the teguments. Head completely devoid of scales, thorax and abdomen covered dorsally and ventrally by scales. Scales as in Figure 9A, a little longer than wide, thoracic scales about 40–50 µm long, with 6–8 rays which extend slightly beyond the margin, abdominal scales slightly larger, with 8–15 rays.

Head prognathous, with some bifid macrosetae inserted in the lateral margins of the cephalic capsule, frons and in the middle of clypeus and labrum. Some dispersed setae are irregularly arranged in the cephalic capsule (Fig. 9B).

Antennae slightly longer than body; in the holotype they are 7.6 mm long. Scape 1.5 times longer than wide and almost twice longer than pedicel (3 times longer in the female), with 3 bifid macrosetae inserted on its apical half, and some additional thin setae of variable length (Fig. 9C). Pedicels of the male with apophyses that appear to be asymmetric. They are subcylindrical but the left apophysis is broader basally and nar-

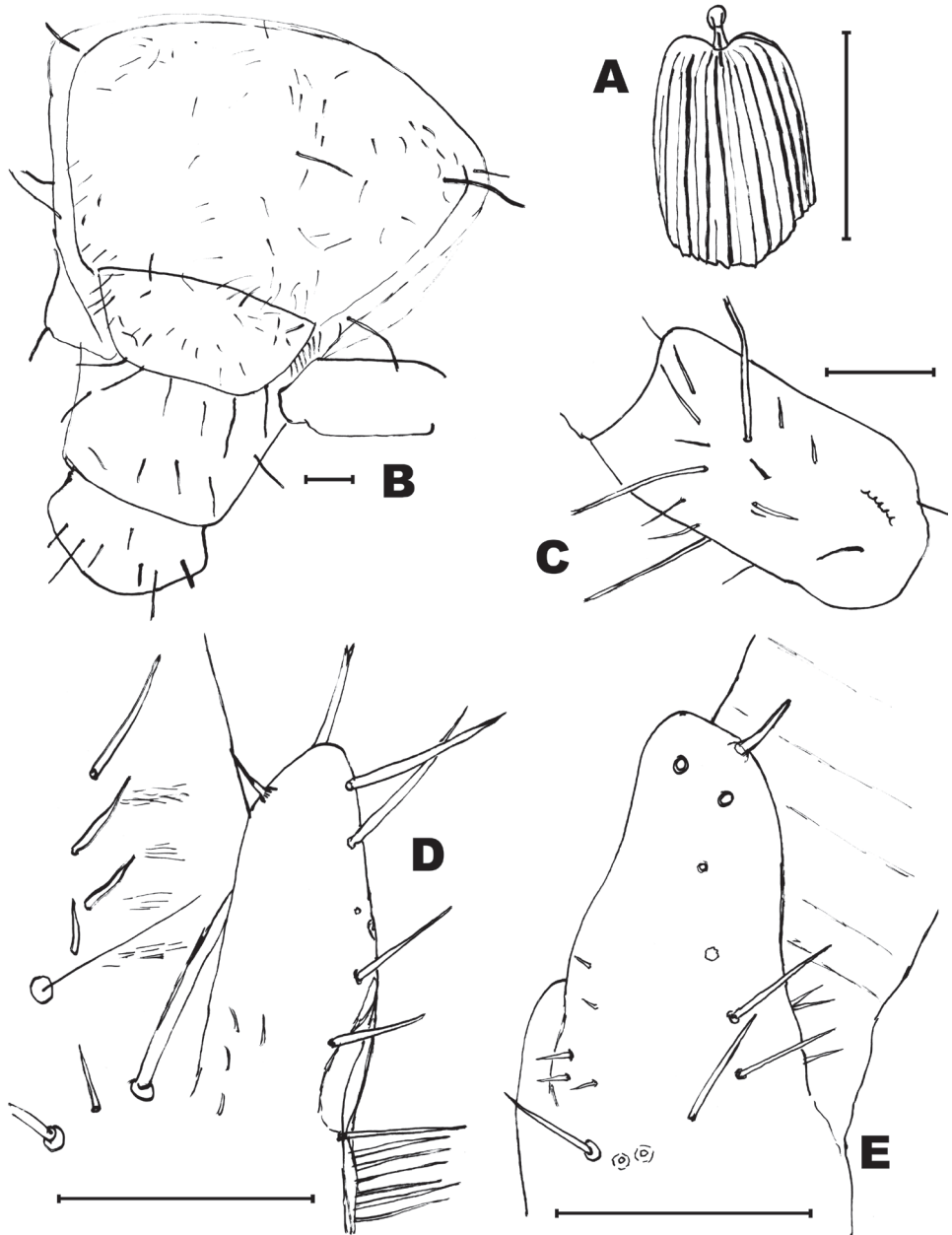


Figure 9. *Lepidospora montaziana* sp. n. **A** abdominal scale **B** head **C** scape **D** apophysis of the right pedicel of the male **E** apophysis of the left pedicel of the male. Scale bars: 0.1 mm (**B–E**); 50 μ m (**A**).

rower in its apical half (ratio length/width at the base: 1.6), with a blunt apex and the right apophysis is slightly longer (ratio length/width at the base: 2.4), without abrupt narrowing in its distal half and apically more acute. Both apophyses are similar in length

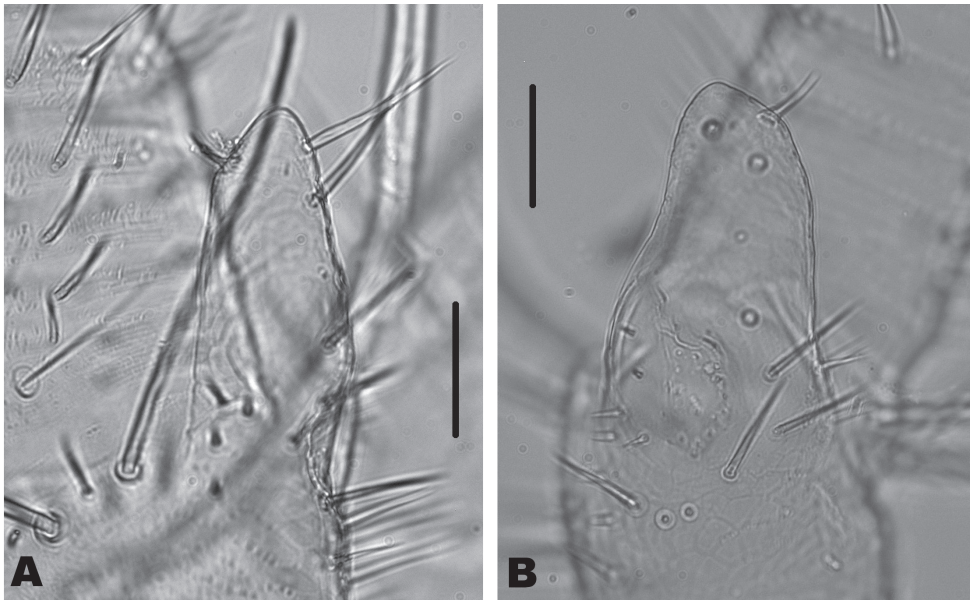


Figure 10. *Lepidospora momtaziana* sp. n. micrographs of the pedicelar apophyses of the male (holotype). **A** right apophysis **B** left apophysis. Scale bar: 0.1 mm.

(their distal end reaches the level of the third annuli); so it can be thought that this different shape could be explained by a different angle of vision because their different position in the slide, but the chaetotaxy of both apophyses does not match; the left apophysis has two insertions of setae nearly at the same level in its apical part and the right apophysis shows two acute setae in the apical part but they are inserted in different positions. Both apophyses have a glandular seta inserted subapically and the right apophysis has a more prolonged apex beyond the insertion of the seta. In the basal part of the apophyses, there is a fovea with several small setae. Three additional long macrosetae are inserted in the distal part of the trunk of the pedicel, just under the limit with the flagellum (compare Figs 9D and 10A with Figs 9E and 10B). Pedicel of the female without apophysis and with five long macrosetae. Basiconic sensilla long, abundant on the flagellum, especially in T-joints, i.e., those annuli bearing trichobothria. Mandibles and maxillae without distinctive features. Last article of maxillary palps only preserved in the holotype, with several (usually 5) apical sensory rods and a subcircular sensilla apically. The three distal articles of these palps (last, penultimate and antepenultimate) with scattered long basiconic sensillae. Apical article of the maxillary palp about 6.8 times longer than wide and 1.15 times longer than the penultimate (Fig. 11A); this latter of similar length than the antepenultimate. Galea with two apical conules (Fig. 11B). Apical article of the labial palp about 1.5–1.7 times longer than wide and 1.5–1.6 times longer than the penultimate, with 6 sensory papillae arranged as usual in the genus (Fig. 11C). Inner side of this article with 5–6 thin-walled basiconic sensilla; outer side with 4–5 similar sensilla, most slightly curved basally and inserted in the basal half of the article.

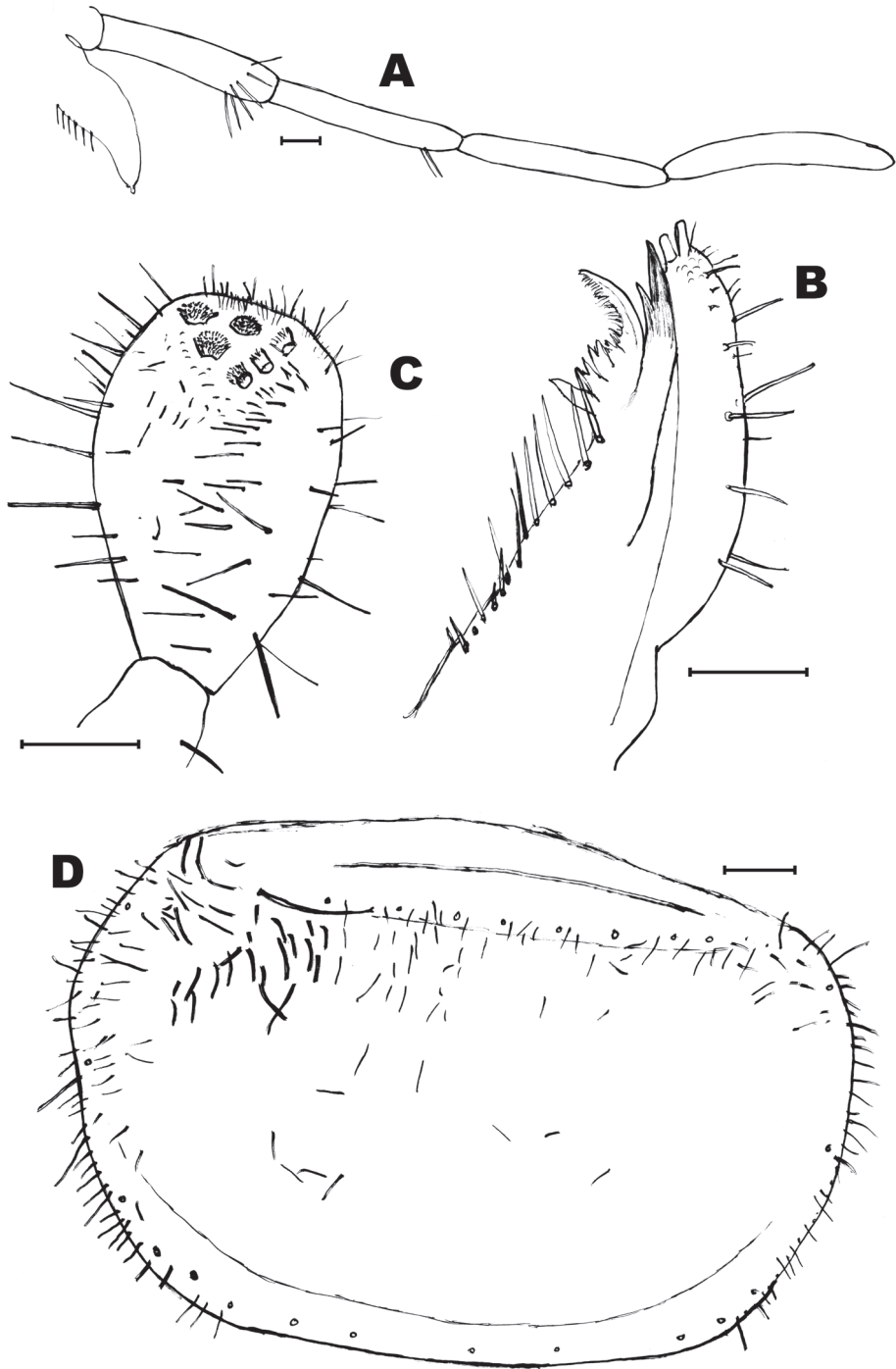


Figure 11. *Lepidospora momtaziana* sp. n. **A** maxillary palp **B** apex of maxilla **C** apical article of the labial palp **D** pronotum (only few macrosetae are preserved but their insertions are indicated). Scale bar: 0.1 mm.

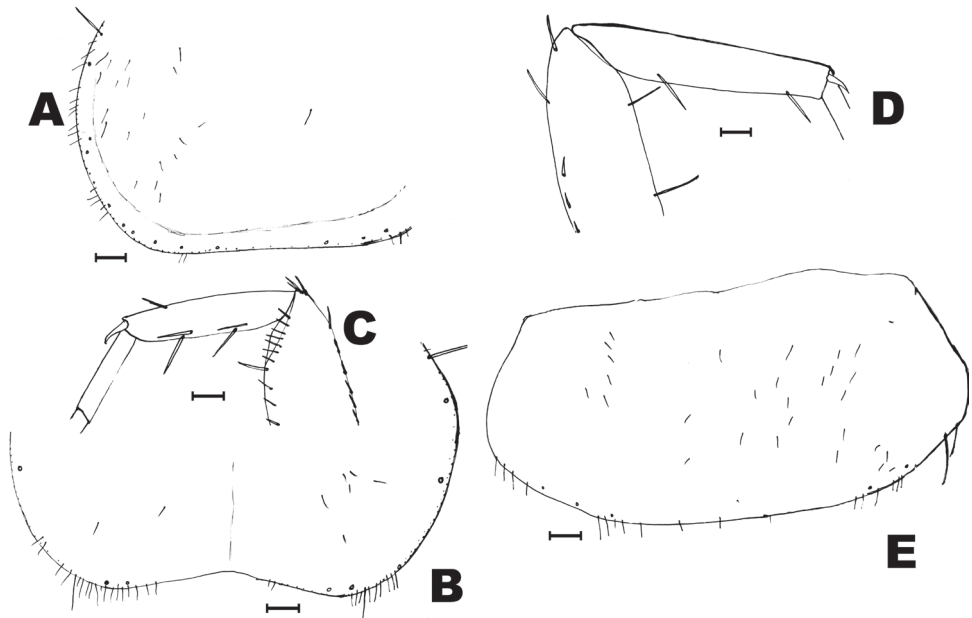


Figure 12. *Lepidospora montaziana* sp. n. **A** mesonotum, lateral and hind margin **B** metanotum, lateral and hind margin **C** protibia **D** metatibia **E** urotergite I. Scale bar: 0.1 mm.

Most thoracic and abdominal macrosetae are lost in both available specimens and only their insertions are visible; when preserved, their length is about $1/4 - 1/5$ of the length of the respective tergite. Nota (Figs 11D, 12A, B) with several bifid macrosetae of variable length irregularly inserted on their lateral and posterior borders; the pronotum also bears these setae (10–14) on its anterior margin, although most of them are lost and only their insertions are visible (Fig. 11D). Moreover, there are a lot of small simple setae over the lateral margins of the nota and in the anterior margin of the pronotum and the posterior margin of the metanotum (Fig. 12B). These thin and short setae (considered as microchaetae) are very scarce in the disc of the nota but there is a significantly higher number in the anterior part of the pronotum of the holotype (Fig. 11D).

Protibiae about 4.2–4.4 times longer than wide, with 2 dorsal and 4–5 ventral spines (apart from a row of 5–7 short spines in the ventro-apical angle of the tibiae (Fig. 12C)). Mesotibiae about 4.5–4.75 times longer than wide, with the same number of distribution of spines than protibiae. Metatibiae about 5.3–5.4 times longer than wide (Fig. 12D) and 1.75 times longer than protibiae, with 1 small dorsal spine (which can be absent) and 4 ventral, two of them inserted very apically on the article. Ventral spines shorter than or as long as the diameter of the tibiae. Tibiae about 1.5–1.6 times longer than the first article of the metatarsi. Metatarsi about 1.3–4.0 times longer than tibiae. Praetarsi with 3 simple claws, the median one shorter than the lateral ones.

Urotergites covered by scales; dorsal and ventral scales similar. Dorsal scales make difficult to discern a faint suture between the tergite and the paratergite. Some abdominal tergites are damaged in the holotype and the urotergal chaetotaxy is more visible in

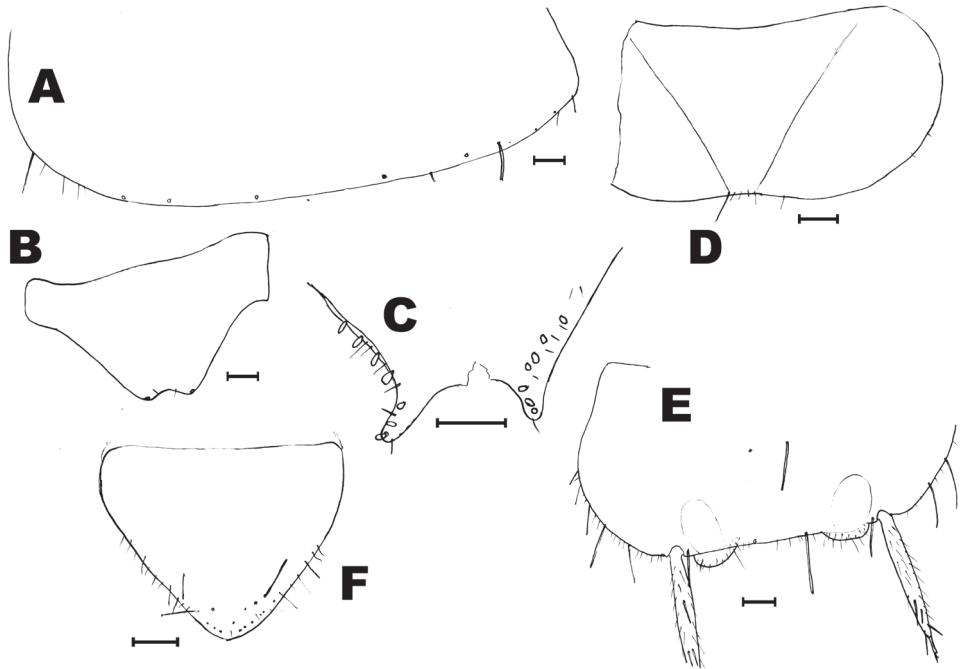


Figure 13. *Lepidospora momtaziana* sp. n., abdomen. **A** urotergite V **B** urotergite X of the female **C** urotergite X of the male, hind margin showing pegs **D** urosternite I **E** urosternite V **F** subgenital plate of the female. Scale bar: 0.1 mm.

the paratype. First urotergite (Fig. 12E) with several small setae inserted in the disc, the remaining urotergites with very few, or completely devoid of, discal setae. The posterior margin of urotergites with 4–5 + 4–5 isolated bifid macrosetae (most of them lost and only their insertions are visible) and with some thin and short acute setae, those of the infralateral region longer (Fig. 13A).

Urotergite X of the male (Fig. 13C) with concave and rounded hind margin and two posterolateral projections which are curved downwards. The posterior part of the tergite bears ventrally 7+7 pegs (on each side, 3 inserted in the posterolateral projection and 4 near the lateral margin of the tergite; on the left side the anterior peg is smaller and thinner than the others, tending to a spiniform shape). Disc of the tergite nearly devoid of setae, only some insertions are visible near the posterior notch and in lateral margins. There are some small and thin setae in these margins, one of them near the apex of the posterolateral projections.

Urotergite X of the female without pegs, its hind margin with a shallow concavity and 1+1 macrosetae inserted in the posterolateral angles (Fig. 13B); the disc, as in the male, nearly without setae.

Urosternite I broken in both available specimens, but the sutures delimiting laterocoxites are visible in the holotype, as well as the setation of the hind margin, consisting in few small setae in the median region and some others in the lateral part (Fig. 13D). Eight pairs of styli, inserted on urosternites II–IX. Eversible vesicles present in urosternites II–VI and

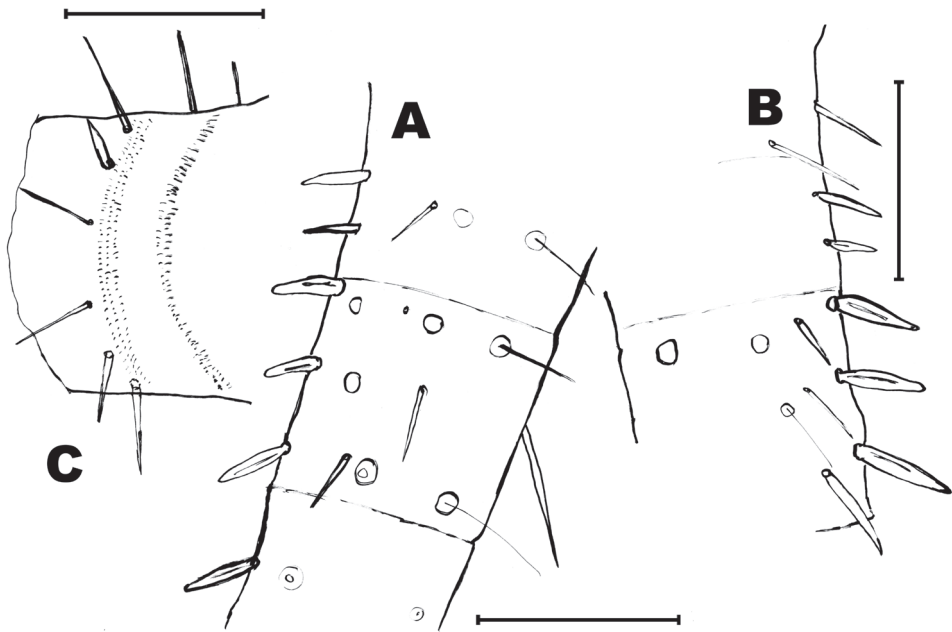


Figure 14. *Lepidospora momtaziana* sp. n., holotype, terminal filaments. **A** basal part of the right cercus. **B** inner margin of the basal part of the left cercus **C** basal portion (only preserved) of appendix dorsalis (=paracercus). Scale bar: 0.1 mm.

pseudovesicles in the urosternite VII. Setation of urosternites II-VII as in Fig. 13E, with 1+1 discal macrosetae, some small setae on the disc, and the hind margin with 1+1 submedian macrosetae (between both vesicles), 1+1 sublateral macrosetae (inserted between vesicles and the basis of the styli) and several acute setae in the outer part, more lateral than styli.

Urosternite VIII of the male entire, of females divided in free coxites. Subgenital plate of the female triangular, with acute hind margin, wider than long (ratio length/width about 0.75), with 1+1 short discal macrosetae (bifid) and several setae on the lateral margins (Fig. 13F).

The genital region of both specimens is damaged, so in the male the hind margin of the urosternite VIII is not visible and the penis and the paramera are lost, and the ovipositor of the female is broken basally, so the length, number of divisions (only 5 are preserved) and the characteristics of the apices of gonapophyses are not known. Terminal filaments probably long but broken basally in the available specimens; maximum preserved length is 0.5 mm. Cerci with 5 acute pegs, longer and thinner than those on the urotergite X (Fig. 14A, B), 1–2 on the proximal division, 3 on the second division and 0–1 on the third division, arranged in a single row. The short basal part of the paracercus that is preserved shows one spiniform small peg in the apical limit of the basal division, the second division is lost (Fig. 14C).

Discussion. This new species of *Lepidospora* can be assigned to the subgenus *Brinckina* Wygodzinsky, 1955 because the absence of scales on the head, so it is compared with the previously described species of this subgenus. Unfortunately, some

characters considered important in the taxonomy of Nicoletiidae cannot be used for this comparison because of the damaged state of the abdominal regions of the two available specimens. In spite of this, the characters described above are enough to state that *Lepidospora* (*Brinckina*) *momtaziana* sp. n. differs from all previously known species of the subgenus *Brinckina*. We present a comparison with seven well distinguished and taxonomically non-problematic species, since the status of *L. (B.) "meridionalis"* var. Silvestri, 1913 and *L. (B.) hemitricha* var. *progressa* Silvestri, 1942 remains doubtful and requires further studies, as Mendes (2002) discussed.

With the previously mentioned limitations, three characters have been considered significant to distinguishing between the new Iranian species and the remaining taxa of the subgenus: the shape and length/width ratio of the pedicellar apophyses of males, the setation of the disc of the nota and the number and arrangement of pegs in terminal filaments (mainly in cerci). The comparison based on these characters is summarized in Table 3. More details about the comparison with each of the species are given below.

It worth mentioning that the shape and length/width ratio of the pedicellar apophysis, a distinctive character that can be used only in adult male specimens, should be described carefully. As Molero et al. (2013) stated, "similar antennae placed in different positions could be interpreted as different shapes, but upon rotating the antennae, similar structures can be recognized". Antennae that are presumably considered as symmetrical show different appearances when illustrated in different positions; for example, see the drawings of Smith and McRae (2016) of the left and right pedicellar apophyses of two male specimens of the same species: are they different because an intraspecific variability or because of being drawn in different positions? If we consider the form that can be interpreted from the drawings of the left apophysis, the length/width ratio is about 2.3, but this parameter is approximately 3 in the drawing of the right apophysis. They are similar in length at the same scale; our experience suggests that both apophyses are identical, but the shape of the transversal section of the apophysis is not circular but elliptical; if the left apophysis seems to be wider it is because it is drawn in a different position (seen from the wider diameter of the ellipse) than the right (seen from the narrower diameter). In the new species from Iran, differences between both pedicellar apophyses are not completely explained by different positions (in the slide), so we conclude that they are actually asymmetrical; the difference is not based only in the length/width ratio but also on the shape of the apical part (narrower than the basal in the left apophysis) and on the different chaetotaxy (being aware of the fact that insertions of detached setae must be accounted for).

The following comparisons of other previously described species are based on illustrations from their original descriptions.

Lepidospora (B.) makapaan Wygodzinsky, 1955 from South Africa (Transvaal) has a lot of pegs on the paracercus but lacks pegs on cerci, a character not shared with any other species of the subgenus, including the new species. Moreover, the chaetotaxy of the head and urosternite I is denser in the South African species and the subgenital plate of females is more rounded apically. Adult specimens of *L. (B.) makapaan* are clearly bigger than adults of the Iranian species, since females of the South African species can reach 16 mm length and their tibia are more than 7 times longer than wide (less than 6 in the new species).

Table 3. Comparing *Lepidospora* (*Brinckina*) *momtaziana* sp. n. with other previously described species of the subgenus *Brinckina*.

SPECIES (geographic origin)	Shape (and ratio length/width) of pedicellar apophysis	Chaetotaxy of the discs of nota	Number and distribution of pegs in cerci
<i>L. (B.) momtaziana</i> sp. n. (Iran)	Asymmetrical, left thumb-like (1.6) and right subcylindrical (2.4)	Sparse and short microchaetae	6 in a single row Proximal division: 1–2 Second division: 3 Third division: 0–1
<i>L. (B.) relictta</i> (Australia)	Symmetrical, subcylindrical (about 3)	Sparse short setulae	4 in a single row Proximal division: 0 Second division: 2 Third division: 2
<i>L. (B.) garambensis</i> (Congo)	Symmetrical, subcylindrical (about 3.8) but somewhat curved	Sparse long setae	3–6 in a single row Proximal division: 0–1 Second division: 2–3 Third division: 1–2
<i>L. (B.) hamata</i> (Congo)	Symmetrical, subcylindrical (about 1.7)	Dense setae	4 in a single row Proximal division: 0 Second division: 3 Third division: 1
<i>L. (B.) alicola</i> (Kenya)	Males unknown	Moderately dense and long setae	Males unknown
<i>L. (B.) hemitricoides</i> (Afghanistan)	Symmetrical, subcylindrical with acute apex (about 2.5?)	Dense setae	Proximal division: 5? 2? Second division: 1? 3? Third division: 0? 1? *
<i>L. (B.) makapaan</i> (South Africa, Transvaal)	Symmetrical, subconical, curved apically (about 2.3)	Few isolated microchaetae	0
<i>L. (B.) hemitricha</i> (China, Vietnam)	Symmetrical, subcylindrical, slightly narrowing towards apex (about 2.5)	Dense and long setae, very dense in prothorax	5 spiniform in a single row Proximal division: 1 Second division: 2 Third division: 2

*There are two ways of interpreting Wygodzinsky's drawings of cerci: the first implies that he did not draw a limit between the proximal and second division but that the limit exists (sometimes it is difficult to discern) in which case the arrangement of pegs would be 2–3–1 as in the new species from Iran; secondly, the aforementioned limit does not exist and, in this case, the arrangement would be 5–1.

Lepidospora (*B.*) *relictta* Smith & McRae, 2016 from northwestern Australia is probably the representative of the subgenus that shows more affinities with the new species from Iran. It is similar because it has pegs on cerci and paracercus and sparse setulae on discs of nota, but males show symmetrical and longer pedicellar apophyses. The number of pegs of the urotergite X is higher (20 against 14 in the new species) and the paracercus (=appendix dorsalis) has 2+2 pegs in the two basal divisions (the Iranian species has only one spiniform seta that can be considered as a peg since it is modified in respect to the remaining setae of the appendix, but nothing can be said about the second division because it is lost).

Males of *L. (B.) hamata* Mendes, 2002 from Congo has a shorter pedicellar apophysis, which is near to the length/width ratio of *L. (B.) momtaziana* sp. n., but the shape is different and apophyses seem to be symmetrical; the glandular seta is almost apical in the African species and more subapical in *L. (B.) momtaziana* sp. n. Moreover, the urotergite X of the male is quite distinct and the species from Congo lacks pegs in the paracercus and the new species shows, at least, one spiniform peg.

Lepidospora (*B.*) *garambensis* Mendes, 2002, described from Congo too, is also devoid of pegs in the paracercus and the apophysis of males is longer. Moreover, mesotibiae of *L. (B.) garambensis* have short strong ventral spines which are absent in the new species.

Males of *L. (B.) alticola* Wygodzinsky, 1965 (from Kenya) are not known. Comparing females of this species with the new one, the labial palp of this African species is stouter, as long as wide (at least 1.5 times longer than wide in *L. (B.) momtaziana* sp. n.) and the discal setae of nota are more abundant and longer (about 1/8 of the total length of the nota in the African species and 1/20 in the Iranian species).

Lepidospora (*B.*) *hemitricha* Silvestri, 1942 and *L. (B.) hemitrichoides* Wygodzinsky, 1962 (from China and Afghanistan, respectively) are similar in bearing pegs on cerci and paracercus, and their apophysis have a similar length/width ratio (approximately 2), but the setation of the disc of their nota is stronger (high number of setae and most setae are longer). Additionally, their urotergites X have a higher number of pegs (12+12 in *L. hemitricha* and about 17+17 in *L. hemitrichoides*) and the pegs on cerci are more spiniform (long and acute) in shape. In *L. hemitricha*, the length/width ratio of their tibiae is lower (about 4 in metatibiae) than in the new species from Iran and males of *L. hemitrichoides* have longer (finger-like) posterolateral angles of the urotergite X, surrounding a deeper median notch, and the number and distribution of spiniform pegs in the basal division of the paracercus is clearly different from the new species (a lot of pegs in three rows in the Afghan species).

Considering the limitations derived from the lack of information about males of *L. alticola* and the doubtful status of some species (see above), *Lepidospora momtaziana* sp. n. can enter in the key of *Lepidospora* made by Mendes (2002) in at step 34 with the following modifications:

- | | |
|------|---|
| 34 | Nota (mainly pronotum) with numerous setae on disc. Ovipositor long, surpassing stylets IX by about 4 times their length. Pegs along male cerci and paracercus. Asiatic species 35 |
| 34' | Nota with few scattered setae on disc (they can be a little more abundant in the anterior part of the pronotum). Ovipositor similar or shorter (its length in <i>L. (B.) momtaziana</i> not known) 34A |
| 34A | Setae on the disc of nota very short, about 1/20 of the length of the notum. Iranian species..... <i>Lepidospora momtaziana</i> sp. n. |
| 34A' | Setae on the disc of nota longer. African species 36 |

Distribution. Known only from the type locality, Momtaz Cave, in Fars province, Iran.

Etymology. The specific name refers to the cave where specimens have been collected. Momtaziana refers to Momtaz, in genitive case, with a feminine ending (-iana) that means “belonging to”.

Habitat. This new species has been collected in the hypogean zone (complete darkness) of Momtaz Cave.

Table 4. Faunistic progress in Iran, comparing the number of species of Microcoryphia and Zygentoma previously known in this country before and after the present survey of subterranean habitats.

Family	Number of species previously known in Iran	Number of species from in Iran after the present survey	Increase of diversity
Machilidae (order Microcoryphia)	5	6	1 (20%)
Lepismatidae (order Zygentoma)	13	16	3 (23%)
Nicoletiidae (order Zygentoma)	0	3	3 (new family for Iran)
Protrinemuridae (order Zygentoma)	1	0	0
Total	19	26	7 (37%)

Conclusions

As a result of the surveys performed in caves in Iran, several new taxa of basal Hexapoda (Microcoryphia and Zygentoma) have been described or reported for the first time in this country. Some of them can be considered strictly subterranean, but others are facultative in this environment (they are usually epigeal or epiedaphic insects but in the climatic conditions of southern Iran they avoid surficial environments and hide at deeper levels of soil or in cavities).

Previous to our studies on subterranean basal hexapods, only five species of Microcoryphia were known from Iran (Table 4), all of them belonging to the family Machilidae; four of them are endemic to the Middle-East region (*Lepismachilis* (*L.*) *hobertandti* Wygodzinsky, 1952; *Silvestrichilis wittmeri* Bitsch, 1970; *Machilanus spinosissimus* Mendes, 1981 and *L. (L.) dominiaki* Mendes, 1985) and the fifth, *Trigoniophthalmus alternatus* (Silvestri, 1904), with a wide distribution over continental Europe, reaching Spain to the west. *Haslundiella iranica* sp. n. represents the sixth species of Microcoryphia known for Iran.

Considering Zygentoma, 14 species of this order were known from Iran in surficial environments, but adding the species described by us in this work and those reported before in a previous paper (Tahami et al. 2018), the number reaches 20, which represents an increase of about 40% in the knowledge of this order (see Table 4).

Moreover, we think that further surveys in other regions and caves of Iran could increase significantly this diversity.

Finally, a key for the eight subterranean basal insects known to date from Iran is given below. For Zygentoma, this key can be considered as complementary to that provided by Kahrarian et al. (2014) for epigeal Lepismatidae.

- 1 Body not flattened, with humped thorax. Paracercus considerably longer than the two cerci. Head with big compound eyes and also with ocelli (order Microcoryphia, family Machilidae) ***Haslundiella iranica* sp. n.**
- Body more or less dorsoventrally flattened, the thorax is not humped. Paracercus subequal in length or longer than cerci. Head usually without ocelli and sometimes without eyes (order Zygentoma) **2**

- 2 Compound eyes present, small, with about 13 ommatidia. Male pedicellus without apophysis. Urosternite VIII of females divided in two coxites. Hind margins of urosternites with macrosetae arranged in dense groups forming one row (comb) and without vesicles (family Lepismatidae)..... **3**
- Eyes absent. Male pedicellus with an apophysis. Urosternite VIII of females divided in two coxites and a submedian subgenital plate. Hind margins of urosternites with isolated macrosetae, not forming combs, some of them with a pair of sublateral vesicles (family Nicoletiidae)..... **6**
- 3 Prosternum strongly reduced. Ovipositor apically provided with strong sclerotized teeth. subfamily Acrotelsatinae. Urotergite X acutely triangular.
..... ***Acrotelsa collaris* (Fabricius, 1793)**
- Prosternum normally developed. Ovipositor usually without spines (primary type). Urotergite trapezoidal, with their hind margin straight or slightly convex or concave, but not acute..... **4**
- 4 With smooth, apically bifid macrosetae. Males with paramera (subfamily Lepismatinae). Hind margin of urotergites I–IX with isolated macrosetae, at most with an infralateral group of 2–3 macrosetae. Urotergite X longer than wide and with concave hind margin.....
..... ***Neoasterolepisma palmonii* (Wygodzinsky, 1942)**
- With feathered macrosetae. Males without paramera. Urotergites I–VIII and X with at least 1+1 combs of macrosetae. Urotergites II–V with 3+3 combs of macrosetae. Urotergite IX without setae. Urotergite X wider than long, with straight hind margin or slightly concave (subfamily Ctenolepismatinae, genus *Ctenolepisma*)..... **5**
- 5 Urosternites without median combs of macrosetae. Urotergite VI with 3+3 combs of macrosetae..... ***Ctenolepisma subterraneum* sp. n.**
- Urosternites II–VI with one median comb of macrosetae. Urotergite VI with 2+2 combs of macrosetae.....
..... ***Ctenolepisma targionii* (Grassi & Rovelli, 1889)**
- 6 Body short, with short antennae and terminal filaments (shorter than half the body length). Pronotum clearly wider than head, abdomen width tapering backwards. Urosternite I entire ... subfamily Atelurinae. All the body covered (including head) with scales.....
..... ***Persiatelurina farsiana* Molero, Tahami, Gaju & Sadeghi, 2018**
- Body subcylindrical, long, with antennae and terminal filaments, when well preserved, longer than body or slightly shorter. Pronotum as wide as or slightly wider than head, abdomen width not clearly tapering backwards. Urosternite I divided in a median sternite and two laterocoxites ... subfamily Coletiniinae, genus *Lepidospora*. Head without scales..... **7**
- 7 Thorax with scales..... ***Lepidospora* (*Brinckina*) *montaziana* sp. n.**
- Thorax without scales.....
..... ***Lepidospora* (*Brinckiletinia*) *malousjanica* Molero et al., 2018**

Acknowledgements

The authors would like to thank Iranian Caving Society and Mr. Mahmoudi, the for-ester of Environment Department for their cooperation in caving and specimen col-lection. Thanks are also given to Naara Torres for the revision of the English version of the manuscript, as English native speaker from U.S.

References

- Christophoryová J, Dashdamirov S, Malek Hosseini M, Sadeghi S (2013) First record of the ge-nus *Megachernes* (Pseudoscorpiones: Chernetidae) from an Iranian cave. *Arachnologische Mitteilungen* 46: 9–16. <https://doi.org/10.5431/aramit4603>
- Irish J (1995) New data of Lepismatidae, mainly from Italy and North East Africa, with notes on the status of *Ctenolepisma rothschildi* Silvestri (Insecta, Thysanura). *Annali del Museo Civico di Storia Naturale “Giacomo Doria”* 90: 559–570.
- Janetschek H (1954) Ueber Felsenspringer der mittelmeeerländer (Thysanura, Machilidae). *Eos* 30 (3–4):163–314.
- Kahrarian M, Molero Baltanás R, Monshizadeh MR, Shenavaee MR (2014) A faunistic study on Lepismatidae (*Zygentoma*) in Kermanshah (Iran). *Entomologia Generalis* 35(1): 53–60. <https://doi.org/10.1127/0171-8177/2014/0063>
- Kahrarian M, Molero R, Gaju M (2016) The genus *Ctenolepisma* (*Zygentoma*: Lepismatidae) in Western Iran, with description of three new species. *Zootaxa* 4093(2): 217–230. <https://doi.org/10.11646/zootaxa.4093.2.4>
- Kaplin VG (1982) New data on the fauna of Thysanura of Mongolia, Kasakhstan and Middle Asia. [In Russian]. *Nasekomye Mongolii* 8: 16–61
- Kaplin VG (1985) A new species of the genus *Ctenolepisma* Esch. (Thysanura, Lepismatidae) from the eastern Karakum Desert. [In Russian]. *Izvestiya Akademii Nauk TSSR, Seriya Biologicheskaya Nauk* 5: 54–65.
- Kashani GM, Malekhosseini M, Sadeghi S (2013) First recorded cave-dwelling terrestrial iso-pods (Isopoda: Oniscidea) in Iran with a description of a new species. *Zootaxa* 3734: 591–596. <https://doi.org/10.11646/zootaxa.3734.5.8>
- Malek-Hosseini MJ, Grismado CJ, Sadeghi S, Bakhshi Y (2015a) Description of the first cave dwelling species of the spider genus *Trilacuna* Tong & Li from Iran (Araneae: Oonopidae). *Zootaxa* 3972: 549–561. <https://doi.org/10.11646/zootaxa.3972.4.6>
- Malek-Hosseini MJ, Muilwijk J, Sadeghi, S, Bakhshi Y (2016a) The Carabid fauna of caves in the southern Zagros Mountains and description of *Laemostenus (Antisphodrus) aequalis* nov.sp. and *Duvalius kileri* nov.sp. from Kohgiluyeh and Boyer-Ahmad Province, Iran (Co-leoptera: Carabidae). *Entomofauna* 37: 185–204.
- Malek-Hosseini MJ, Sadeghi S, Bakhshi Y, Dashan M (2016b) Ectoparasites (Insecta and Acari) Associated with Bats in South and South-Western Caves of Iran. *Ambient Science* 3(1): 22–28. <https://doi.org/10.21276/ambi.2016.03.1.ra03>

- Malek-Hosseini MJ, Zamani A, Sadeghi S (2015b) A survey of cave-dwelling spider fauna of Kohgiluyeh & Boyer-Ahmad and Fars provinces, Iran (Arachnida: Araneae). *Revista Ibérica de Aracnología* 27: 90–94.
- Mendes LF (1988) Revisão do género *Lepisma* s. lat. (Zygentoma, Lepismatidae). *Boletim da Sociedade Portuguesa de Entomologia*, supl. 2: 1–236.
- Mendes LF (2002) Some new data and descriptions of thysanurans (Zygentoma: Nicoletiidae) from Central and Eastern Africa. *Annales du Musée royal de l’Afrique Centrale, Zoologie* 290: 87–127.
- Molero-Baltanás R, Bach de Roca C, Gaju Ricart M (1999) *Neoasterolepisma caeca*, nueva especie de Lepismatidae de Canarias (Apterygota, Zygentoma). *Vieraea* 27: 87–96.
- Molero-Baltanás R, Gaju-Ricart M, Bach de Roca C (2000) On the taxonomic use of the distribution pattern of the antennal asteriform sensilla in *Neoasterolepisma* and *Tricholepisma* (Insecta, Zygentoma, Lepismatidae). *Pedobiologia* 44: 248–256. [https://doi.org/10.1078/S0031-4056\(04\)70045-1](https://doi.org/10.1078/S0031-4056(04)70045-1)
- Molero R, Bach C, Sendra A, Montagud S, Barranco P, Gaju M (2013) Revision of the genus *Coletinia* (Zygentoma: Nicoletiidae) in the Iberian Peninsula, with descriptions of nine new species. *Zootaxa* 3615(1): 1–60. <https://doi.org/10.11646/zootaxa.3615.1.1>
- Smith G, McRae J (2016) Further short range endemic troglobitic silverfish (Zygentoma: Nicoletiidae; Subnicoletiinae and Coletiniinae) from north-western Australia. *Records of the Western Australian Museum* 31: 41–55. [https://doi.org/10.18195/issn.0312-3162.31\(1\).2016.041-055](https://doi.org/10.18195/issn.0312-3162.31(1).2016.041-055)
- Tahami MS, Gorochoy AV, Sadeghi S (2017a) Cave and burrow crickets of the subfamily Bothriophylacinae (Orthoptera: Myrmecophilidae) in Iran and adjacent countries. *Zoosystematica Rossica* 26: 241–275. https://www.zin.ru/journals/zsr/content/2017/zr_2017_26_2_Tahami.pdf
- Tahami MS, Merkl O, Sadeghi S (2016) *Leptodes* of Iran, with description of six new cavernicolous species (Coleoptera: Tenebrionidae: Pimeliinae: Leptodini). *Annales Zoologici* 66(4): 589–606. <https://doi.org/10.3161/00034541ANZ2016.66.4.012>
- Tahami MS, Molero R, Gaju M, Sadeghi S (2018) Discovery of representatives of the family Nicoletiidae (Insecta: Zygentoma) from caves of Iran, with descriptions of two new supraspecific taxa. *Zootaxa* 4369: 253–269. <https://doi.org/10.11646/zootaxa.4369.2.6>
- Tahami MS, Muilwijk J, Lohaj R, Sadeghi S (2017b) Study of *Laemostenus* species across Zagros and Central zone of Iran, with the description of seven new cavernicolous species and notes on subgenus *Iranosphodrus* (Coleoptera: Carabidae: Sphodrini). *Zootaxa* 4344: 115–136. <https://doi.org/10.11646/zootaxa.4344.1.4>
- Tahami MS, Růžička J, Sadeghi S, Jakubec P, Novak M (2017c) Small carrion beetles (Coleoptera: Leiodidae: Cholevinae) from caves in Iran, with additional taxonomical notes on *Anemadus sen-gleti* and *Catops farsicus*. *Zootaxa* 4303: 509–520. <https://doi.org/10.11646/zootaxa.4303.4.4>
- Tahami MS, Zamani A, Sadeghi S, Ribera C (2017d) A new species of *Loxosceles* Heineken & Lowe, 1832 (Araneae: Sicariidae) from Iranian caves. *Zootaxa* 4318: 377–387. <https://doi.org/10.11646/zootaxa.4318.2.10>
- Wygodzinsky P (1942) Second contribution towards the knowledge of Diplura and Thysanura from Palestine. *Revista Brasileira de Biologia* 2(1): 29–46

Four new troglophilic species of *Loxosceles* Heinecken & Lowe, 1832: contributions to the knowledge of recluse spiders from Brazilian caves (Araneae, Sicariidae)

Rogério Bertani¹, Diego M. von Schimonsky^{2,3},
Jonas E. Gallão^{2,3}, Maria E. Bichuette²

1 Laboratório Especial de Ecologia e Evolução, Instituto Butantan, Av. Vital Brasil, 1500 CEP 05503-900, São Paulo, São Paulo, Brazil **2** Laboratório de Estudos Subterrâneos, Departamento de Ecologia e Biologia Evolutiva, Universidade Federal de São Carlos campus São Carlos, São Paulo, Brazil **3** Programa de Pós Graduação em Biologia Comparada – Faculdade de Filosofia, Ciências e Letras de Ribeirão Preto - FFCLRP, Universidade de São Paulo – USP, Ribeirão Preto, São Paulo, Brazil

Corresponding author: Rogério Bertani (bertani.rogerio@gmail.com)

Academic editor: Miquel Arnedo | Received 13 June 2018 | Accepted 1 November 2018 | Published 13 December 2018

<http://zoobank.org/6877DA0E-7A92-4EE2-8F33-7D05B337AE73>

Citation: Bertani R, von Schimonsky DM, Gallão JE, Bichuette ME (2018) Four new troglophilic species of *Loxosceles* Heinecken & Lowe, 1832: contributions to the knowledge of recluse spiders from Brazilian caves (Araneae, Sicariidae). ZooKeys 806: 47–72. <https://doi.org/10.3897/zookeys.806.27404>

Abstract

Four new species of recluse spiders from Brazilian caves are described with both males and females. *Loxosceles ericsoni* Bertani, von Schimonsky & Gallão, **sp. n.** and *L. karstica* Bertani, von Schimonsky & Gallão, **sp. n.** both occur in caves in the Peruaçu region, located in the northern area of the state of Minas Gerais; *L. karstica* **sp. n.** is additionally found in the Serra do Ramalho karst area, located in the southwestern region of the state of Bahia. These two species belong to the *gaucho* group. *Loxosceles carinhanha* Bertani, von Schimonsky & Gallão, **sp. n.** and *L. cardosoi* Bertani, von Schimonsky & Gallão, **sp. n.** occur exclusively in caves of the Serra do Ramalho karst area and belong to the *rufescens/amazonica* species group. The discovery of two additional and highly distinct species in the *rufescens/amazonica* group (*L. carinhanha* **sp. n.** and *L. cardosoi* **sp. n.**) increases the debate on the origin, evolution, and geographical distribution of this widely distributed group of recluse spiders in the New and Old World. The presence of three species (*L. ericsoni* **sp. n.**, *L. carinhanha* **sp. n.**, and *L. cardosoi* **sp. n.**) with marked differences in morphological characters in a relatively small area indicates that the region seems to be an important center for *Loxosceles* diversity, which remains poorly studied.

Keywords

Bahia, brown spider, karst area, Minas Gerais, taxonomy

Introduction

The genus *Loxosceles* Heinecken & Lowe, 1832, known as brown or recluse spiders, comprises 134 species (World Spider Catalog 2018) from the New World, Africa, Europe, and Asia. Many species are of medical concern due to the potent venom they produce, which can cause severe necrosis following a bite (Gertsch 1967, Isbister and Fan 2011). Most of the species found in the New World were described by Gertsch and Mulaik (1940), Gertsch (1958, 1967, 1973), and Gertsch and Ennik (1983). After these significant revisions, very few species were described (Wang 1994, Martins et al. 2002), but more recently, *Loxosceles* is again receiving attention with several new species described (Ribera and Planas 2009, Duncan et al. 2010, Bertani et al. 2010, González-Sponga 2010, Gonçalves-de-Andrade et al. 2012, Sánchez-Ruiz and Brescovit 2013, Planas and Ribera 2015, Cala-Riquelme et al. 2015, Fukushima et al. 2017, Tahami et al. 2017; Lotz 2017; Brescovit et al. 2017; Souza and Ferreira 2018).

In South America, Gertsch (1967) distinguished four groups of species, *gaucho*, *laeta*, *spadicea*, and *amazonica*. The *gaucho* group now has six species in Brazil, as follows: *L. gaucho* Gertsch, 1967; *L. adelaida* Gertsch, 1967; *L. similis* Moenkhaus, 1898; *L. chapadensis* Bertani, Fukushima & Nagahama, 2010; *L. niedeguidonae* Gonçalves-de-Andrade, Bertani, Nagahama & Barbosa, 2012; *L. troglobia* Souza & Ferreira, 2018, and one species from Paraguay, *L. variegata* Simon, 1897. The *spadicea* group has three species recorded in Brazil: *L. intermedia* Mello-Leitão, 1934; *L. hirsuta* Mello-Leitão, 1931; and *L. anomala* (Mello-Leitão, 1917); and one species in Bolivia, *L. spadicea* Simon, 1907. The *laeta* group is the largest, with 24 species described by Gertsch (1967). A single native species was described in Brazil, *L. puortoi* Martins, Knysak & Bertani, 2002, and one was introduced, *L. laeta* (Nicolet, 1849). It is especially diverse in the Peruvian Andes. Gertsch (1967) considered the *amazonica* group to have a single species, *L. amazonica* Gertsch, 1967, from Brazil. Recently, it was proposed that this species belongs to an Old World group, *rufescens* (Fukushima et al. 2017), and two additional species from Brazil were described: *L. williansoni* Fukushima, Gonçalves-de-Andrade & Bertani, 2017 and *L. muriciensis* Fukushima, Gonçalves-de-Andrade & Bertani, 2017 (Fukushima et al. 2017). Phylogenetic analyses using molecular (Binford et al. 2008, Duncan et al. 2010) or morphological approach (Magalhães et al. 2017) were recently published, but they included a limited subset of *Loxosceles* species, or focused mainly on the *rufescens* group (Binford et al. 2008, Duncan et al. 2010).

Loxosceles are secretive spiders found under rocks, ground litter, and loose bark; in the holes of trees, tree trunks, and natural openings in cliffs and banks; and in caves (Gertsch 1967). The majority of *Loxosceles* found in caves are troglaphiles, which means that they have source populations both inside and outside caves, completing its life cycle in both environments, however, troglaphitic species (obligatory and exclusive subterranean source population) may be found (*sensu* Trajano 2012). There are 15 described

species of *Loxosceles* in Brazil, and only four, *L. adelaida*, *L. similis*, *L. willianilsoni*, and *L. troglobia* (the only troglomorphic species in Brazil), occur in caves. However, it is worth mentioning that the majority of the records of *Loxosceles* in Brazilian caves are still at a generic level (Trajano 1987, Pinto-da-Rocha 1995, Cordeiro et al. 2014, Gallão and Bichuette 2015). Worldwide, this genus has been recorded in caves in Iran, Thailand, South Africa, and Namibia (e.g., Chomphuphuang et al. 2016, Tahami et al. 2017, Lotz 2017). It is also noteworthy that, for some caves in Namibia and South Africa, there are records of at least seven species, two of them coexisting in one cave in South Africa (*L. parramae* Newlands, 1981 and *L. speluncarum* Simon, 1893) (Lotz 2017).

The aim of this paper is to describe four new *Loxosceles* species with a discussion about distribution and diversity of this genus in Brazilian caves.

Materials and methods

Study sites

Studied regions are in the transition zone of the Cerrado and Caatinga morphoclimatic domains (Ab'Saber 1977), and, according to the Köppen-Geiger classification (Peel et al. 2007), the climate is tropical semi-arid, with a well-defined dry period between April and September and an average annual temperature of 24 °C and a maximum rainfall of 800–1000 mm (INMET 2017).

Peruaçu region, in the northern area of the state of Minas Gerais in southeastern Brazil

The Janelão, Bonita, and Boquete Caves (Figs 1–3) are located in Peruaçu Caves National Park (PCNP), in the state of Minas Gerais in southeastern Brazil, and are under legal protection. The region is covered by extensive limestone outcrops of the Bambuí geomorphological group (Piló and Kohler 1991) and is home to the richest

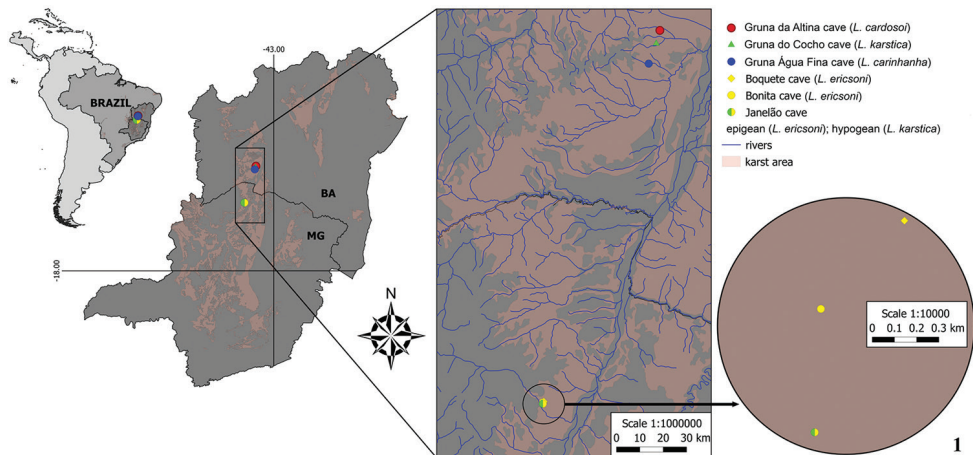
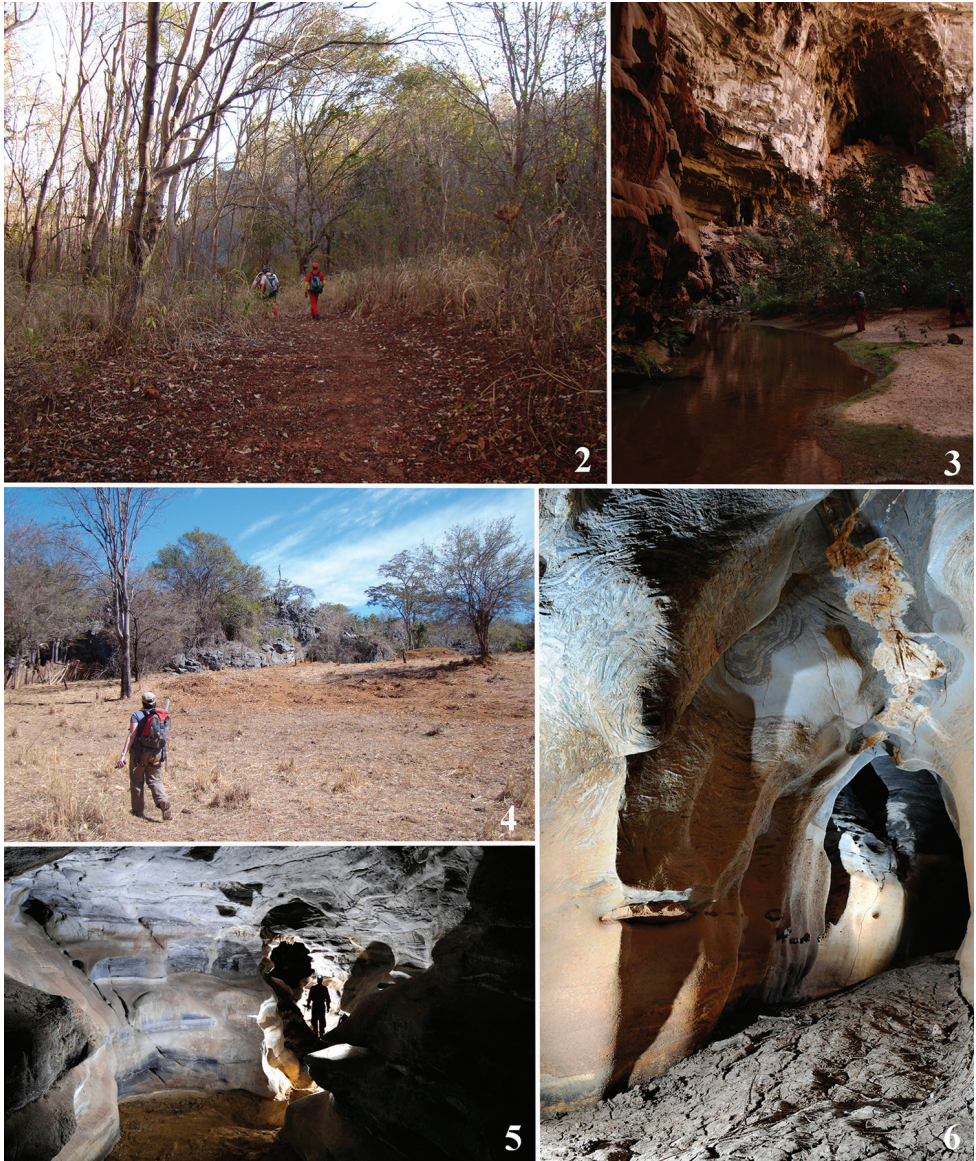


Figure 1. Map showing records of *L. ericsoni* sp. n., *L. karstica* sp. n., *L. carinhanha* sp. n., and *L. cardosoi* sp. n



Figures 2–6. Habitats. **2** Caatinga vegetation at Peruçu Caves National Park, Januária, state of Minas Gerais, Brazil **3** Janelão Cave **4** Caatinga vegetation at Serra do Ramalho karst area, Carinhanha, state of Bahia, Brazil **5** Gruna da Altina Cave **6** Gruna Água Fina Cave. Photographs by PP Rizzato (**2–4**), A Gambarini (**5, 6**).

cave in Minas Gerais, Olhos d'Água Cave, with at least 12 obligatory cave species of troglobites (Trajano et al. 2016, Gallão and Bichuette 2018).

Serra do Ramalho karst area, state of Bahia, northeastern Brazil

The Serra do Ramalho karst area (Figs 1, 4–6) comprises several limestone outcrops of the Bambuí geomorphological group, including several large cave systems, some reaching

several kilometers in length (Auler et al. 2001). The region is one of high subterranean diversity, and there is no legal protection for this region (Trajano et al. 2016). The main threats are deforestation for agriculture and pastureland, in addition to potential mining projects for cement production and mineral products (Gallão and Bichuette 2018).

Specimens

Gertsch (1967) was used as the basis for species descriptions. Structures from the left side of the specimens were used, or, when the right side was used, the figures were mirrored to show them as coming from the left side to allow for easy comparison. A Leica LAS Montage and LAS 3D module mounted on a Leica M205C dissecting microscope were used for image capture and measurements of spider structures. Left legs and palps were measured from the dorsal aspect of the left side. All measurements are in millimeters. The copulatory organs of females were dissected and digested with a commercial protein remover for contact lenses (with pancreatin) for several minutes in order to observe the internal structure; when necessary, they were also cleared with clove oil.

Abbreviations:

ALE anterior lateral eye,
PLE posterior lateral eye,
PME posterior median eye.

Most specimens were collected inside caves and fixed with ethanol 70%. Epigean collections were conducted in the cave surroundings. Specimens are deposited at **LES** – Laboratório de Estudos Subterrâneos, Universidade Federal de São Carlos, São Carlos (curator ME Bichuette); and at **MZUSP** – Museu de Zoologia da Universidade de São Paulo (USP), São Paulo (curator R Pinto-da-Rocha).

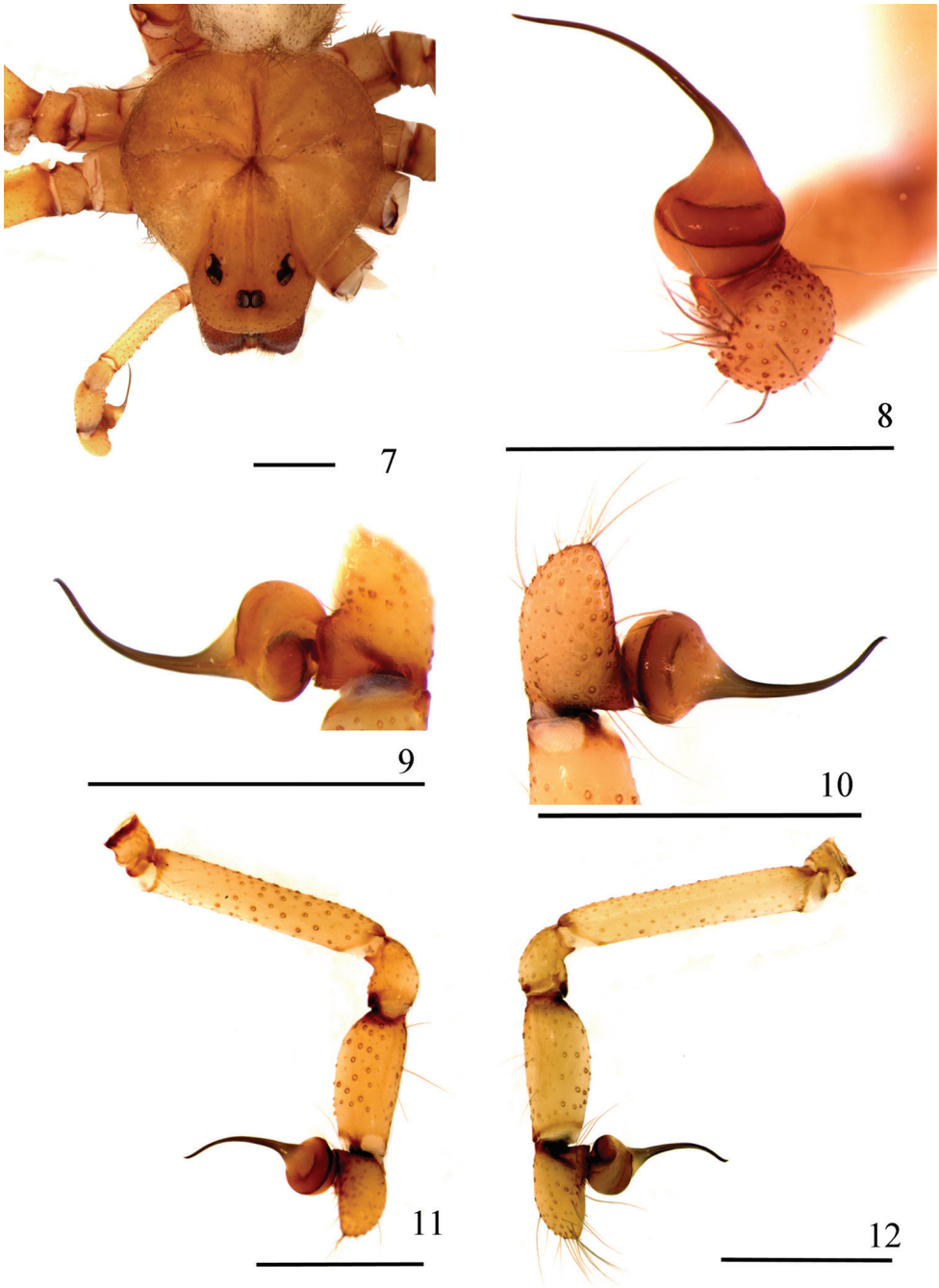
Taxonomy

Loxosceles ericsoni Bertani, von Schimonsky & Gallão, sp. n.

<http://zoobank.org/E39A83F9-474A-4657-ABB8-5F914EA6416F>

Figs 1, 7–17, 55

Type material. Male holotype (MZUSP 74427) and female paratype (MZUSP 74429), BRAZIL: *Minas Gerais*, Januária, Epigean Janelão Cave (15°06'S, 44°14'W) 600 m a.s.l., M.E. Bichuette, P.P. Rizzato, and J.E. Gallão leg., 22.vii.2012; Boquete Cave (15°04'S, 44°17'W) 681 m a.s.l., 1 female paratype, same collectors and date (MZUSP 74430); Bonita Cave (15°06'S, 44°14'W) 661 m a.s.l., paratypes 4 females, same collectors and date (LES 14592).



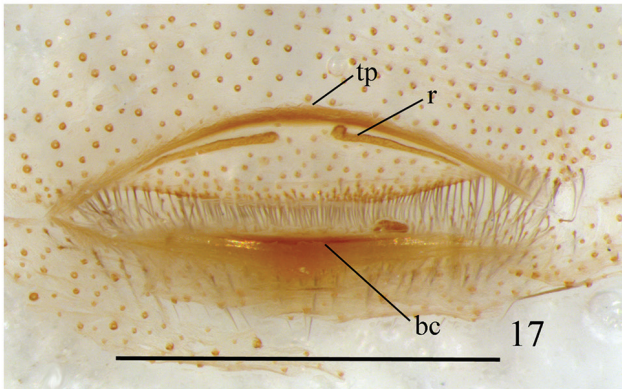
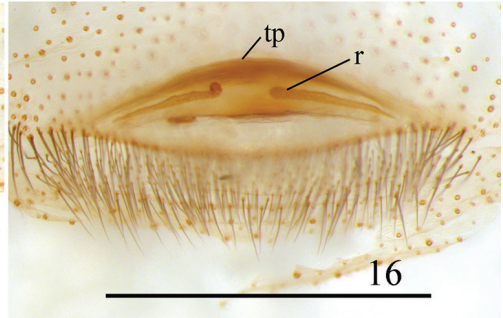
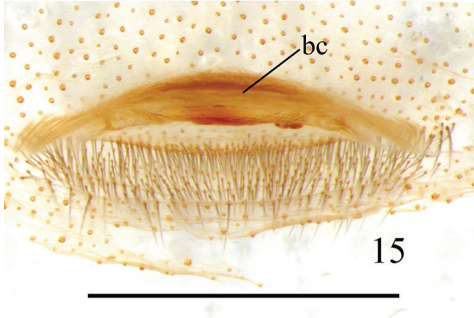
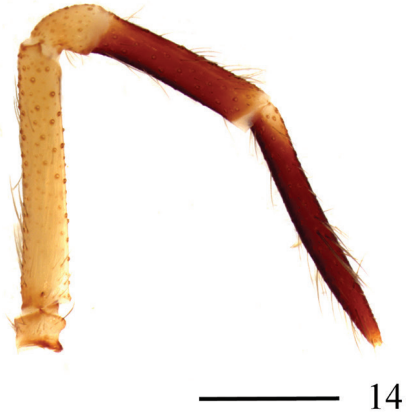
Figures 7–12. *Loxosceles ericsoni* sp. n., holotype male (MZUSP 74427) **7** carapace and palps **8–10** left palpal bulb **8** dorsal **9** retrolateral **10** prolateral **11, 12** left palp **11** prolateral **12** retrolateral. Scale bar: 1 mm.

Other material examined. BRAZIL, *Minas Gerais*: Januária, epigeal habitats near Janelão Cave (15°06'S, 44°14'W) 600 m a.s.l., 2 immatures, M.E. Bichuette, P.P. Rizzato and J.E. Gallão leg., 22.vii.2012 (MZUSP 74428); Boquete Cave, 681 m a.s.l., 1 female, 2 immatures, M.E. Bichuette, P.P. Rizzato, and J.E. Gallão leg., 23.vii.2012 (LES 14593), 2 immatures, same collectors and date (MZUSP 74431); Bonita Cave, 681 m a.s.l., 3 immatures, same collectors and date (LES 14594).

Diagnosis. Males of *Loxosceles ericsoni* sp. n. resemble those of *L. karstica* sp. n. by the palpal tibia length being less than 2 and more than 1.4 times the palpal cymbium length. They can be distinguished from *L. karstica* sp. n. by the longer cymbium and slender embolus (Figs 11, 12). Females of *L. ericsoni* sp. n. differ from those of all other *Loxosceles* species by the extremely narrow sclerotized transversal plate and the two straight, very long, and slender receptacles (Figs 15–17).

Description. *Male holotype*: Total length 6.85. Carapace 3.20 long, 3.04 wide. Eye sizes and interdistances: ALE 0.23, PME 0.21, PLE 0.22, PME-PLE 0.04, PME-ALE 0.25; clypeus 0.35. Leg formula II, I, IV, III. Leg lengths: leg I: femur 8.73, patella 1.23, tibia 10.71, metatarsus 10.68, tarsus 1.93, total 33.28; II (right leg, left missing): 11.87, 1.27, 15.01, 15.80, 1.70, 45.65; III: 8.46, 1.15, 8.65, 11.22, 1.59, 31.07; IV: 9.29, 1.23, 9.73, 12.42, 1.80, 34.47. Palp: femur 1.53 long, 0.27 wide; patella 0.45 long, 0.32 wide; tibia 0.87 long, 0.35 wide; cymbium 0.62 long, 0.33 wide. Labium 0.63 long, 0.56 wide. Sternum 1.58 long, 1.60 wide. Femur I 2.7 times as long, tibia I 3.3 times as long and leg I 10.4 as long as carapace. Palpal femur 5.6 times longer than wide, tibia 2.5 times longer than wide, cymbium longer than wide (Figs 11, 12). Bulb suboval and slightly longer than half cymbium length. Embolus slender, long, gently curved and ending in a short and steep curvature on apex, approximately 2.4 times longer than bulb length in retrolateral view, without carina (Figs 8–10). Cephalic region of carapace with some sparse long setae (Fig. 7). Carapace with light brown pars cephalica and border (Fig. 7). Legs and palp light brown, covered by short, greyish setae. Coxae, endites, and sternum light brown.

Female paratype: Total length 9.37. Carapace 4.04 long, 3.55 wide. Eye sizes and interdistances: ALE 0.26, PME 0.21, PLE 0.24, PME-PLE 0.01, PME-ALE 0.56; clypeus 0.42. Leg formula II, I, IV, III. Leg lengths: leg I: femur 8.41, patella 1.42, tibia 10.05, metatarsus 9.41, tarsus 1.87, total 31.16; II: 9.70, 1.32, 11.66, 12.34, 1.92, 36.94; III: 7.98, 1.33, 7.58, 9.35, 1.51, 27.75; IV: 8.48, 1.34, 8.64, 10.98, 1.89, 31.33. Palp: femur 2.05 long, 0.35 wide; patella 0.58 long, 0.38 wide; tibia 1.27 long, 0.26 wide; tarsus 1.94 long, 0.20 wide. Labium 0.69 long, 0.66 wide. Sternum 2.18 long, 1.96 wide. Femur I 2.1 times as long, tibia I 2.5 times as long, and leg I 7.7 as long as carapace. Palpal femur 5.8 times longer than wide, tibia 4.9 longer than wide, tarsus not incrassate (Fig. 14). Spermathecae sclerotized transverse plate extremely narrow. Two receptacles almost straight, long, slender, parallel to transverse sclerotized plate (Figs 15–17). Dorsal part of the bursa copulatrix with a central area medially sclerotized (Fig. 17). Cephalic region of carapace with some sparse long setae (Fig. 13). Carapace with light brown pars cephalica and border (Fig. 13). Legs light brown,



Figures 13–17. *Loxosceles ericsoni* sp. n., paratype female (MZUSP 74429) **13** carapace and palp **14** left palp, prolateral **15–17** spermathecae **15** dorsal, with bursa copulatrix over receptacles **16** ventral **17** dorsal, bursa copulatrix unfolded below. Abbreviations: bc bursa copulatrix, r receptacle, tp transverse sclerotized plate. Scale bar: 1 mm.

covered by short, greyish setae. Palp light brown, except reddish brown tibia and tarsus (Fig. 14). Coxae and sternum light brown. Endites and labium brown.

Etymology. The specific name is in honor of Ericson Cernawsky Igual from Grupo Pierre Martin de Espeleologia (GPME) for his contribution to Brazilian speleology and his commitment to the conservation of caves.

Remarks. *Loxosceles ericsoni* sp. n. females have highly modified spermathecae (Figs 15–17). Although they have a transverse plate, it is very narrow and does not connect directly to the two receptacles (Figs 16, 17). The receptacles themselves are two long, slender tubes positioned parallel to the transverse plate and converging to the center. Despite the modified female genitalia, it is possible to include this species in the *gaucho* group by the male palpal morphology, as they have a cymbium almost the same length as the palpal tibia (Figs 11, 12).

***Loxosceles karstica* Bertani, von Schimonsky & Gallão, sp. n.**

<http://zoobank.org/1E1BBD45-081B-44DF-9ED1-DC1F1581F466>

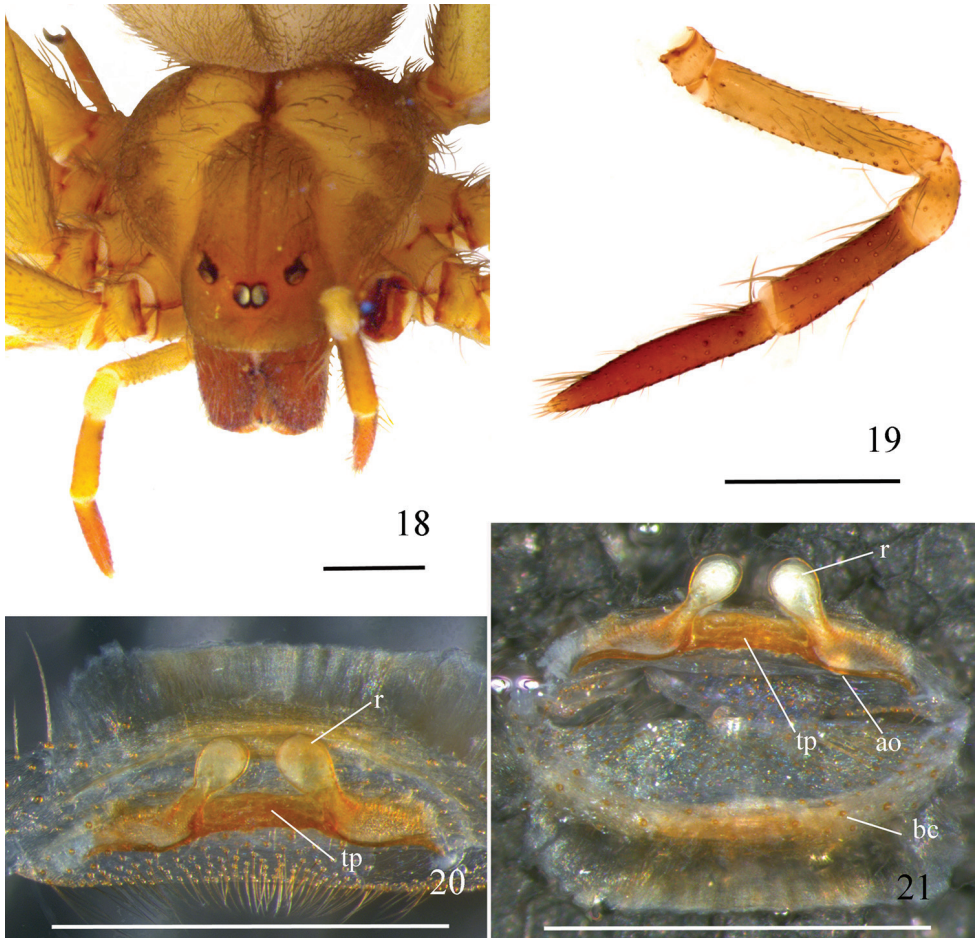
Figs 1, 18–27

Material examined. Female holotype (MZUSP 74432), male paratype (MZUSP 74433), 2 female paratypes (LES 14712), 2 male and 2 female paratypes (MZUSP 74434), 3 female paratypes (MZUSP 74435), 3 male and 3 female paratypes (LES 14595), BRAZIL: *Minas Gerais*, Januária, Janelão Cave (15°06'S, 44°14'W) 600 m a.s.l., M.E. Bichuette, P.P. Rizzato and J.E. Gallão leg., 22.vii.2012.

Other material examined. BRAZIL, *Minas Gerais*: Januária, Janelão Cave (15°06'S, 44°14'W) 600 m a.s.l., 2 immatures, M.E. Bichuette, P.P. Rizzato and J.E. Gallão leg., 22.vii.2012 (LES 14596), 1 immature, same collectors and date (LES 14713); *Bahia*: Carinhanha, Gruna do Cocho Cave (13°36'S, 43°46'W) 514 m a.s.l., 3 females, M.E. Bichuette, N. Hattori and J.E. Gallão leg., 02.vi.2012 (LES 14597).

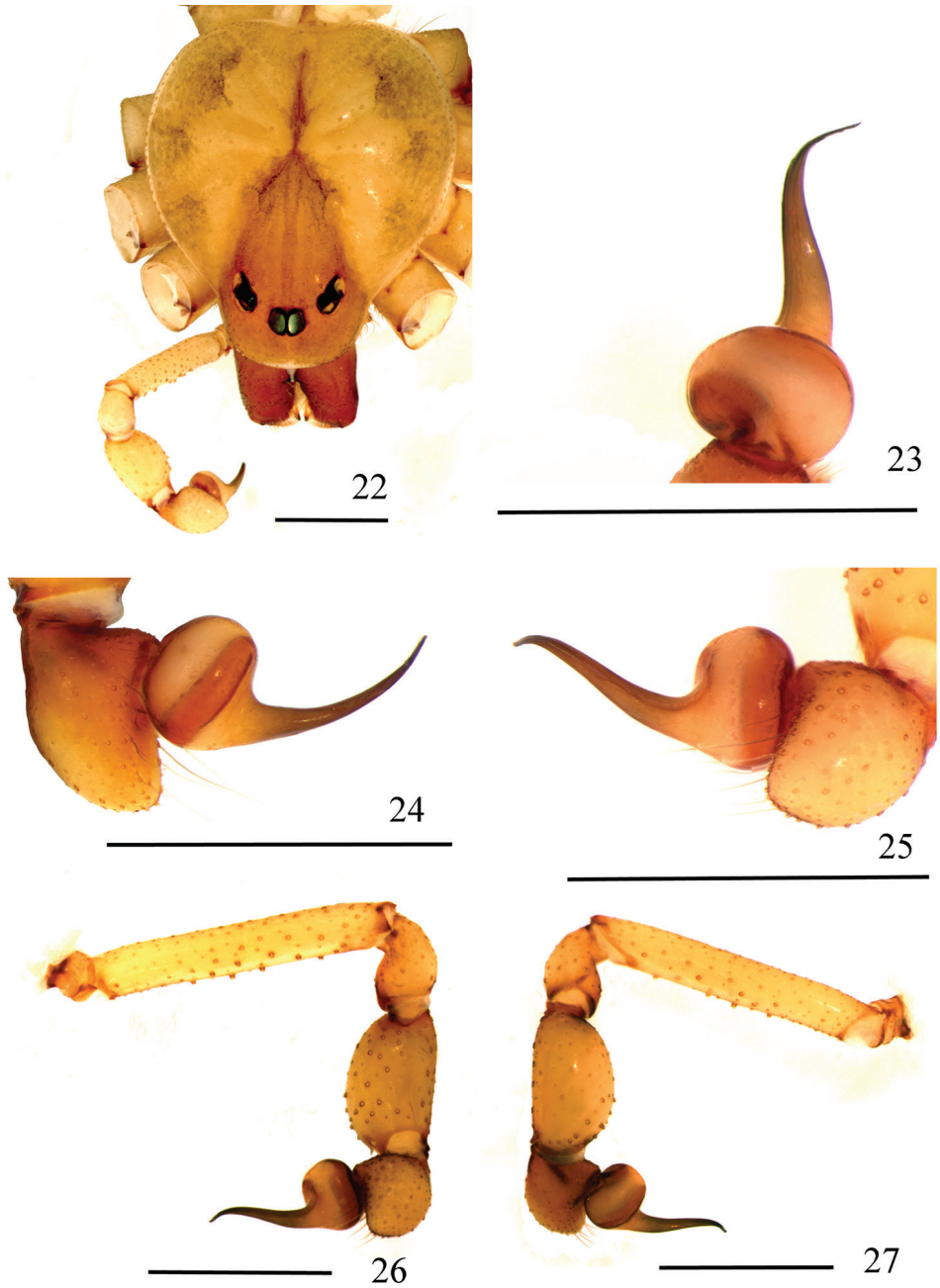
Diagnosis. Males of *Loxosceles karstica* sp. n. resemble those of *L. ericsoni* sp. n. by the palpal tibia length more than 1.4 and less than 2.0 times the cymbium length. They can be distinguished from those of *L. ericsoni* sp. n. by the shorter cymbium and stouter embolus (Figs 26, 27). Females of *L. karstica* sp. n. resemble those of *L. similis*, *L. chapadensis*, and *L. niedeguidonae* by the spermathecae having the sclerotized transversal plate with two long and straight receptacles. They differ from the females of the species above by the short, sclerotized transverse plate with the receptacles positioned at an angle of 45° to the inner side (Figs 20, 21). Additionally, they can be distinguished from females of *L. chapadensis* by the dorsal part of the bursa copulatrix medially sclerotized (Fig. 21) and from *L. niedeguidonae* by the non-incrassated palpal tarsus (Fig. 19).

Description. *Female holotype*: Total length 8.60. Carapace 3.58 long, 3.16 wide. Eye sizes and interdistances: ALE 0.24, PME 0.21, PLE 0.24, PME-PLE 0.05, PME-ALE 0.20; clypeus 0.32. Leg formula II, I, IV, III. Legs length: leg I: femur 7.49, patella 1.18, tibia 8.10, metatarsus 7.79, tarsus 1.79, total 26.35; II: 8.29, 1.25, 9.01, 9.05, 1.74, 29.34; III: 6.39, 1.28, 6.32, 7.17, 1.53, 22.69; IV: 7.41, 1.31, 7.43, 8.42,



Figures 18–21. *Loxosceles karstica* sp. n., holotype female (MZUSP 74432) **18** carapace and palp **19** left palp, prolateral **20, 21** spermathecae **20** ventral **21** dorsal, bursa copulatrix unfolded below. Abbreviations: ao atriobursal orifice, bc bursa copulatrix, r receptacle, tp transverse sclerotized plate. Scale bar: 1 mm.

1.58, 26.15. Palp: femur 1.44 long, 0.24 wide; patella 0.52 long, 0.34 wide; tibia 1.02 long, 0.29 wide; tarsus 1.41 long, 0.24 wide. Labium 0.80 long, 0.58 wide. Sternum 1.90 long, 1.74 wide. Femur I 2.1 times as long, tibia I 2.2 times as long, and leg I 7.3 as long as carapace. Palpal femur 6 times longer than wide; tibia 3.5 longer than wide; tarsus not incrassate (Fig. 19). Spermathecae sclerotized transverse plate short with almost-straight receptacles positioned at an angle of 45° to the inner side (Figs 20, 21). Dorsal part of the bursa copulatrix medially sclerotized (Fig. 21). Cephalic region of carapace with some sparse, long setae (Fig. 18). Carapace with dark-brown pars cephalica and border (Fig. 18). Legs brown, covered by short, greyish setae. Palp light brown, except for reddish brown tibia and tarsus (Fig. 19). Coxae and sternum light brown. Endites and labium brown.



Figures 22–27. *Loxosceles karstica* sp. n., paratype male (MZUSP 74433) **22** carapace and palp **23–25** left palpal bulb **23** dorsal **24** prolateral **25** retrolateral **26, 27** left palp **26** prolateral **27** retrolateral. Scale bar: 1 mm.

Male paratype: Total length 6.56. Carapace 3.06 long, 2.76 wide. Eye sizes and interdistances: ALE 0.26, PME 0.21, PLE 0.20, PME-PLE 0.04, PME-ALE 0.17; clypeus 0.32. Leg formula II, I, IV, III (inferred from male MZUSP 74434; see below). Leg lengths: leg I: missing; II: femur 9.39, patella 1.22, tibia 10.58, metatarsus 11.69, tarsus 0.92, total 33.80; III: missing; IV: 7.91. 1.24. 8.06. 9.50. 1.64. 28.35. Palp: femur 1.72 long, 0.29 wide; patella 0.51 long, 0.35 wide; tibia 0.84 long, 0.48 wide; cymbium 0.57 long, 0.44 wide. Labium 0.52 long, 0.44 wide. Sternum 1.67 long, 1.57 wide. Femur I 2.6 times as long, tibia I 3.1 times as long, and leg I 9.9 as long as carapace (inferred from male MZUSP 74434; see below). Palpal femur 5.9 times longer than wide, tibia 1.7 times longer than wide, cymbium oval (Figs 26, 27). Bulb suboval and a little smaller than cymbium. Embolus curved from its basis, approximately 1.8 times longer than bulb length in retrolateral view, without carina (Figs 23–25). Cephalic region of carapace covered by some sparse setae (Fig. 22). Entire pars cephalica dark-brown, carapace border dark-brown but slightly faded (Fig. 22). Legs, palps, endites, coxae, sternum, and labium light brown.

Remarks. The male specimen in better condition to be chosen as paratype lacks legs I and III. For this reason, another male (MZUSP 74434), not in condition to serve as type, had legs measured as follows: leg I: femur 8.25, patella 1.16, tibia 9.88, metatarsus 10.33, tarsus 2.10, total 31.72; II: 9.89, 1.23, 11.72, 13.07, 2.02, 37.93; III: 7.49, 1.06, 7.51, metatarsus broken, tarsus missing; IV: 8.21, 1.06, 8.72, 10.24, tarsus missing. Carapace: 3.20 long, 2.94 wide.

The new species *L. karstica* sp. n. has genitalic characteristics shared with other species of the *gaucho* group distributed in the southern regions of Brazil and Paraguay, as *L. gaucho*, *L. similis*, *L. adelaida*, and *L. variegata*, which have palpal tibia that are short and incrassate in males (Figs 26, 27) and the large spermathecae transverse plate in females (Figs 20, 21). It also shares characteristics with the species of the *gaucho* group that are more distributed in the northern part of Brazil, as *L. chapadensis* and *L. niedeguidonae*, as they have a longer palpal tibia in males and a spermathecae transverse plate that is almost as short as in the new species but with differences in the bursa copulatrix sclerotization and the size and shape of receptacles.

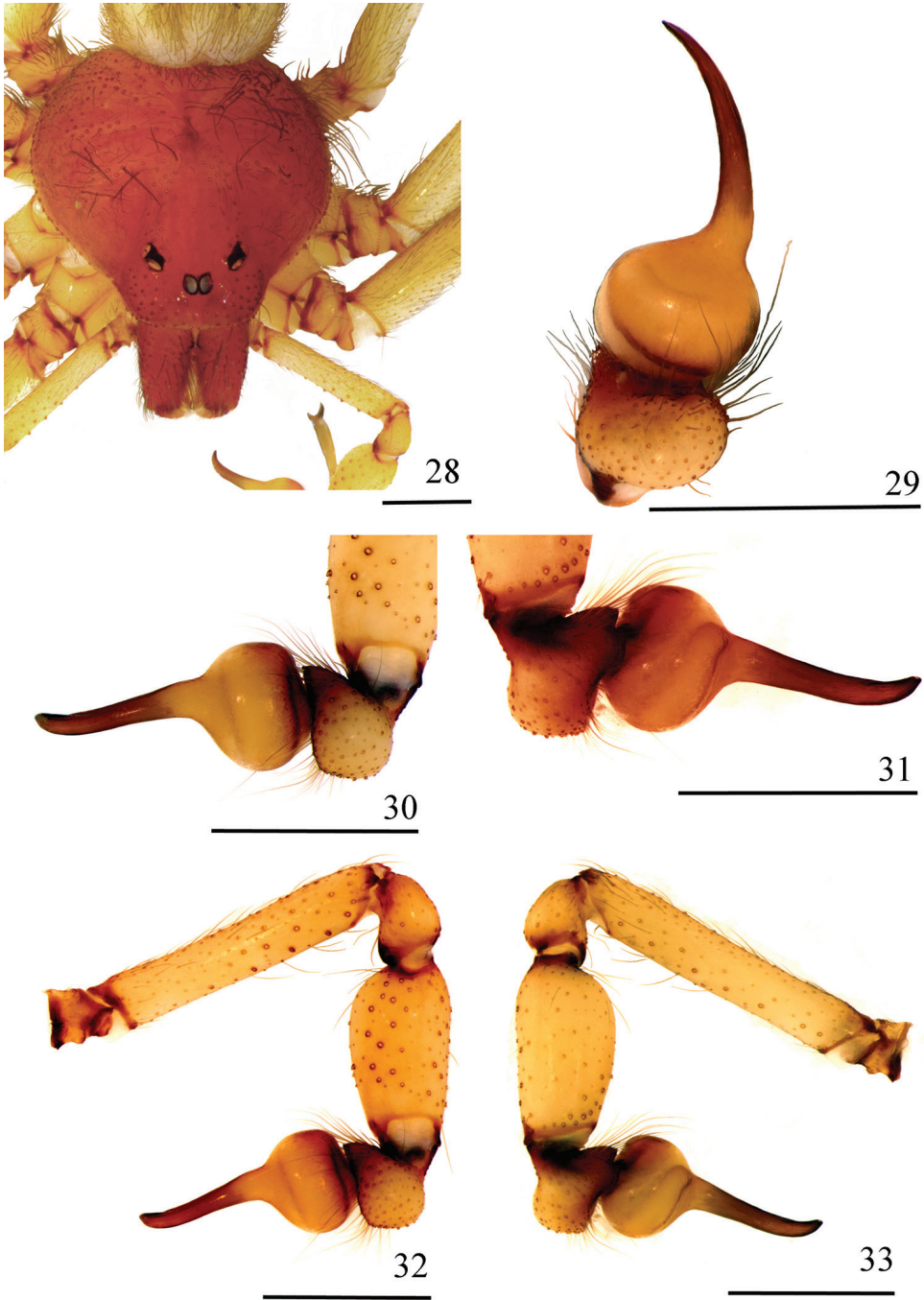
Etymology. The specific name refers to karst, a word used to define terrain with distinctive hydrology and landforms that arise from a combination of high rock solubility and well-developed porosity. *Loxosceles karstica* sp. n. occurs in two important karst areas of Brazil (Peruaçu and Serra do Ramalho).

***Loxosceles carinhanha* Bertani, von Schimonsky & Gallão, sp. n.**

<http://zoobank.org/F90FD902-CBA1-40A1-9B59-506D75D722D3>

Figs 1, 28–41

Material examined. Male holotype (MZUSP 74436) and female paratype (MZUSP 74437), 1 female paratype (MZUSP 74438), 1 female paratype (LES 14709), BRAZIL: *Bahia*, Carinhanha, Gruna Água Fina cave (13°41'S, 43°48'W) 484 m a.s.l., M.E. Bichuette, N. Hattori and J.E. Gallão leg., 29.v.2012.



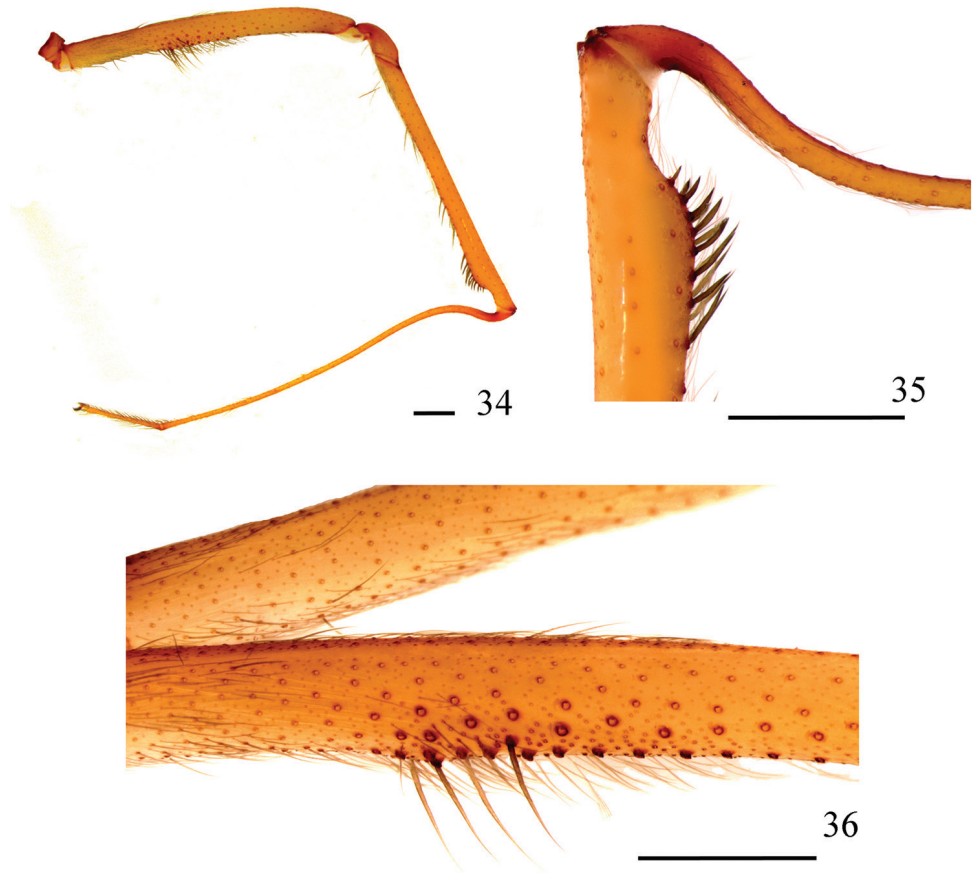
Figures 28–33. *Loxosceles carinhanba* sp. n., holotype male (MZUSP 74436) **28** carapace and palp **29–31** left palpal bulb **29** dorsal **30** prolateral **31** retrolateral **32, 33** left palp **32** prolateral **33** retrolateral
Scale bar: 1 mm.

Other material examined. BRAZIL, *Bahia*: Carinhanha, Gruna Água Fina Cave (13°41'S, 43°48'W) 484 m a.s.l., 1 female and 2 immatures, M.E. Bichuette, N. Hattori and J.E. Gallão leg., 29.v.2012 (MZUSP 74439).

Diagnosis. Males of *Loxosceles carinhanha* sp. n. can be distinguished from those of all other *Loxosceles* species by the thick embolus (Figs 29–31), a strong curvature on basal metatarsus I, and a constriction on distal tibia I (Figs 34, 35). Females of *L. carinhanha* sp. n. resemble females of *L. cardosoi* sp. n. by having spermathecae as a large, weakly sclerotized pouch with two large receptacles on its distal portion. Females of *L. carinhanha* sp. n. can be distinguished from those of *L. cardosoi* sp. n. by the spermathecae lacking a sclerotized transverse plate and dorsal parts of bursa copulatrix having only a small sclerotized triangular area (Figs 39–41).

Description. *Male holotype*: Total length 7.32. Carapace 3.63 long, 3.39 wide. Eye sizes and interdistances: ALE 0.22, PME 0.22, PLE 0.21, PME-PLE 0.05, PME-ALE 0.27; clypeus 0.38. Leg formula II, IV, III, I. Leg lengths: leg I: femur 7.18, patella 1.44, tibia 6.68, metatarsus 9.29, tarsus 2.18, total 26.77; II femur 9.69, patella 1.51, tibia 10.87, metatarsus 13.34, tarsus 2.23, total 37.64; III: 7.56, 1.33, 7.88, 9.97, 1.70, 28.44; IV: 8.37, 1.41, 8.54, 11.92, 2.16, 32.40. Palp: femur 1.92 long, 0.34 wide; patella 0.54 long, 0.41 wide; tibia 1.12 long, 0.57 wide; cymbium 0.61 long, 0.45 wide. Labium 0.89 long, 0.49 wide. Sternum 1.87 long, 1.74 wide. Femur I 1.9 times as long, tibia I 1.8 times as long and leg I 7.4 as long as carapace. Palpal femur 5.6 times longer than wide; tibia 2.0 times longer than wide; cymbium oval (Figs 32, 33). Bulb suboval and slightly larger than cymbium. Embolus thick and straight, with a curvature on apex, approximately 1.3 times longer than bulb length in retrolateral view, without carina (Figs 29–31). Femur I prolateral median area with a series of enlarged setae (Figs 34, 36). Metatarsus I strongly curved on its basal portion. Distal tibia I abruptly narrow, with a series of strong macrosetae before the constriction (Figs 34, 35). Cephalic region of carapace, fovea, and thoracic striae with long, greyish setae (Fig. 28). Carapace and chelicerae uniformly reddish (Fig. 28). Abdomen, legs, and palp light brown, covered by short, greyish setae. Coxae and sternum light brown; labium and endites slightly darker.

Female paratype: Total length 9.30. Carapace 3.99 long, 3.25 wide. Eye sizes and interdistances: ALE 0.20, PME 0.20, PLE 0.22, PME-PLE 0.05, PME-ALE 0.34; clypeus 0.41. Leg formula II, I, IV, III. Leg lengths: leg I: femur 6.79, patella 1.30, tibia 7.12, metatarsus 7.47, tarsus 1.82, total 24.50; II: 7.97, 1.40, 8.69, 9.30, 1.98, 29.34; III: 6.69, 1.29, 6.42, 7.48, 1.69, 23.57; IV: 7.23, 1.35, 7.20, 9.21, 1.69, 26.68. Palp: femur 1.61 long, 0.28 wide; patella 0.54 long, 0.34 wide; tibia 1.07 long, 0.26 wide; tarsus 1.67 long, 0.23 wide. Labium 0.67 long, 0.54 wide. Sternum 1.98 long, 1.68 wide. Femur I 1.7 times as long, tibia I 1.8 times as long and leg I 6.1 as long as carapace. Palpal femur 5.7 times longer than wide, tibia 4.1 longer than wide, tarsus not incrassate (Fig. 38). Spermathecae are a large, weakly sclerotized pouch with two large receptacles on its distal portion. Dorsal parts of bursa copulatrix have a small, sclerotized triangular area (Figs 39–41). Carapace with some sparse, long, greyish setae (Fig. 37). Carapace light brown, cephalic area, fovea, and border darker (Fig. 37).



Figures 34–36. *Loxosceles carinhanha* sp. n., holotype male (MZUSP 74436), left leg I **34** proteral **35** detail of tibia and metatarsus joint, showing metatarsus curvature and macrosetae on distal tibia **36** detail of macrosetae on median portion of femur. Scale bar: 1 mm.

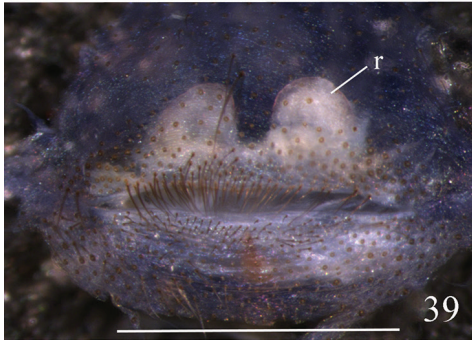
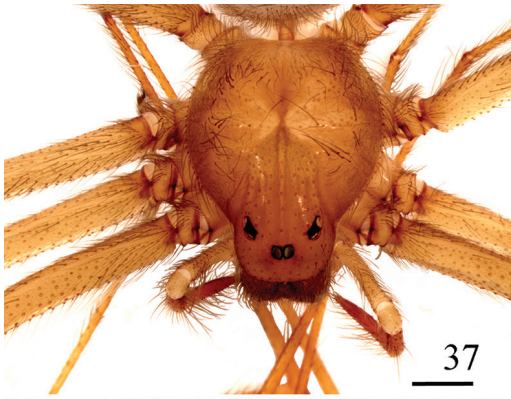
Chelicerae reddish brown. Abdomen greyish, legs light brown, both covered by short greyish setae. Palp femur and patella light brown, tibia and tarsus reddish brown (Fig. 38). Coxae and sternum light brown, labium and endites brown.

Etymology. The specific name refers to the type locality of the species, Carinhanha, a municipality in the southwestern section of the state of Bahia, Brazil. The region possesses several cave systems with high diversity and a fragile subterranean fauna.

Remarks. *Loxosceles carinhanha* sp. n. and *L. cardosoi* sp. n. males have a uniformly reddish carapace (Figs 28, 42) instead of the brown marked carapace characteristic of the groups *gaucho* and *rufescensamazonica*, and femur I has macrosetae on its proteral median area (Figs 36, 48), which is exclusive of the two species. They occur in closer areas and are probably sister species. The inclusion of the two species in one of the groups defined by Gertsch (1967) for South American *Loxosceles* is not simple question. They could fit in either *gaucho* or *rufescensamazonica* groups. Males of *gaucho*

group have the cymbium and tibia subequal in length (Gertsch 1967). However, two species described more recently has slightly longer and slender tibia (*L. chapadensis* and *L. niedeguidonae*). Even though the tibia is not incrassate in these species, the cymbium is larger than the bulb, projecting forward. Considering the variation of tibia length and width in this group, we consider the cymbium size a better character to diagnose males of *gaucho* group. Males of the *rufescens/amazonica* group have the cymbium considerably shorter than tibia. More important, however, is they are never much more larger than the bulb. Based in this criterion, both *L. carinhanha* sp. n. and *L. cardosoi* sp. n. can be included in the *rufescens/amazonica* group (Figs 32, 33, and 46, 47). Concerning females, those of the *gaucho* group are readily recognizable by “the seminal receptacles attached to immovable, sclerotized, transverse plate” (Gertsch 1967). We noted that in species of *gaucho* group the receptacles are always slender and strongly sclerotized, except the apex and can be another diagnostic character. Those of the *rufescens/amazonica* group have the “seminal receptacles with a cluster of small, globular lobes at apex” (Gertsch 1967). More recently, at least two species were known to have a single large lobe at apex, *L. mahan* Planas & Ribera, 2015 from Canary Islands and *L. willianilsoni*, from Brazil (Fukushima et al. 2017). We consider that the main characters shared by females of *rufescens/amazonica* group is the spermathecae triangular shape, two free receptacles (not attached to a transverse sclerotized plate) with large basal transverse openings with or without sclerotized edges and two dark sclerotized lateral bands with distinct levels of sclerotization depending on the species (see Planas and Ribera 2015 and Fukushima et al. 2017 for spermathecae variation). *Loxosceles cardosoi* sp. n. females have a transverse sclerotized plate (compatible with those species of *gaucho* group) and the receptacles are short (contrary to *rufescens/amazonica* group) and broad (as in the *rufescens/amazonica* group). A single dark sclerotized band is present (another characteristic of *rufescens/amazonica* group). The bursa copulatrix is strongly sclerotized. The putative sister species, *L. carinhanha* sp. n. has spermathecae weakly sclerotized lacking a transverse sclerotized plate and the receptacles are free. The bursa copulatrix is weakly sclerotized, except for a central triangular area. In favor of the inclusion of *L. cardosoi* sp. n. and *L. carinhanha* sp. n. in *rufescens/amazonica* group are the short cymbium in males and the broad and no sclerotized receptacles in females. Additionally, *L. carinhanha* sp. n. spermathecae have a single dark sclerotized band. There is no supporting character for the inclusion of males in the *gaucho* group. In females, *L. cardosoi* sp. n. has the characters transverse sclerotized plate and short receptacles, which are lacking in *L. carinhanha* sp. n. Therefore, it seems more parsimonious to include the two species in the *rufescens/amazonica* group, elevating to five the number of species of this group in South America. These two species are very distinctive of the other species of the group both in the New and the Old World.

It has been proposed the origin of *Loxosceles rufescens* group in the Old World with a posterior introduction of *L. amazonica* during portuguese colonization of Brazil beginning in 1500 (Duncan et al. 2010). One of the evidences for the introduction hypothesis was the lack of other related species in South America (Duncan et al. 2010). Recently, Fukushima et al. (2017) described two species related with *L. amazonica* and



Figures 37–41. *Loxosceles carinhanha* sp. n., paratype female (MZUSP 74437) **37** carapace and palps **38** left palp, prolateral **39–41** spermathecae **39** ventral **40** dorsal, with bursa copulatrix over receptacles **41** dorsal, bursa copulatrix unfolded below. Abbreviations: bc bursa copulatrix, r receptacle, sta sclerotized triangular area. Scale bar: 1 mm.

L. rufescens from Brazil and argued contrary to this possibility for the short time (500 years) for speciation taking place. The discovery of two additional and very distinctive species reinforces the proposal of Fukushima et al. (2017). As the *Loxosceles* diversity in South America is still largely unknown, it is necessary more efforts to collect and describe species from more remote areas of Brazil, mainly those in the northeastern and central western regions, as the areas under study here, which seems to be a hot spot for *Loxosceles* diversity.

***Loxosceles cardosoi* Bertani, von Schimonsky & Gallão, sp. n.**

<http://zoobank.org/FB08FAF6-0DFD-4E30-8C29-088423627E1F>

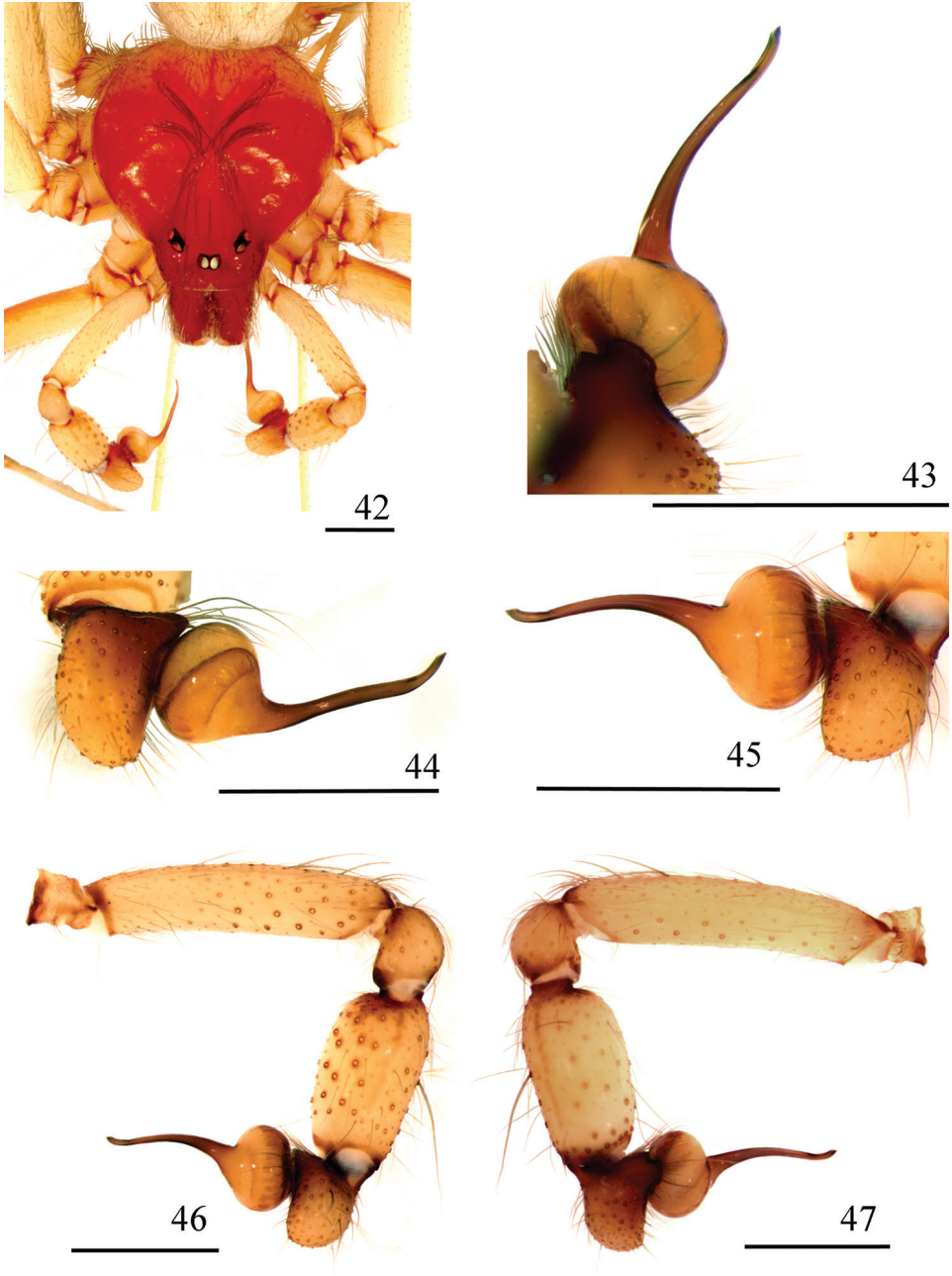
Figs 1, 42–54, 56, 57

Material examined. Male holotype (MZUSP 74440) and female paratype (MZUSP 74441), 1 male, 4 females paratypes (MZUSP 74442), 2 males, 4 females paratypes (LES 14710), BRAZIL: *Bahia*, Carinhanha, Gruna da Altina cave (13°33'S, 43°45'W) 496 m a.s.l., M.E. Bichuette, N. Hattori and J.E. Gallão leg., 01.vi.2012.

Other material examined. BRAZIL, *Bahia*: Carinhanha, Gruna da Altina Cave (13°33'S, 43°45'W) 496 m a.s.l., 10 immatures, M.E. Bichuette, N. Hattori and J.E. Gallão leg., 01.vi.2012 (LES 14711).

Diagnosis. Males of *Loxosceles cardosoi* sp. n. resemble those of *L. carinhanha* sp. n. by having a group of macrosetae on the median prolateral area of femur I (Fig. 48). They can be distinguished from the males of *L. carinhanha* sp. n. by the slender embolus with a gentle curvature on its median area ending in a strong curvature on its apex (Figs 43–45) and the straight metatarsus I. Females of *L. cardosoi* sp. n. resemble those of *L. carinhanha* sp. n. by having spermathecae as a large, weakly sclerotized pouch with two large receptacles on its distal portion. Females of *L. cardosoi* sp. n. can be distinguished from those of *L. carinhanha* by the spermathecae having a sclerotized transverse plate, one dark sclerotized band reaching the basal area of each receptacle and dorsal and ventral parts of bursa copulatrix strongly sclerotized (Figs 51–54).

Description. *Male holotype*: Total length 7.54. Carapace 3.70 long, 3.54 wide. Eye sizes and interdistances: ALE 0.23, PME 0.20, PLE 0.19, PME-PLE 0.02, PME-ALE 0.23; clypeus 0.30. Leg formula II, IV, III, I. Leg lengths: leg I: femur 7.39, patella 1.38, tibia 8.25, metatarsus 9.26, tarsus 1.77, total 28.05; II: 10.12, 1.43, 12.41, 13.65, 2.06, 39.67; III: 8.05, 1.36, 8.04, 9.82, 1.52, 28.79; IV: 8.67, 1.38, 9.04, 11.74, 2.03, 32.86. Palp: femur 2.10 long, 0.47 wide; patella 0.57 long, 0.51 wide; tibia 1.27 long, 0.67 wide; cymbium 0.72 long, 0.52 wide. Labium 0.89 long, 0.52 wide. Sternum 1.85 long, 1.82 wide. Femur I 2.0 times as long, tibia I 2.2 times as long, and leg I 7.6 as long as carapace. Palpal femur 4.5 times longer than wide, tibia 1.9 times longer than wide, cymbium oval (Figs 46, 47). Bulb suboval and approximately same size as cymbium. Embolus slender, with a gentle curvature to dorsal aspect on its middle and a strong curvature on apex, approximately two times longer than bulb length in retrolateral view, without carina (Figs 44, 45). Cephalic region of



Figures 42–47. *Loxosceles cardosoi* sp. n., holotype male (MZUSP 74440) **42** carapace and palp **43–45** left palpal bulb **43** dorsal **44** prolateral **45** retrolateral **46, 47** left palp **46** prolateral **47** retrolateral. Scale bar: 1 mm.

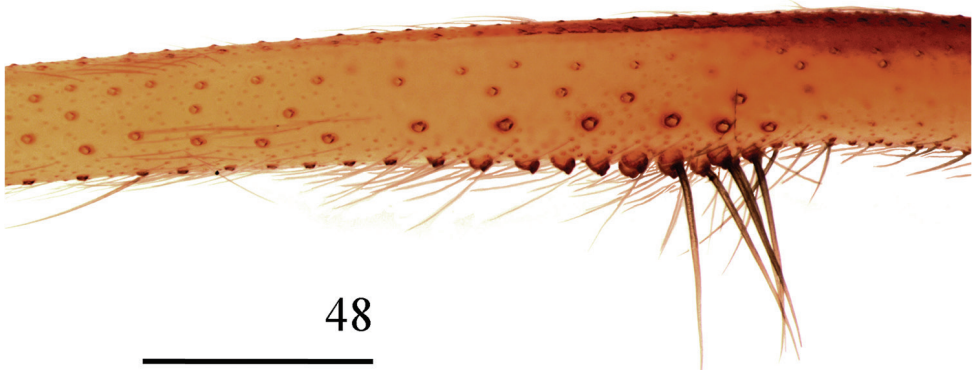


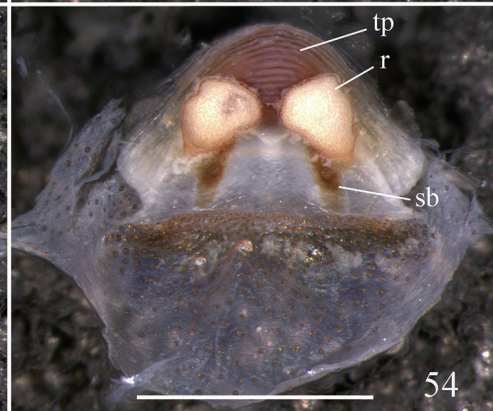
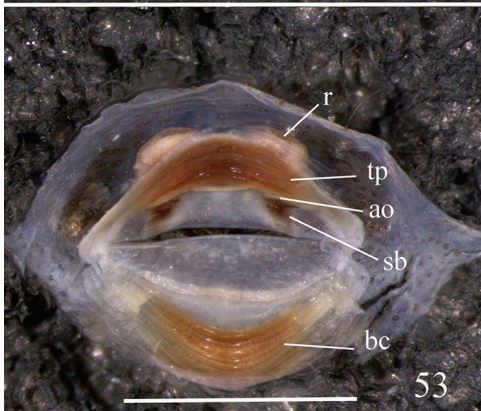
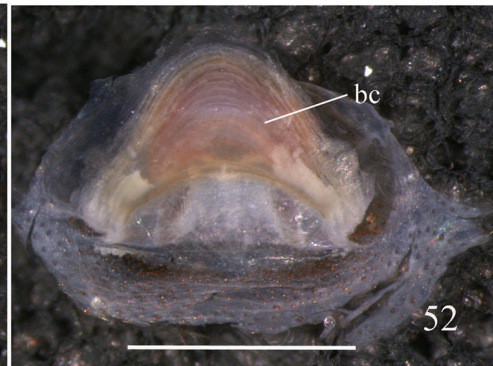
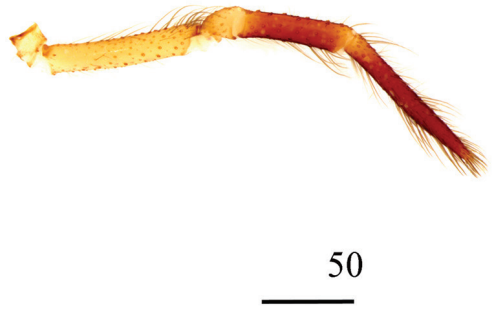
Figure 48. *Loxosceles cardosoi* sp. n., holotype male (MZUSP 74440), left leg I, detail of macrosetae on median portion of femur. Scale bar: 1 mm.

carapace, fovea and thoracic striae with long, greyish setae forming a pattern (Fig. 42). Carapace and chelicerae uniformly reddish (Fig. 42). Abdomen, legs and palp light brown, covered by short, greyish setae. Femur I dorsally brown on its base. Coxae and sternum light brown, labium and endites brown. Femur I prolateral median area with a series of macrosetae (Fig. 48).

Female paratype: Total length 9.15. Carapace 4.05 long, 3.49 wide. Eye sizes and interdistances: ALE 0.26, PME 0.24, PLE 0.22, PME-PLE 0.04, PME-ALE 0.36; clypeus 0.49. Leg formula II, IV, I, III. Leg lengths (left): leg I: femur 7.45, patella 1.42, tibia 8.24, metatarsus 8.30, tarsus 1.69, total 27.10; II: 8.87, 1.48, 9.87, 10.22, 1.80, 32.24; III: 7.30, 1.48, 7.00, 8.17, 1.48, 25.43; IV: 8.10, 1.48, 8.20, 9.91, 1.73, 29.42. Palp: femur 1.36 long, 0.31 wide; patella 0.36 long, 0.41 wide; tibia 1.18 long, 0.29 wide; tarsus 1.78 long, 0.22 wide. Labium 0.66 long, 0.64 wide. Sternum 2.13 long, 1.79 wide. Femur I 1.8 times as long, tibia I 2.0 times as long, and leg I 6.7 as long as carapace. Palpal femur 4.4 times longer than wide, tibia 4.0 longer than wide, tarsus not incrassate (Fig. 50). Spermathecae are a large weakly sclerotized pouch with two large receptacles on its distal portion, a broad transverse sclerotized plate, and one dark sclerotized band reaching the basal area of each receptacle. Dorsal and ventral parts of bursa copulatrix strongly sclerotized (Figs 51–54). Cephalic region of carapace, fovea, and thoracic striae with long, greyish setae (Fig. 49). Carapace light brown, cephalic area slightly darker (Fig. 49). Chelicerae brown. Abdomen and legs light brown, covered by short, greyish setae. Palp femur and patella light brown, tibia and tarsus reddish brown (Fig. 50). Coxae and sternum light brown; labium and endites brown.

Etymology. The specific name is in honor of Dr. João Luiz Costa Cardoso, a physician who worked for several years at the Hospital Vital Brazil, Instituto Butantan, São Paulo, Brazil, treating bites and stings of venomous animals and publishing several related articles.

Remarks. See remarks under *L. carinhanha* sp. n.



Figures 49–54. *Loxosceles cardosoi* sp. n., paratype female (MZUSP 74441) **49** carapace and palp **50** left palp, prolateral **51–54** spermathecae **51** ventral, cuticle not removed **52** dorsal, with bursa copulatrix over receptacles **53** dorsal, bursa copulatrix unfolded below **54** ventral, cuticle removed. Abbreviations: ao atrio-bursal orifice, bc bursa copulatrix, r receptacle, sb sclerotized bar, tp transverse sclerotized plate. Scale bar: 1 mm.



Figures 55–57. Living specimens in their habitats. **55** *Loxosceles ericsoni* sp. n. female, Bonita Cave, Peruaçu Caves National Park, Januária, state of Minas Gerais, Brazil **56, 57** *Loxosceles cardosoi*, Gruna da Altina Cave, Serra do Ramalho karst area, Carinhanha, state of Bahia, Brazil. **56** Female **57** Male. Photographs by PP Rizzato (**55**), ME Bichuette (**56, 57**).

Discussion

According to Trajano and Carvalho (2017), troglomorphic populations are easily found more in subterranean habitats than in epigeal habitats, probably by the differences in species dynamics. Generally, troglomorphs present higher densities in subterranean habitats and low densities on the surface and they can move between them (Trajano and Carvalho 2017). The presence of individuals at all ages in subterranean habitats is one of the strongest pieces of evidence for troglomorphic populations, contemplating such distribution along the years including different annual cycles.

Autapomorphic states, known as troglomorphisms in troglobitic species, evolving because the subterranean habitats (by natural selection, neutral mutation or even pleyotropy) are relevant clues to state if a species are obligatory and exclusive cave-dwelling, however, this method is only valid when used in a comparative method.

Loxosceles karstica sp. n., *L. carinhanha* sp. n. and *L. cardosoi* sp. n., only found inside caves, do not show any troglomorphisms, at least morphological, such as elongated appendices, reduction of visual organs, sclerotization degree or pigmentation, when compared with other *Loxosceles* species, as observed in *L. troglobia*, the only troglobitic representative of *Loxosceles* in Brazil (Souza and Ferreira 2018). It is noteworthy that epigeal habitats for these species are very dry, mainly in the winter season in Brazil, which may lead not to find these species in the surface, however, individuals of this new *Loxosceles* species may be encountered in suitable habitats on epigeal surface. Presence of troglomorphisms do not define troglobitic species, but in most cases are cause of the incompatibility of troglobitic species living in epigeal habitats (Trajano and Carvalho 2017), as seen in *L. troglobia*.

The presence of three new species (*L. ericsoni* sp. n., *L. carinhanha* sp. n., and *L. cardosoi* sp. n.) with very distinct morphological characteristics in a relatively small area (Fig. 1) indicates that the regions of Peruaçu and Serra do Ramalho are important centers for *Loxosceles* distribution, which remains poorly studied.

The karst areas of Peruaçu and Serra do Ramalho have different conservation statuses. Peruaçu's caves are under legal protection as part of a National Park (Peruaçu Caves National Park-PCNP), and part of its cave fauna is included in the Brazilian RedList (at present, four species); by contrast, the Serra do Ramalho karst area has no legal protection, and the main strategy to protect its karst, caves, and cave fauna is to use the Brazilian RedList, since six of the 14 troglobites are included on this list (Gallão and Bichuette 2018). Both areas are included in the governmental program for priority areas for conservation (PAN), but until now, no action has been proposed. The main threats to both regions are deforestation in Itacarambi and Januária and deforestation together with mining projects in the Serra do Ramalho karst area (Gallão and Bichuette 2018). Although the new species of *Loxosceles* described herein are not obligatorily cave-dwelling, they are endemic to two regions with a high degree of endemism of troglobites and are part of a fragile community, representing a strong argument for protection of these regions' cave fauna.

Acknowledgements

We are grateful to Vandeir B. de Jesus ("Branco") and Reinaldo dos Santos for help with field trips in the Peruaçu region and to the Peruaçu Caves National Park administrators for their support. We are grateful to the Fundação de Amparo à Pesquisa do Estado de São Paulo (FAPESP) 2012/01093-0 and 2015/19976-3 for RB, 2010/08459-4 for MEB; to the Conselho Nacional de Desenvolvimento Científico e Tecnológico (CNPq) research fellow 307704/2017-3 for RB, research fellow 303715/2011-1 and

308557/2014-0 for MEB, and PhD scholarship 142276/2013-8 for JEG; to Coordenação de Aperfeiçoamento de Pessoal de Nível Superior (CAPES) for PhD scholarship for DMVS and master scholarship for JEG. We also thank the Instituto Chico Mendes de Conservação da Biodiversidade (ICMBio) for collection permits (20165 and 28992), Ricardo Pinto-da-Rocha (MZUSP) for providing a repository for a portion of the specimens, Ivan Magalhães and Facundo Labarque for comments and suggestions on the manuscript. MEB especially thanks Grupo Bambuí de Pesquisas Espeleológicas (GBPE) for presenting Serra do Ramalho and Peruaçu karst areas and bringing the attention to these two relevant areas.

References

- Ab'Saber AN (1977) Os domínios morfoclimáticos na América do Sul: primeira aproximação. Geomorfologia. Instituto de Geografia da Universidade de São Paulo: São Paulo 52: 1–22.
- Auler A, Rubbioli E, Brandi R (2001) As grandes cavernas do Brasil. Grupo Bambuí de Pesquisas Espeleológicas, Belo Horizonte, 228 pp.
- Bertani R, Fukushima CS, Nagahama RH (2010) *Loxosceles chapadensis* (Araneae: Sicariidae): a new recluse spider species of the *gaucho* group from Brazil. The Journal of Arachnology 38: 364–367. <https://doi.org/10.1636/A09-92.1>
- Binford GJ, Callahan MS, Bodner MR, Rynerson MR, Nuñez PB, Ellison C, Duncan R (2008) Phylogenetic relationships of *Loxosceles* and *Sicarius* spiders are consistent with western Gondwanan vicariance. Molecular Phylogeny and Evolution 49: 538–553. <https://doi.org/10.1016/j.ympev.2008.08.003>
- Brescovit AD, Taucare-Ríos A, Magalhães ILF, Santos AJ (2017) On Chilean *Loxosceles* (Araneae: Sicariidae): first description of the males of *L. surca* and *L. coquimbo*, new records of *L. laeta* and three remarkable new species from coastal deserts. European Journal of Taxonomy 388: 1–20. <https://doi.org/10.5852/ejt.2017.388>
- Cala-Riquelme F, Gutiérrez-Estrada MA, Daza EF (2015) The genus *Loxosceles* Heineken & Lowe 1832 (Araneae: Sicariidae) in Colombia, with description of new cave-dwelling species. Zootaxa 4012(2): 396–400. <https://doi.org/10.11646/zootaxa.4012.2.12>
- Chomphuphuang N, Deowanish S, Songsangchote C, Sivayyapram V, Thongprem P, Warrit N (2016) The Mediterranean recluse spider *Loxosceles rufescens* (Dufour, 1820) (Araneae: Sicariidae) established in a natural cave in Thailand. Journal of Arachnology 44(2): 142–147. <https://doi.org/10.1636/R15-61>
- Cordeiro LM, Borghezán R, Trajano E (2014) Subterranean biodiversity in the Serra da Bodoquena karst area, paraguay river basin, Mato Grosso do Sul, Southwestern Brazil. Biota Neotropica 14(3): 1–28. <https://doi.org/10.1590/1676-06032014011414>
- Duncan RP, Rynerson MR, Ribera C, Binford GJ (2010) Diversity of *Loxosceles* spiders in northwestern Africa and molecular support for cryptic species in the *Loxosceles rufescens* lineage. Molecular Phylogenetics and Evolution 55: 234–248. <https://doi.org/10.1016/j.ympev.2009.11.026>

- Fukushima CS, de Andrade RMG, Bertani R (2017) Two new Brazilian species of *Loxosceles* Heineken & Lowe, 1832 with remarks on *amazonica* and *rufescens* groups (Araneae, Sicariidae). *ZooKeys* 667: 67–94. <https://doi.org/10.3897/zookeys.667.11369>
- Gallão JE, Bichuette ME (2015) Taxonomic distinctness and conservation of a new high biodiversity subterranean area in Brazil. *Anais da Academia Brasileira de Ciências* 87(1): 209–217. <https://doi.org/10.1590/0001-3765201520140312>
- Gallão JE, Bichuette ME (2018) Brazilian obligatory subterranean fauna and threats to the hypogean environment. *ZooKeys* 746: 1–23. <https://doi.org/10.3897/zookeys.746.15140>
- Gertsch WJ (1958) The spider genus *Loxosceles* in North America, Central America, and the West Indies. *American Museum Novitates* 1907: 1–46. <http://digitallibrary.amnh.org/handle/2246/4535>
- Gertsch WJ (1967) The spider genus *Loxosceles* in South America (Araneae, Scytodidae). *Bulletin of the American Museum of Natural History* 136: 117–174. <http://digitallibrary.amnh.org/handle/2246/1989>
- Gertsch WJ (1973) A report on cave spiders from Mexico and Central America. *Bulletin of the Association for Mexican Cave Studies* 5: 141–163.
- Gertsch WJ, Ennik F (1983) The spider genus *Loxosceles* in North America, Central America, and the West Indies (Araneae, Loxoscelidae). *Bulletin of the American Museum of Natural History* 175: 264–360. <http://digitallibrary.amnh.org/handle/2246/981>
- Gertsch WJ, Mulaik S (1940) The Spiders of Texas, I. *Bulletin of the American Museum of Natural History* 77: 307–340. <http://digitallibrary.amnh.org/handle/2246/875>
- Gonçalves-de-Andrade RM, Bertani R, Nagahama RH, Barbosa MFR (2012) *Loxosceles niedeguidonae* (Araneae, Sicariidae) a new species of brown spider from Brazilian semi-arid region. *ZooKeys* 175: 27–36. <https://doi.org/10.3897/zookeys.175.2259>
- González-Sponga MA (2010) Biodiversidad. Arácnidos de Venezuela. Descripción de seis especies nuevas del género *Loxosceles* Heineken & Lowe, 1832 (Araneae: Scytodidae: Loxoscelinae). *Boletín, Academia de Ciencias Físicas, Matemáticas y Naturales de Venezuela* 68(2): 31–49.
- INMET (2017) Instituto Nacional de Meteorologia. <http://www.inmet.gov.br/portal/> [accessed April 2017]
- Isbister GK, Fan HW (2011) Spider bite. *Lancet* 378: 2039–47. [https://doi.org/10.1016/S0140-6736\(10\)62230-1](https://doi.org/10.1016/S0140-6736(10)62230-1)
- Lotz LN (2017) An update on the spider genus *Loxosceles* (Araneae: Sicariidae) in the Afrotropical region, with description of seven new species. *Zootaxa* 4341(4): 475–494. <https://doi.org/10.11646/Zootaxa.4341.4.2>
- Magalhães ILF, Brescovit AD, Santos AJ (2017) Phylogeny of Sicariidae spiders (Araneae: Haplogynae), with a monograph on Neotropical *Sicarius*. *Zoological Journal of the Linnean Society* 179(4): 767–864. <https://doi.org/10.1111/zoj.12442>
- Martins R, Knysak I, Bertani R (2002) A new species of *Loxosceles* (Araneae: Sicariidae) of the *laeta* group from Brazil (Araneae: Sicariidae). *Zootaxa* 94: 1–6. <https://doi.org/10.11646/zootaxa.94.1.1>

- Peel MC, Finlayson BL, McMahon TA (2007) Updated world map of the Köppen-Geiger climate classification. *Hydrology and Earth System Sciences Discussions* 42: 439–473. <https://doi.org/10.5194/hessd-4-439-2007>
- Piló LB, Köhler HC (1991) Do Vale do Peruaçu ao São Francisco: uma viagem ao interior da terra. In: *Anais do III Congresso da Associação Brasileira do Estudo do Quaternário*, Belo Horizonte.
- Pinto-da-Rocha R (1995) Sinopse da fauna cavernícola do Brasil (1907–1994). *Papéis Avulsos de Zoologia* 39(6): 61–173.
- Planas E, Ribera C (2015) Description of six new species of *Loxosceles* (Araneae: Sicariidae) endemic to the Canary Islands and the utility of DNA barcoding for their fast and accurate identification. *Zoological Journal of the Linnean Society* 174: 47–73. <https://doi.org/10.1111/zoj.12226>
- Ribera C, Planas E (2009) A new species of *Loxosceles* (Araneae, Sicariidae) from Tunisia. *ZooKeys* 16: 217–225. <https://doi.org/10.3897/zookeys.16.232>
- Sánchez-Ruiz A, Brescovit, AD (2013) The genus *Loxosceles* Heineken & Lowe (Araneae: Sicariidae) in Cuba and Hispaniola, West Indies. *Zootaxa* 3731(2): 212–222. <https://doi.org/10.11646/zootaxa.3731.2.2>
- Souza MFVR, Ferreira RL (2018) A new highly troglomorphic *Loxosceles* (Araneae: Sicariidae) from Brazil. *Zootaxa* 4438(3): 575–587. <https://doi.org/10.11646/zootaxa.4438.3.9>
- Tahami MS, Zamani A, Sadeghi S, Ribera C (2017) A new species of *Loxosceles* Heineken & Lowe, 1832 (Araneae: Sicariidae) from Iranian caves. *Zootaxa* 4318(2): 377–387. <https://doi.org/10.11646/zootaxa.4318.2.10>
- Trajano E (1987) Fauna cavernícola brasileira: composição e caracterização preliminar. *Revista Brasileira de Zoologia* 3(8): 533–561. <https://doi.org/10.1590/S0101-81751986000400004>
- Trajano E (2012) Ecological classification of subterranean organisms. In: White WB, Culver DC (Eds) *Encyclopedia of Caves*. Elsevier Academic Press, Amsterdam, 275–277. <https://doi.org/10.1016/B978-0-12-383832-2.00035-9>
- Trajano E, Gallão JE, Bichuette ME (2016) Spots of high diversity of troglobites in Brazil: the challenge of measuring subterranean diversity. *Biodiversity and Conservation* 25(10): 1805–1828. <https://doi.org/10.1007/s10531-016-1151-5>
- Trajano E, Carvalho MR (2017) Towards a biologically meaningful classification of subterranean organisms: a critical analysis of the Schiner-Racovitza system from a historical perspective, difficulties of its application and implications for conservation. *Subterranean Biology* 22: 1–26. <https://doi.org/10.3897/subtbiol.22.9759>
- Wang JF (1994) Two new species of spiders of the genus *Loxosceles* from China. *Journal of Hebei Normal University (nat. Sci. Ed., Suppl.)*: 13–15.
- World Spider Catalog (2018) World Spider Catalog. Version 19.0. Natural History Museum Bern, online at <https://wsc.nmbe.ch/>, accessed on [accessed May 2018]

***Parasogata* gen. n., a new genus of the tribe Delphacini with descriptions of two new species from China (Hemiptera, Fulgoromorpha, Delphacidae)**

Zheng-Xiang Zhou^{1,2}, Lin Yang¹, Xiang-Sheng Chen^{1,3,4}

1 Institute of Entomology, Guizhou University, Guiyang, Guizhou, 550025, P.R. China **2** College of Agriculture, Anshun University, Anshun, 561000, P.R. China **3** Guizhou Key Laboratory for Plant Pest Management of Mountainous Region, Guizhou University, Guiyang, Guizhou, 550025, P.R. China **4** Special Key Laboratory for Development and Utilization of Insect Resources of Guizhou, Guizhou University, Guiyang, Guizhou, 550025, P.R. China

Corresponding author: *Xiang-Sheng Chen* (chenxs3218@163.com)

Academic editor: *Mike Wilson* | Received 6 May 2018 | Accepted 10 November 2018 | Published 13 December 2018

<http://zoobank.org/17F67E8D-764D-4802-9E8E-4E256742C773>

Citation: Zhou Z-X, Yang L, Chen X-S (2018) *Parasogata* gen. n., a new genus of the tribe Delphacini with descriptions of two new species from China (Hemiptera, Fulgoromorpha, Delphacidae). ZooKeys 806: 73–85. <https://doi.org/10.3897/zookeys.806.26394>

Abstract

A new planthopper genus *Parasogata* **gen. n.** (Delphacidae: Delphacinae: Delphacini) was described and illustrated with two new species *P. binaria* **sp. n.** and *P. furca* **sp. n.** from south China. A key to species of the new genus is also given.

Keywords

Delphacid, distribution, Fulgoroidea, new taxa, planthopper

Introduction

The planthopper tribe Delphacini Leach, 1815 is the largest clade of Delphacidae, occurring in all ecoregions (excluding Antarctica) and including approximately 1652 species in 319 genera (Bourgoin 2018). In China, 259 species in 135 genera are known (Ding 2006; Dong and Qin 2012; Hou et al. 2013, 2014a, b; Qin 2005, 2006, 2007; Qin et al. 2006, 2008, 2009a, b, 2010, 2011, 2012, 2014; Ren et al. 2015).

Here, a new genus, *Parasogata* gen. n., with two new species, *P. binaria* sp. n. and *P. furca* sp. n., are described and illustrated from China. The new genus is assigned to the Delphacini because the spinal formula of the hind leg 5–7–4, tibial spur large, thin, flattened and bearing a row of fine, black-tipped teeth on the posterior margin; genital diaphragm developed, suspensorium present. The similarities and affinities of the new genus with similar genera are compared and discussed. A key to the species of the new genus is also provided.

Materials and methods

Terminology of morphological and measurements follow Yang and Yang (1986) and the morphological terminology of female genitalia follows Bourgoin (1993). Measurements of body length equal the distance between the apex of vertex and tip of tegmen. All measurements are in millimeters (mm). Dry specimens were used for the description and illustration. Color pictures for adult habitus were obtained by KEYENCE VHX-1000. External morphology was observed under a stereoscopic microscope Leica Mz 12.5 and characters were measured with an ocular micrometer. The genital segments of the examined specimens were macerated in 10% KOH and drawn from preparations in glycerin jelly using Olympus CX41 and Leica MZ 12.5 stereomicroscope. Illustrations were scanned with Canon CanoScan LiDE 200 and imported into Adobe Photoshop 6.0 for labeling and plate composition.

The type specimens of the new species are deposited in the Institute of Entomology, Guizhou University, Guiyang, Guizhou Province, China (**GUGC**).

Taxonomy

Genus *Parasogata* gen. n.

<http://zoobank.org/C168D41B-DB7F-4841-BCCC-EF3299BD2EC6>

Figs 9–60

Type species. *Parasogata binaria* sp. n.

Diagnosis. This genus is readily recognized by its large size and vertex, pronotum and mesonotum bearing an uninterrupted white fascia. The genus is most similar to *Sogata* Distant, 1906 but separately by the phallus being up-curved (down-curved in *Sogata* (Ding 2006: figs 281–283)), with a row processes at subapically (without process in *Sogata*).

Description. General color of male yellowish white to brown (Figs 9–12, 35–38). Vertex, pronotum and mesonotum with an uninterrupted white fascia (Figs 9, 35). Vertex, frons, face, antennae yellowish brown to yellowish white (Figs 9–12, 35–38). Pronotum and mesonotum yellowish white (Figs 13, 39). Forewings and hindwings hyaline (Figs 9–12, 35–38). Legs yellowish white (Figs 10, 36). Abdomen yellow (Figs 10, 36). Head including eyes narrower than pronotum (Figs 13, 15, 39, 41). Vertex

subquadrate, anterior margin arched, lateral carinae with slightly concave, submedian carinae uniting at apex. Frons with single median carina, longer in middle line than wide at widest part, widest at apex (Figs 14, 16, 40, 42). Y-shaped carina feeble (Figs 13, 15, 39, 41). Antennae cylindrical, with basal segment shorter than second, reaching frontoclypeal suture (Figs 14, 16, 40, 42). Pronotum with lateral carinae almost attaining hind margin (Figs 13, 15, 39, 41). Posttibial spur with 29–32 distinct teeth along hind margin.

Male genitalia. Anal segment collar-shaped, lateroapical angles produced into processes (Figs 24–25, 50–51). Pygofer in profile wider ventrally than dorsally, laterodorsal angles not produced, in posterior view with opening wider than long, lateral margins well defined, lateral quadrate areas strongly sclerotized, medioventral process absent (Figs 21–23, 47–49). Diaphragm broad (Figs 23, 49). Aedeagus long, tubular, with a row processes at subapically, slightly upward apically (Figs 26, 52). Genital styles simple, widely divergent apically (Figs 27–28, 53–54). Suspensorium large (Figs 29, 55).

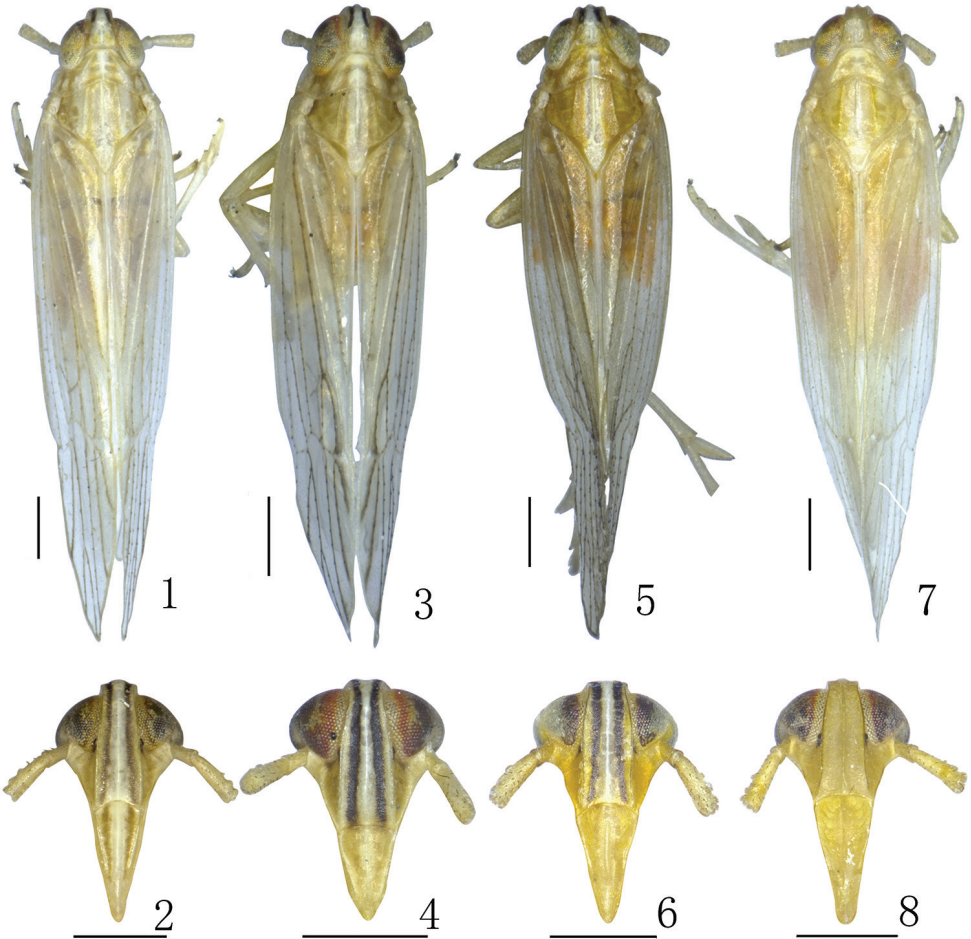
Etymology. This generic name “*Parasogata*” refers to its strong similarity to *Sogata*. The name is to be treated as feminine.

Distribution. China.

Remarks. The genus *Parasogata* gen. n. resembles *Sogata* Distant, 1906, *Neometopina* Yang, 1989, *Neunkanodes* Yang, 1989 and *Lisogata* Ding, 2006 in vertex, pronotum and mesonotum with an uninterrupted white fascia, frons with median carina single (Figs 1–8), but differs from these genera by anal segment with two pairs of processes, or with a pair of forked processes (without process in *Lisogata*); aedeagus not forked at half of apex (with forked at half of apex in *Neometopina* and *Neunkanodes*); aedeagus with processes and decurved dorsad apically (without process and decurved ventrad apically in *Sogata*) (Table 1).

Table 1. Differences among *Parasogata* and similar genera.

	<i>Parasogata</i> gen. n.	<i>Neometopina</i>	<i>Sogata</i>	<i>Neunkanodes</i>	<i>Lisogata</i>
Size (mm)	4.72–5.20	4.62–4.82	4.20–4.70	4.40–4.90	4.40–4.70
Frons color	Black with median carina yellowish white	Brown with median carina yellowish white	Black with median carina yellowish white	Brown with median carina yellowish white	Yellow
Y-shaped carina	Feeble	Distinct	Feeble	Feeble	Feeble
Lateral carinae of pronotum	Almost attaining hind margin	Almost attaining hind margin	Almost attaining hind margin	Conspicuous not attaining hind margin	Almost attaining hind margin
Number of teeth of hind tibial spur	29–32	20–23	18–23	23–24	30–38
Hind margin of male pygofer	Not produced	Not produced	Not produced	Produced caudad, lobe-like	Not produced
Processes of male anal segment	Two pairs or one pair with bifurcation	One pair	One pair	One pair	None
Apex of aedeagus	Unforked	Forked	Unforked	Forked	Unforked
Inner basal angle of genital styles	None	None	None	Protruding	None



Figures 1–8. Dorsal and frontal view **1, 2** *Neometopina penghuensis* Yang, 1989 **3, 4** *Sogata dohertyi* Distant, 1906 **5, 6** *Neunkanodes formosana* Yang, 1989 **7, 8** *Lisogata zhejiangensis* Ding, 2006. Scale bar: 0.5 mm.

Revised couplets to the key to Chinese Delphacini by Ding (2006)

- 70 Pygofer in profile with posterior margin produced caudad in a lobe (Ding 2006: fig. 314)..... *Neunkanodes* Yang
- Pygofer in profile not produced **71a**
- 71a Aedeagus without processes, apically decurved ventrally (Ding 2006: figs 281–283)..... *Sogata* Distant, 1906
- Aedeagus with distinct processes, apically recurved dorsally (Figs 26, 52).....
..... *Parasogata* gen. n.

Key to species of genus *Parasogata* gen. n. (male)

- 1 Pronotum brown except median carina yellowish white (Figs 13, 17); anal segment with two pairs of processes, each with apex not forked (Figs 24–25) *P. binaria* sp. n.
- Pronotum yellow except median carina yellowish white (Figs 39, 43); anal segment with a pair of processes, each with apex forked (Figs 50–51) *P. furca* sp. n.

***Parasogata binaria* sp. n.**

<http://zoobank.org/ACC2E082-45A0-4653-9B55-52B8E0182662>

Figs 9–34

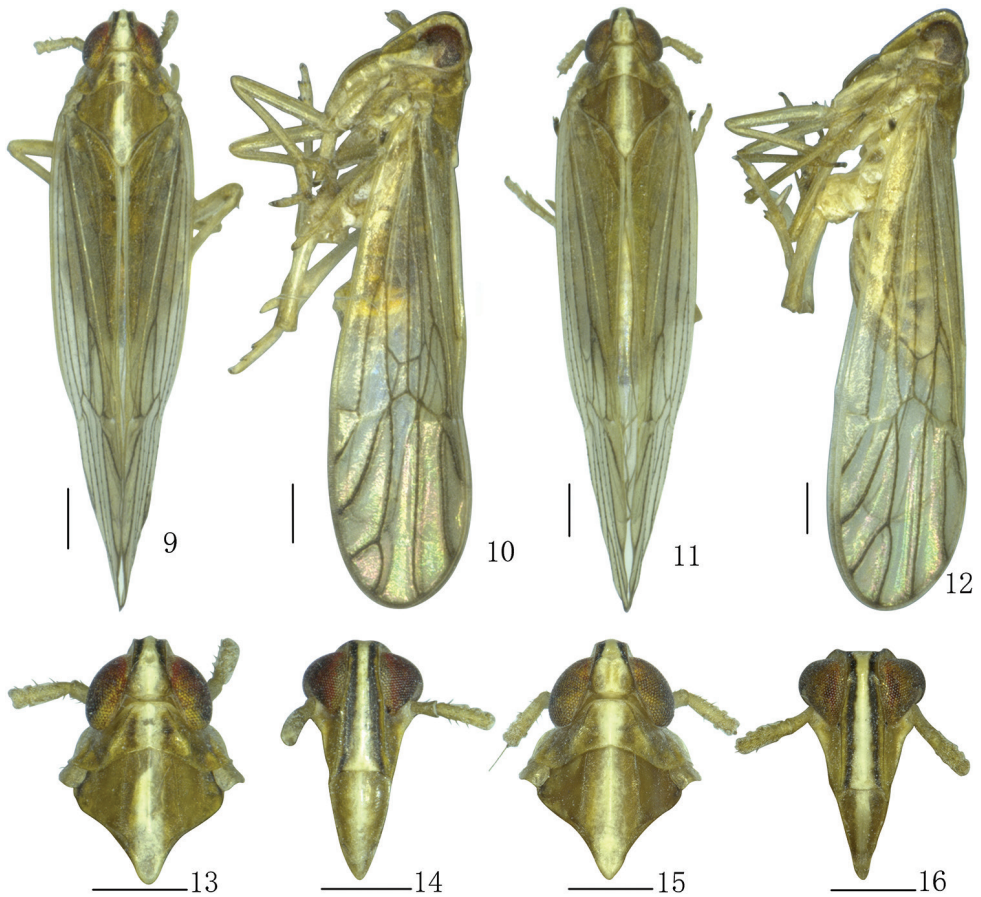
Type material. Holotype: ♂, CHINA, Yunnan: Daweishan National Natural Reserve (22°81'N, 103°79'E), 18 Aug. 2017, Y.-J. Sui. Paratypes: 1♂1♀, same data as holotype; 1♂2♀♀, same data as holotype except, 22 Aug. 2017, Q. Luo; 6♂♂5♀♀, same data as holotype except, 19 Aug. 2017, N. Gong.

Measurements. Body length (from apex of vertex to apex of forewing): male 5.10–5.20 mm (n = 9); female 5.90–6.00 mm (n = 8); forewing length: male 4.30–4.42 mm (n = 9); female 5.10–5.12 mm (n = 8).

Diagnosis. Big-sized species with general color yellowish white to yellowish brown, anal segment with two pairs of spinose processes; aedeagus with ten processes subapically and with irregular teeth on ventral side of apex, constriction and bluntly rounded at apex (Fig. 26).

Description. *Coloration.* General color yellowish white to yellowish brown. Head yellowish brown (Figs 13–16). Vertex yellowish white, except along lateral margin dark brown (Figs 13–16). Frons black, except median carinae yellowish white and lateral margins yellowish brown (Fig. 14). Clypeus and genae yellowish brown (Fig. 14). Rostrum yellowish brown, with apex brown. Eyes generally yellow to brown (Figs. 9–16), ocelli dark brown (Figs 10, 12, 14, 16). Antennae yellow (Figs 13–16). Pronotum and mesonotum yellowish brown, except media carinae yellowish white (Figs 13, 15). Forewings with veins dark brown (Figs 9–12). Hindwings pale white, with veins brown. Legs yellowish white to pale yellow, tibiae pale yellow basally, tarsomeres yellowish white (Figs 10, 12). Abdomen brown, except lateral margins yellow (Figs 9–12).

Structure. Head including eyes narrower than pronotum, ratio 0.77:1 (Figs 13, 15). Vertex with anterior margin arched, lateral carinae slightly concave, submedian carinae uniting at apex, longer than wide at base, ratio 1.28:1, narrower at apex than at base, ratio 0.64:1 (Figs 13, 17). Frons longer in middle line than wide at widest part, ratio 2.28:1 (Figs 14, 18), lateral carinae nearly straight (Figs 14, 18). Postclypeus wider at base than frons at apex, slightly longer than wide at base (Figs 14, 18). An-

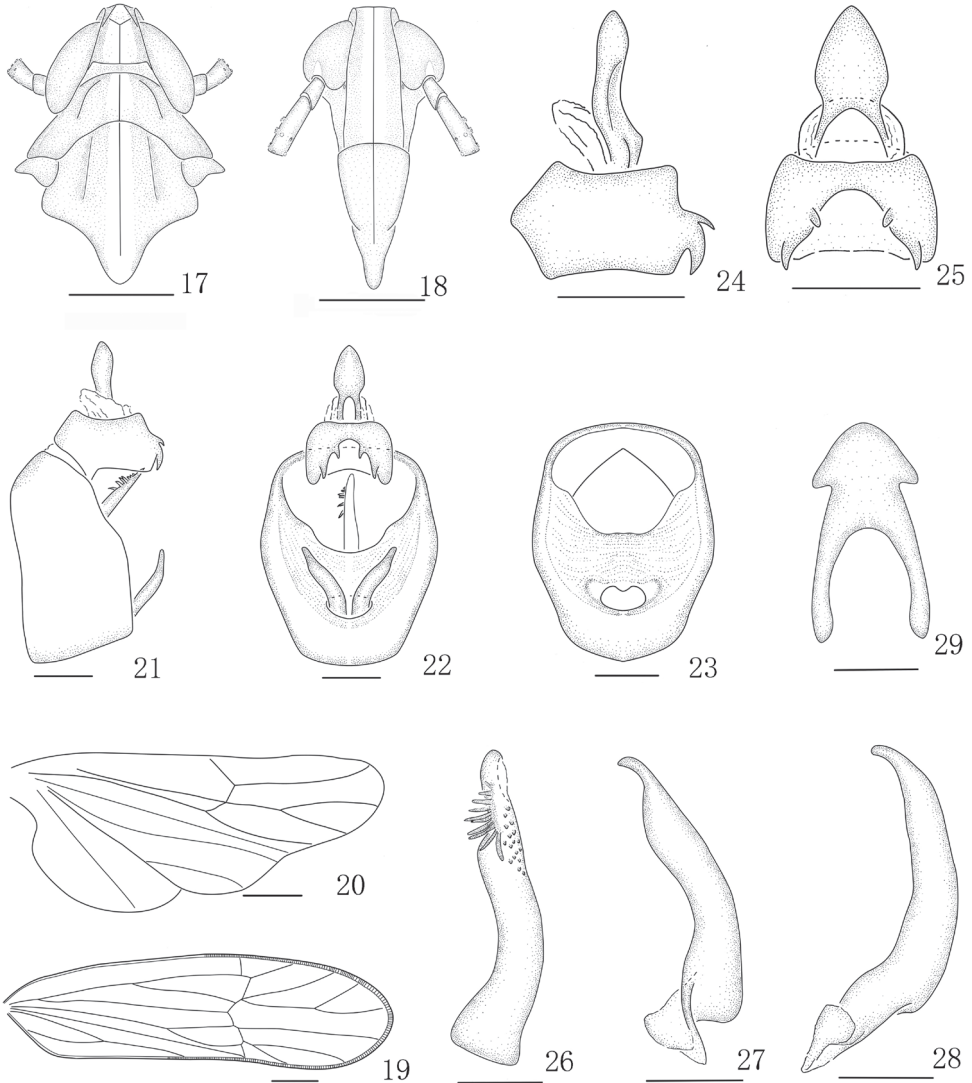


Figures 9–16. *Parasogata binaria* sp. n. **9, 10** Male habitus (dorsal and lateral views) **11, 12** Female habitus (dorsal and lateral views) **13** Male head and thorax, dorsal view **14** Male front **15** Female head and thorax, dorsal view **16** Female front. Scale bar: 0.5 mm.

tennae cylindrical, basal segment longer than wide, ratio 1.55:1, shorter than second, ratio 0.42:1 (Figs 14, 18). Pronotum shorter than vertex, ratio 0.75:1 (Figs 13, 17). Mesonotum longer than pronotum and vertex combined, ratio 1.25:1 (Figs 13, 17). Posttibial spur with approximately 30–32 distinct teeth along hind margin. Forewings longer than widest part, ratio 3.48:1, widest at apical 1/4 (Figs 10, 12, 19).

Male genitalia. Anal segment with two pairs of spinose processes, upper pair smaller (Figs 24–25). Pygofer quadrate in posterior view (Figs 21–23). Diaphragm broad, transparent (Fig. 23). Aedeagus with ten processes subapically and with irregularity teeth at ventral of apex, constriction and blunt rounded at apex (Fig. 26). Genital styles with inner margin arched and outer margin concave in caudal view, distinctly constricted at apex (Figs 27–28). Suspensorium large and arrow-shaped (Fig. 29).

Female genitalia. Gonocoxa VIII at base of inner margin arched (Fig. 31). Gonapophyses VIII with apex sharp, with ventral margin membranous at half of apex, dorsal



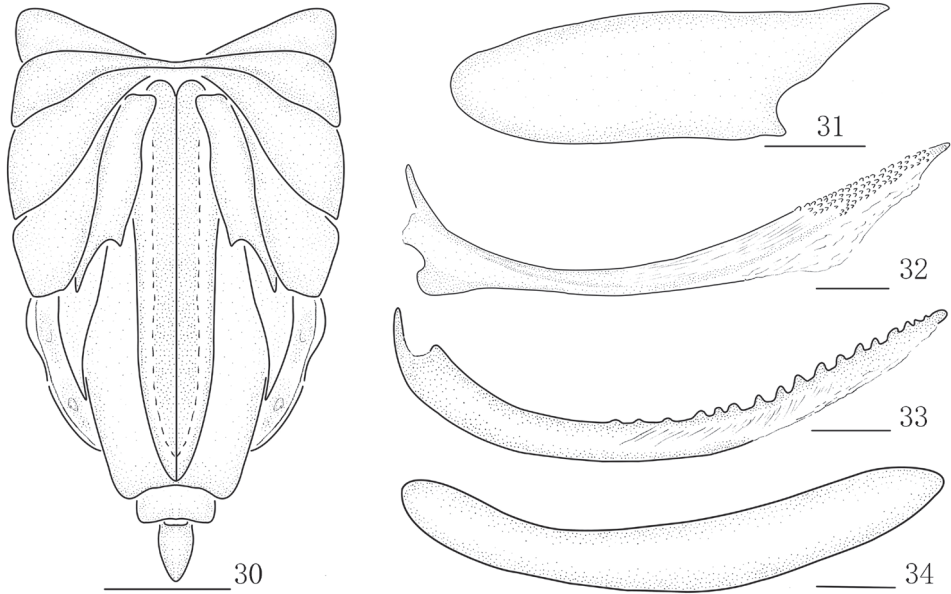
Figures 17–29. *Parasogata binaria* sp. n. male **17** Head and thorax, dorsal view **18** Front **19** Forewing **20** Hindwing **21** Genitalia, lateral view **22** Genitalia, caudal view **23** Diaphragm, caudal view **24** Anal segment, left view **25** Anal segment, caudal view **26** Aedeagus, left view **27** Genital style, caudal view **28** Genital style, left view **29** Suspensorium. Scale bars: 0.5 mm (**17–23**); 0.2 mm (**24–25**); 0.1 mm (**26–29**).

aspect with several small teeth apically (Fig. 32). Gonapophyses IX long, sclerotized, curved basally, narrowing towards apex, with approximately 17 teeth, abruptly reduced and indistinct at apex (Fig. 33). Gonoplasts twisted, long and stripe-shaped (Fig. 34).

Report hosts. None.

Distribution. China (Yunnan).

Etymology. The specific epithet is from the Latin word *binaria* (bipartite), referring to the anal segment with two pairs of processes.



Figures 30–34. *Parasogata binaria* sp. n., female **30** Abdomen, ventral view **31** Gonocoxa VIII **32** Gonapophysis VIII **33** Gonapophysis IX **34** Gonoplac. Scale bars: 0.5 mm (**30**); 0.2 mm (**31–34**).

Remarks. The species is similar to *Sogata dohertyi* (Distent, 1906), but can be distinguished by anal segment with processes cross (not cross in *Sogata dohertyi*), aedeagus with a row processes (without process in *Sogata dohertyi*).

***Parasogata furca* sp. n.**

<http://zoobank.org/85CEB0C9-63CD-42F2-B312-9AD19FAD4F40>

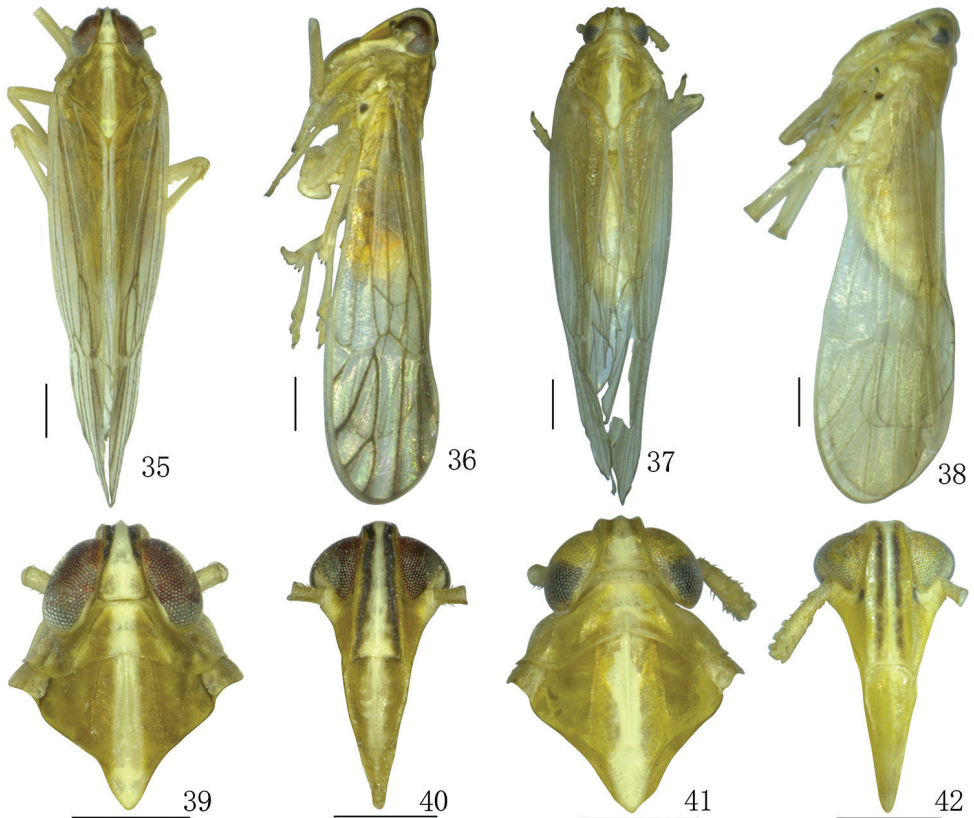
Figs 35–60

Type material. Holotype: ♂, **CHINA, Guizhou:** Wangmo County, Zhexiang (24°97'N, 106°15'E), 7 Jul. 2016, H.-X. Li and L.-J. Yang. Paratypes: 3♂♂, same data as holotype: 2♂♂1♀, **Yunnan:** Yuanjiang County, Donggezhen (23°69'N, 101°82'E), 26 Aug. 2014, Z.-X. Zhou.

Measurements. Body length (from apex of vertex to apex of forewing): male 4.72–4.84 mm (n = 6), female 5.10–5.22 mm (n = 1); forewing length: male 3.61–3.93 mm (n = 6); female 4.42–4.51 mm (n = 1).

Diagnosis. Big-sized species with General color yellow, anal segment with a pair of spinose processes, forked apically (Figs 50–51); aedeagus with eight processes and with many irregularity ventral teeth at subapically (Fig. 52).

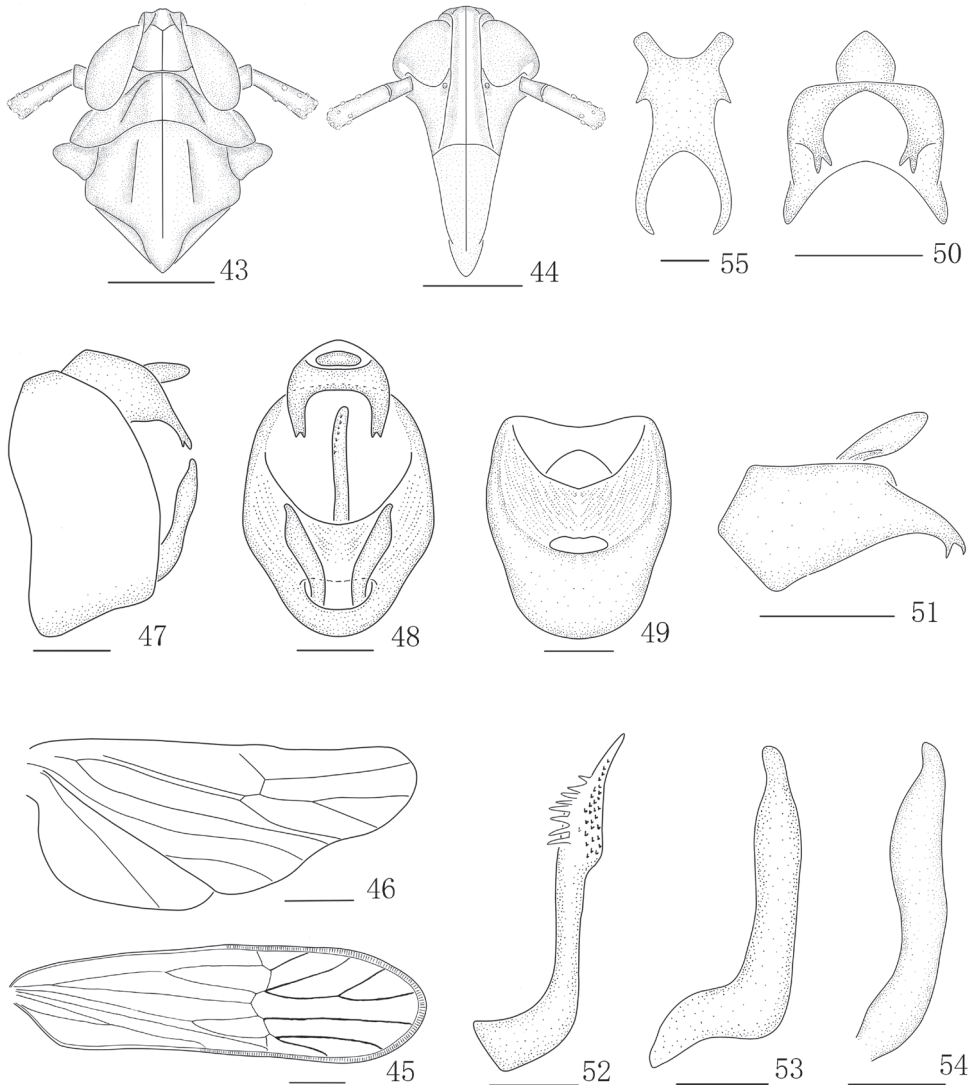
Description. *Coloration.* Head yellow. Vertex yellowish white to black (Figs 39, 41). Frons black except middle carinae yellowish white and lateral margin yellowish brown (Figs 40, 42). Clypeus and genae yellow (Figs 40, 42). Rostrum yellowish brown,



Figures 35–42. *Parasogata furca* sp. n. **35, 36** Male habitus (dorsal and lateral views) **37, 38** Female habitus (dorsal and lateral views) **39** Male head and thorax, dorsal view **40** Male front **41** Female head and thorax, dorsal view **42** Female front. Scale bar: 0.5 mm.

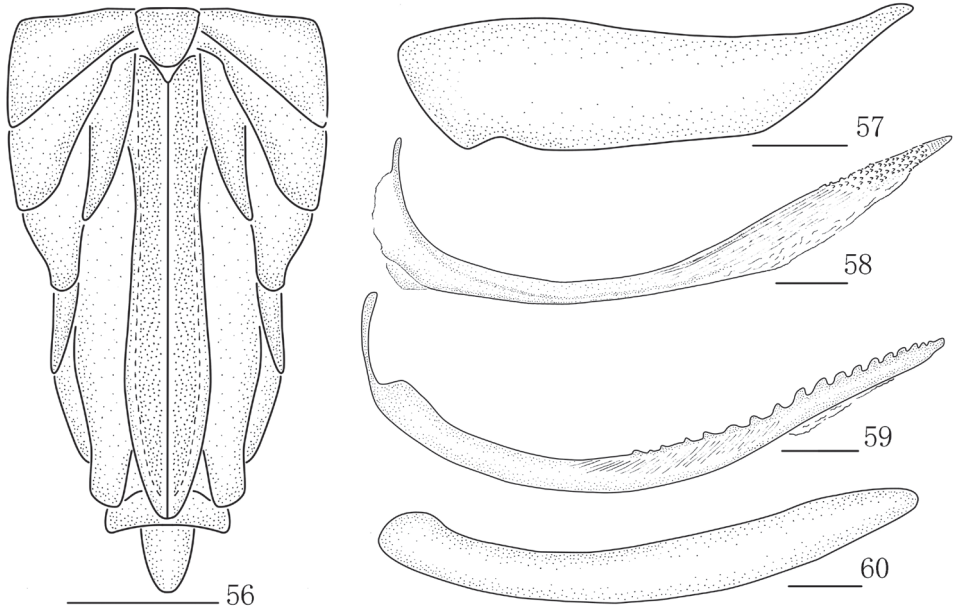
with apex brown. Eyes generally yellow to brown (Figs 35–42), ocelli yellowish brown (Figs 36, 38, 40, 42). Antennae yellow (Figs 35–42). Pronotum and mesonotum with carinae yellowish brown (Figs 39, 41). Forewings with veins dark brown (Figs 35–38). Hindwings pale white, veins brown. Legs yellowish white to pale yellowish; tibiae yellow basally, tarsomeres yellowish white (Figs 36, 38). Abdomen yellow (Figs 35–38).

Structure. Head including eyes narrower than pronotum, ratio 0.79:1 (Figs 39, 43). Vertex with anterior margin transverse, lateral carinae with slightly concave, longer than wide at base, ratio 1.22:1, narrower at apex than at base, ratio 0.55:1 (Figs 39, 43). Frons longer in middle line than wide at widest part, ratio 1.83:1, lateral carinae straight (Figs 40, 44). Postclypeus wider at base than frons at apex, slightly longer than wide at base (Figs 41, 46). Antennae cylindrical, basal segment longer than wide, ratio 1.55:1, shorter than second, ratio 0.38:1 (Figs 39–44). Pronotum shorter than vertex, ratio 0.67:1 (Figs 36, 38, 40, 42, 44). Mesonotum longer pronotum and vertex combined, ratio 1.21:1 (Figs 39, 43). Forewings longer than widest part, ratio 3.85:1, widest at apical 1/4 (Figs 35–38, 45). Posttibial spur with approximately 29–32 distinct teeth along hind margin.



Figures 43–55. *Parasogata furca* sp. n., male **43** Head and thorax, dorsal view **44** Front **45** Forewing **46** Hindwing **47** Genitalia, lateral view **48** Genitalia, caudal view **49** Diaphragm, caudal view **50** Anal segment, caudal view **51** Anal segment, left view **52** Aedeagus, left view **53** Genital style, left view **54** Genital style, caudal view **55** Suspensorium. Scale bars: 0.5 mm (**43–49**); 0.2 mm (**50, 51**); 0.1 mm (**52–55**).

Male genitalia. Anal segment with a pair of spinose processes, forked apically (Figs 50–51). Pygofer quadrate in caudal view (Figs 47–49). Diaphragm broad, transparent, dorsal margin arched (Fig. 49). Aedeagus with eight processes and with many irregularity ventral teeth at subapically (Fig. 52). Genital styles with lateral margins arched in caudal view, with two lateral margins almost parallel in profile (Figs 53–54). Suspensorium large and X-shaped, with a process at each lateral margin (Fig. 55).



Figures 56–60. *Parasogata furca* sp. n., female **56** Abdomen, ventral view **57** Gonocoxa VIII **58** Gonapophysis VIII **59** Gonapophysis IX **60** Gonoplac. Scale bars: 0.5 mm (**56**); 0.2 mm (**57–60**).

Female genitalia. Gonocoxa VIII with base of inner margin slightly concave (Fig. 57). Gonapophyses VIII with apex sharp, ventral margin membranous at half of apical, in dorsal margins with several small teeth at half of apical (Fig. 58). Gonapophyses IX long, sclerotized, curved basally and narrowing towards apex, serrated caudad in distal, with approximately 18 teeth, abruptly reduced and indistinct at apex (Fig. 59). Gonoplacs twisted (Fig. 60).

Report hosts. None.

Distribution. China (Guizhou, Yunnan).

Etymology. The specific epithet is from the Latin word *furca* (forked), indicating the anal segment produced lateroapical angles forked.

Remarks. This species is similar to *Parasogata binaria* sp. n., but can be distinguished by the anal segment with a single pair of processes (two pairs of processes in *Parasogata binaria* sp. n.), suspensorium with dorsal margin hunch-up (with dorsal margin concave in *Parasogata binaria* sp. n.).

Acknowledgments

We wish to express our sincere thanks to Prof. M.D. Webb (The Natural History Museum, London, UK) and J.F. Campodonico (University of Chile, Chile) for helpful suggestions on the revision of the early draft of the manuscript. We are grateful to

all collectors of specimens. This work was supported by the National Natural Science Foundation of China (No. 31472033), the program of Science and Technology Innovation Talents Team, Guizhou Province (No.20144001) and the Program of Excellent Innovation Talents, Guizhou Province (No. 20154021).

References

- Bourgoin T (1993) Female genitalia in Hemiptera Fulgoromorpha, morphological and phylogenetic data. *Annales de la Société Entomologique de France (Nouvelle Série)* 29: 225–244.
- Bourgoin T (2018) FLOW (Fulgoromorpha Lists On The Web): a world knowledge base dedicated to Fulgoromorpha. Version 8, updated 20 November 2018. <http://hemiptera-databases.org/flow/> [accessed 25 November 2018]
- Ding JH (2006) *Fauna Sinica. Insecta Vol. 45. Homoptera Delphacidae*. Editorial Committee of Fauna Sinica, Chinese Academy of Science. Science Press, Beijing, 776 pp.
- Dong AP, Qin DZ (2012) A new species in the Oriental delphacid genus *Miranus* Chen & Ding (Hemiptera: Fulgoroidea) from China. *Entomotaxonomia* 34(1): 45–49.
- Hou XH, Yang L, Chen XS (2013) Revision of the genus *Neometopina* (Hemiptera, Fulgoromorpha, Delphacidae) from China. *ZooKeys* 307: 97–104. <https://doi.org/10.3897/zookeys.307.4660>
- Hou XH, Chen XS (2014a) Revision of the planthopper genus *Nycheuma* Fennah (Hemiptera, Fulgoromorpha, Delphacidae). *ZooKeys* 462: 47–57. <https://doi.org/10.3897/zookeys.462.6657>
- Hou XH, Yang L, Chen XS (2014b) Revision of the Oriental genus *Neunkanodes* Yang (Hemiptera, Fulgoromorpha, Delphacidae) with descriptions of two new species. *Zootaxa* 3795(2): 174–180. <https://doi.org/10.11646/zootaxa.3795.2.6>
- Qin DZ (2005) A new genus and a new species of Delphacini (Hemiptera, Fulgoroidea, Delphacidae) from China. *Acta Zootaxonomica Sinica* 30(4): 791–793.
- Qin DZ (2006) Synopsis of two genera of Delphacidae, with descriptions of three new species (Hemiptera, Fulgoroidea). *Acta Zootaxonomica Sinica* 31(2): 392–397.
- Qin DZ, Zhang YL (2006) A new genus and a new species of Delphacini (Hemiptera, Fulgoroidea, Delphacidae) from China. *Zootaxa* 1204: 61–68.
- Qin DZ (2007) Two new species of the Chinese endemic delphacid genus *Neuterthron* Ding (Hemiptera: Fulgoromorpha) from Yunnan and Shaanxi Provinces. *Zootaxa* 1547: 59–64.
- Qin DZ, Chen XS, Lin YF (2008) Revision of the Delphacid genus *Altekon* Fennah (Hemiptera, Fulgoroidea), with description of a new record species from China. *Acta Zootaxonomica Sinica* 33(4): 813–815.
- Qin DZ, Zhang YL (2009a) A new species of *Longtania* Ding from China and redescription of the male genitalia of *Platyttibia ferruginea* Ding (Hemiptera, Fulgoroidea, Delphacidae). *Zootaxa* 1979: 62–68.
- Qin DZ, Chen XD, Men QL (2009b) A new record species of the genus *Megadelphax* Wanger and description of *Eurybregma Nigrolineata* Scott (Hemiptera, Fulgoroidea, Delphacidae) from China. *Acta Zootaxonomica Sinica* 34(3): 654–658.

- Qin DZ, Wang SY, Lin YF (2010) Two new record species of Delphacidae (Hemiptera, Fulgoroidea) from China. *Acta Zootaxonomica Sinica* 35(4): 925–929.
- Qin DZ, Chen XD, Lin YF (2011) New record of the genus *Trichodelphax* Vilbaste from China with redescription of *T. Lukjanovitshi* (Hemiptera, Fulgoroidea, Delphacidae). *Acta Zootaxonomica Sinica* 36(1): 202–204.
- Ren FJ, Xie Q, Qin DZ (2014) *Kakuna taibaiensis* sp. n. and a newly recorded species of *Dicranotropis* (Hemiptera, Fulgoroidea, Delphacidae) from China. *ZooKeys* 545: 67–74.
- Ren FJ, Xie Q, Qin DZ (2015) *Mestus cruciatus*, a new delphacid species from southwest China with some remarks on the genus (Hemiptera, Fulgoromorpha, Delphacidae). *ZooKeys* 444: 119–130.
- Yang JT, Yang CT (1986) Delphacidae of Taiwan (I) Asiracinae and the tribe Tropidocephalini (Homoptera: Fulgoroidea). *Taiwan Museum Special Publication* 6: 1–79.

Revision of the Oriental species of *Calleida* Latreille (*sensu lato*). Part 2: the *C. discoidalis* species group (Coleoptera, Carabidae, Lebiini)

Hongliang Shi¹, Achille Casale²

¹ *Beijing Forestry University, College of Forestry, Beijing 100083, China* ² *Università di Sassari, Italy (Zoologia); private: Corso Raffaello 12, 10126 Torino, Italy*

Corresponding author: *Hongliang Shi* (shihl@bjfu.edu.cn)

Academic editor: *B. Guérouguiev* | Received 2 October 2018 | Accepted 14 November 2018 | Published 13 December 2018

<http://zoobank.org/1D8F8513-85FF-49F1-9DDD-3B655ADB4611>

Citation: Shi H, Casale A (2018) Revision of the Oriental species of *Calleida* Latreille (*sensu lato*). Part 2: the *C. discoidalis* species group (Coleoptera, Carabidae, Lebiini). ZooKeys 806: 87–120. <https://doi.org/10.3897/zookeys.806.30051>

Abstract

The *C. discoidalis* species group of the genus *Calleida* Latreille from Asia (in the sense of Casale and Shi 2018) is revised with six species recognized. Four new species are described: *C. piligera* Shi & Casale, **sp. n.** (type locality: Taiwan: Siling, 24.65°N, 121.42°E); *C. cochinchinae* Casale & Shi, **sp. n.** (type locality: Vietnam: “Cochinchina”); *C. yunnanensis* Shi & Casale, **sp. n.** (type locality: Yunnan: Caiyanghe, 22.60°N, 101.12°E); and *C. luzonensis* Casale & Shi, **sp. n.** (type locality: Philippines: Nagtipunan, 16.22°N, 121.60°E). *C. fukiensis* Jedlička, 1963 is confirmed as an available and valid species name, and *C. suenonii* Kirschenhofer, 1986 is newly synonymized with it. A phylogenetic analysis of Oriental *Calleida* species, based on adult morphological characters, is performed. The results show that the monophyly of most species groups in Oriental *Calleida* is accepted, but the *C. discoidalis* group appears polyphyletic and comprises three lineages. However, because many species relationships in the cladogram lack significant supporting, presently the *C. discoidalis* group was remained to use for morphological convenience. Five types of female reproductive tracts were recognized, corresponding to five branches in the cladogram.

Keywords

Calleida, character evolution, Oriental, spermatheca, taxonomy

Introduction

Calleida Latreille, 1824 is a genus of Lebiini Calleidina (Coleoptera, Carabidae) with rich species diversity mainly distributed in tropical and subtropical regions of the Americas, Sub-Saharan Africa and Southeast Asia (Casale 1998). These small to medium-sized and beautiful carabid beetles generally have vivid metallic color, but species identifications are very difficult in many cases. Our first contribution to the Oriental species of *Calleida* (Casale & Shi, 2018) provided a primary infra-generic taxonomy with nine species groups recognized and species revisions of six species groups.

As the second part of our contributions to the Oriental species of *Calleida*, the present paper is mainly dedicated to revision of the *C. discoidalis* species group. This group is defined as follows: abdominal sternite VII with four or more setae in males (two or more on each side), six or more setae in females (three or more on each side); abdominal sternite VII notched in males (Figs 2, 5); endophallus with two short copulatory pieces. This species group contains six known species distributed in China, Laos, Vietnam, and the Philippines. Two of them were described previously, and four are here described as new species.

At the beginning of our work, we included all Oriental species with multisetose abdominal sternite VII (four or more setae on abdominal sternite VII in males and six or more in females) in the *C. discoidalis* group. But *C. puncticollis* Shi & Casale, although with multisetose abdominal sternite VII, was recognized as very different from all other members both from external and genital characters. Thus, we erected a separate group to accommodate this species (Casale and Shi 2018). Even so, the members of the so-called *C. discoidalis* group are easily distinguishable by external features and different to each other in female genital characters, but this group is only supported by one external morphological character. Based on this, the *C. discoidalis* group is inferred to be paraphyletic or polyphyletic, and seems to be composed of three lineages with different female genital characters. However, it is difficult to define these lineages as distinct groups or move them to other groups based on the external and male genital characters. Therefore, we proposed the *C. discoidalis* group as a simple “group of convenience” to make identifications of species and species groups easier (Casale and Shi 2018).

When studying morphologies of each species, we found that the female reproductive tract (especially the spermatheca) has very important value of inferring species relationships of the Oriental *Calleida*. Thus, a preliminary phylogenetic analysis was performed to solve the systematic position of each species of the non-monophyletic *C. discoidalis* group, and moreover to interpret female genitalic evolution and evaluate its taxonomic value in the genus.

Materials and methods

Materials

This contribution was based primarily on the examination of *Calleida* specimens from different collections which are indicated with abbreviations:

BMNH	British Museum of Natural History, London, U.K.
CCA	Collection of Achille Casale, Torino, Italy
CCCC	Collection of Changchin Chen, Tianjin, China
CDG	Collection of Augusto Degiovanni, Bubano di Mordano (Modena), Italy
CPB	Collection of Peter Bulirsch, Prague, Czech Republic
CRS	Collection of Riccardo Sciaky, Milano, Italy
HBUM	Museum of Hebei University, Baoding, China
IZAS	Institute of Zoology, Chinese Academy of Science, Beijing, China
MNHN	Muséum National d'Histoire Naturelle, Paris, France
NHMW	Naturhistorisches Museum, Wien, Austria
NMNST	National Museum of Natural Science, Taipei, China
NMPC	Národní Přírodovědecké Muzeum, Prague, Czech Republic
SCAU	South China Agriculture University, Guangzhou, China
SMTD	Staatliches Museum für Tierkunde, Dresden, Germany
SYUM	Sun Yat-sen University Museum, Guangzhou, China
ZMFK	Zoologisches Forschungsmuseum Alexander Koenig, Bonn, Germany
ZSM	Zoologische Staatssammlungen, München, Germany

Methods

The methods, terminology and taxonomic treatment follow our previous work (Casale and Shi 2018). The phylogenetic reconstruction was performed using WIN-PAUP v. 4.0b10 software. The cladograms were created with FigTree v. 1.4.0 and trees were edited with Adobe Photoshop software. Parameters used in the analyses are listed in associated text.

Abbreviations

TL: body total length, from the anterior margin of clypeus to the apex of elytra, measured along the suture. **L**: overall length, from apex of mandibles to apex of elytra, measured along the suture. **PL**: length of pronotum, as linear distance from the anterior to the basal margin, measured along the midline. **PW**: maximum width of pronotum, as greatest transverse distance of pronotum. **EL**: length of elytra, as linear distance from the basal ridge to the apex, measured along the suture. **EW**: maximum width of elytra, as greatest transverse distance of two closed elytra.

Taxonomy

Key to species of *Calleida discoidalis* species group (in the sense of Casale and Shi 2018)

- 1 All intervals of elytra with strong metallic lustre, uniformly green, bluish or cupreous, without any trace of a dull reddish patch on disc **2**
- Elytra metallic green or bluish, with a reddish patch on the posterior half of disc, sometimes the reddish patch vague or narrow, but at least the inner three intervals with metallic lustre very faint (Figs 22, 23) **4**
- 2 Elytra with basal ridge incomplete, extended only from shoulder to the fourth interval; elytral disc metallic bluish green to bluish purple; basal three antennomeres reddish yellow, the rest ones distinctly darkened; femora distinctly bicolor, with basal part yellowish and apical part almost black (Fig. 2); abdominal sternite VII with six or rarely seven setae in females (Casale and Shi 2018: fig. 5). S. China [1] ***Calleida fukiensis* Jedlička**
- Elytra with basal ridge complete, extended from shoulder to the parascutellar stria; elytral disc metallic green to cupreous; antennae and femora uniformly reddish, or with apical antennomeres and apex of femora only weakly darkened; abdominal sternite VII with eight or more setae in females (Fig. 13) .2
- 3 Head and pronotum dark brown, without trace of metallic lustre (Figs 9–11); elytra metallic green, or with cupreous reflection; body form stouter (EL/EW = 1.65–1.75). S. China (Taiwan, Shaanxi, Shanghai, Guangxi, Guizhou, Guangdong, Sichuan) [2] ***Calleida piligera* Shi & Casale, sp. n.**
- Dorsal side, including head and pronotum, evenly metallic green (Fig. 19), with marked cupreous reflection, more evident at apex of elytra; body form slenderer (EL/EW = 1.84). S. Vietnam (“Cochinchina”) [3] ***Calleida cochinchinae* Casale & Shi, sp. n.**
- 4 Head, pronotum and legs brownish, markedly darkened; elytra dark metallic green, with obvious reflections of cupreous red or purple on lateral and apical areas (Figs 22, 23). Pronotum elongate and narrow (PW/PL: 1.07–1.13), elytra very elongate (EL/EW = 1.72–1.75). China (Yunnan), Laos [4] ***Calleida yunnanensis* Shi & Casale, sp. n.**
- Head, pronotum, and legs red to reddish yellow; elytra bright metallic green or a little bluish, not reddish or cupreous on lateral or apical areas. Pronotum more transverse (ratio WP/PL = 1.17–1.24), elytra short and wider (EL/EW = 1.52–1.65). Philippine Islands **5**
- 5 Head, pronotum and elytral patch dark reddish; elytral disc metallic bluish green; elytral patch usually wider, occupying the inner five or six intervals (Figs 32, 33); smaller beetles (L = 10 mm). Mindanao [5] ***Calleida discoidalis* Heller**
- Head, pronotum and elytral patch reddish yellow; elytral disc bright metallic green; elytral patch usually narrower, occupying the inner three to five intervals (Figs 36, 38, 39); larger beetles (L = 10.5–11.0). E. Luzon [6] ***Calleida luzonensis* Casale & Shi, sp. n.**

[1] *Calleida fukiensis* Jedlička, 1963

Figs 1–8, Map 1

Callida onoha ab. *fukiensis* Jedlička, 1953: 146 (type locality: China: “Fukien”; holotype deposited in ZFMK), unavailable name.

Callida fukiensis Jedlička, 1963: 437, available name.

Calleida suenisoni Kirschenhofer, 1986: 324 (type locality: China: Zhejiang; holotype deposited in ZMUC, paratypes in NHMW), **new synonymy**.

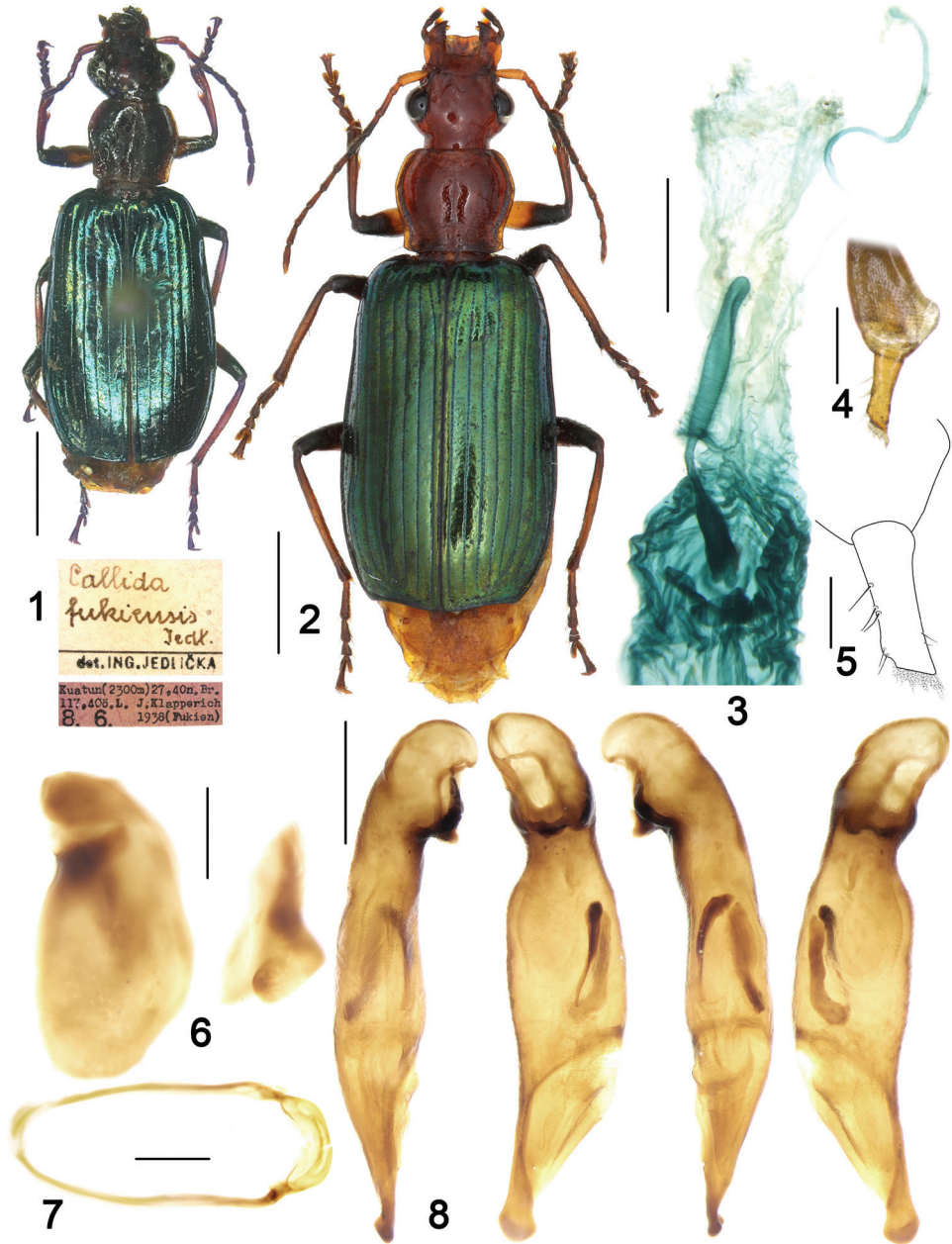
Type materials. *C. fukiensis*, **holotype**: female, examined through photo (Fig. 1), “Kuatun (2300 m), 27,40n. Br. 117,40ö.L. J. Klapperich 8.6.1938 (Fukien)”, “*Callida fukiensis* Jedl., det. ING. JEDLIČKA” (ZFMK). *C. suenisoni*, **paratypes**: 1 male, “China, Hangchow 30°18'N, 120°07'E, 9.X.1921 Elgin Suenson leg.” (NHMW). 1 male, “China, Tien Mu Shan 30°23'N, 119°37'E, 19.VI.1937”, “paratypus”, “*Callida* (*Callidiola*) *suenisoni* m. det. Kirschenhofer 83” (NHMW).

Notes on the type material. *C. fukiensis*: This species was originally described based on a single specimen (holotype by monotypy) from “Kuatun, Fukien” (= Guadun, Fujian) deposited in ZFMK (Jedlička 1953). We examined this specimen through photograph (Fig. 1) thanks to the help of Dr Dirk Ahrens, the curator of ZFMK. We examined five further specimens in Jedlička’s collection (NMPC) subsequently identified by himself as *C. fukiensis*, not belonging to the type series. Three of them are corresponding to the holotype (see material examined below), while the other two actually belong to a different species, *C. klapperichi* Jedlička and *C. jelineki* Casale & Shi, respectively.

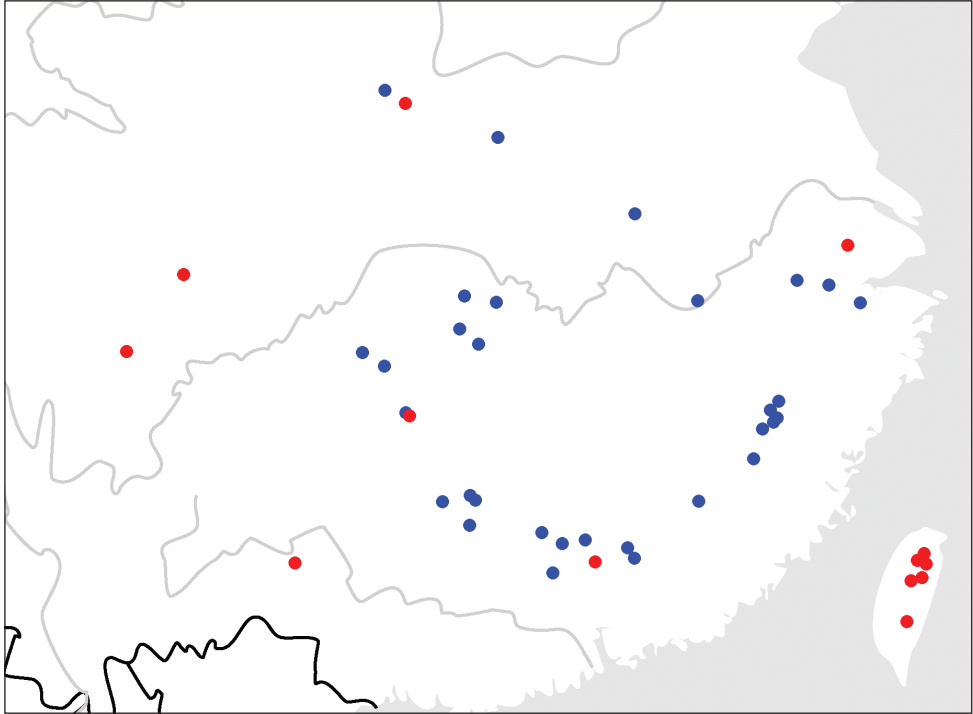
C. suenisoni: This species was described based on the male holotype and eleven paratypes, with type locality: China, Tien-Mu-Shan (= Tianmushan, Zhejiang), 30°23'N, 119°37'E. We did not examine the holotype deposited in ZMUC, but the two examined paratypes (one of them from the type locality) plus one additional male specimen from the type locality, and the original description with male genitalia illustrations (Kirschenhofer, 1986) are enough to recognize this species as identical to *C. fukiensis*. It is noticeable that the original literature erroneously reported that this species has two apical setae on the abdominal sternite VII in males, and four in females. But actually it has four (two on each side) setae in males, and usually six (three on each side) in females.

Taxonomic remarks. Jedlička (1953) described *Calleida fukiensis* as an “aberration” of *Calleida onoha* Bates, 1873. Later Jedlička (1963) treated this taxon as a distinct species and provided a brief description. According to the International Code of Zoological Nomenclature, *C. fukiensis* Jedlička, 1953 is an unavailable infrasubspecific name, but *C. fukiensis* Jedlička, 1963 is available, whereas this name has been later ignored in recent catalogues (Lorenz 2005; Kabak 2017).

From the examination of abundant material for this species, including the type material cited above, we proved that the morphological features of these two taxa are coincident. So we treat *C. suenisoni* Kirschenhofer, 1986 as a junior synonym of *Calleida fukiensis* Jedlička, 1963.



Figures 1–8. *Calleida fukiensis* Jedlička. **1** Habitus and labels of holotype (female, Fukien, ZMFK) **2** Habitus (female, Guizhou, IZAS) **3** Female reproductive tract (Shaanxi) **4** Gonocoxa (Shaanxi) **5** Gonocoxite II (Shaanxi) **6** Left and right parameres of aedeagus (Fujian) **7** male sternite IX (Fujian) **8** Median lobe of aedeagus, right-lateral, ventral, left-lateral, and dorsal views (Fujian). Scale bars: 2.0 mm (**1**, **2**), 0.5 mm (**3**, **7**, **8**), 0.2 mm (**4**, **6**), 0.1 mm (**5**).



Map I. Distributions for species in the *C. discoidalis* group: *C. fukiensis* Jedlička (blue); *C. piligera* sp. n. (red).

Non-type materials examined. Fujian: 1 female, “Kuatun. Fukien. China. 27.6.46. (Tschung Sen.)” [type locality], “*fukiensis* Jedl. Det. Ing. Jedlička” (NMPC). 1 male, “Fujian, Chong’an, Xingcun, Sangang, 740 m”, “1960.V.17, leg. Pu Fuji” (IZAS). 1 male, “Fujian, Chong’an, Xingcun, Sangang, 740 m”, “1960.VII.18, leg. Pu Fuji” (IZAS). 1 female, “Fujian, Chong’an, Xingcun, Sangang, 900 m”, “1960.VI.26, leg. Zuo Yong” (IZAS). 1 male, “Fujian, Chong’an, Xingcun, Sangang, 740 m”, “1960.VI.24, leg. Zuo Yong” (IZAS). 1 female, “Fujian, Chong’an, Xingcun, Sangang, 740 m, light trap”, “1960.VI.30, leg. Zhang Yiran” (IZAS). 1 female, “Fujian, Chong’an, Xingcun, Sangang, 740 m”, “1960.VI.28, leg. Zhang Yiran” (IZAS). 1 female, “Fujian, Chong’an, Xingcun, Sangang, 720 m”, “1960.V.7, leg. Jiang Shengqiao” (IZAS). 1 female, “Fujian, Chong’an, Xingcun, Sangang, 720 m”, “1960.VI.24, leg. Jiang Shengqiao” (IZAS). 1 male, “Fujian, Chong’an, Xingcun, Tongmuguan, 740–850 m”, “1960.VII.24, leg. Zhang Yiran” (IZAS). 1 male, “Fujian, Jianyang, Huangkeng, Guilin, 290–310m”, “1960.VIII.4, leg. Pu Fuji” (IZAS). 1 female, “Fujian, Jianyang, Huangkeng, Dazhulan, 900–1170 m”, “1960.VII.5, leg. Pu Fuji” (IZAS). 1 female, “Fujian, Jianyang”, “1965.V.23, leg. Li Hongxing” (IZAS). 1 female, “Fujian, Jianyang, Guilin, 1979.VII.14, leg. Chen Chong” (IZAS). 1 female, “Wuyishan, Niyang, 570 m”, “1997.VIII.2, leg. Zhang Youwei” (IZAS). 1 female, “Fu-

jian, Wuyishan, Pikeng, 520 m”, “1997.VII.14, leg. Wang Jiashe” (IZAS). 1 female, “Fujian, Wuyishan, Pikeng, 520 m”, “1997.VII.21, leg. Wu Yanyu” (IZAS). 1 female, “Wuyishan, Xianfengling, 1200 m”, “1997.VI.26, leg. Wu Yanyu” (IZAS). 1 female, “CHINA, Fujian Province, Wuyi Shan, ca860 m, 27°74'N, 117°66'E 9.VI.2001, leg. J. Cooter” (CCA). 1 male, “Fukien. Shaowu. Chine. 1937. Klapperich”, “*fukiensis* n. sp. det. Ing. Jedlička” (NMPC). 1 female, “Fujian, Jiangle, 1985.X.9, leg Zeng Fanchun” (IZAS). 1 male, “Fujian, Jiangle, Longqishan”, “1991.V. 30, leg. Liu Hong” (IZAS). 1 female, “Fujian, Jiangle, Longqishan, Yujiaping, 800 m”, “1991.V. 28, leg. Li Hongxing” (IZAS). 1 female, “Fujian, Jiangle, Longqishan, 600m”, “1991.VI. 27, leg. Yang Longlong” (IZAS). 1 male, “Fujian, Jiangle, Longqishan”, “1991.V. 16, leg. Li Wenzhu” (IZAS). **Zhejiang**: 1 male, “Tiemushan, July, 19, 35” (IZAS). 1 female, “Tiemushan, August, 18, 35” (IZAS). 1 female, “T’ienmo Shan, 20.9.1953” (IZAS). 1 male “China, Tien Mu Shan 30°23'N, 119°37'E, 17.VI.1937, Elgin Suenson leg.” (CRS) (as *C. suensoni*). 1 male, “Shaohing, July, 12, 35” (IZAS). **Jiangxi**: 1 female, “Jiangxi, Ruijin, Baying”, “1980.VIII.16” (IZAS). 1 male, 2 females, “Jiangxi, Jilianshan”, “1979.IX.30, leg. Yu Peiyu” (IZAS). **Henan**: 2 males, “Henan, Luoshan, Dongzhai, 2005.VII.14–15, leg. Gao Chao, Wang Jiliang” (HBUM). **Hubei**: 1 female, „Hubei, Hefeng, 1989.VII.28, 870m, leg. Li Yongkun“ (IZAS). 1 female, “Hubei, Wudangshan, Laoying, 2004.IX.7, leg. Zhang Zhisheng, Chen Huiming” (HBUM). 1 female, “Hupeh Prov. China. River by city wall of Hwangmei. Hwangmei Distr. 1933.VIII.3, leg. Y.W. Djou” (SYUM). **Hunan**: 1 female, “CHINA, Hunan Prov., Shimen Country, Hupingshan”, “2008.6.19–25 d, leg. Tang Guo” (IZAS). 1 male, “Hunan, Yongshun Coun., Shanmuhe forestry centre, 600m”, “1988.VIII.4, leg. Wang Shuyong” (IZAS). 1 female, “Hunan, Yongshun Coun., Shanmuhe forestry centre, 600m”, “1988.VIII.6, leg. Wang Shuyong” (IZAS). 1 male, “Hunan, Yongshun Coun., Shanmuhe forestry centre, 600–820 m”, “1988.VIII.7, leg. Wang Shuyong” (IZAS). 1 female, “Hunan, Yongshun County, Shanmuhe forestry centre, 600 m”, “1988.VIII.5, leg. Zhang Xiaochun” (IZAS). 2 males, 1 female, “Hunan, Yuanling, Jiemuxi, 2004.VIII.2–11, leg. Wang Jianfeng, Wang Jiliang” (HBUM). 1 female, “Hunan, Jianghua Coun., Sanjiangwei”, “1978.VI., leg. Peng Jianwen, Yin Shicai” (IZAS). **Guangdong**: 1 male, 1 female, “Guangdon, Nanling, leg. Wang L.” (SCAU). 1 female, “Guangdong, Huaiji” (SCAU). 1 female, “Guangdong, Lianxian”, “1965.VI.27, leg. ZhangYouwei” (IZAS). 1 female, “Guangdong, Shixing, Chebal-ing, Zhangdongshui; sweep net, 24.72320N, 114.25640E”, “354m, 2008.VII.27; day, leg. Tang Guo” (IZAS). **Guangxi**: 1 female, “Guangxi, Xing’an, Tongren”, “1985.VII.2, leg. Liao Subai” (IZAS). 1 female, “Guangxi, Xing’an, Jinshi, 2005.VII” (IZAS). 1 male, “Guangxi, Xing’an, Jinshi, 2007.VII” (IZAS). 1 female, “Guangxi, Xing’an, Mao’ershan” (IZAS). 1 male, 1 female, “Guangxi, Longsheng, Sanmen, 300 m”, 1963.VI.27, leg. Wang Chunguang” (IZAS). 1 female, “Guangxi, Longsheng, Sanmen, 300 m”, 1963.VI.28, leg. Shi Yongshan” (IZAS). 1 male, “Guangxi, Lingchuan, Lingtian, 225 m, 1984.VI.3” (IZAS). 1 female, “Guangxi, Lingchuan, Lingtian, 240, 1984.VI.6”, “8417” (IZAS). **Guizhou**: 2 males, 2 females, “Guizhou,

Yanhe, Mayanghe, Daheba, 300m, 2007.IX.17–30, leg. Liu Ye” (IZAS). 2 males, “Guizhou, Yanhe, Daheba, 450–700m, 2007.VI.5–12, leg. Song Qiongzhong” (IZAS). 1 female, “Guizhou, Yanhe, Daheba, 450–700m, 2007.VI.5–12, leg. Zhang Pei” (IZAS). 1 male, “Guizhou, Jiangkou, Fanjingshan, 550m”, “1988.VII.13, light trap, leg. Yang Xingke” (IZAS). 2 females, “Guizhou, Daozhen, Yuheba, 2004.V.25, leg. Yu Yang” (HBUM). 2 males, 1 female, “Guizhou, Daozhen, Xiannüdong, 2004.VIII.24–26, leg. Yang Xiujian, Hua Huiran” (HBUM). **Shaanxi**: 1 female, “China, Shaanxi, Foping, Changjiaoba, Shangshawo; 33.59716N, 108.01366E; 33.59212N, 108.02235E”, “1107–1215m, 2007.5.29, day, leg. Shi Hongliang” (IZAS). 1 female, “Shaanxi, Foping, 890 m, 1999.VI.26, leg. Zhang Youwei” (IZAS). **Shanxi**: 1 male, “Swan-ping. Mongolei.”, “ex Orig. Saml. J. Breit Wien”, “Museum J. Frey. Tutzing”, “*fukiensis* Jedl. Det. Ing. Jedlička” (NMPC).

Diagnosis. With the character states of the *Calleida discoidalis* species group, but different from all other known species by the combination of the following features: (1) elytra metallic bluish green to bluish purple; (2) antennae and femora distinctly bicolor: basal three antennomeres reddish, the following darkened, femora with basal half reddish, apical blackish; (3) elytral basal border only extended from the shoulders to interval 4; (4) abdominal sternite VII with four setae in males (two on each side), six setae in females (three on each side, in some specimens with one additional seta on one side). This species is unique amongst all known Asiatic *Calleida* species by its incomplete elytral basal ridge. From all other species of the *C. discoidalis* group, and from all other *Calleida* species in China, *C. fukiensis* can be easily distinguished by its bluish elytra and bicolored femora.

Description. *General features* as in Fig. 2. Small to medium-sized: L = 7.7–9.1 mm.

Colour: Head, pronotum and scutellum reddish orange to maroon; palpomeres and apex of mandible dark brown to blackish; apical palpomere light yellow at apex; the basal three antennomeres, and base of fourth yellow reddish, distal antennomeres dark brown, the second to fourth antennomeres a little darkened in some specimens; elytra bluish green to bluish purple, with marked metallic reflection and sutural area darker; epipleura metallic dark blue; ventral side orange yellow; legs yellowish to reddish brown, with apical third of femur and base of tibia blackish; tarsomeres dark brown on the dorsal side.

Lustre and microsculpture: Head and pronotum shiny, with highly effaced microsculpture; elytra shiny, with fine but distinct isodiametric reticulate microsculpture and marked metallic lustre.

Head: Smooth or very finely and sparsely punctate; frons with oblique, faint wrinkles at sides; supraorbital furrows deep, interrupted before the level of hind edge of eyes; genae longer than the half length of eyes; temporae swollen, gradually narrowed towards the neck constriction; apical labial palpomere securiform, truncate at apex in males, less tumid and not truncate in females; mentum with lateral lobes triangular, the inner margins oblique; median tooth obtuse, with two short setae, inserted in the middle part of the tooth.

Pronotum: Transverse-cordiform (ratio PW/PL = 1.13–1.18), greatest width at approximate anterior third; lateral margins arcuate near the middle, slightly sinuate anteriorly to the posterior angles; posterior angles almost rectangular or slightly acute in some specimens; lateral expansions narrow; disc slightly convex, with sporadic transverse wrinkles and fine punctures.

Elytra: Elongate (ratio EL/EW = 1.64–1.68), with basal ridge only extended from the shoulders to the fourth interval; striae moderately deep, finely punctate, punctures gradually weakened in the apical part of elytra; intervals flat, finely and sparsely punctate; the eighth interval slightly tumid near apex; umbilicate series of composed of 15 pores along stria 8; apical truncation straight or slightly concave; outer apical angle thickened but not angulate.

Ventral side: Prosternum, lateral area of metasternum, and metepisterna finely pubescent; abdominal sternites with sparse and short accessory setae; sternite VII with four setae in males (two on each side), six setae in females (seldom with one additional seta on one side) (Casale and Shi 2018: figs 2, 5); apical margin of abdominal sternite VII distinctly notched in males, straight in females.

Male genitalia (Figs 6–8): Median lobe of aedeagus slightly bent, its middle part strongly expanded in dorsal view; dorsal and ventral margins slightly curved in lateral view; apical orifice pleuropic left; apical lamina flat and rounded, apex expanded and thickened; endophallus with two chitinized copulatory pieces, located in the middle area near the left lateral margin, long and narrow, close to each other at base, V-shaped; left paramere depressed on the dorsal side; right paramere not emarginate at apex.

Female genitalia (reproductive tract Fig. 3 and gonocoxa Figs 4, 5): Spermatheca digitiform, as long as the pedicel, with long basal projection; surface faintly and finely whorled; spermathecal pedicel with basal half expanded, apical half slender, with an indistinct apical protuberance; spermathecal gland duct laterally inserted at base of the projection, long and slender, about twice length as spermatheca; glandular area slightly incrassate, about two thirds as long as gland duct, base with very weakly defined atrium. Gonocoxite II sub-rectangular, as long as three times the basal width; base slightly wider than apex; inner margin with several setae, extending from the basal third to apex; outer margin distinctly curved at middle, only slightly setose in the apical third; apex obliquely truncate, with irregular membranous extension on the outer part.

Geographical distribution and habitat. Endemic to China, but widespread and known from several provinces of South China: Zhejiang, Fujian, Jiangxi, Henan, Hubei, Hunan, Guangdong, Guangxi, Guizhou, Shaanxi. *C. fukiensis* is one of the most widely spread *Calleida* species in China (Map 1).

We examined one male in NMPC labeled as “Swan-ping, Mongolei”, referring to Shuo-ping Fu, an old name for the region around Youyu county (39.98N, 112.47E, 1300 m) in northernmost Shanxi. This locality is far from all other confirmed localities of this species. We consider it to be a dubious record and was not included in the distribution map.

This species was mainly found in evergreen broad-leaf forest of southern China. Some specimens were collected on vegetation or by light trap.

[2] *Calleida piligera* Shi & Casale, sp. n.

<http://zoobank.org/DB98BF02-9165-4B11-A8B9-CCE0E9420930>

Figs 9–18, Map 1

Type locality. Taiwan, Taoyuan county, Siling (24.65N, 121.42E, 1100 m).

Type materials. **Holotype**, male, “Taiwan, Taoyuan, Fuhsing, Siling; leg. Changchin Chen, 1995.V.28, C.C.C.C.” (NMNST, Fig. 9). **Paratypes** (a total of 23 specimens): **Taiwan**: 2 males, 1 female, same data as holotype (CCA, CCCC). 1 male, 1 female, “Taiwan, Nantou, Ren’ai, Sungkang, 2000 m, leg. Chinchu Lo, 1995.VI.23” (CCCC). 1 female, “Taiwan, Nantou, Ren’ai, Sungkang; 2000 m; leg. Chinchu Lo, 1995.VI.2” (CCCC). 1 female, “Taiwan, Nantou, Ren’ai, Sungkang, leg. Changchin Chen, 1994.VIII.16” (CCCC). 1 male, “Taiwan, Taitung, Hsiang Yang; leg. Wensin Lin; 2008.IV.26N” (CCCC). 2 females, “Taiwan, Ilan, Tatung, Siyuan, leg. Changchin Chen, 1998.V.30” (CCCC). 1 female, “Taiwan, Hsinchu, Jianshi, leg. Changchin Chen, 1994.VI.11” (CCCC). 3 females, “Taiwan, Hualien, Sioulin, Bi-lyu Scared Tree, leg. Changchin Chen, 1995.V.2” (CCA, CCCC). **Shaanxi**: 1 male, “China, Shaanxi, Ningshan, Huoditang; 33.43368N, 108.44747E”, “1538m, 2007.VI.2, beating, leg. Shi Hongliang” (IZAS). **Shanghai**: 1 female “Shanghai”, “Coll. Armitage”, “Museum Paris Coll. R. Oberthür, 1952” (MNHN). **Guangdong**: 1 male, “Guangdong, Shimentai N.R. leg. Tian M.Y” (SCAU). 1 female “Guangdong” (CCA). **Guangxi**: 1 male, “Guangxi, Tianlin, Cenwanglaoshan; 1200–1300 m; 2002.V.28, leg. Yang Xiujuan” (HBUM). **Guizhou**: 1 female, “Guizhou, Fanjingshan, Heiwanhe; 1200 m; 2002.VI.4; leg. Song Qiongzhang” (IZAS). 1 male, “Guizhou, Fanjingshan, N27°89.962’, E108°70.826’; 1500–2000 m;”, “2008.VII.3, light trap; leg. Li Yu, B08L9135” (CCCC). **Sichuan**: 1 male “China, Sichuan, Qingchenghou Shan 70 km NW Chengdu 1500 m 6.–13.VIII.2010 S. Murzin” (ZSM). 1 female, “West Sichuan Gongga Shan (Moxi env.) 3000 m 22.V–10.VI.1993 leg. V. Beneš” (CPB).

Specific epithet. In Latin, *piligera* means setose. The specific name is referred to the remarkable high number of setae on the abdominal sternite VII in both sexes.

Diagnosis. With the character states of the *Calleida discoidalis* species group, but differing from all other known species by the combination of: (1) elytra uniformly metallic green or cupreous green, without discal patch; (2) head and pronotum brownish, without metallic lustre; (3) abdominal sternite VII with eight or more setae in both males and females; (4) pronotum only with a few fine punctures along the median furrow.

Compared with *Calleida fukiensis*, the new species differs by the complete elytral basal ridge that reaches the parascutellar stria, the much higher number of setae on abdominal sternite VII, and the different body colour.

In this species group, the new species is somewhat similar to *C. yunnanensis* sp. n., but differs from that species by the elytra lacking any trace of discal reddish patch, and males with more than eight setae on the terminal ventrite. Amongst the other *Calleida* species of China, the new species is similar to *C. klapperichi* Jedlička, 1963 in general appearance, but can be readily distinguished by the number of setae on abdominal sternite VII.

Description. *General features* as in Figs 10, 11. Medium-sized: L = 9.5–11.0 mm.

Colour: Head dark brown, mouth part and antennae yellowish brown; pronotum dark brown, with lateral expansions yellowish; scutellum reddish brown; elytra uniformly metallic green, usually with cupreous reflection, without reddish discal patch; elytral suture and lateral margins yellowish brown; epipleura yellowish brown; ventral side and legs yellowish brown, femora darkened in some specimens.

Lustre and microsculpture: Head without microsculpture; pronotum mostly without distinct microsculpture, except some fine transverse meshes near the discal transverse wrinkles, and faint isodiametric meshes on the middle part of the basal area; elytra with distinct microsculpture in an isodiametric mesh.

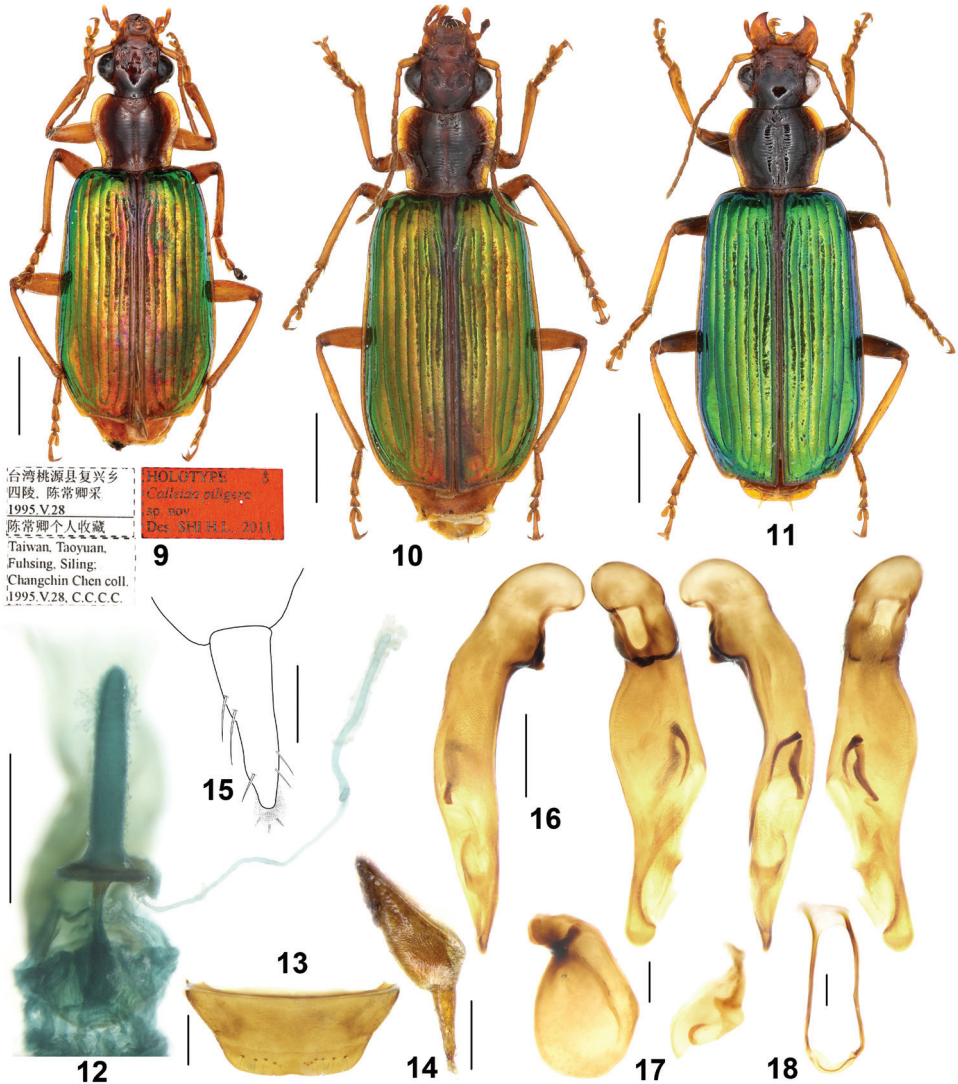
Head: Moderately convex; frons with a few very fine punctures and oblique wrinkles laterally, distinct or very faint; supraorbital furrows deep, extended to the level of posterior edge of eyes; temporae not swollen, gradually narrowed towards the neck; genae shorter than the half length of eyes; antennae reaching the basal fifth of elytra; terminal labial palpomere strongly securiform with truncate apex in males, only slightly expanded in female; mentum lateral lobes with outer margins slightly arcuate, inner margins oblique, mentum tooth near triangular, rounded at apex, with two short setae inserted in middle part of the tooth.

Pronotum: Transverse (ratio PW/PL = 1.19–1.28), with its maximum width at about the anterior third; lateral margins gradually arcuate near the middle, straight or slightly sinuate before the posterior angles which are obtusely rounded; lateral expansions widened, explanate in front; disc slightly convex, with distinct transverse wrinkles and with a few fine punctures along only the median furrow; median furrow distinct, but interrupted before both the anterior and posterior margins.

Elytra: Elongate (ratio EL/EW = 1.65–1.75), with basal border complete, reaching the parascutellar stria; striae distinct, finely punctate, the punctures gradually weakened in the apical part; intervals slightly convex, finely and sparsely punctate; intervals without additional setigerous pores; third to fifth intervals slightly depressed at the basal fourth; eighth interval slightly tumid at apex; umbilicate series of 15–16 pores along eighth stria; apical truncation slightly concave; lateral margins distinctly thickened at the outer apical angles, which are obtusely rounded.

Ventral side: Prosternum, lateral area of metasternum, and metepisterna with fine pubescence; abdominal sternites with dense and long accessory setae; abdominal sternite VII with 8–12 setae in both male and female (four to six on each side) (Fig. 13), usually not regularly arranged in a row; apical margin of abdominal sternite VII distinctly notched in male, straight or slightly emarginate in female.

Male genitalia (Figs 16–18): Median lobe bent, pleuropic left; in ventral aspect middle portion strongly widened, right lateral margin strongly sinuate; apical lamella flat, a little shorter than basal width, fully rounded at apex. Endophallus with two chitinized copulatory pieces close to left lateral margin of the median lobe, their apex adjacent to the base of the apical orifice, close to each other at base, V-shaped, the ventral one sinuate and acerate, the dorsal one a little wider. Left paramere dorsally depressed, about 1.5 times as long as wide; right paramere not emarginate.



Figures 9–18. *Calleida piligera* sp. n. **9** Habitus and labels of holotype (male, Taiwan, NMNST) **10** Habitus (female paratype, Taiwan, IZAS) **11** Habitus (female paratype, Taiwan, IZAS) **12** Female reproductive tract (paratype, Taiwan, IZAS) **13** Female sternite VII (paratype, Taiwan, IZAS) **14** Gonocoxa (paratype, Taiwan, IZAS) **15** Gonocoxite II (paratype, Taiwan, IZAS) **16** Median lobe of aedeagus, right-lateral, ventral, left-lateral, and dorsal views (holotype) **17** Left and right parameres of aedeagus (holotype) **18** Male sternite IX (holotype). Scale bars: 2.0 mm (**9–11**), 0.5 mm (**12, 13, 16, 18**), 0.2 mm (**14, 17**), 0.1 mm (**15**).

Female genitalia (reproductive tract Fig. 12 and gonocoxa Figs 14, 15): Spermatheca digitiform, twice longer than the pedicel, surface not whorled, base with an evident basal sclerotized plate (annulus receptaculi); spermathecal pedicel with basal part a little expanded, apical part slender; spermathecal gland duct laterally inserted at the basal surface of the plate, very long and slender, a little longer than spermatheca;

glandular area slightly incrassate, a little shorter than gland duct, base with very small atrium. Gonocoxite I moderately wide, with microsculpture; gonocoxite II subulate, apex sharp, length about three times as basal width; inner margin with several setae, extending from the basal third to apex, outer margin only slightly setose in the apical third; both outer and inner margins straight; apical margin with membranous extension and short setae.

Geographical distribution and habitat. Widely distributed in several provinces of south China: Taiwan, Shaanxi, Shanghai, Guangdong, Guangxi, Guizhou and Sichuan (Map 1). Common at mid-high elevations (ca 2000m) in Taiwan, but apparently rare in Chinese continental provinces. This species was mainly found in evergreen broad-leaf forest. Some specimens were collected by beating from vegetation or in light trap.

Remarks. From many important morphological aspects, *C. piligera* sp. n. is very peculiar in the *C. discoidalis* species group: (1) the base of spermatheca has an evident annulus receptaculi, surface not whorled; in contrast spermatheca is without such structure and surface more or less whorled in all other known species; (2) terminal ventrite with four or more setae on each side in males; in contrast usually with two (exceptionally three) setae on each side in males for all other known species; and (3) gonocoxite II subulate, apex narrowed and sharp in contrast to gonocoxite II with apex more or less oblique truncated in all other known species. The similarities of spermatheca lead us to hypothesize a relationship of the new species to the *C. terminata* species group, in which all known species have spermatheca with annulus receptaculi and without whorled surface (Casale and Shi 2018: figs 55, 60). But, in several other aspects, such as shape of the male genitalia, setation on the terminal ventrite, and shape of elytral apical outer angles, the new species does not accord with the *C. terminata* group at all. As discussed above, the *C. discoidalis* group is probably not monophyletic. As we just erected it as a group of convenience to accommodate species with similar multiple setation of the abdominal sternite VII and male genitalia character, the question of species relationship must await a future answer.

In most specimens, the elytra are metallic green, with distinct cupreous reflection (Figs 9, 10), but in two females from Songgang (Taiwan: Nantou), the elytra are vivid green, without cupreous reflection (Fig. 11).

[3] *Calleida cochinchinae* Casale & Shi, sp. n.

<http://zoobank.org/D4CD66E9-39FF-4DE6-BFE6-CA1C3448DF5B>

Figs 19–21, Map 2

Type locality. S. Vietnam: “Cochinchina”.

Type material. Holotype, female, “MUSEUM PARIS Cochinchine, Baudouin d’Aulne 1897”, “*Calleida cochinchine*” (MNHN, Fig. 19).

Specific epithet. The name is derived from the former name of the southern province of Vietnam of the former French empire (1862–1954), as indicated in the original label of the holotype.

Diagnosis. This brilliant new species is distinct amongst all Asiatic *Calleida* species for: (1) abdominal sternite VII with five setae on each side in females (males unknown); (2) head, pronotum and ventral side uniformly metallic green, with marked cupreous reflection; (3) elytra rather elongate; (4) elytral apical margin strongly concave, with margins thickened at the outer apical angles but not angulate. *C. cochinchinae* can be easily distinguished from all other species in the *C. discoidalis* species group by its special coloration, but might be confused with *C. viet* Casale & Shi, also from South Vietnam, which has similar completely metallic greenish dorsal surface. Different from that species, the new species has a more elongate shape (EL/EW = 1.84, contrasting to 1.68 in *C. viet*), less prominent elytral outer apical angles, and multisetose abdominal sternite VII (males unknown, but supposed multisetose also).

Description. *General features* as in Fig. 19. Medium to large-sized: L = 12.0 mm (female holotype). Body elongate and slender, dorsal and ventral side completely metallic.

Colour: Head, pronotum, elytra (epipleura included), and ventral side uniformly metallic green with marked cupreous reflection, more evident at the elytral base and apex; clypeus and labrum blackish, palpomeres dark brownish with yellowish apex for the terminal segments; antennae and legs reddish yellow; legs with faint metallic green reflection; apex of femora, and all tarsomeres dark brownish.

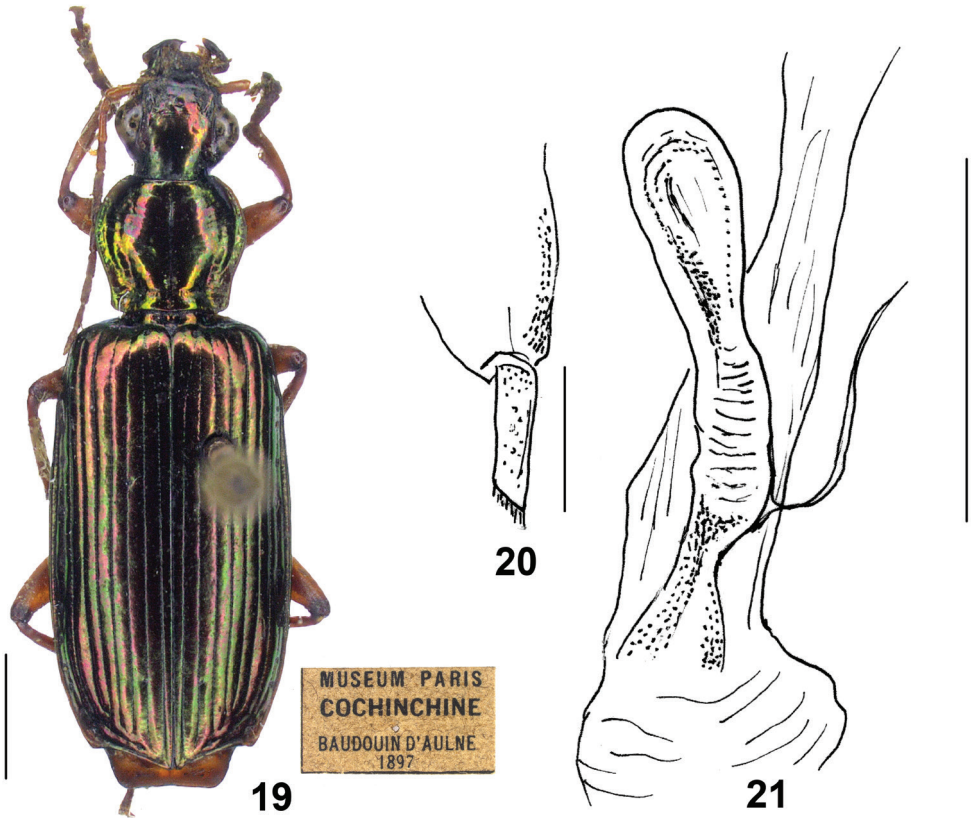
Lustre and microsculpture: Dorsal surface rather shiny and polished; head and pronotum with vanished microsculpture; elytra with faint but distinct microsculpture in isodiametric meshes.

Head: Slightly convex, almost impunctate; frons with very faint transverse wrinkles at sides; supraorbital furrows moderately deep, vanished anteriorly to the half of the inner edge of eyes; temporae barely swollen, narrowed towards the neck; genae short, as long as the half length of eyes. Antennae short, only slightly exceeding the humeral angles of elytra. Terminal labial palpomere markedly dilated in females (probably securiform in males); mentum lateral lobes with outer margins straight, the inner margins oblique; mentum tooth obtusely truncate at apex, with two short setae inserted at the middle part of tooth.

Pronotum: Roundish-cordate (ratio PW/PL = 1.14), with its maximum width at about the anterior third; lateral expansions moderately wide; lateral margins reflexed and arcuate at the middle, distinctly sinuate before the posterior angles which are obtuse, not pointed at apex. Disc slightly convex, with deep transverse wrinkles and with a few punctures along the median furrow; median furrow deep, widened at base and reaching the posterior margin.

Elytra: Elongate (ratio EL/EW = 1.84), with basal ridge complete, extended to the parascutellar stria; striae deep, finely punctate; intervals flat, very finely and sparsely punctate; intervals 7–8 moderately tumid at apex; umbilicate series of 13 (right elytron) to 15 (left elytron) pores along the eighth stria; apical truncation oblique, markedly concave, margins thickened at outer apical angles, which are obtusely prominent, not angulate.

Ventral side: Glabrous; in the female holotype, abdominal sternite VII with five setae on each side, apical margin almost straight, slightly excised at middle. Male sternum unknown.



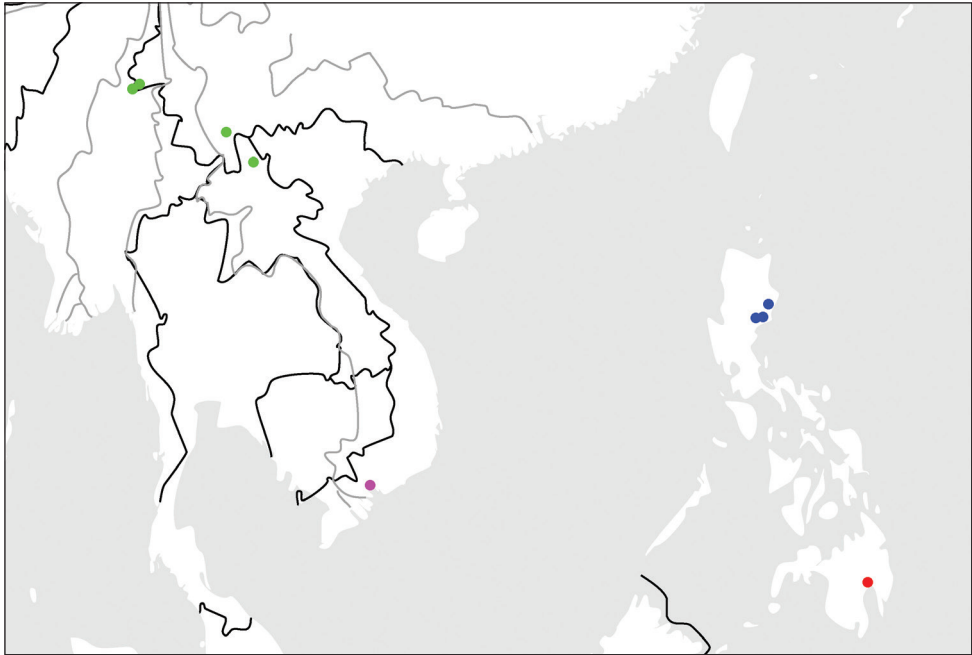
Figures 19–21. *Calleida cochinchinae* sp. n. **19** Habitus and labels of holotype (female, Cochinchine, MNHN) **20** Gonocoxite II (holotype) **21** Female reproductive tract (holotype). Scale bars: 2.0 mm (**19**), 0.2 mm (**20**), 0.5 mm (**21**).

Male genitalia: Unknown.

Female genitalia (reproductive tract Fig. 21 and gonocoxa Fig. 20): Spermatheca slightly dilated to apex, a little longer than the pedicel, base without projection; surface distinctly whorled; spermathecal pedicel markedly dilated at the basal two thirds, slender in the apical third; spermathecal gland duct laterally inserted, rest portion not examined (damaged in the only available individual). Gonocoxite I wide; gonocoxite II subulate, elongate, a little narrowed to apex, about four times as long as wide at base; inner margin setose in the apical fourth; both outer and inner margins straight; apex obliquely truncate, with membranous setose extension.

Geographical distribution and habitat. Only known from the single holotype female from Vietnam: “Cochinchina”, without further information on the type locality in the label (Fig. 19 and Map 2). No data are available on the habitat, which should be located in tropical forests of the region.

Remarks. From the rather elongate habitus and peculiar female genital characters, *C. cochinchinae* sp. n. is different from all other known species in the *C. discoidalis*



Map 2. Distributions for species in the *C. discoidalis* group: *C. cochinchinae* sp. n. (magenta); *C. yunnanensis* sp. n. (green); *C. discoidalis* Heller (blue); *C. luzonensis* sp. n. (red).

species group, but surprisingly accords with the *C. lativittis* species group. Amongst all examined species of Asiatic *Calleida*, only *C. cochinchinae* and species in the *C. lativittis* group (two species with female genitalia examined of three species of the group; Casale and Shi 2018) have the following character combinations of the female reproductive tract: spermatheca without basal projection or plate, and the spermathecal gland duct inserted on the lateral side of spermatheca. Thus, we inferred a relationship of the new species with the *C. lativittis* species group rather than to other species of the *C. discoidalis* group, which was erected as a “group of convenience” to accommodate species with similar multisetose abdominal sternite VII. This relationship was also supported by our phylogenetic analysis (Fig. 43).

[4] *Calleida yunnanensis* Shi & Casale, sp. n.

<http://zoobank.org/A9F123C3-A55D-44D3-AE29-6564D5D82A58>

Figs 22–31, Map 2

Type locality. Yunnan, Pu’er city, Caiyanghe (22.60N, 101.12E, 1700 m).

Type materials. Holotype: Male, “Yunnan, Simao, Caiyanghe national reserve, 1700 m, 2007.VII.28, leg. Zhao Yongshuang” (IZAS, Fig. 22). **Paratypes** (a total of 8 specimens): **Yunnan:** 2 females, same data as holotype (IZAS and CCA). 1 female, “Yunnan, Simao, Caiyanghe national reserve, Liechang, 2009.III.7, leg. Zhu Xiaoyu”

(CCCC). 1 male, “Yunnan, Ruili, Mengxiu, 2150 m, 2005.VIII.3, leg. Mao Benyong” (HBUM). 1 female, “Yunnan, Ruili, Nongdao, Dengga, 1000 m, 2006.VIII.1, leg. Liu Biao” (IZAS). 1 female, “Yunnan, Ruili, Nongdao, Dengga to Mafengshan, 23.95285N, 97.59808E – 23.94485N, 97.55647E”, “927–1207 m, 2009.VIII.10, leg. Shi Hongliang, beating” (IZAS). 1 female, “Yunnan, Ruili, Nongdao, Wudian-shan, 920m, 2015-IX-11, beating on vegetation, Yang Xiaodong leg.” (CCCC). **Laos:** 1 female, “Haut Mekong, Pou Lan. 13.V.1918. R.V. de Salvaza”, “1961”, “Brit. Mus. 1921-89” (BMNH).

Specific epithet. The name of the new species refers to its type locality: Yunnan, China.

Diagnosis. With the character states of the *C. discoidalis* species group, but different from all other known species by the combination of: (1) elytra metallic green, with evident lustre of cupreous red or purple; (2) elytral discal reddish patch not well defined; (3) head, disc of pronotum and legs brownish, markedly darkened; (4) elytra with several very small additional setae on odd intervals; (5) abdominal sternite VII with two (seldom three) setae on each side in males, four or more in females; (6) median lobe of aedeagus with a cuneiform projection on the ventral side.

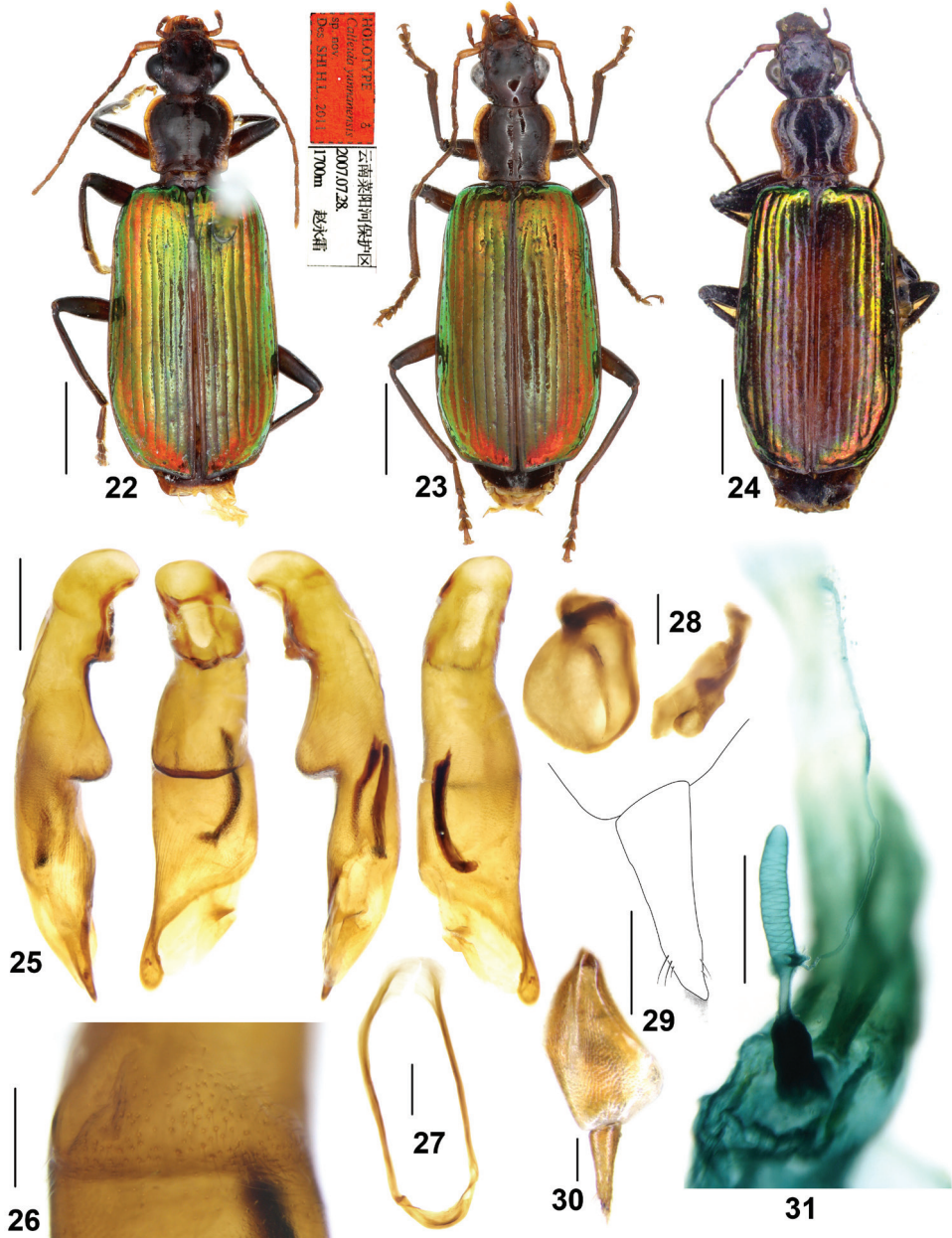
In this species group, *C. yunnanensis* sp. n. is somewhat similar to the two species (*C. discoidalis* and *C. luzonensis*) from the Philippines based on the presence of a reddish patch on elytral disc. But from the other two, *C. yunnanensis* can be distinguished by: (1) the darker color on head, pronotum, legs and ventral side; (2) the presence of cupreous reddish hue on elytra; (3) narrower pronotum and elytra; and (4) the characters of aedeagus which has a peculiar projection on the median lobe ventral surface.

In southern Yunnan, *C. yunnanensis* sp. n. is sympatric with *C. quadricollis* Straneo and one undescribed species belonging to the *C. splendidula* species group. These three species are similar in general features and coloration, but *C. yunnanensis* sp. n. can be readily distinguished by its higher number of setae on the terminal ventrite in both sexes.

Description. *General features* as in Figs 22–24. Medium-sized: L = 9.4–9.8 mm.

Colour: Head dark reddish brown, vertex distinctly darker, approximate piceous; mouth parts and antennae yellowish brown, terminal palpomere with light yellow apex. Pronotum dark brown, with lateral expansions yellowish brown and disc slightly lighter along the median furrow; scutellum reddish brown. Elytra metallic green with marked cupreous reddish or purplish reflection, more evident in the apical area; metallic reflection gradually fainter toward the suture, forming a vague discal reddish brown patch almost without metallic lustre on the apical half or two thirds, not reaching elytral base, widest near elytral apical third or fourth, occupying the inner three or four intervals, sometimes the fifth interval also partly brownish; lateral margins, elytral suture, and epipleura brownish with faint metallic reflection. Ventral side reddish brown to dark brown, with metacoxae and adjacent metasternal area generally lighter; legs brown, femora gradually darker to apex, tibiae infusate at base, tarsomeres yellowish brown.

Lustre and microsculpture: Dorsal surface moderately shiny and polished; head and pronotum with vanished microsculpture; elytra with faint microsculpture in isodiametric meshes, more evident in females.



Figures 22–31. *Calleida yunnanensis* sp. n. **22** Habitus and labels of holotype (male, Yunnan, IZAS) **23** Habitus (female paratype, Yunnan, IZAS) **24** Habitus (female paratype, Laos, NHML) **25** Median lobe of aedeagus, right-lateral, ventral, left-lateral, and dorsal views (holotype) **26** Cuneiform projection on median lobe, ventral view (holotype) **27** Male sternite IX (holotype) **28** Left and right parameres of aedeagus (holotype) **29** Gonocoxite II (paratype, Yunnan, IZAS) **30** gonocoxa (paratype, Yunnan, IZAS) **31** Female reproductive tract (paratype, Yunnan, IZAS). Scale bars: 2.0 mm (**22–24**), 0.5 mm (**25, 27, 31**), 0.2 mm (**26, 28, 30**), 0.1 mm (**29**).

Head: Slightly convex, almost impunctate; frons with oblique wrinkles aside, weakly defined or very faint; supraorbital furrows moderately deep, vanished at half of the inner edge of eyes; temporae moderately swollen, gradually narrowed towards the neck; genae longer than the half length of eyes; antennae reaching the basal fifth of elytra; terminal labial palpomere strongly securiform with truncate apex in males, also dilated but less so in females; mentum lateral lobes with outer margins straight, inner margins oblique; mentum tooth obtuse with apex truncate or slightly rounded, with two short setae inserted at the base of tooth.

Pronotum: Sub-quadrate (ratio PW/PL = 1.07–1.13), with its maximum width near anterior third; lateral expansions moderately wide; lateral margins arcuate at the middle, more or less sinuate before the posterior angles; posterior angles rectangular or obtuse, sometimes slightly pointed at apex; disc weakly convex, sometimes with very faint transverse wrinkles and a few punctures along the median furrow; median furrow distinct, but not reaching anterior nor posterior margins.

Elytra: Elongate (ratio EL/EW = 1.72–1.75), with basal border complete, extended to the parascutellar stria; striae distinct, finely punctate, with punctures gradually weakened in the apical part; intervals flat, finely and sparsely punctate; the third, fifth and seventh intervals each with more than 10 very small additional pores, slightly larger than interval punctures, each bearing one short seta, setae a little longer in the basal area of intervals; the eighth interval distinctly tumid near apex; umbilicate series of 15–16 pores along the eighth stria; apical truncation straight or very weakly concave; lateral margins distinctly thickened at the outer apical angles, which are obtusely rounded.

Ventral side: Mostly glabrous, lateral areas of prosternum at apex and metasternum with a few short setae; abdominal sternites sparsely pubescent. Abdominal sternite VII with two (the holotype bearing three setae on the right side) setae on each side in males, the inner seta placed a little forward; with four to six setae on each side in females, with the outer second seta placed a little forward; apical margin of abdominal sternite VII distinctly notched in males, straight in females.

Male genitalia (Figs 25–28): Median lobe of aedeagus pleuropic left, peculiarly shaped, with a conspicuous cuneiform projection near the middle of the ventral side (Fig. 25); apical surface of the projection bearing numerous fine setae (Fig. 26), almost perpendicular to the surface of the ventral margin; right lateral surface finely and longitudinally wrinkled before the apical orifice; apical lamina flat, a little longer than the basal width, rounded at apex. Endophallus with two chitinized copulatory pieces, close to the left lateral side of the median lobe, adjacent to each other at base, nearly V-shaped. Left paramere rounded, longitudinally depressed on the dorsal side, raised at base, about one and a half times longer than wide; right paramere slightly emarginate.

Female genitalia (reproductive tract Fig. 31 and gonocoxa Figs 29, 30): Spermatheca digitiform, not so straight as in the species treated above, nearly as long as the pedicel, with a stout triangular basal projection (much shorter than in *C. fukiensis*); surface distinctly whorled; spermathecal pedicel markedly dilated at the basal two thirds, apical third slender; spermathecal gland duct laterally inserted at base of the projection,

very long and slender, about 1.5 times as long as spermatheca; glandular area barely incrassate, about same length as gland duct, base with atrium not protuberant. Gonocoxite I wide, with microsculpture; gonocoxite II narrow, approximate subulate, three times as long as wide at base; inner margin setose in the apical fourth; both outer and inner margins straight; apex obliquely truncate with membranous setose extension.

Geographical distribution and habitat. Known from two localities of southern and southwest Yunnan, and northern Laos (Luang Namtha) (Map 2). In southern Yunnan, this species was found in a mountain rainforest and an evergreen broad-leaf forest at middle elevation (ca 1000 m). One specimen was collected by beating shrubs along a dirt path.

Remarks. We examined one female from northern Laos (Fig. 24), labeled as “Haut Mekong. Pou Lan.” (R.V. de Salvaza) (BMNH) probably referring to Ban Phou Lan (20.555N, 101.001E, 890 m) in Luang Namtha Province. Different from other specimens in Yunnan, this specimen from Laos has the elytra almost completely greenish, only with very faint reddish hue, 12 setae in female abdominal sternite VII, and a little wider gonocoxite II. Besides the above minor differences, all characters including the female reproductive tract have no significant difference from the typical *C. yunnanensis* from Yunnan, China. So at moment we attribute this specimen to *C. yunnanensis*, although its distribution is a little distant.

[5] *Calleida discoidalis* Heller, 1921

Figs 32–35, Map 2

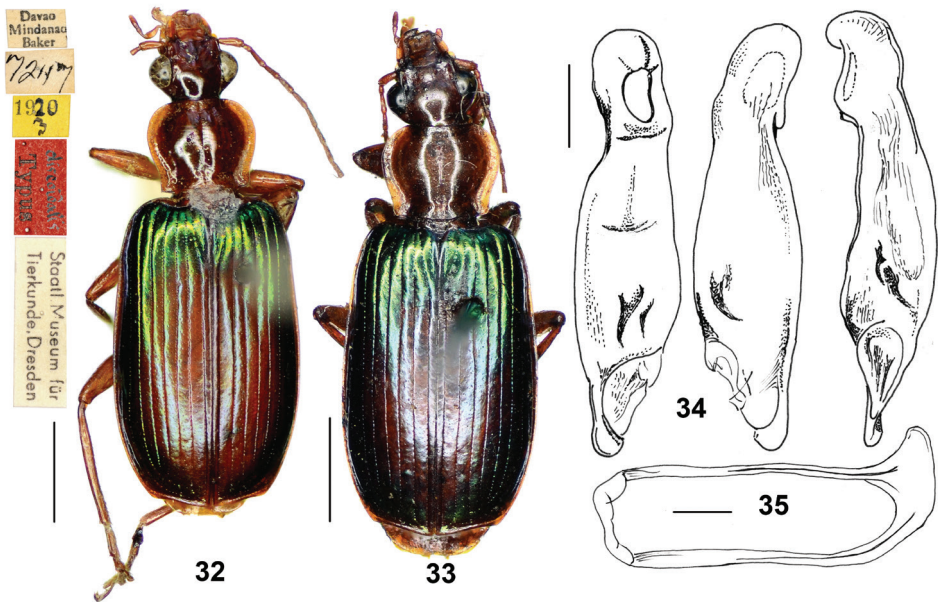
Callida discoidalis Heller, 1921: 529 (type locality: Philippines: Mindanao, Davao; holotype deposited in SMTD); Jedlička 1963: 436.

Type material examined. **Holotype**, male, “Davao Mindanao Baker”, “7247”, “1920/3”, “discoidalis. Typus”, “Staatl. Museum für Tierkunde. Dresden” (SMTD, Fig. 32).

Non-type materials examined. 1 female, “Davao Mindanao Baker”, “Ex Mus. Coll. Agric. Phil. Is.”, “*Callida discoidalis* Heller compared with type H.E.A.”, “H.E. Andrewes Coll. B. M. 1945-97.” (BMNH). 1 female, “Davao Mindanao Baker” (CCA, ex Straneo collection).

Diagnosis. *C. discoidalis* is distinct within the *Calleida discoidalis* group for its evident reddish spot on the inner five or six intervals of the elytra, markedly contrasting with the lateral metallic bluish green intervals, and for having the head, antennae, pronotum, legs and ventral side completely reddish yellow. *C. discoidalis* is similar to *C. luzonensis* n. sp., from which is distinct by several characters stressed in the key to species (and see diagnosis of *C. luzonensis* below).

C. discoidalis could be confused with *C. splendidula*, sympatric in the Philippines, for their similar habitus and colour, and the evident reddish patch on the elytral disc in both species. It is, however, easily recognized by the latter for the multisetose ab-



Figures 32–35. *Calleida discoidalis* Heller. **32** Habitus and labels of holotype (male, Mindanao, SMTD) **33** Habitus (female, Mindanao, NHML) **34** median lobe of aedeagus, ventral, dorsal, and left-lateral dorsal views (holotype) **35** Male sternite IX (holotype). Scale bars: 2.0 mm (**32**, **33**), 0.5 mm (**34**, **35**).

dominal sternite VII (in *C. splendidula*, the abdominal sternite VII bears only one seta on each side in males, two in females), generally larger size, and for the different shape of aedeagus.

Description. The original description provided by Heller (1921), here completed with some additional characters, is sufficient to distinguish this taxon.

General features as in Figs 32–33. Medium-sized species: TL = 9.5–10.0 mm; L = 10.0–10.5 mm.

Colour: Head, antennae, pronotum, underside and legs reddish yellow. Elytra dark metallic green, with trace of bluish; disc with an evident reddish patch, one-half to two-thirds as long the elytra length, widest in apical third of elytra, occupying the inner five or six intervals; reddish patch not reaching elytral base, narrowed to apex, only with the first interval reddish at apex.

Lustre and microsculpture: Moderately shiny; head and pronotum with obsolete microsculpture; elytra with faint but distinct microsculpture in isodiametric meshes.

Head: Smooth; genae short, moderately swollen; neck constriction evident.

Pronotum: Wider than head, cordate, markedly transverse (ratio PW/PL = 1.17–1.23). Lateral margins widened and arcuate in front, reflexed and sinuate in the basal third; lateral expansions wide; posterior angles obtuse; disc with shallow transverse wrinkles. In one examined specimen, exceptionally the left side bears two antero-lateral setae.

Elytra: Moderately elongate (ratio EL/EW = 1.62–1.65), depressed, with basal border complete, extended to the parascutellar stria; striae deep, finely punctate; intervals convex at base, flattened on disc; intervals 7–8, slightly tumid at apex; apical margin obliquely truncate, with outer apical angles slightly thickened at the outer apical angles, which are obtusely rounded.

Ventral side: Abdominal sternites with sparse, short but evident pubescence. Abdominal sternite VII with two setae on each side in males, four on each side in females.

Male genitalia: As in Figs 34–35, median lobe of aedeagus slightly bent, its distal-middle part moderately dilated in dorsal view; dorsal and ventral margins slightly curved and undulate in lateral view; apical orifice pleuropic left; apical lamina flat, rounded at apex, slightly thickened in lateral aspect. Endophallus with two chitinized copulatory pieces, located in the apical half near the left lateral margin; the dorsal one larger in size, longish, markedly bent and acuminate at apex; the ventral one small, spine-like. Left paramere depressed on the dorsal side; right paramere not curved at apex.

Female genitalia: Not examined.

Geographical distribution and habitat. Only known from the Mindanao Island in the Philippines (Map 2) from a very few specimens. Probably found in tropical forests.

Remarks. We examined five other specimens from Philippines in the collection of BMNH, identified as “*discoidalis*”, which actually belong to *C. splendidula* (Fabricius).

[6] *Calleida luzonensis* Casale & Shi, sp. n.

<http://zoobank.org/0AB89DFC-F6A5-49C7-A45D-219EA1AAEC0A>

Figs 36–42, Map 2

Type locality. Philippines, Luzon, Nagtipunan (16.22N, 121.60E).

Type materials. Holotype: male, “Philippines-E Luzon Nagtipunan, Quirino V-2014” (CCA, Figs 36, 37). **Paratypes:** 2 females, same data as holotype, but “July 2014” and “August 2014” (CCA, CRS). 1 female, “Filippine VIII.2014 Dindin, Isabela, eastern Luzon, racc. loc. leg.” (CDG). 1 male, “Eastern Luzon, Sierra Madre, Madela, Tapsoy, Quirino”, “June 2016” (BMNH). 1 male, “Filippine: VIII.2014 Sierra Madre, Tapsoy, Quirino, Eastern Luzon, Ismael leg.” (CCA). 1 female, “Filippine: VIII.014 Nagtipunan, Quirino, Eastern Luzon, Ismael leg.” (CDG). 1 male, “Filippine: Tapsoy, Quirino, Eastern Luzon VIII.2014 (local collectors)” (CDG). 2 females, “Philippine: Luzon, Quirino, Maddela, Disimongal, Sierra Madre. Mar. 2016, local collector” (IZAS).

Specific epithet. The new species is named after its type locality: Luzon Island, Philippines.

Diagnosis. *C. luzonensis* sp. n. is distinct amongst all Asiatic *Calleida* species but close to *C. discoidalis* for: (1) elytra with evident reddish patch on the inner three to five intervals, markedly contrasting with the lateral metallic green intervals; (2) head, antennae, pronotum, legs and underside uniformly yellow reddish; (3) terminal ventrite

with two setae on each side in males, three or more setae in females. The new species is closest to *C. discoidalis* from Mindanao Island, both having very similar external features. Comparing with *C. discoidalis*, *C. luzonensis* sp. n. has the following differences: (1) elytral discal reddish patch usually more reduced, narrower and more prolonged; (2) elytra metallic region generally lighter and more vivid; (3) body size generally a little larger (L = 10.5–11.0mm). The following differences in the median lobe of aedeagus support these two species as distinct: (1) in *C. luzonensis* sp. n. the median lobe smaller in size, shorter and stouter, length about 1.9 mm; in *C. discoidalis* median lobe length about 2.6 mm; (2) in *C. luzonensis* sp. n. apical lamina wider and less developed, length 0.6 time as the basal width, apex not thickened in lateral aspect, versus in *C. discoidalis*, apical lamina longer and more developed, length 0.7 times the basal width, apex a little thickened in lateral aspect; (3) left margin markedly prominent near middle in dorsal aspect in *C. luzonensis* sp. n., and evenly curved in *C. discoidalis*.

As with *C. discoidalis*, *C. luzonensis* might be confused with *C. splendidula*, a sympatric species in the Luzon Island (Philippines) based on their similar habitus and colour, and the evident reddish patch on the elytral disc in both species. Moreover, in one female paratype from Dindin, Isabela (Fig. 39), the reddish patch on the elytral disc is extended from the base to apex only on the sutural interval, and extended on the second and third intervals only near the apex. Therefore, the elytra appear almost completely metallic green and particularly similar to those of *C. splendidula* “var.” *unicolor* Jedlička, which is widely distributed in Philippines.

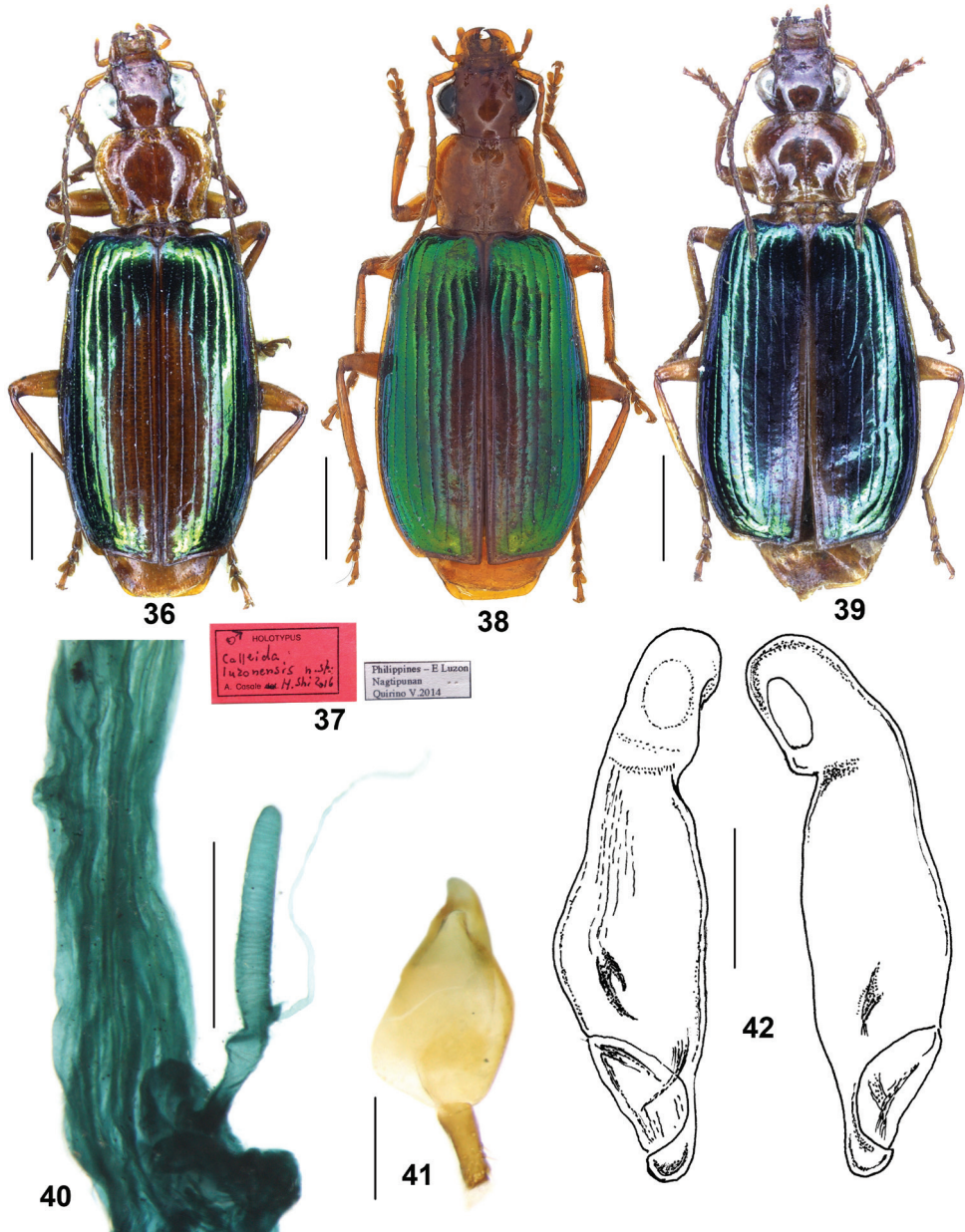
The new species is, however, easily recognized from the latter by the larger size, the multisetose abdominal sternite VII (in the species belonging to *C. splendidula* group, abdominal sternite VII bears only one seta on each side in males, two in females), and for the different aedeagal shape.

Description. *General features* as in Figs 36, 38, 39. Medium-sized species: TL = 10.0–10.5 mm; L = 10.5–11.0 mm.

Colour: Head, antennae, pronotum, underside and legs bright reddish yellow. Elytra bright metallic green, disc with an evident reddish patch, generally one-half to two-thirds as long as the elytra length, widest in apical third of elytra, occupying the inner three to five intervals; reddish patch not reaching elytral base, narrowed to apex, only with the first interval reddish at apex. In one examined specimen (Fig. 39), the reddish patch is rather reduced, extended only to the second and third intervals, thus the elytra are almost completely metallic green.

Lustre and microsculpture: Dorsal surface moderately shiny and polished; head and pronotum with vanished microsculpture; elytra with faint but distinct microsculpture in isodiametric meshes.

Head: Slightly convex, almost impunctate; supraorbital furrows shallow, vanished a little behind the anterior edge of eyes; temporae moderately swollen, gradually narrowed towards the neck; genae shorter than half the length of eyes; antennae reaching the basal fifth of elytra; terminal labial palpomere strongly securiform with truncate apex in males, also dilated much less so in females.



Figures 36–42. *Calleida luzonensis* sp. n. **36** Habitus of holotype (male, Luzon, CCA) **37** Labels of holotype **38** Habitus (female paratype, Luzon, IZAS) **39** Habitus (female paratype, Luzon, CCA) **40** Female reproductive tract (paratype, Luzon, IZAS) **41** Gonocoxa (paratype, Luzon, IZAS) **42** Median lobe of aedeagus, dorsal and ventral views (holotype). Scale bars: 2.0 mm (**36**, **38**, **39**), 0.5 mm (**40**, **42**), 0.2 mm (**41**).

Pronotum: Wider than head, transverse-cordate (ratio PW/PL = 1.19–1.24), depressed on disc. Lateral margins widened and arcuate in front, reflexed and sinuate in the basal third; lateral expansions wide; basal foveae wide, very deep; posterior angles obtuse; disc with shallow transverse wrinkles.

Elytra: Moderately elongate (ratio EL/EW = 1.52–1.65), slightly widened in the posterior third, depressed; basal border complete, extended to the parascutellar stria; striae punctate; intervals subconvex at base, flattened on disc, sparsely punctate; the eighth intervals slightly tumid near apex; apical margin obliquely truncate, weakly concave, with margin slightly thickened at the outer apical angle, which is obtusely rounded.

Ventral side: Abdominal sternites with sparse and short pubescence. Abdominal sternite VII with two setae on each side in males, three to five setae on each side in females.

Male genitalia: As in Fig. 42, median lobe of aedeagus with general features as in *C. discoidalis*, but smaller in size, L = 1.9 mm, more widened and stouter; apical orifice pleuropic left; left margin prominent near middle in dorsal aspect; apical lamina less developed, rounded distally, length about three-fifths as long as the basal width in dorsal aspect; apex not thickened in lateral aspect. Endophallus with two chitinized, small sized, spine-like copulatory pieces, located in the middle area near the left lateral margin, close to each other at base. Left paramere depressed on the dorsal side; right paramere not curved at apex.

Female genitalia (reproductive tract Fig. 40 and gonocoxa Fig. 41): Spermatheca digitiform, about two times length of pedicel, surface faintly whorled, with a very small basal projection; spermathecal pedicel straight, apex markedly swollen; spermathecal gland duct laterally inserted on the basal projection, about same length as spermatheca; glandular area not incrassate, about half length as gland duct, base with small protuberant atrium. Gonocoxite II sub-rectangular, 2.5 times long as the basal width, a little narrowed to apex, apex wildly truncate, not oblique; setose from the middle to apex on both inner and outer margins; outer margin a little curved; apex with membranous extension.

Geographical distribution and habitat. Only known from eastern Luzon Island (Quirino and Isabela provinces) in the Philippines (Map 2). Probably found in tropical forests by local collectors.

Phylogeny and character evolution

As a conclusion of the preliminary character analysis (see remarks under each species and species groups in text and our previous contribution: Casale and Shi 2018), we suggested that the female reproductive tract has important value in infrageneric taxonomy of *Calleida*. Moreover, in some species groups, the *C. splendidula* group in particular, the male genitalia are very homogeneous and make species delimitation difficult, but detailed studies of the female genitalia, especially the spermathecal characters, are expected to facilitate a solution in future studies. To interpret the evolution of female reproductive tract characters better, and to reveal the position of each species in the non-monophyletic *C. discoidalis* group, a very preliminary attempt of phylogenetic analysis was conducted.

Characters and matrix

A total of 24 characters were selected, which included nine female genital characters, four male genital characters, four sexual dimorphic characters, and seven external characters. Two of the characters were multistate, whereas the others were binary. Although all characters were unordered in the phylogenetic analysis (without demonstration of character polarities), the supposed plesiomorphic states were coded “0”. A total of 18 species containing representatives of all nine species groups (defined in Casale and Shi 2018) of Asiatic *Calleida* was included in the phylogenetic analysis, but two of them lacked female or male genitalia characters respectively. The Australia-Asiatic genus *Anomotarus* was selected as out-group. The information on the matrix is found in Table 1. The character coding is shown below:

- 1 Spermathecal basal projection: (0) absent, (1) present.
- 2 Spermatheca basal sclerotized plate (*annulus receptaculi*): (0) absent, (1) present.
- 3 Whorl on spermatheca: (0) strong, (1) absent or very faint.
- 4 Apical protuberance of spermathecal pedicel: (0) absent, (1) present.
- 5 Spermathecal pedicel shape: (0) near straight, (1) strongly curved or curled.
- 6 Spermathecal pedicel length: (0) less than or subequal to spermatheca, (1) longer than spermatheca.
- 7 Spermathecal gland duct insertion: (0) ventrally, (1) laterally.
- 8 Spermathecal glandular area: (0) not or weakly incrassate, (1) distinctly inflated.
- 9 Gonocoxite II apex: (0) subulate, (1) oblique truncate.
- 10 Ventral lobe on aedeagus: (0) absent, (1) present.
- 11 Male aedeagus venter: (0) plain or lobed, (1) ridged or markedly concaved.
- 12 Primary (ventral) copulatory piece of endophallus: (0) shorter than half length of median lobe, (1) longer than length of median lobe, flagellum-like, (2) absent or very weakly defined.
- 13 Secondary (dorsal) copulatory piece of endophallus: (0) well chitinized, (1) absent or very weakly defined.
- 14 Apex of abdominal sternite VII in males: (0) straight, (1) notched.
- 15 Setae on each side of male abdominal sternite VII: (0) one seta, (1) normally two, exceptionally three setae, (2) three or more setae.
- 16 Setae on each side of female abdominal sternite VII: (0) two setae, (1) three or more setae.
- 17 Female terminal labial palpomere: (0) same as in males, securiform, (1) less dilated than in males.
- 18 Antennomeres I–III except primary setae: (0) glabrous, (1) with accessory setae.
- 19 Pronotum anterior angles: (0) glabrous, (1) setose.
- 20 Elytra: (0) uniformly metallic, (1) disc with reddish patch.
- 21 Elytral apical margin: (0) straight or weakly concaved, (1) strongly concaved.
- 22 Elytral outer apical angles: (0) rounded or obtuse, (1) sharply angulate.
- 23 Elytral margins on apical outer angles: (0) more or less thickened, (1) not thickened.
- 24 Ratio elytra length/width: (0) between 1.5 to 1.75, (1) greater than 1.8.

Table 1. Characters matrix for Asiatic *Calleida* and the out-group *Anomotarus stigmula*. “?” = missing data.

Taxa / Character	000000000111111111122222 123456789012345678901234
<i>Anomotarus stigmula</i> (Chaudoir)	000000011002000010000010
<i>C. gressittiana</i> Casale & Shi	?????????001110011100010
<i>C. puncticollis</i> Shi & Casale	000000000002102100000010
<i>C. excelsa</i> Bates	000000111000010011110011
<i>C. jelineki</i> Casale & Shi	000000111000010010100011
<i>C. corporaali</i> Andrewes	011000101100110010001100
<i>C. viet</i> Casale & Shi	011000101100110010001100
<i>C. borneensis</i> Shi & Casale	1011111010000010010001000
<i>C. doriae</i> Bates	101100100010010010000000
<i>C. lepida</i> Redtenbacher	101101100010010010000000
<i>C. sultana</i> Bates	101101100010010010100000
<i>C. cf. splendidula</i> (Fabricius)	101011101000010010010000
<i>C. tenuis</i> Andrewes	101011101000010010000000
<i>C. onoha</i> Bates	101001101000010010000000
<i>C. luzonensis</i> sp. n.	100000101000011110010000
<i>C. cochinchinae</i> sp. n.	0000001?1??????100010011
<i>C. piligera</i> sp. n.	011000100000012110000000
<i>C. fukiensis</i> Jedlička	100000101000011110000000
<i>C. yunnanensis</i> sp. n.	100000101100011110010000

Most of the materials used in the phylogenetic analysis were cited in the present and our previous contribution (Casale and Shi 2018). Localities for examined materials of species not cited previously are shown below:

Anomotarus stigmula (Chaudoir): India (Andhra Pradesh)

Calleida lepida Redtenbacher: China (Jiangxi)

Calleida sultana Bates: China (Yunnan)

Calleida cf. splendidula (Fabricius): China (Guangxi)

Calleida tenuis Andrewes: Malaysia (Sabah)

Calleida onoha Bates: Japan (Okinawa)

Phylogenetic analysis

The phylogeny reconstruction was performed using WIN-PAUP* Version 4.0b10 with the following parameters: Optimality criterion = parsimony; all characters were unordered; starting tree(s) was obtained via stepwise addition; addition sequence: random; number of replicates = 1000; number of trees held at each step during stepwise addition = 10; branch-swapping algorithm: TBR; steepest descent option not in effect; initial ‘MaxTrees’ setting = 100; ‘MulTrees’ option in effect; topological constraints not enforced; trees unrooted; bootstrap method with heuristic search; and number of bootstrap replicates = 1000. Branches with bootstrap values greater than 50% were maintained.

Both the equal weighting (EW) method and the successive weighting (SW) method were used in the phylogeny reconstruction. But, because of a limited number of characters, several branches in the cladogram with EW method were not expanded. So, only the cladogram generated with the SW analyses is presented in Fig. 43. In the SW analysis, 66 most parsimonious trees were obtained. The length and indices for each most parsimonious tree were as follow: Tree length = 25.6–26.4; consistency index (CI) = 0.682–0.704; retention index (RI) = 0.812–0.830; and rescaled consistency index (RC) = 0.554–0.584.

Results

In the cladogram generated with the SW method, the monophyly for each species group was corroborated with the exception of the *C. discoidalis* group which was posited as a polyphyletic group (blue color branches in the cladogram). Several relationships among species groups were suggested with relatively high reliabilities.

In our previous contribution (Casale and Shi 2018), two rather isolated lineages in the Asiatic *Calleida* were proposed mainly on their special male endophallus characters. One of them, the *C. puncticollis* species group, formed the earliest branch of Asiatic *Calleida* in the cladogram. In contrast, another primary lineage, the *C. gressittiana* group, did not form an isolated clade in the cladogram. Instead, it was grouped in the *C. lativittis* group, but because *C. gressittiana* is the only species with female genitalia unknown, this relationship is questionable.

The polyphyletic *C. discoidalis* group was composed of three isolated lineages. **Lineage I** containing only one known species, *C. cochinchinae*, was suggested as a relatively early branch in the cladogram. A monophyletic or paraphyletic group of lineage I + *C. lativittis* group was presumed, supported by the similarities on female reproductive tract shape (type II) and elongate elytra (character 24). **Lineage II** containing only one known species, *C. piligera*, was suggested as the sister group of the *C. terminata* group by a moderately high bootstrap value (= 66). Such relationship was also well founded by the presence of the basal plate on female reproductive tract (type IV). **Lineage III** containing four known species (three species selected in the phylogenetic analysis, which belong to the *C. discoidalis* group). The monophyly of lineage III was well supported (= 81) and can be also inferred by the similar female reproductive tracts (type IV).

Five species groups and two lineages of the *C. discoidalis* group formed a monophyletic clade (= 70), containing more than 80% described species of Asiatic *Calleida*. Under this clade, the *C. splendidula* group, *C. borneensis* group, *C. doriae* group, and *C. chloroptera* group are closer to each other than to the other branches. The closer relationships among them were also supported by their similar female reproductive tracts (type V).

The monophyly of these four groups and their relationships were unresolved in the cladogram, but it was suggested that the *C. doriae* group + *C. chloroptera* group are monophyletic (= 81), and *C. borneensis* is close to *C. splendidula* group.

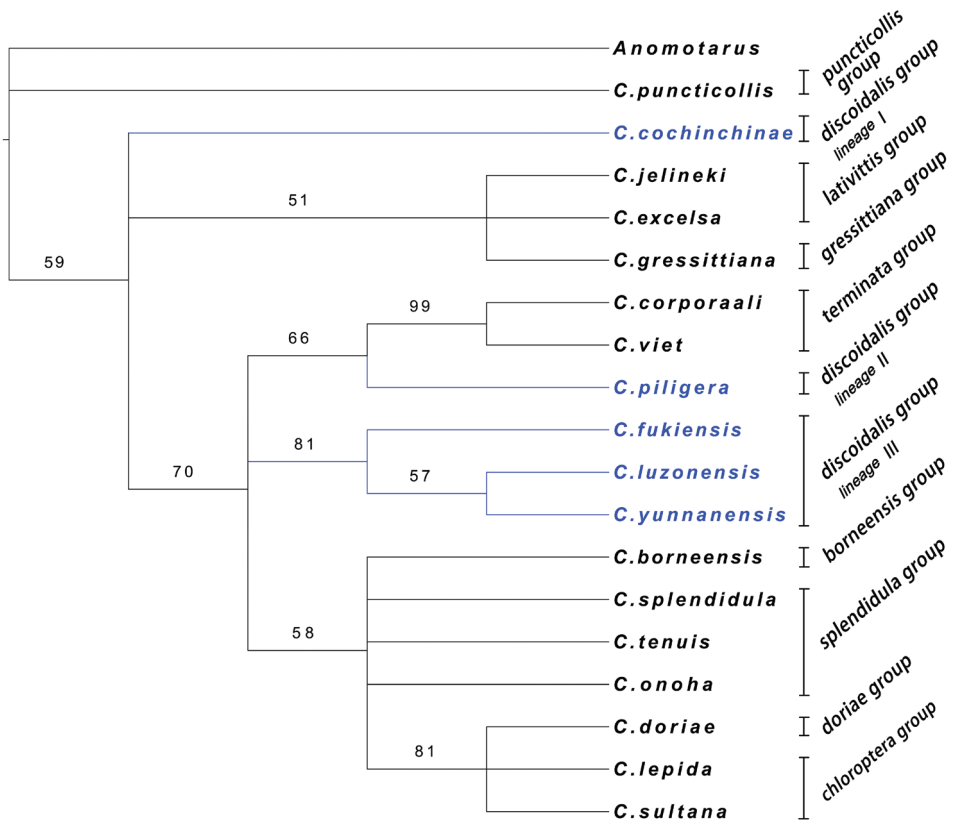


Figure 43. Cladogram of Asiatic *Calleida* species relationships obtained by the SW method with bootstrap values greater than 50%. Species group membership is shown in the right side. The polyphyletic *C. discoidalis* species group is in blue.

Character evolution for female reproductive tract

The character evolution analysis was based on the cladogram obtained with the SW analysis. In this cladogram, only the eight characters (1–8) of female reproductive tract were analyzed. Character evolution was marked on the branches. For homoplastic transformations, the maximum parsimonious assumption was accepted with parallelisms priority to reversals. Spermathecae for all available species contained in the phylogenetic analysis were illustrated in Fig. 44.

Three of the eight female reproductive tract characters were considered having apomorphic conditions (solid spots in Fig. 44), with spermathecal gland duct insertion (char. 7) transformed from ventrally to laterally, which supported the *C. puncticollis* group as the earliest branch of Asiatic *Calleida*. The presence of a well sclerotized basal plate (char. 2) supported the monophyly of the *C. terminata* group + *C. discoidalis* group lineage II, both with well defined type III spermathecae. The elongate spermathe-

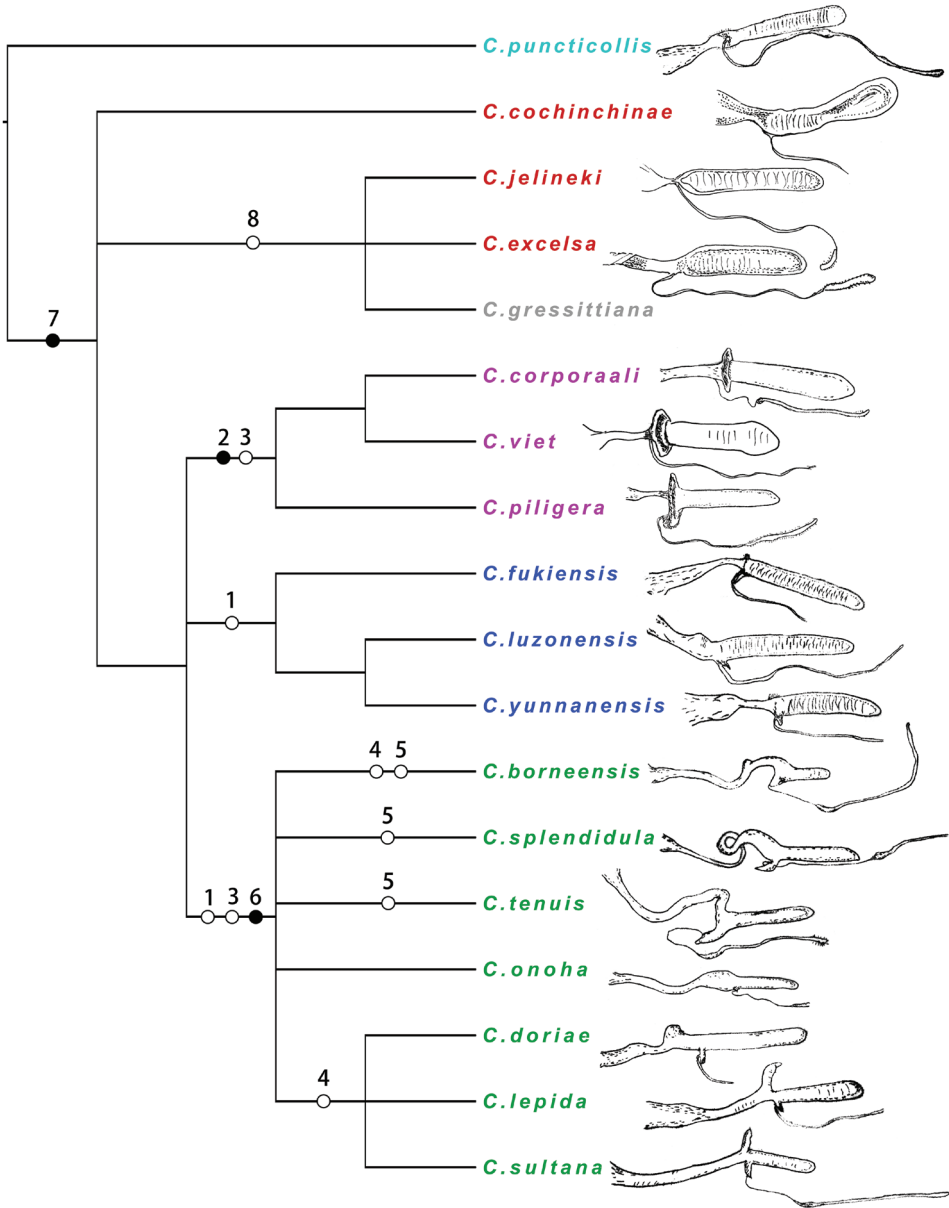


Figure 44. Possible character evolutions for female reproductive tracts in Asiatic *Calleida* species. Solid spots represent apomorphies; empty circles represent homoplasy. Five types of spermathecae are shown in different colors on taxa: type I (cyan), type II (red), type III (purple), type IV (blue), type V (green).

ecal pedicel (char. 6) supported a monophyletic clade of four species groups (*C. splendidula*, *C. borneensis*, *C. doriae*, and *C. chloroptera* groups) with spermatheca type V.

The remaining five characters had homoplastic or ambiguous transformations (empty circles in Fig. 44). Two of them (char. 1 and char. 3) were considered important,

supporting three monophyletic clades (corresponding to female reproductive tract type III, type IV, and type V). But, the apomorphic transformation assumptions of these two characters were conflicted on solving relationships among these three clades. Two other characters (char. 4 and char. 5) only transformed inside the monophyletic clade of *C. splendidula* group + *C. borneensis* group + *C. doriae* group + *C. chloroptera* group, but they did not support a phylogenetic relationship except for the monophyly of *C. doriae* group + *C. chloroptera* group, which was supported by the presence of apical protuberance of spermathecal pedicel (char. 4).

Female reproductive tract category

Five types of female reproductive tracts were recognized corresponding to five lineages in the cladogram (different colors in Fig. 44). Four of them were suggested as monophyletic, while the monophyly of the type II was neither supported nor objected by the cladogram.

- Type I** Spermatheca distinctly whorled; spermathecal gland duct ventrally inserted; spermathecal base and pedicel apex not modified. Type I was supposed to be a very special and isolated type in Asiatic *Calleida*, only represented by the *C. puncticollis* group. In this species, also the absence of copulatory piece in endophallus is unique.
- Type II** Similar to type I, but spermathecal gland duct laterally inserted. Present in the *C. lativittis* group and lineage I of the *C. discoidalis* group. The type II also showed several primary characters, but can be separate from type I by the different position of spermathecal gland duct insertion.
- Type III** Spermatheca not or very faintly whorled; spermatheca with a well sclerotized basal plate (*annulus receptaculi*); spermathecal pedicel narrow and short. Present in the monophyletic clade of *C. terminata* group + *C. discoidalis* group lineage II. Type III is well recognized for its highly modified *annulus receptaculi*. The modified spermathecal base and the not or very faintly whorled spermatheca suggest a relationship to the type V.
- Type IV** Spermatheca distinctly whorled, with a distinct basal projection; spermathecal pedicel short and partly expanded; atrium very weakly defined. Present in lineage III of the *C. discoidalis* group.
- Type V** Present in the monophyletic clade of *C. splendidula* group + *C. borneensis* group + *C. doriae* group + *C. chloroptera* group, containing more than half of described Asiatic *Calleida* species. Type V is a highly modified and diverse type, recognized by the not or very faintly whorled spermatheca, strongly elongate spermathecal pedicel, and the presence of spermathecal basal projection. The elongate spermathecal pedicel is curved or curled, and/or has an apical protuberance in some taxa. The variable spermathecal pedicel in type V could be important in species definition of the *C. splendidula* group.

Conclusion

The phylogeny reconstruction partly supported the monophyly of most species groups, but the *C. discoidalis* group was proved to be polyphyletic with three isolated lineages. Some relationships amongst species groups were solved, but many branches had relatively low bootstrap value, while some others were unexpanded. Because of the above insufficiency, we did not tend to revise the definition of species groups on the phylogeny results, and just regard it as a very preliminary attempt to reveal species relationships.

The results of character evolution analysis showed that the female reproductive tract has very important taxonomic value in *Calleida*. Five distinct types of female reproductive tracts were recognized, corresponding to four monophyletic and one paraphyletic branches in the cladogram. Future studies are expected to solve character transformation polarity and better evaluate taxonomic value, when more materials will be examined, such as Afrotropical and Neotropical *Calleida* species, and allied genera of Calleidina such as the African genus *Lipostratia* Chaudoir and the Australian genus *Demetrida* White.

Acknowledgements

We wish to thank the following curators and colleagues for access to materials under their care: Mr Changchin Chen (CCCC), Mr Augusto De Giovanni (CDG), Dr David Wrase (ZSM), Dr Riccardo Sciaky (CRS), Dr Peter Bulirsch (CPB), Prof. Guodong Ren (HBUM), Dr Hongbin Liang (IZAS), Dr Thierry Deuve, Ms H el ene Perrin and Ms Azadeh Taghavian (MNHN), Dr Max Barclay, Ms Beulah Garner and Ms Christine Taylor (BMNH), Dr Eric Kirschenhofer (NHMW), Dr Josef Jel inek, Dr Ji r ı H ajek and Martin Fik a cek (NMPC), Dr Olaf J ager (SMTD), Prof. Mingyi Tian (SCAU), and Prof. Hong Pang (SYUM). Special thanks are to Dr Dirk Ahrens (ZMFK) for his help of taking photograph of holotype of *C. fukiensis*. This work was partially supported by the Special Fund for Forest Scientific Research in the Public Welfare (No. 201504304) and the Natural Science Foundation of China (No. 31401992).

References

- Casale A (1998) Phylogeny and biogeography of Calleidina (Coleoptera: Carabidae: Lebiini): a preliminary survey. In: Ball GE, Casale A, Vigna Taglianti A (Eds) Phylogeny and Classification of Caraboidea. Proceedings of a Symposium. 28 August, 1996, Florence, Italy. XX International Congress of Entomology. Atti Museo regionale di Scienze naturali, Torino, 381–428.
- Casale A, Shi HL (2018) Revision of the Oriental species of *Calleida* Latreille (*sensu lato*). Part 1: introduction, groups of species, and species of six species groups (Coleoptera: Carabidae: Lebiini). *Zootaxa* 4442(1): 1–42. <https://doi.org/10.11646/zootaxa.4442.1.1>

- Heller KM (1921) New Philippine Coleoptera. *The Philippine Journal of Science* 19: 523–627. <https://doi.org/10.5962/bhl.part.1235>
- Kabak I (2017) Lebiini: Calleidina. In: Löbl I, Löbl D (Eds) *Catalogue of Palaearctic Coleoptera*. Vol. 1. Archostemata – Myxophaga – Adepaga. Revised and Updated Edition. Brill NV, Leiden, 580–582.
- Jedlička A (1953) Neue Carabiden aus der chinesischen Provinz Fukien. *Entomologische Blätter*, Krefeld 49: 141–147.
- Jedlička A (1963) Monographie der Truncatipennen aus Ostasien, Lebiinae-Odacanthinae-Brachyninae (Coleoptera, Carabidae). *Entomologische Abhandlungen und Berichte aus dem Staatlichen Museum fuer Tierkunde in Dresden* 28: 269–579.
- Kirschenhofer E (1986) Neue Arten truncatipenner Carabidae der palaearktischen und orientalischen Region unter besonderer Berücksichtigung der Aufsammlungen Eigin Suensons in Ostasien (Coleoptera, Carabidae). *Entomofauna* 7(23): 317–348.
- Lorenz W (2005) *Systematic List of Extant Ground Beetles of the World (Insecta Coleoptera Geadphaga: Trachypachidae and Carabidae Incl. Paussinae, Cicindelinae, Rhysodinae)*, second edition. Wolfgang Lorenz, Tutzing, Germany, 530 pp.

Nine new species of *Clada* from Madagascar (Coleoptera, Ptinidae)

Petr Zahradník¹, Miloš Trýzna²

1 Forestry and Game Management Research Institute, Strnady 136, CZ-150 00 Praha 5-Zbraslav, Czech Republic **2** Czech University of Life Sciences, Faculty of Forestry and Wood Sciences, Department of Forest Protection and Entomology, Kamýčká 1176, CZ-165 21 Praha 6-Suchbát, Czech Republic

Corresponding author: Petr Zahradník (zahradnik@vulhm.cz)

Academic editor: T.K. Philips | Received 29 October 2018 | Accepted 17 September 2018 | Published 13 December 2018

<http://zoobank.org/996E3193-C180-461C-B3E5-82BB5E0014A1>

Citation: Zahradník P, Trýzna M (2018) Nine new species of *Clada* from Madagascar (Coleoptera, Ptinidae). ZooKeys 806: 121–140. <https://doi.org/10.3897/zookeys.806.21916>

Abstract

Nine new species of the genus *Clada* (s. str.) Pascoe, 1887 (Bostrichoidea: Ptinidae: Eucradinae) are described from Madagascar: *Clada* (*Clada*) *barclayi* sp. n., *C. (C.) dimbyi* sp. n., *C. (C.) fasciata* sp. n., *C. (C.) lalae* sp. n., *C. (C.) madagascarensis* sp. n., *C. (C.) mamyi* sp. n., *C. (C.) njakai* sp. n., *C. (C.) obesa* sp. n., and *C. (C.) rindrai* sp. n. No species of this genus were previously known from Madagascar. Photographs of the dorsal habitus and drawings of the male and female antennae and aedeagi of most of these species are given.

Keywords

Afrotropical region, *Clada*, Coleoptera, Madagascar, new species, Ptinidae, taxonomy

Introduction

Madagascar is a large island (almost 600 mil. km²) with diverse natural conditions influenced by various geographical and climatic conditions, and also by an exceptionally rich tree flora. Most species of Ptinidae are xylophagous or fungivorous. No recent papers on the family Ptinidae from this region have been published, except the subfamily Ptininae (Bellés 1987, 1991; Philips 2005).

Many descriptions of species (almost all of them endemics in Madagascar, a few of them also occur on some neighbouring islands or in continental Africa, and a few are widely distributed or cosmopolitan) are known from older descriptions by M. Pic and some other authors. These descriptions tend to be very short, without pictures, only some of them are modern with illustrations, especially of the aedeagus. Madagascar's fauna of Ptinidae is surely richer. This is our first contribution on this family from Madagascar.

The subfamily Eucradinae LeConte, 1861 contains two tribes, Eucradini LeConte, 1861, with the North American genus *Eucrada* LeConte, 1861 and Hedobiini Mulsant et Rey, 1868, with five genera distributed worldwide, *Anhedobia* Nakane, 1963, *Clada* Pascoe, 1887, *Hedobia* Dejean, 1821, *Neohedobia* Fisher, 1919 and *Ptinomorphus* Mulsant et Rey, 1868. Sexual dimorphism is typical of all species in the tribe Eucradini. Males have more pectinate antennae, and females less pectinate. Genera in the tribe Hedobiini have slightly serrate antennae. Only the genus *Clada* is atypical, with serrate antennae in both sexes in some species, while in others, the antennae of the male are pectinate, and those of the female serrate, and in some species antennae are pectinate in both sexes. White (1974) placed this genus in the subfamily Dryophilinae LeConte, 1861, while other authors have put it in the subfamily Eucradinae. The lateral edge of the pronotum in the subfamily Eucradinae is absent, but the subfamily Dryophilinae has the lateral edge distinct. Moreover, genera of the subfamily Dryophilinae have filiform antennae.

The genus *Clada* (Eucradinae: Hedobiini) contains two subgenera, *Taiwanoclada* Sakai, 1987 from Taiwan with only one species, and the nominal subgenus with 50 species from the Palaearctic, Oriental, and Afrotropical regions. From the sub-saharan African and southern African regions, the following species are known:

<i>C. (C.) basilewskyi</i> Español, 1969	Tanzania
<i>C. (C.) costipennis</i> Kolbe, 1897	Tanzania
<i>C. (C.) flabellicornis</i> Pic, 1936	Zaire
<i>C. (C.) granulata</i> Español, 1972	South Africa
<i>C. (C.) humeralis</i> Pic, 1926	Congo, Kenya, Tanzania
<i>C. (C.) laticollis</i> Pic, 1947	Ethiopia, Kenya
<i>C. (C.) lineatipennis</i> Pic, 1926	Ivory Coast
<i>C. (C.) longicornis</i> Pic, 1934	Kenya
<i>C. (C.) multistriata</i> Pic, 1952	Benin
<i>C. (C.) rugosa</i> Pic, 1915	Benin, Ivory Coast
<i>C. (C.) waterhousei</i> Pascoe, 1887	South Africa

In Madagascar, no species of the genus *Clada* were known. Overall, only 48 species and subspecies of Ptinidae are known from Madagascar, 18 from the subfamily Ptiniinae, one from Ernobiinae, five from Anobiinae, seven from Xyletininae, seven from Mesocoelopodinae, and ten from Dorcatominae (Español 1969a; Pic 1896, 1912a, b, 1949, 1952).

Materials and methods

We have studied all the original descriptions of species in the subgenus *Clada* from Central and South Africa and also some other descriptions from neighbouring countries (including India, with some similar species) (Español 1969b, 1972; Kolbe 1897; Pascoe 1887; Pic 1915, 1926, 1934, 1936, 1947, 1952). Specimens of new species have been given a red printed label with the following text: “Holotype” or “Paratype”. On the second white printed label is the following text: “name of species. sp. n., P. Zahradník et M. Trýzna det.”.

The type materials are deposited in the following collection:

- NHMUK** Natural History Museum, London, U.K.
MTDC Miloš Trýzna collection, Děčín, Czech Republic
FGMRI Forestry and Game Management Research Institute, Jíloviště, Czech Republic (P. Zahradník)
LBVC Lukáš Blažej collection, Varnsdorf, Czech Republic

Descriptions

Clada (Clada) barclayi sp. n.

<http://zoobank.org/3024EF07-9FDF-4F02-AC93-8AE41CCEB249>

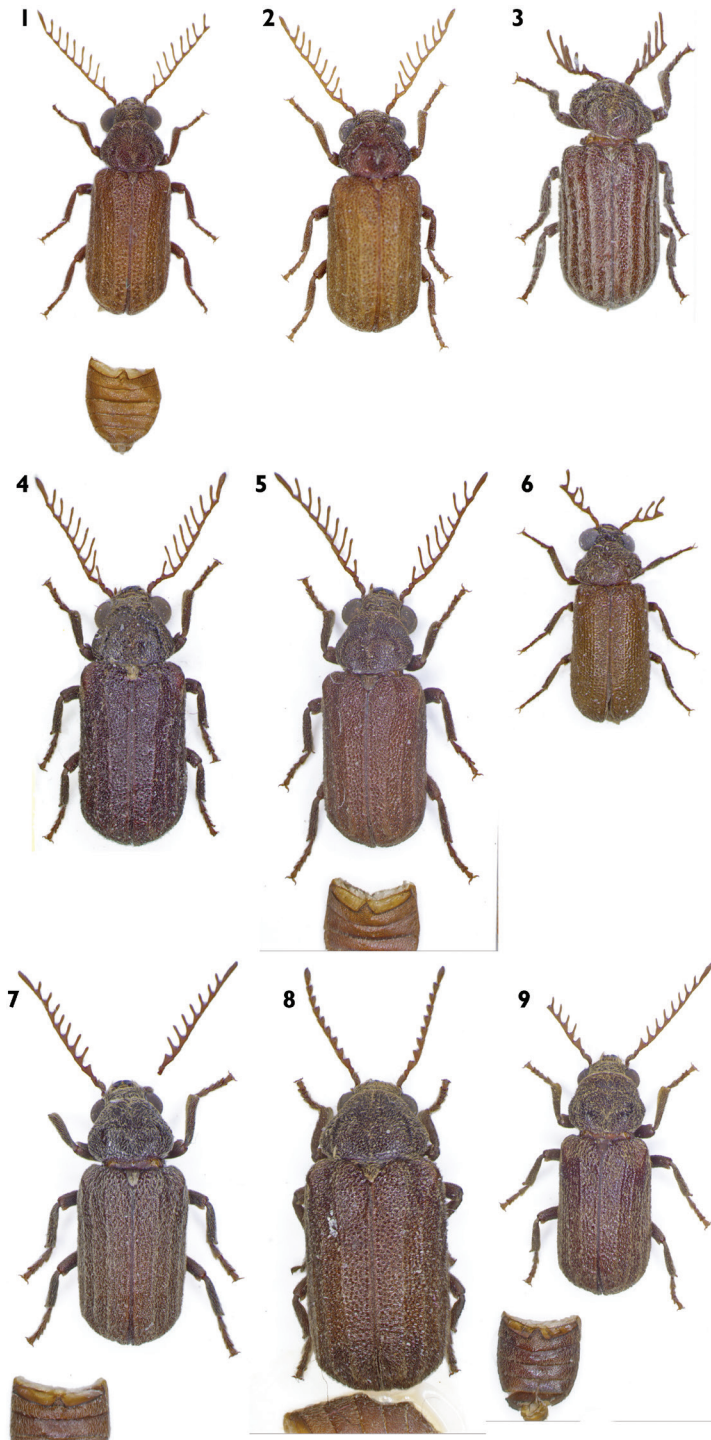
Figs 1, 10, 19a, b, 28

Type material. Holotype male: Madagascar, Mahajanga prov., Ampatika env., Mahajamba riv., 17.–19.xi.1995, I. Jeniš lgt. (FGMRI). **Paratype (1):** 1 female, Madagascar, Morondava prov., Maronfandilia, 4.–5.xii.1995, J. Stolarczyk lgt. (FGMRI).

Differential diagnosis. This species is similar to *C. (C.) humeralis* Pic, 1926, but differs by lighter colour of the elytra and missing lighter humeri. Fully differs by shape of the aedeagus. Fully differs by shape of the aedeagus. For differences from other Madagascan species, see key.

Description. Male (holotype). Elongate-elliptical, transversally convex. Body length 5.8 mm, maximum width 2.2 mm (Figure 1). Ratio length:width of elytra 1.7. Body light brown, also antennae, maxillary and labial palpi and legs, only pronotum and head darker. Pubescence yellowish white.

Head matt shiny, with double punctation – first coarse, dense, umbilicate, distance between punctures approximately the same as their diameter; second is very fine, punctures almost touching. Pubescence recumbent or semi-erect, long, inclined more or less forwards. Anterior part of head with shallow deepening. Clypeus with shallow transverse depression. Eyes large, globular with short erect sparse pubescence. Frons 1.6 times as wide as diameter of eye, from dorsal view. Antennae consisting of eleven antennomeres, 3rd to 10th pectinate (Figure 19a). First antennomere robust, twice as long as wide; second smallest, one-half as long as first, almost as wide as long. 3rd 1.4 times



Figures 1–9. Habitus. **1** *C. (C.) barclayi* sp. n. **2** *C. (C.) dimbyi* sp. n. **3** *C. (C.) fasciata* sp. n. **4** *C. (C.) lalae* sp. n. **5** *C. (C.) madagascarensis* sp. n. **6** *C. (C.) mamyi* sp. n. **7** *C. (C.) njakai* sp. n. **8** *C. (C.) obesa* sp. n. **9** *C. (C.) rindrai* sp. n.

as wide as long, 4th to 8th 2.1 as wide as long; 9th and 10th 1.7 times as wide as long. Apical antennomere longest, oblong oval, 5 times as long as wide. All antennomeres on margin with short erect dense setae. Apical maxillary palpomere long, spindle shaped.

Pronotum convex, matt shiny, rounded, transverse (ratio length:width of pronotum 0.8); widest on one half, but only slightly. Base of pronotum finely bordered. Middle of pronotum at base with small, blunt swelling, posteriorly slightly sharpened. Surface of pronotum with double punctation: one coarse, dense, umbilicate, distance between punctures approximately one-half their diameter; other one is very fine, punctures almost touching. Pubescence short, sparse, recumbent, inclined more or less forwards.

Scutellum almost triangular, narrow, 1.4 times as long as wide, dense recumbent pubescence, inclined backwards.

Elytra oval, transversally convex, shiny, with distinct humeri. Each elytron with five fine costae, almost invisible, but apex more distinct. Surface of elytra with double punctation: one coarse, dense, umbilicate, distance between punctures approximately the same as their diameter; the other one is very fine, punctures almost touching. Pubescence relatively sparse, recumbent or semi-erect, inclined backwards. Posterior margin of each elytron with approximately 25 small teeth.

Legs stout, with short and dense recumbent pubescence. All tarsi robust, same length as tibia. 1st metatarsomere as long as 2nd and 3rd together, same width, slightly emarginate on top, 4th slightly shorter than previous, more emarginate, almost to 2/3 of their length. 5th same length as 3rd and 4th together, rectangular, wider on the top, with two large claws, without teeth.

For *aedeagus* see Figure 28.

Female. Habitually the same as male, only antennae serrate (Figure 19b). 1st antennomere robust with dense long erect hairs. 2nd small, as wide as 1st, half as long as previous, as long as wide. Antennomeres 3th to 10th serrate. 3rd and 4th twice longer than wide; 5th 2.3 longer than wide; 6th twice longer than wide; 7th 1.7 times longer than wide; 8th to 10th twice longer than wide. Apical antennomere longest, oblong oval, 3.3 times longer than wide. Body length 6.8 mm, maximum width 2.9 mm. Ratio length:width of elytra 1.8.

Name derivation. Patronym, dedicated to our friend and colleague Maxwell VL Barclay (Natural History Museum, London).

Biology. Unknown.

Distribution. This species is found in the western part of Madagascar (Figure 10).

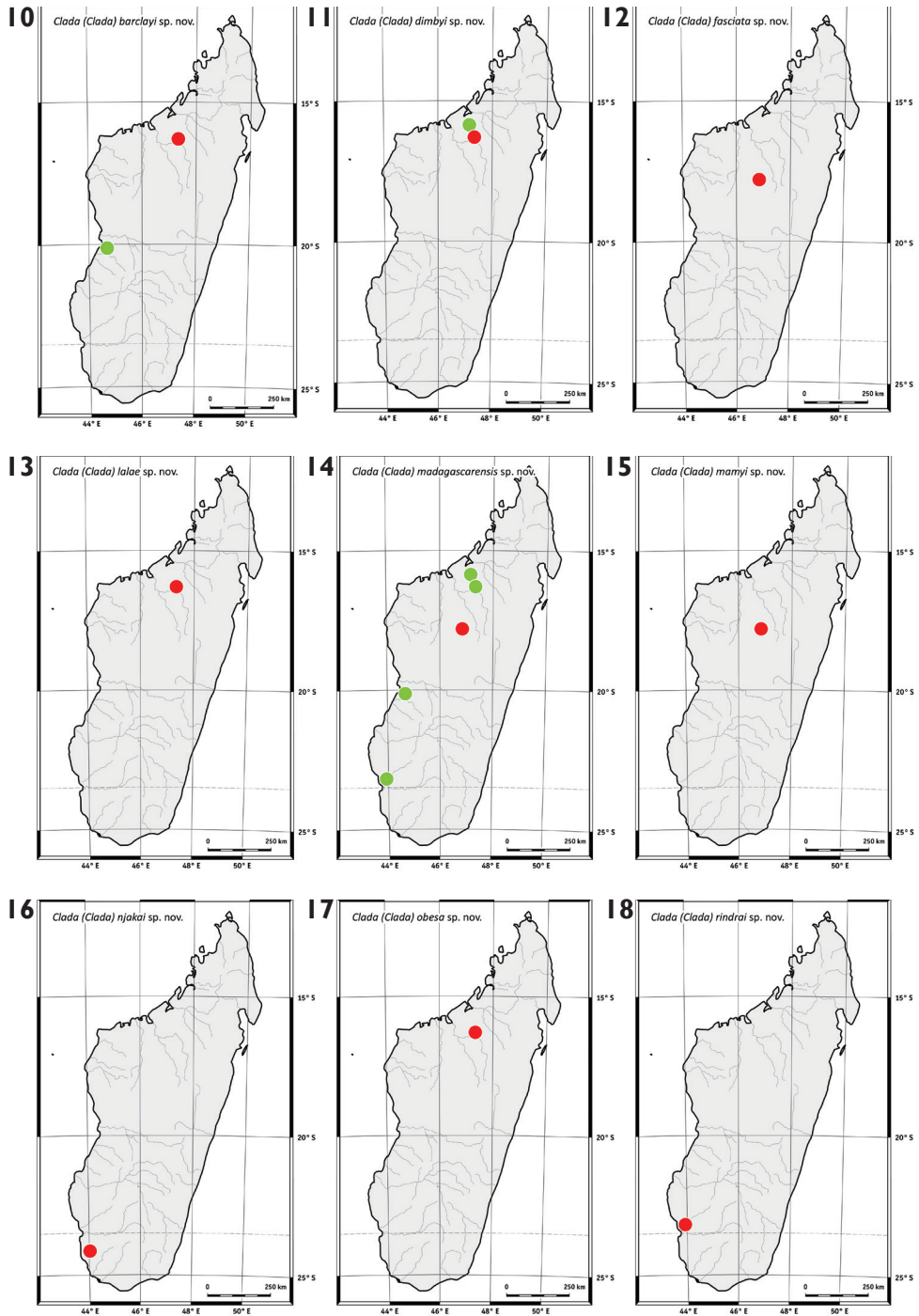
***Clada (Clada) dimbyi* sp. n.**

<http://zoobank.org/1591559C-96BE-4553-B410-39F33E8C2167>

Figs 2, 11, 20, 29

Type material. Holotype male: Madagascar, Mahajanga prov., Mahajamba riv., Ampatika env., 17.–19.xi.1995, I. Jeniš lgt. (FGMRI). **Paratype(1):** 1 male, Madagascar, Mahajanga prov., Ambodimanga, Ankolia riv., 14.–15.xi.1995, J. Stolarczyk lgt. (FGMRI).

Differential diagnosis. The species is similar to *C. (C.) humeralis* Pic, 1926, but differs by the lighter colour of the elytra and absence of lighter coloured humeri. Fully



Figures 10–18. Maps of distribution. **10** *C. (C.) barclayi* sp. n. **11** *C. (C.) dimbyi* sp. n. **12** *C. (C.) fasciata* sp. n. **13** *C. (C.) lalae* sp. n. **14** *C. (C.) madagascarensis* sp. n. **15** *C. (C.) mamyi* sp. n. **16** *C. (C.) njakai* sp. n. **17** *C. (C.) obesa* sp. n. **18** *C. (C.) rindrai* sp. n.

differs by shape of the aedeagus. Fully differs by shape of the aedeagus. For differences from other Madagascan species, see key.

Description. Male (holotype). Elongate-elliptical, transversally convex. Body length 5.9 mm, maximum width 2.9 mm (Figure 2). Ratio length:width of elytra 1.6. Body light brown, head and pronotum brown, antennae and legs partly darker. Pubescence white.

Head matt-shiny, with double punctation – one coarse, dense, umbilicate, distance between punctures approximately the same as their diameter; other is very fine, punctures almost touching. Pubescence recumbent or semi-erect, long, mostly inclined forwards, partly to centre of head, on vertex backwards. Clypeus with shallow, transverse depression. Eyes large, globular with short erect sparse pubescence. Frons twice as wide as diameters of eye, in dorsal view. Antennae consisting of eleven antennomeres; 3rd to 10th pectinate (Figure 20). 1st antennomere robust, twice as long as wide; 2nd smallest, only 1/3 as long as 1st, as long as wide, the same width as 1st. 3rd 1.3 times as wide as long; 4th and 5th 2.1 times as wide as long; 6th, 7th and 9th 1.9 times as wide as long; 8th twice wider as long; 10th 1.6 times as wide as long. Apical antennomere longest, oblong oval, 5.7 times as long as wide. All antennomeres with short recumbent pubescence, only 1st and 2nd with a few long semi-erect setae. Apical maxillary palpomere long, spindle shaped.

Pronotum convex, matt-shiny, transverse (ratio length:width of pronotum 0.8); widest in posterior 2/3. Base of pronotum finely bordered. Middle of pronotum at base with a small blunt swelling, posteriorly slightly sharpened. Surface of pronotum with coarse, dense, umbilicate punctation, distance between punctures smaller than their diameter. Pubescence long, sparse, recumbent, inclined more or less forwards.

Scutellum large, longitudinally trapezoidal, 1.2 times as long as wide, densely recumbent pubescence, inclined backwards, surface shining with fine, dense punctures.

Elytra oval, transversally convex, shiny, with distinct humeri. Each elytron with five very fine costae. Surface of elytra irregularly punctated with punctures of different diameters, coarse, dense, umbilicate. Pubescence relatively sparse, recumbent, on sides also semi-erect, inclined backwards. Posterior margin of each elytron with approximately 25 very small teeth.

Legs stout, with short and dense recumbent pubescence. Mesotibia on the apex with short forked projection. All tarsi robust, the same length as tibia. 1st metatarsomere as long as 2nd and 3rd together, the same width, slightly emarginate on top, 4th slightly shorter than previous, more emarginate, almost to 2/3 of their length. 5th the same length as 3rd and 4th together, rectangular, wider on the top, with two large claws, without teeth.

For *aedeagus* see Figure 29.

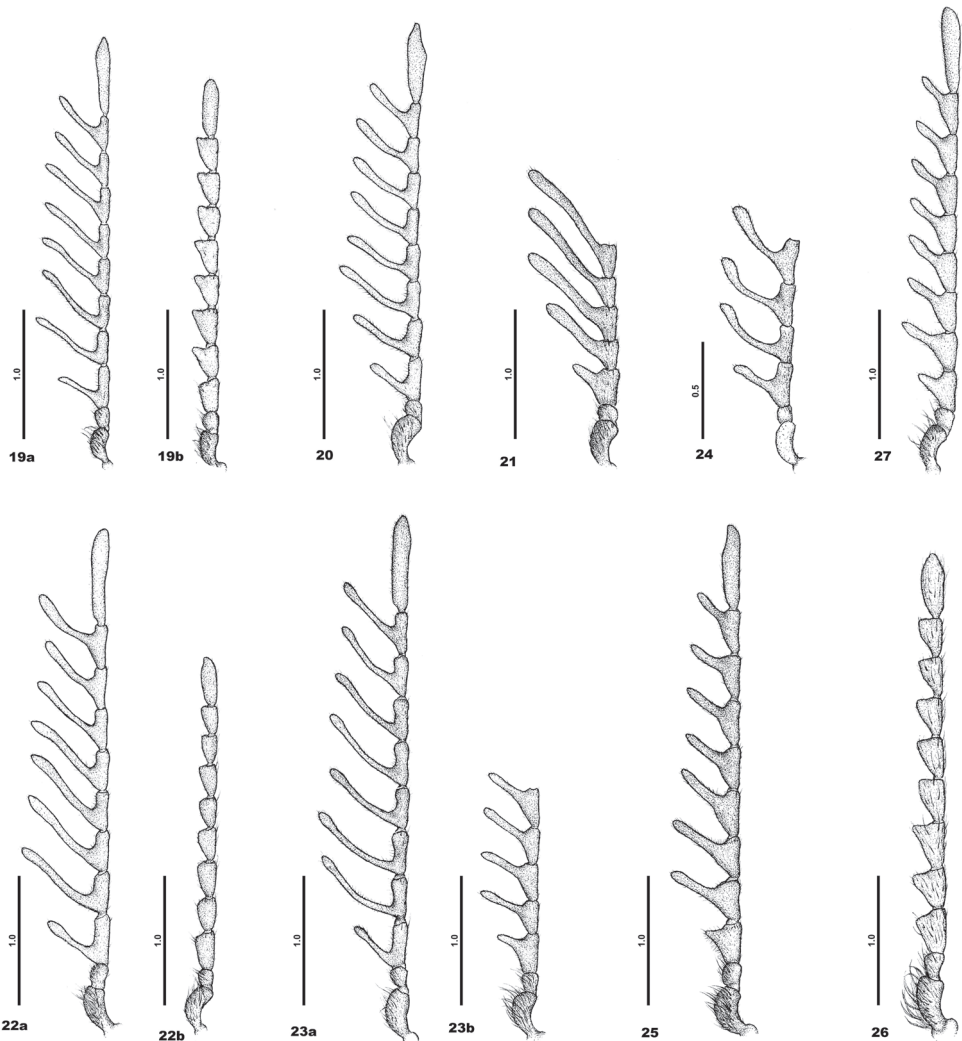
Female. Unknown.

Variability. Without visible variability.

Name derivation. Patronymic, dedicated to Dr Dimby Raharinjanahary from Madagascar National Parks, Antananarivo (Chargé des Bases de données de suivibio-diversité et recherche).

Biology. Unknown.

Distribution. This species is found in the northwestern part of Madagascar (Figure 11).



Figures 19–27. Antennae. **19** *C. (C.) barclayi* sp. n. – a male, b female **20** *C. (C.) dimbyi* sp. n. – male **21** *C. (C.) fasciata* sp. n. – male **22** *C. (C.) lalae* sp. n. – a male, b female **23** *C. (C.) madagascarensis* sp. n. – a male, b female **24** *C. (C.) mamyi* sp. n. – male **25** *C. (C.) njakai* sp. n. – male **26** *C. (C.) obesa* sp. n. – female **27** *C. (C.) rindrai* sp. n. – male.

***Clada (Clada) fasciata* sp. n.**

<http://zoobank.org/B411F2DE-4892-46F4-842E-6B0E1A9FD67D>

Figs 3, 12, 21, 30

Type material. Holotype male: Madagascar, Antananarivo prov., Manankazo env., 15.–17.xii.1996, I. Jeniš lgt. (FGMRI).

Differential diagnosis. The species is similar to *C. (C.) lineatipennis* Pic, 1926, which has black coloured elytra, and *C. (C.) costipennis* Kolbe, 1897, *C. (C.) flabel-*

licornis Pic, 1936 and *C. (C.) multistriata* Pic, 1952 whose males have pectinated antennae. Differs also by shape of the aedeagus. For differences from other Madagascan species, see key.

Description. Male (holotype). Elongate-elliptical, transversally convex. Body length 6.0 mm, maximum width 2.6 mm (Figure 3). Ratio length:width of elytra 1.7. Body, including antennae, maxillary and labial palpi and legs, brown. Only pronotum piceous brown. Pubescence white.

Head shiny, with double punctation – first coarse, dense, umbilicate, distance between punctures approximately the same as their diameter; other very fine, punctures almost touching. Pubescence more or less recumbent, long, inclined backwards; on vertex inclined backwards. Clypeus with transverse depression. Eyes large, globular with short erect sparse pubescence. Frons 3 times as wide as diameters of the eye, from dorsal view. Antennae probably consisting of eleven antennomeres (they are damaged, only 7 antennomeres remain), from 4th pectinate (Figure 21). 1st antennomere robust, twice as long as wide; 2nd as wide as 1st, 0.3 as long as 1st, 0.8 times as wide as long. 3rd strongly serrate, 1.1 times as wide as long. 4th and 5th 2.5 times as wide as long. 6th 3 times as wide as long; 7th 2.7 times as wide as long. All antennomeres with very short recumbent dense pubescence, 1st also with sparse long semi-erect setae. Apical maxillary palpomere long, slim, spindle shaped.

Pronotum convex, matt-shiny, transverse (ratio length:width of pronotum 0.7); widest in middle. Middle of the pronotum with blunt small swelling. Surface of pronotum with coarse, dense, umbilicate punctation; punctures almost touching. Pubescence long, dense, semi-erect, inclined more or less from middle of pronotum to all sides.

Scutellum large, triangular, narrow, 1.2 times as long as wide, very densely recumbent pubescence, inclined backwards, surface shining, finely punctated; punctures almost touching.

Elytra oval, transversally convex, shining, humeri almost absent. Each elytron with six fine costae, covered with white recumbent dense pubescence, inclined backwards and from sides of costa to their centre. Surface of elytra with double punctation – one coarse, dense, umbilicate, almost touching; other is very fine, punctures also almost touching. Pubescence between stripes relatively sparse, recumbent or semi-erect, inclined backwards. Posterior margin of each elytron with approximately 20 small teeth, almost invisible.

Legs stout, with long, dense, recumbent pubescence. All tarsi robust, same length as tibia. 1st metatarsomere as long as 2nd and 3rd together, same width, slightly emarginate on top, 4th slightly shorter than previous, more emarginate, almost to 2/3 of their length. 5th the same length as 3rd and 4th together, rectangular, wider on the top, with two large claws, without teeth.

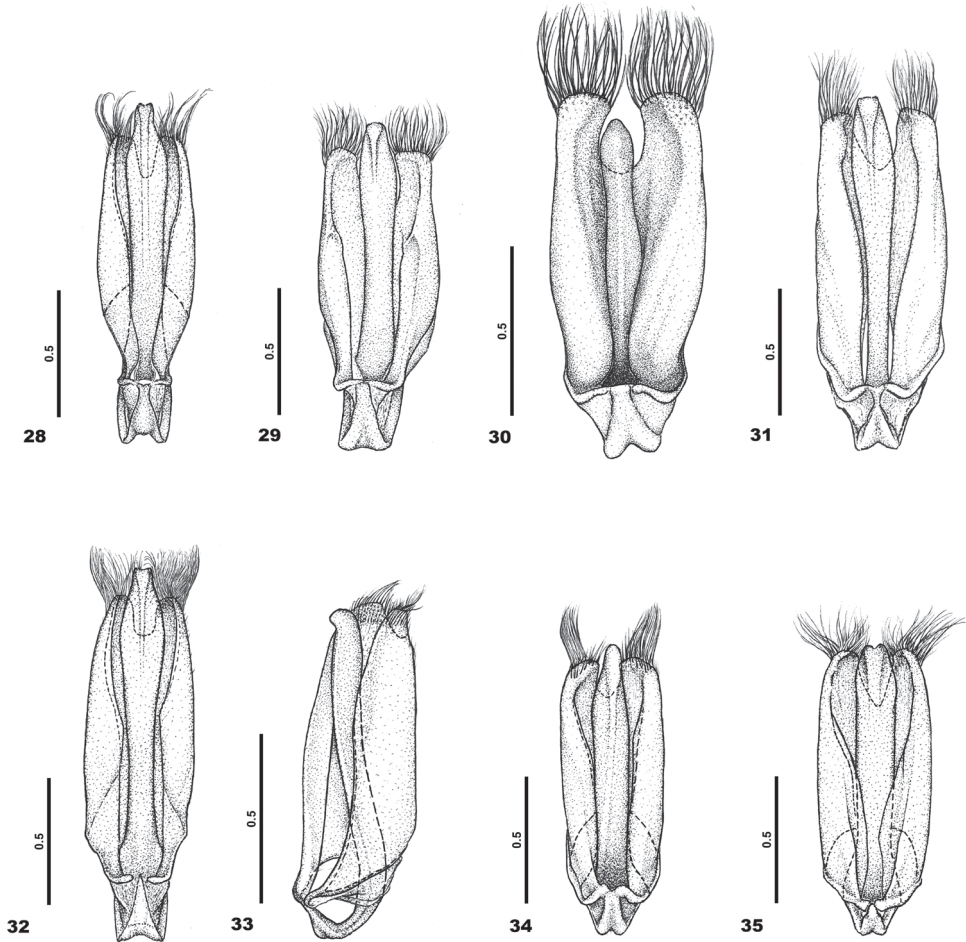
For *aedeagus* see Figure 30.

Female. Unknown.

Name derivation. Derived from the rows of dense recumbent hairs on elytra, from Latin word *fascia*, meaning stripe.

Biology. Unknown.

Distribution. This species is found in the central part of Madagascar (Figure 12).



Figures 28–35. Aedeagus in dorsal view. **28** *C. (C.) barclayi* sp. n. **29** *C. (C.) dimbyi* sp. n. **30** *C. (C.) fasciata* sp. n. **31** *C. (C.) lalae* sp. n. **32** *C. (C.) madagascarensis* sp. n. **33** *C. (C.) mamyi* sp. n. **34** *C. (C.) njakai* sp. n. **35** *C. (C.) rindraï* sp. n.

***Clada (Clada) lalae* sp. n.**

<http://zoobank.org/F199462F-C7C5-4735-8C77-618D7CCF3053>

Figs 4, 13, 22a, b, 31

Type material. Holotype male: Madagascar, Mahajanga prov., Mahajamba riv., Ampatika env., 17.–19.xi.1995, I. Jeniš lgt. (FGMRI). **Paratypes (5):** 2 males, 1 female, the same data as holotype; 2 males, Madagascar, Mahajanga prov., Ampatika env., 17.–20.xii.1995, J. Stolarczyk lgt. (FGMRI).

Differential diagnosis. This species is similar to *C. (C.) humeralis* Pic, 1926, but differs by the lighter colour of the elytra. Fully differs by shape of the aedeagus. For differences from other Madagascan species, see key.

Description. Male (holotype). Elongate-elliptical, transversally convex. Body length 7.0 mm, maximum width 2.9 mm (Figure 4). Ratio length:width of elytra 1.7. Body dark brown; antennae, maxillary and labial palpi and legs lighter. Pubescence white.

Head matt, clypeus shiny, with coarse, dense, umbilicate punctation; distance between punctures approximately the same as their diameter. Pubescence recumbent, long, dense, inclined mostly forwards. Clypeus with shallow transverse depression. Eyes large, globular with long erect sparse pubescence. Frons 2.1 times as wide as diameter of eye, from dorsal view. Antennae consisting of eleven antennomeres, 3rd to 10th pectinate (Figure 22a). 1st antennomere robust, three times as long as wide; 2nd smallest, twice shorter than 1st, as long as wide, almost same width as 1st. 3rd 0.8 times shorter than wide; 4th and 6th to 8th 0.5 times shorter than wide; 9th and 10th 0.6 times shorter than wide and the 10th 0.7 times shorter than wide. Apical antennomere longest, oblong oval, 5 times as long as wide. All antennomeres with short recumbent pubescence, only 1st and 2nd with a few long semi-erect setae. Apical maxillary palpomere long, spindle shaped.

Pronotum convex, matt, transverse (ratio length:width of pronotum 0.7); widest in posterior 2/3. Base of pronotum finely bordered. Middle of pronotum in posterior part with blunt small swelling, posteriorly slightly sharpened. Surface of pronotum with coarse, dense, umbilicate, distance between punctures the same as their diameter. Pubescence short, sparse, recumbent, inclined more or less forwards, in posterior part of pronotum backwards.

Scutellum large, longitudinally rectangular, 1.3 times as long as wide, densely recumbent pubescence, inclined backwards, surface shinning with fine dense puncture.

Elytra oval, transversally convex, shiny, with distinct humeri. Each elytron with fine costae. Surface of elytra irregularly wrinkled, with double punctation – one coarse, dense, umbilicate, punctures almost touching; other is very fine, punctures also almost touching. Pubescence relatively sparse, recumbent, on sides also semi-erect and sporadically also erect, inclined backwards. Posterior margin of each elytron with approximately 25 very small teeth.

Legs stout, with short and dense recumbent pubescence. All tarsi slim, slightly shorter than tibia. 1st metatarsomere as long as 2nd and 3rd together, and same length as 5th. 2nd the same length as 3rd and 4th together. 4th emarginate approximately to 1/2 of their length. 5th long and robust with two large claws, without teeth.

For *aedeagus* see Figure 31.

Female. Habitually the same as male, only antennae serrate (Figure 22b). Body length 8.1 mm, maximum width 3.2 mm.

Variability. Body length 5.4–8.1 mm, maximum width 2.2–3.2 mm.

Name derivation. Patronym, dedicated to Dr Lala Harivelo Ravaomanarivo Raveloson (University of Antananarivo, Faculty of Sciences, Department of Entomology).

Biology. Unknown.

Distribution. This species is found in the northwestern part of Madagascar (Figure 13).

***Clada (Clada) madagascarensis* sp. n.**

<http://zoobank.org/32F329CB-F712-49DB-80E6-F28B4EE00B18>

Figs 5, 14, 23a, b, 32

Type material. Holotype male: Madagascar, Mahajanga distr., Ampatika env., 17.–20. xi.1995, J. Stolarczyk lgt. (FGMRI). **Paratypes (21):** 4 males and 1 female, the same data as holotype (FGMRI); 10 males, Madagascar, Morondava distr., Kirindy, 23.–25. xi.1997, J. Stolarczyk lgt. (FGMRI 4 ex., LBVC 2 ex., MTDC 2 ex., NHMUK 2 ex.); 1 male: Madagascar, Mahajanga distr., Ambodimanga env., 14.–16.xi.1995, J. Stolarczyk lgt. (FGMRI); 2 males: Madagascar, Morondava distr., Maronfandilia, 4.v.1995, J. Stolarczyk lgt. (FGMRI); 2 male: Madagascar, Mahajanga prov., Mahajamba riv., Ampatika env., 17.–19.xi.1995, I. Jeniš lgt. (FGMRI); 1 female: Madagascar, Toliara env., 23.–27.xi.1996, J. Stolarczyk lgt. (FGMRI).

Differential diagnosis. This species is similar to *C. (C.) humeralis* Pic, 1926, but differs by the lighter colour of the elytra and missing lighter humeri. Both sexes have pectinate antennae, while the female of *C. (C.) humeralis* Pic, 1926 has serrate antennae. Fully differs by shape of the aedeagus. For differences from other Madagascan species, see key.

Description. Male (holotype). Elongate-elliptical, transversally convex. Body length 6.0 mm, maximum width 2.5 mm (Figure 5). Ratio length:width of elytra 1.6. Whole body brown, only antennae, palp slightly lighter and pronotum slightly darker. Pubescence white.

Head shiny, with double punctation – one coarse, dense, umbilicate, distance between punctures approximately the same as their diameter, sometimes almost touching; other one is very fine, punctures almost touching. Pubescence recumbent or semi-erect, long, inclined mostly forwards. Clypeus with shallow transverse depression. Eyes large, globular with short erect sparse pubescence. Frons twice as wide as diameters of the eye, from dorsal view. Antennae consisting of eleven antennomeres, 4th to 10th pectinate (Figure 23a). 1st antennomere robust, twice as long as wide; 2nd smallest, only 1/3 long as 1st, as wide as long, same width as the 1st. 3rd serrate, as long as wide; 4th to 8th twice long as wide; 9th 1.7 times as wide as long; 10th 1.5 times as wide as long. Apical antennomere longest, oblong oval, 6.6 times as long as wide. All antennomeres with short recumbent pubescence, only 1st with a few long semi-erect setae. Apical maxillary palpomere long, spindle shaped.

Pronotum convex, matt-shiny, transverse (ratio length:width of pronotum 0.7); widest in middle. Base of pronotum finely bordered. Middle of pronotum at base with blunt small swelling, posteriorly slightly sharpened. Surface of pronotum with double punctation – one coarse, dense, umbilicate, distance between punctures approximately the same as their diameter; other one is very fine, punctures almost touching. Pubescence long, sparse, recumbent, inclined more or less to middle of pronotum.

Scutellum large, longitudinally trapezoidal, narrow, almost as long as wide, densely recumbent pubescence, inclined backwards, surface almost invisible.

Elytra oval, transversally convex, shining, with distinct humeri. Each elytron with five very fine costae, more distinct on second half of elytron. Surface of elytra irregular

punctated, puncture coarse, dense, umbilicate. Pubescence relatively sparse, recumbent, inclined backwards. Posterior margin of each elytron with approximately 25 very small teeth.

Legs stout, with short and dense recumbent pubescence. All tarsi robust, same length as tibia. 1st metatarsomere as long as 2nd and 3rd together, same width, slightly emarginate on top, 4th slightly shorter than previous, more emarginate, almost to 2/3 of their length. 5th is same length as 3rd and 4th together, rectangular, wider on the top, with two large claws, without teeth.

For *aedeagus* see Figure 32.

Female. Antennae less pectinate than in male (damaged, only six antennomeres remain – Figure 23b). Body length 5.7 mm, maximum width 2.1 mm.

Variability. Body length 5.7–7.1 mm, maximum width 2.1–2.8 mm.

Name derivation. Latin adjective, referring to the occurrence of the new species in Madagascar.

Biology. Unknown.

Distribution. This species is found in the western part of Madagascar (Figure 14).

***Clada (Clada) mamyi* sp. n.**

<http://zoobank.org/C07FB3A7-6981-4570-920C-220305AC455F>

Figs 6, 15, 24, 33

Type material. Holotype male: Madagascar, Antananarivo prov., Manankazo env., 15.–17.xii.1996, I. Jeniš lgt. (FGMRI).

Differential diagnosis. Differs from other species of this genus from sub-saharan and southern African regions by a lack of elytral costae. Fully differs by shape of the aedeagus. For differences from other Madagascan species, see key.

Description. Male (holotype). Elongate-elliptical, transversally convex. Body length 3.9 mm, maximum width 1.6 mm (Figure 6). Ratio length:width of elytra 1.7. Body brown, head and pronotum darker, antennae lighter. Pubescence white.

Head shining, with coarse, dense, umbilicate punctated, distance between punctures approximately the same as their diameter. Pubescence recumbent, short, sparse, inclined mostly forwards. Clypeus with shallow transverse depression. Eyes large, globular with very short erect sparse pubescence, almost invisible. Frons 1.3 times as wide as diameter of the eye, from dorsal view. Antennae probably consisting of eleven antennomeres (they are damaged, only 6 antennomeres remain – Figure 24), 3rd to 6th pectinate. 1st antennomere robust, three times as long as wide; 2nd smallest, 3 times shorter than 1st, as long as wide, same width as 1st. 3rd 1.2 times wider as long; 4th 1.3 times wider than long; 5th and 6th 2.2 times wider than long. Other antennomeres are slightly damaged or missing. All antennomeres without pubescence. Apical maxillary palpomere short, spindle shaped.

Pronotum convex, matt-shiny, transverse (ratio length:width of pronotum 0.6); widest in middle. Base of pronotum finely bordered. Pronotum without swelling. Surface

of pronotum with coarse, dense, umbilicate, distance between punctures smaller than their diameter. Pubescence long, sparse, recumbent, inclined more or less forwards.

Scutellum large, longitudinally almost rectangular, 1.1 times as long as wide, densely recumbent pubescence, inclined backwards, surface shining with fine dense puncture.

Elytra oval, transversally convex, shining, humeri almost indistinct. Each elytron with only very fine quasi-costae. Surface of elytra with double punctation – one coarse, dense, umbilicate, punctures almost touching; other one is very fine, punctures also almost touching. Pubescence relatively sparse, recumbent, on sides also semi-erect, inclined backwards. Posterior margin of each elytron with approximately 25 very small teeth.

Legs stout, with short and dense recumbent pubescence. All tarsi slim, 1.2 as long as tibia. 1st metatarsomere as long as 2nd to 4th together, and same length as 5th. 2nd is same length as 3rd and 4th together. 4th only slightly emarginate. 5th long and slim with long slim claws, without teeth.

For *aedeagus* see Figure 33.

Female. Unknown.

Name derivation. Patronym, dedicated to Dr Mamy A Rakotoarijaona from Madagascar National Parks, Antananarivo (Directeur des Opérations).

Biology. Unknown.

Distribution. This species is found in the central part of Madagascar (Figure 15).

Clada (Clada) njakai sp. n.

<http://zoobank.org/D3CD1585-C840-41A0-9290-E8FFCD375206>

Figs 7, 16, 25, 34

Type material. Holotype male: Madagascar, Toliara prov., Tsimanampetsotsa N. P., Mitoho camp, 24°02.898'S, 43°45.138'E, 10 m a. s. l., 12.–13.i.2014, M. Trýzna leg.

Paratypes (15): 1 male: the same data as holotype; 13 males: Madagascar, Toliara prov., Tsimanampetsotsa N. P., Andranovao camp, 24°01.505'S, 43°44.306'E, 15 m a. s. l., 14.–15.i.2014, M. Trýzna leg. (FGMRI 7 ex., LBVC 2 ex., MTDC 2 ex., NHMUK 2 ex.).

Differential diagnosis. This species is similar to *C. (C.) humeralis* Pic, 1926, but differs by the lighter colour of the elytra and missing lighter humeri. Fully differs by shape of the aedeagus. For differences from other Madagascan species, see key.

Description. Male (holotype). Elongate-elliptical, transversally convex. Body length 5.3 mm, maximum width 2.1 mm (Figure 7). Ratio length:width of elytra 1.8. Whole body dark brown, only antennae, maxillary and labial palpi and humeri on elytra moderately lighter. Pubescence yellowish-white.

Head matt-shiny, with double punctation – one coarse, dense, umbilicate, distance between punctures approximately the same as their diameter; other one very fine, punctures almost touching. Pubescence recumbent or semi-erect, short, inclined backwards; on sides of head semi-erect and long, inclined forwards. Clypeus with shallow transverse depression. Eyes large, globular with short erect sparse pubescence. Frons twice as wide as diameters of eye, from dorsal view. Antennae consisting of eleven antennomeres, 4th

to 10th pectinate (Figure 25). 1st antennomere robust, twice as long as wide; 2nd smallest, only one-half length of 1st, as long as wide, slightly narrower than 1st. 3rd serrate, as long as wide; 4th and 5th 1.8 times wider than long; 6th and 7th 1.5 times wider than long; the 8th and 9th 1.3 times wider as long; and 10th 1.1 times as wide as long. Apical antennomere is longest, oblong oval, 4.3 times as long as wide. All antennomeres on margin with short erect dense setae. Apical maxillary palpomere long, spindle shaped.

Pronotum convex, matt-shiny, rounded, transverse (ratio length:width of pronotum 0.7); widest at 2/3 posteriorly. Base of pronotum finely bordered. Middle of pronotum at base with blunt small swelling, posteriorly slightly sharpened. Surface of pronotum with double punctation, one coarse, dense, umbilicate, distance between punctures approximately the same as their diameter; other one is very fine, punctures almost touching. Pubescence long, sparse, recumbent, inclined more or less to middle of pronotum.

Scutellum triangular, narrow, 1.3 times as long as wide, very densely recumbent pubescence, inclined backwards, surface is not visible.

Elytra oval, transversally convex, shining, with distinct humeri. Each elytron with five fine costae, almost invisible, but apex more distinct. Surface of elytra with double punctation, one coarse, dense, umbilicate, distance between punctures approximately the same as their diameter; other one is very fine, punctures almost touching. Pubescence relatively sparse, recumbent or semi-erect, inclined backwards. Posterior margin of each elytron with approximately 25 small teeth.

Legs stout, with short and dense recumbent pubescence. All tarsi robust, same length as tibia. 1st metatarsomere as long as 2nd and 3rd together, same width, slightly emarginate on top, 4th slightly shorter than previous, more emarginate, almost to 2/3 of their length. 5th is same length as 3rd and 4th together, rectangular, wider on the top, with two large claws, without teeth.

For *aedeagus* see Figure 34.

Female. Unknown.

Variability. Body length 4.7–7.1 mm, maximum width 1.8–2.8 mm.

Name derivation. Patronym, dedicated to Adolphe Randrianjaka (University of Antananarivo, Faculty of Sciences, Department of Entomology), whom we called Njaka.

Biology. Unknown. All specimens were collected at light.

Distribution. This species is found in the southwestern part of Madagascar (Figure 16).

***Clada (Clada) obesa* sp. n.**

<http://zoobank.org/D6AB5731-53E8-4709-9FDB-61614AE6B6F9>

Figs 8, 17, 26

Type material. Holotype female: Madagascar, Mahajanga prov., Ampatika env., Mahajamba riv., 10.–12.xii.1996, I. Jeniš lgt. (FGMRI).

Differential diagnosis. Differs from other African species by the shape of the body, which is very arched. For differences from other Madagascan species, see key.

Description. Female (holotype). Short, elongate-elliptical, extremely strongly transversally convex (any other species from genus *Clada* Pascoe, 1887 is not so convex). Body length 8.0 mm, maximum width 4.4 mm (Figure 8). Ratio length:width of elytra 1.6. Body dark brown, pronotum piceous-black, legs dark brown, antennae and maxillary and labial palpi lighter, brown. Pubescence yellowish white.

Head matt; dense, coarse, umbilicate punctation, with long recumbent or semi-erect dense pubescence, with sparse long erect setae, inclined more or less forwards, only on vertex partly inclined to middle or backwards. Clypeus with deep transversal furrow, frons flattened. Eyes large, globular with short erect sparse brown pubescence. Frons wide, 2.9 times as wide as diameter of eye (from dorsal view). Antennae consisting of eleven antennomeres, serrate (Figure 26). 1st antennomere robust, twice as long as wide, with dense long erect hairs; 2nd small, as wide as 1st, only one-half of their length, as long as wide. 3rd slightly serrate, 1.5 times as long as wide. Antennomeres 4th to 10th serrate; 4th 1.1 times as long as wide, 5th 1.5 times as long as wide; 6th 1.3 times as long as wide, 7th to 10th 1.6 times as long as wide, 11th oblong oval, 2.6 times as long as wide. Apical maxillary palpomere long, spindle shaped.

Pronotum convex, matt shining, transverse (ratio length:width of pronotum 0.7), widest in last third. Base of pronotum finely bordered. Middle of pronotum at base with high blunt swelling, on their sides shallow, almost invisible rounded depression. Surface of pronotum coarsely, densely, umbilicate punctate, distance between punctures smaller than their diameter, almost touching. Pubescence short, recumbent or semi-erect, inclined largely backwards, on sides inclined obliquely backward, on anterior margin inclined from sides to middle; from anterior margin to swelling in middle arranged to narrow strip.

Scutellum large, almost triangular (on top slightly rounded), 1.2 times as long as wide. Surface distinct with dense and coarse umbilicate punctation, with short, dense, recumbent pubescence inclined backwards.

Elytra short oval, transversally strongly convex, shining, with distinct humeri. Each elytron slightly irregular bent, with fifth costae, which are only slightly visible (especially from lateral view). Surface of elytra with double punctation. One very coarse, dense, umbilicate, irregular, diameter between punctures smaller than their diameter. Other one relatively fine, dense; punctures almost touching. Pubescence short, sparse, inclined backwards.

Legs stout, with short and dense recumbent pubescence. All tarsi robust, same length as tibia. 1st metatarsomere as long as 2nd and 3rd together, same width, slightly emarginate on top, 4th slightly shorter than previous, more emarginate, almost to 2/3 of their length. 5th is same length as 3rd and 4th together, rectangular, wider on the top, with two large claws, without teeth.

Male. Unknown.

Name derivation. Derived from the shape of body, from the Latin *obesus* for plump.

Biology. Unknown.

Distribution. This species is found in the northwestern part of Madagascar (Figure 17).

***Clada (Clada) rindrai* sp. n.**

<http://zoobank.org/55124B57-580F-4909-A8BC-79414B5C1B23>

Figs 9, 18, 27, 35

Type material. Holotype male: Madagascar, Toliara prov., Toliara env., 23.–27. xi.1996, J. Stolarczyk lgt. (FGMRI).

Differential diagnosis. This species is similar to *C. (C.) humeralis* Pic, 1926, but differs by the lighter colour of the elytra and missing lighter humeri. Fully differs by shape of the aedeagus. For differences from other Madagascan species, see key.

Description. Male (holotype). Elongate-elliptical, transversally convex. Body length 6.6 mm, maximum width 2.5 mm (Figure 9). Ratio length:width of elytra 1.5. Body brown, pronotum darker; antennae, maxillary and labial palpi and legs lighter. Pubescence yellowish white.

Head matt-shiny, with double punctation – one coarse, dense, umbilicate, distance between punctures approximately the same as their diameter; other one is very fine, almost invisible, punctures almost touching. Pubescence semi-erect, long, in anterior part inclined forwards, in posterior part inclined more or less backwards. Clypeus with shallow transverse depression, shiny. Eyes large, globular with long erect dense pubescence. Frons 2.7 times as wide as diameter of the eye, from dorsal view. Antennae consisting of eleven antennomeres, 4th to 10th pectinate (Figure 27). 1st antennomere robust, 2.5 times as long as wide; 2nd smallest, almost triangular, only one-half long as the 1st, as long as wide, slightly narrower as the 1st. The 3rd strongly serrate, as long as wide, 1.8 times as width of 1st. 4th to 9th 1.4 times as wide as long; 10th 0.9 times shorter as long. Apical antennomere is longest, oblong oval, 5.7 times as long as wide. All antennomeres on margin with short erect dense setae. Apical maxillary palpomere long, spindle shaped.

Pronotum convex, matt-shiny, rounded, transverse (ratio length:width of pronotum 0.8); widest at 2/3 posteriorly. Base of pronotum finely bordered. Middle of pronotum at base with blunt small swelling, posteriorly slightly sharpened. Surface of pronotum with double punctation – one coarse, dense, umbilicate; distance between punctures approximately one half of their diameter, some punctures almost touching; other one is very fine, punctures almost touching. Pubescence long, dense, semi-erect, inclined more or less to middle of pronotum, only on sides inclined to margin.

Scutellum triangular with blunt top, narrow, 1.8 times as long as wide, very sparse and short recumbent pubescence, inclined backwards.

Elytra oval, transversally convex, shiny, with distinct humeri. Each elytron with five fine costae, almost invisible, but apex more distinct. Surface of elytra with double punctation, one coarse, dense, umbilicate, distance between punctures approximately the same as their diameter; other one is very fine, punctures almost touching. Pubescence relatively sparse, recumbent partly also semi-erect, inclined backwards. Posterior margin of each elytron with approximately 25 small teeth.

Legs stout, with short and dense recumbent pubescence. All tarsi robust, same length as tibia. 1st metatarsomere as long as 2nd and 3rd together, same width, slightly emarginate on top. 4th slightly shorter than previous, more emarginate, almost to 2/3 of their length. 5th is same length as 3rd and 4th together, rectangular, wider on the top, with two large claws, without teeth.

For *aedeagus* see Figure 35.

Female. Unknown

Name derivation. Patronym, dedicated to Mr Rindra Andriamahefasoa (Chef de Volet Conservation et Recherche, Andasibe-Mantadia National Park).

Biology. Unknown.

Distribution. This species is found in the southwestern part of Madagascar (Figure 18).

Key to *Clada* (s. str.) from Madagascar

- 1 Body extremely strongly convex, large species (8 mm), quite differ by shape of body from other species of this genus; between swelling and posterior margin of pronotum wide flattened (only female holotype known)..... *Clada (Clada) obesa* sp. n.
- Body convex, smaller (maximum 7 mm), between swelling and posterior margin only very slim flattened (males)..... 2
- 2 Elytra with distinct longitudinal rows of dense recumbent hairs, aedeagus Fig. 30 *Clada (Clada) fasciata* sp. n.
- Elytra without distinct rows of dense recumbent hairs 3
- 3 Elytra with very fine quasi costae or without distinct costae, eyes with very short hairs, aedeagus Fig. 33 *Clada (Clada) mamyi* sp. n.
- Elytra with more or less distinct costae, eyes with distinct hairs..... 4
- 4 The 3rd antennomere serrate 5
- The 3rd antennomere pectinate 6
- 5 Swelling on pronotum sharpened, aedeagus Fig. 34 *Clada (Clada) njakai* sp. n.
- Swelling on pronotum blunt, aedeagus Fig. 35..... *Clada (Clada) rindra* sp. n.
- 6 Lateral projection of the 3rd antennomere shorter than the length of this antennomere, aedeagus Fig. 32 *Clada (Clada) madagascarensis* sp. n.
- Lateral projection of the 3rd antennomere longer than the length of this antennomere 7
- 7 Elytra yellow-brown..... 8
- Elytra dark brown, aedeagus Fig. 31..... *Clada (Clada) lalae* sp. n.
- 8 The 2nd antennomere as long as wide, aedeagus Fig. 29 *Clada (Clada) dimbyi* sp. n.
- The 2nd antennomere distinctly longer than wide, aedeagus Fig. 28..... *Clada (Clada) barclayi* sp. n.

Table 1. Main distinguishing characters of species of the genus *Clada* (s. str.) from the Southern African Region and Madagascar.

Species	Antennae		Costae/rows of hairs	Colour of elytra	Figure of aedeagus
	male	female			
<i>C. (C.) barclayi</i> sp. n.	P	S	yes/no	light brown	Zahradník & Trýzna
<i>C. (C.) basilewskyi</i> Español, 1969	S		yes/no	dark brown	Español, 1969b
<i>C. (C.) costipennis</i> Kolbe, 1897	P		yes/yes	dark brown	Absent
<i>C. (C.) dimbyi</i> sp. n.	P		yes/no	light brown	Zahradník & Trýzna
<i>C. (C.) fasciata</i> sp. n.	S		yes/yes	Brown	Zahradník & Trýzna
<i>C. (C.) flabellicornis</i> Pic, 1936	P		yes/yes	Rusty	absent
<i>C. (C.) granulata</i> Español, 1972	S		yes/no	Black	Español, 1972
<i>C. (C.) humeralis</i> Pic, 1926	P	S	yes/no	black (piceous)	absent
<i>C. (C.) lalae</i> sp. n.	P	S	yes/no	dark brown	Zahradník & Trýzna
<i>C. (C.) laticollis</i> Pic, 1947			yes/no	black-piceous (immature light brown)	absent
<i>C. (C.) lineatipennis</i> Pic, 1926			yes/yes	black (piceous)	absent
<i>C. (C.) longicornis</i> Pic, 1934	F	F	yes/no	Rusty	absent
<i>C. (C.) madagascarensis</i> sp. n.	P	P	yes/no	Brown	Zahradník & Trýzna
<i>C. (C.) mamyi</i> sp. n.	P		no/no	Brown	Zahradník & Trýzna
<i>C. (C.) multistriata</i> Pic, 1952	P		yes/yes	black (piceous)	absent
<i>C. (C.) njakai</i> sp. n.	P		yes/no	dark brown	Zahradník & Trýzna
<i>C. (C.) obesa</i> sp. n.		S	yes/no	dark brown	absent
<i>C. (C.) rindrai</i> sp. n.	P		yes/no	Brown	Zahradník & Trýzna
<i>C. (C.) rugosa</i> Pic, 1915	P		yes/no	Rusty	no
<i>C. (C.) waterhousei</i> Pascoe, 1887	P		yes/no	rusty or black	no

Abbreviations: F-filiform; P-pectinate; S-serrate

Acknowledgements

We would like to thank Dr Lala Harivelo Ravaomanarivo Raveloson (University of Antananarivo, Faculty of Sciences, Department of Entomology), Dr Mamy A. Rakotoarijaona (Directeur des Opérations, Madagascar National Parks, Antananarivo), and Dr Dimby Raharinjanahary (Chargé des Bases de données de suivibiodiversité et recherche, Madagascar National Parks, Antananarivo) for supporting our research project: 'Étude à long terme de la biodiversité des groupes choisis d'insectes: Coléoptères, Héétéroptères, Homoptères, Lépidoptères et quelque famille de Micro Lépidoptères nocturne dans les localités préalablement sélectionnées en considération de la recherche et la protection de la biodiversité dans les aires protégées de Madagascar. Analyse des risques potentiels d'influencer négativement la biodiversité dans les régions étudiées'. This work was supported by the Internal Grant Agency (IGA no. 20124364, IGA no. A28 16), Faculty of Forestry and Wood Sciences, Czech University of Life Sciences, Prague and by the project of the Ministry of Agriculture of the Czech Republic, Resolution RO0116 (reference number 10462/2016-MZE-17011). We are indebted to Lukáš Blažej (Varnsdorf, Czech Republic) for drawings of antennae and aedeagi and Maxwell VL Barclay for proofreading the manuscript.

References

- Bellés X (1987) *Xylodes (Diegous) excavaticollis* n. sp. de Madagascar (Col., Ptinidae). Bulletin de la Société Entomologique de France 102: 29–31.
- Bellés X (1991) Insectes Coléoptères Ptinidae. Faune de Madagascar. 77. Muséum National d'Histoire Naturelle Paris. Faune de Madagascar 77: 1–122.
- Español F (1969a) Notas sobre anóbidos (Col.). XXXVII.-XXXIX. [XXXVII. Más datos sobre los *Stagetus* del África tropical; XXXVIII. Dos nuevos *Stagetus* del Asia paleártica; XXXIX. Un nuevo Anobiinae de Madagascar]. Publicaciones del Instituto de Biología Aplicada 46: 49–64.
- Español F (1969b) Notas sobre anóbidos (Col.). XLI. Contribución al conocimiento de las *Clada* Pasc. Africanas. Miscelánea Zoológica (Barcelona) 2(4): 39–46.
- Español F (1972) Notas sobre anóbidos (Col.). LVI.-LVIII. [LVI. Los *Xyletinus* Latr. de Madagascar; LVII. Descripción de dos nuevas especies del África meridional; LVIII. Sobre un nuevo género de Xyletininae de las islas Canarias]. Publicaciones del Instituto de Biología Aplicada 52: 49–65.
- Kolbe HJ (1897) Coleopteren. Die Käfer Deutsch-Ost-Afrikas. Berlin: D. Reimer, 367 pp. <https://doi.org/10.5962/bhl.title.53492>
- Pascoe FLS (1887) Notes on Coleoptera, with Descriptions of new Genera and Species. Part VI. The Annals and Magazine of Natural History (5)20: 8–20 + 1 pl.
- Philips TK (2005) *Acanthaptinus triplehorni*, a new genus and species of spider beetle (Coleoptera: Ptinidae) from Madagascar. Annales Zoologici 55: 483–587.
- Pic M (1896) Ptinidae recueillis à Madagascar par M. Charles Alluaud 1893 [Col.]. Bulletin de la Société Entomologique de France 1896: 352–355.
- Pic M (1912a) Coleopterorum Catalogus. Pars 41 – Ptinidae. In: Junk W, Schenkling S (Eds) Coleopterorum Catalogus. W. Junk, Berlin, 46 pp.
- Pic M (1912b) Coleopterorum Catalogus. Pars 48 – Anobiidae. In: Junk W, Schenkling S (Eds) Coleopterorum Catalogus. W. Junk, Berlin, 92 pp.
- Pic M (1915) Descriptions abrégées diverses. Mélanges Exotico-entomologiques 12: 3–20.
- Pic M (1926) Nouveautés diverses. Mélanges Exotico-entomologiques 45: 1–32.
- Pic M (1934) Nouveautés diverses. Mélanges Exotico-entomologiques 63: 1–36.
- Pic M (1936) Nouveaux Coléoptères de l'Afrique Occidentale. Revue de Zoologie et de Botanique Africaines 29: 34–36.
- Pic M (1947) Coléoptères du globe (suite). L'Échange, Revue Linnéenne 63: 1–4.
- Pic M (1949) Nouveaux Coléoptères de Madagascar. Mémoires de L'Institut Scientifique de Madagascar, Série A 3: 341–345.
- Pic M (1952) Mission A. Villiers au Togo et au Dahomey (1950) VI. Coléoptères diverses. Bulletin de l'Institut Français d'Afrique Noire 14: 97–119.
- Pic M (1953) Coléoptères nouveaux de Madagascar. Mémoires de l'Institut Scientifique de Madagascar, Série E 3: 253–278.
- White RE (1974) Type-species for world genera of Anobiidae (Coleoptera). Transactions of the American Entomological Society 99: 415–475.

Analysis of temporal diversification of African Cyprinidae (Teleostei, Cypriniformes)

Mariam I. Adeoba¹, Kowiyou Yessoufou²

1 Department of Zoology, University of Johannesburg, Kingsway Campus PO Box 524, Auckland Park 2006, South Africa **2** Department of Geography, Environmental management and Energy studies, University of Johannesburg, Kingsway Campus PO Box 524, Auckland Park 2006, South Africa

Corresponding author: *Mariam I. Adeoba* (mariamsalami@yahoo.co.uk)

Academic editor: *M. E. Bichuette* | Received 15 April 2018 | Accepted 2 October 2018 | Published 13 December 2018

<http://zoobank.org/EC645E25-3F17-4F36-ACCD-CE3946FA767F>

Citation: Adeoba MI, Yessoufou K (2018) Analysis of temporal diversification of African Cyprinidae (Teleostei, Cypriniformes). ZooKeys 806: 141–161. <https://doi.org/10.3897/zookeys.806.25844>

Abstract

Recent evidence that freshwater fishes diversify faster than marine fishes signifies that the evolutionary history of biodiversity in freshwater system is of particular interest. Here, the evolutionary diversification events of African Cyprinidae, a freshwater fish family with wide geographic distribution, were reconstructed and analysed. The overall diversification rate of African Cyprinidae is 0.08 species per million year (when extinction rate is very high, i.e., $\epsilon = 0.9$) and 0.11 species per million year (when $\epsilon = 0$). This overall rate is lower than the rate reported for African Cichlids, suggesting that African freshwaters might be less conducive for a rapid diversification of Cyprinidae. However, the observed diversification events of African Cyprinidae occurred in the last 10 million years. The temporal pattern of these events follows a non-constant episodic birth-death model (Bayes Factor > 28) and the rate-constant model never outperformed any of the non-constant models tested. The fact that most diversification events occurred in the last 10 million years supports the pattern reported for Cyprinidae in other continent, e.g., Asia, perhaps pointing to concomitant diversification globally. However, the diversification events coincided with major geologic and paleo-climatic events in Africa, suggesting that geological and climatic events may have mediated the diversification patterns of Cyprinidae on the continent.

Keywords

climate change, extinction, fish, geological rift, speciation

Introduction

The standing biodiversity, i.e., the diversity of life that we are witnessing today, is the result of countless speciation and extinction events that have occurred in the past (Jablonski 1995; May et al. 1995; Niklas 1997). An important body of literature has been devoted to explain not only what drives these macro-evolutionary events (ecological or stochastic forces) but also their temporal dynamics (Morrison et al. 2004; Williams and Reid 2004; Xiang et al. 2005; Kozak et al. 2006; Weir 2007; Phillimore and Price 2008). These studies explored specific questions: i) did macro-evolutionary events occur at a constant rate with species accumulating exponentially over time? Alternatively, ii) did they occur at non-constant rates with bursts of speciation at the origin (owing to availability of empty niches) followed by a rate decrease over time (adaptive radiation)?

In macro-evolutionary studies, fossil records are believed to track better the temporal dynamic of species accumulation (Raup 1976; Jablonski 1995; Niklas 1997). However, a number of limitations preclude a common or frequent use of fossil records. First, we do not always have fossil records for several taxonomic groups of interest (Raup 1976; Jablonski 1995; Niklas 1997; Peters and Foote 2002). This is especially the case for taxonomic groups with soft body parts or those that occur in arid environments because they are rarely fossilized. Second, it is difficult to identify punctuated events (e.g., mass extinction) in fossil records, and as a result, the analysis of fossil records “can give the impression that the diversity of life has increased inexorably through time” (Crisp and Cook 2009).

In the face of the limitations of fossil records for macro-evolutionary studies, DNA-based phylogenies provide a commonly used alternative approach (e.g., Harvey et al. 1994; Rüber and Zardoya 2005). Most recent studies employed the phylogenetic approach to investigate the dynamics of species accumulation over time, and these dynamics are best interpreted when represented graphically in the form of lineages-through-time plot (LTT plot). Various theoretical scenarios of LTT plots are plausible as described in Crisp and Cook (2009). First, the tempo and mode of species accumulation can be constant over time corresponding to a linear semi-log LTT plot due to a constant ratio birth/death through time. Second, the pattern can depart from a linear semi-log LTT plot showing a concave or convex line as a result of single rate decrease or increase, respectively. Third, a pattern of early rapid radiation that later slows down can also be observed. This is known as adaptive radiation and is thought to be driven by ecological opportunities (i.e., the need to fill empty niches trigger a rapid radiation, which slows down over time as the proportion of empty niches decrease with time). Characteristics of LTT plot corresponding to adaptive radiation are steep slope at the origin and the slope flattens progressively. Finally, when the LTT plot has an anti-sigmoidal shape, this is indicative of a constant radiation punctuated by mass extinction events (Crisp and Cook 2009).

In the literature, the adaptive radiation is the most commonly reported scenario irrespective of the taxonomic groups studied (Shaw et al. 2003; Kadereit et al. 2004; Machordom and Macpherson 2004; Morrison et al. 2004; Williams and Reid 2004; Xiang et al. 2005; Kozak et al. 2006; Weir 2006; Phillimore and Price 2008; Seehausen

2015). Nonetheless, it is important to highlight that these studies are biased not only towards plants but specifically towards plant groups of exceptionally high diversification rate (Baldwin and Sanderson 1998; Richardson et al. 2001; Verboom et al. 2003; Klak et al. 2004; Kay et al. 2005; Hughes and Eastwood 2006; García-Maroto et al. 2009; Valente et al. 2010). In the animal kingdom, similar high radiations were also reported in the Cambrian era (see Rokas et al. 2005) but Rokas et al.'s study was very broad as it focused on Metazoa in general. Even studies that explored more specifically the diversification patterns of vertebrate also focused on groups that showed relatively high diversification rate (e.g., birds, Moyle et al. 2009). For fish, particular attention has been given to the African Cichlids (McCune 1997; Verheyen et al. 2003; Day et al. 2008), again because this group of fish showed spectacular diversification rates (8.29–62.15 species per million years in the Lake Victoria; Verheyen et al. 2003).

However, the phylogenetic approach too has some limitations, with the most commonly cited limitation being the lack of complete DNA data for most lineages of interest. For example, in the vertebrate group, we only have DNA sequences (COI) for 67% of extant bird species (Jetz et al. 2012), 55% of mammals (Bininda-Emonds et al. 2007), 45% of squamate reptiles (Pyron et al. 2013) and the lowest proportion of available DNA sequences is for fishes (27%; Rabosky et al. 2013). Consequently, we have a poor understanding of the evolutionary history and diversification patterns of several vertebrate groups due to unavailability of complete DNA data. Although several statistical approaches have been proposed to simulate complete sampling (e.g., see Pybus and Harvey 2000), a complete DNA- and/or taxonomic-based phylogeny would always be better for ecological and evolutionary studies than simulated phylogenies (see Rabosky 2015). Interestingly, owing to the ongoing global DNA barcoding campaign, an impressive volume of DNA sequences is increasingly made available in public repositories (www.boldsystems.org) and these sequences can be used for taxonomic, ecological, and evolutionary studies. Even when complete DNA sequences are not yet available for a particular taxonomic group of interest (e.g., African Cyprinidae), a recent improvement in methodological approaches now allows the reconstruction of a comprehensive phylogenetic tree (see Thomas et al. 2013) without any simulation. Thomas et al.'s approach (see details in Material and Method Section) combines taxonomic information with the available incomplete DNA sequences to assemble a complete phylogenetic tree. The resulting phylogeny from Thomas et al.'s approach is showed multiple times to be suitable for the analysis of diversification rates and evolutionary processes (e.g., Jetz et al. 2012) especially when trait data are not involved (see Rabosky 2015).

In the present paper, Thomas et al.'s approach was used to assemble a complete phylogeny for the African Cyprinidae. A higher proportion of the African freshwater ichthyofauna belongs to the family Cyprinidae after the cichlids (Skelton et al. 1991). For example, 24 genera and 539 species of Cyprinidae are recognized in Africa (Froese and Pauly 2017). They are distributed from the northern to southern Africa, with their mature sizes ranging from small (30 mm SL) to larger size (900 mm SL) (Skelton et al. 1991). The aim of the present Chapter was to understand the evolutionary processes that shaped the current diversity of the fish family Cyprinidae in Africa. Specifically,

four questions were investigated. First, what is the overall rate of the evolutionary processes (speciation and extinction events) that led to the observed diversity of Cyprinidae in Africa? ii) How does this rate compare to the rates reported for African Cichlids? iii) Have diversification rates of African Cyprinidae changed significantly through time? iv) Is there evidence that African Cyprinidae experienced mass extinction events?

Materials and methods

Assembling a fully sampled phylogeny of the African Cyprinidae

The recent approach of Thomas et al. (2013) was used to assemble a complete phylogeny, as we do not have a complete matrix of DNA sequences for all species. This approach requires taxonomic information and DNA data. The DNA data used are the COI matrix that we recently assembled and published (see details in Adeoba et al. 2018). These DNA sequences were used to first reconstruct a constraint tree. With regard to DNA data, three types of species (types 1, 2 and 3) are distinguished: “type 1 species” are species for which COI sequences are available; “type 2 species” are species for which COI sequences are missing but they are congeners of type 1; “type 3 species” have no COI sequences and are not congeners of type 1. In this study, there are 138 type 1 species, 388 type 2 species, and 13 type 3 species.

To assemble the constraint tree, an XML file was generated using the COI sequences of the type 1 species, in the program BEAUTi, and this file was used to reconstruct a dated constraint tree based on a Bayesian MCMC approach implemented in the BEAST program. Next, the GTR + I + Γ model was selected as the best model of sequence evolution based on the Akaike information criterion evaluated using MODELTEST (Nylander 2004). In addition, a Yule process was selected as the tree prior with an uncorrelated relaxed lognormal model for rate variation among branches. Also, the COI sequences of the following species were used as outgroups and for calibration purpose (He et al. 2008; Tang et al. 2010; Wang et al. 2012): *Barbonymus altus* (Günther, 1868), *Barbonymus schwanenfeldii* (Bleeker, 1854), *Barbus barbatus* (Linnaeus, 1758), *Carrassius auratus* (Linnaeus, 1758), *Carrassius gibelio* (Bloch, 1782), *Gyrinocheilus aymonieri* (Tirant, 1883), *Hybognathus argyritis* Girard, 1856, *Myxocyprinus asiaticus* (Bleeker, 1864), *Paramisgurnus dabryanus* Dabry de Thiersant, 1872, *Phoxinus phoxinus* (Linnaeus, 1758), *Pseudorasbora parva* (Schlegel, 1842), *Rhinichthys umatilla* (Gilbert & Evermann, 1894), *Tinca tinca* (Linnaeus, 1758) and *Vimba vimba* (Linnaeus, 1758). For calibration purpose, following Wang et al. (2012) and Cavender (1991), the root node of Cyprinidae was constrained to 55.8 million years (My) and the split between *Tinca* and the modern leuciscins was constrained to 18.0 My. In addition, the lineage *Barbus* was calibrated to 13 My following Zardoya and Doadrio (1999). Monte Carlo Markov chains were run for 50 million generations with trees sampled every 1000 generations. Log files, including prior and likelihood values, as well as the effective sample size (ESS) were examined using TRACER (Rambaut and

Drummond 2007). ESS values were all > 200 for the age estimates. The first 25% of the resulting 50,000 trees were discarded as burn-in, and the remaining trees were combined using TREEANNOTATOR (Rambaut and Drummond 2007) to generate a maximum clade credibility (MCC) tree (the constraint tree).

To integrate the types 2 and 3 species into the constraint tree, a simple taxon definition file that lists all three types of species along with their taxonomic information (here genus names) was formed. Using the constraint tree and the taxon definition file, an MrBayes input file was first generated as implemented in the R library PASTIS (Thomas et al. 2013), and then a dated complete phylogeny using MrBayes 3.2. (Ronquist and Huelsenbeck 2003) was reconstructed under a relaxed-clock model with node-age calibrations indicated above.

In the 10,000 resulting trees, the topology of species with DNA-sequences remains fixed, and the unsampled species (types 2 and 3) were assigned randomly within their genera. In an early study, Kuhn et al. (2011) demonstrated that similar approach to that of Thomas et al. (2013) generates conservative placements of types 2 and 3 species with respect to divergence times and diversification rate estimation, which is, following Rabosky (2015), a significant advance for diversification studies.

Data analysis

All analyses were done in R (R Development Core Team 2011). To understand how the observed diversity of African Cyprinidae was accumulated over time, multiple approaches described below were used.

First, the net diversification rate (speciation minus extinction) was estimated using Magallón and Sanderson's method (Magallón and Sanderson 2001) implemented in the R library GEIGER (Harmon et al. 2007) under two scenarios: no extinction ($\epsilon = 0$) and high extinction rate ($\epsilon = 0.9$).

Second, the observed net diversification rates were compared to those reported for Cichlids in various African lakes (Lake Malawi and Lake Victoria).

Third, to assess whether the diversification rates of African Cyprinidae have changed significantly through time, the gamma statistic (Pybus and Harvey 2000), the LTT (Lineage-Through-Time) plot and several evolutionary models were tested on the African Cyprinidae dataset. The value of gamma was calculated on the phylogenetic tree of Cyprinidae using the R package LASER (Rabosky 2006). If $\gamma < 0$, this implies a decreasing speciation of Cyprinidae over time whereas $\gamma > 0$ is indicative of an increasing speciation toward the present day (Pybus and Harvey 2000).

To test if the value of gamma departs significantly from zero, the observed value of gamma was compared, using confidence interval, to the expected value of gamma under a constant-rate birth-death model. To this end, an MCMC (Markov chain Monte Carlo) simulation was performed to estimate the posterior probability distribution of gamma under this constant-rate model. Specifically, the constant-rate birth-death model was parameterized by drawing rate parameters from the joint posterior densities inferred from

the phylogenetic tree of Cyprinidae. This parameterized model was used to simulate 1000 phylogenies, and these simulated phylogenies were used to calculate the expected value of gamma. Then, the observed value of gamma was compared to the posterior-predictive distribution of the expected value of gamma. If the observed value falls near the centre of the simulated distribution, then the diversification rates of African Cyprinidae are constant over time. If not, it means that the diversification of the African Cyprinidae has significantly changed over time (Höhna et al. 2015), i.e., some diversification shifts have occurred.

In addition, the 1000 phylogenies that were simulated were used to reconstruct the posterior-predictive distribution of the corresponding LTT plots (1000 simulated LTT plots). The observed LTT plot for African Cyprinidae was then reconstructed and compared to the simulated LTT plots. If the observed LTT plot falls within the simulated LTT plots, this means that the diversification rate of African Cyprinidae has been constant over time. Otherwise, the diversification of African Cyprinidae has experienced some evolutionary shifts. Next, the observed LTT plot was also compared to the various scenarios predicted and summarized above in the Introduction (Crisp and Cook 2009). Furthermore, the evolutionary models that explain the diversification patterns depicted by the observed LTT plot of the African Cyprinidae were identified. The models tested include a constant-rate birth-death model and three rate-variation models. The rate-variation models include a birth-death model with an exponentially decreasing speciation rate, a birth-death model with piecewise-constant rates (i.e., rates of speciation and extinction change over time but the diversification rate remains constant; Höhna 2015) and a birth-death model of evolution punctuated by a mass-extinction event. The best of these models was selected based on Bayes Factors (Baele et al. 2013) whose values were interpreted following Jeffreys (1961) (Suppl. material 1: Table S1).

Finally, to investigate whether African Cyprinidae experienced some mass extinctions events (if so, when), the CoMET [Compound Poisson Process (CPP) on Mass Extinction Time] approach was used (May et al. 2016). This approach has the advantage of being able not only to fit all possible birth-death models to the data at hand but also to specifically model mass extinction events. Briefly explained, the CoMET approach treats the number of speciation-rate shifts, extinction-rate shifts, mass-extinction events, as well as the parameters associated with these events as random variables, and then estimates their joint posterior distribution. For this analysis, hyperpriors was set both *a priori* and empirically as implemented in the R package TESS (Höhna et al. 2015). The results of *a priori* hyperpriors are reported below as they are similar to that of the empirically set priors.

Results

The phylogenetic tree of African Cyprinidae is presented in a study that is currently under review and provided here as Suppl. material 1. Based on this tree, the overall diversification rate of African Cyprinidae is 0.08 species per million year (when extinction rate is very high, i.e., $\epsilon = 0.9$) and 0.11 species per million year (when $\epsilon = 0$). This overall rate is lower than the rate reported for African Cichlids (see details in Discussion below).

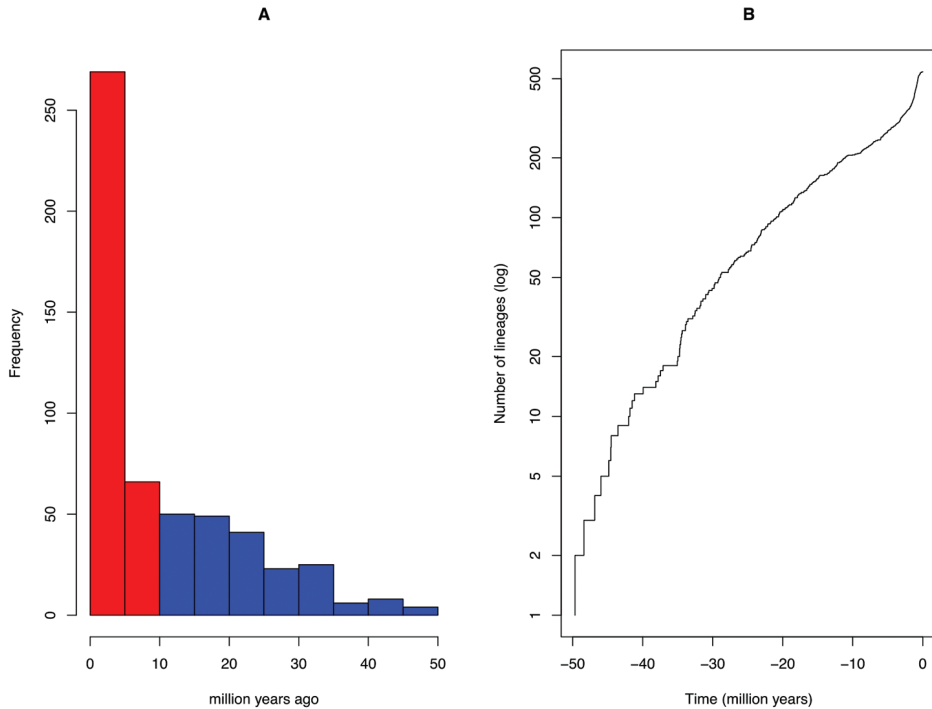


Figure 1. Diversification patterns of African Cyprinidae. **A** Histogram depicting the frequency of branching time on the phylogeny of African Cyprinidae; red colour shows the most frequent branching events which occurred the last 10 million years; blue colour indicates earlier branching events i.e., prior to 10 million years ago **B** lineage-through-time plot of the phylogeny of African Cyprinidae.

Most diversification events occurred in the last 10 million years (my) (Figure 1A), and the temporal pattern of these events, represented as an LTT plot (Figure 1B), follows an anti-sigmoidal shape, which is indicative of an overall constant diversification punctuated by a mass extinction event.

To assess whether there was a significant rate variation over the diversification period, the gamma statistic was first calculated ($\gamma = 6.23$), and this positive gamma value (which is indicative of an increase diversification rate over time) is significantly different from the expected gamma under a rate-constant diversification model (Confidence Interval CI = 0.80–4.31; Figure 2A). This suggests that a non-constant diversification model is best suitable to explain the accumulation of African Cyprinidae over time. This result is also supported by the comparative analysis of the observed LTT plot of the African Cyprinidae with the simulated LTT plots under a rate-constant diversification (Figure 2B). This comparative analysis clearly showed that the observed LTT plot is different from the expected ones (Figure 2B).

Given this evidence of non-constant diversification, the next step was to identify the best model for the diversification pattern of African Cyprinidae. The non-constant episod-

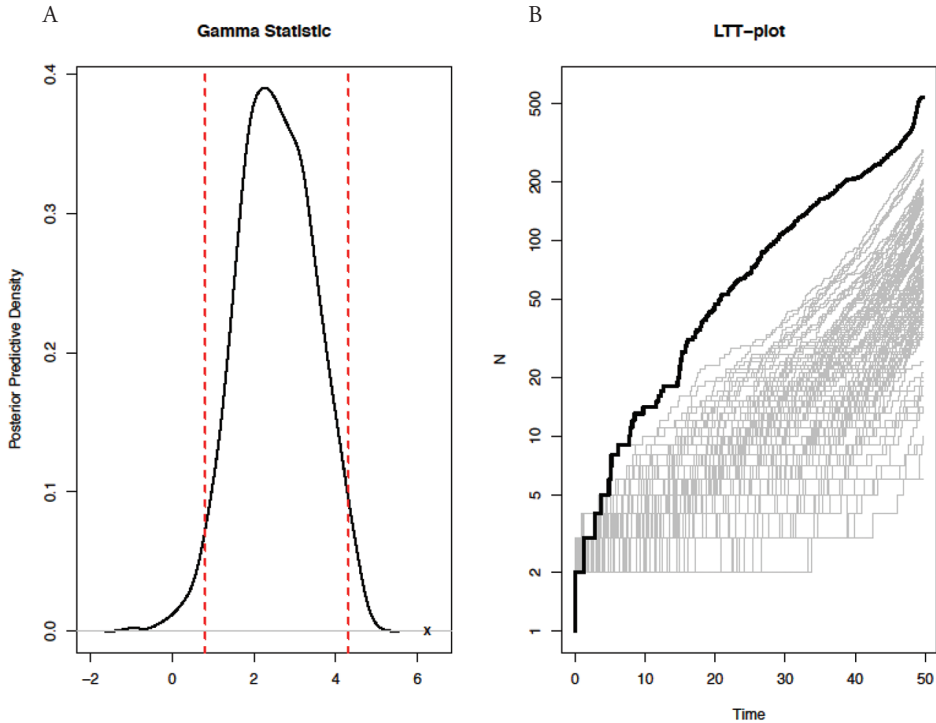


Figure 2. Comparative analysis of the fit of observed diversification pattern of African Cyprinidae to the constant-rate birth-death model using posterior-predictive simulation. Left panel (**A**): The posterior-predictive distribution for the gamma statistic; the dashed red lines indicate the 95% credible interval, and the “x” indicates the location of the value of the observed gamma statistic. Right panel (**B**): Lineage-through-time plot for the simulated phylogenies (grey) and for the phylogeny African Cyprinidae (bold black).

ic birth-death model was decisively supported (see BF interpretation in Table 1) as the best model explaining the diversification pattern of the African Cyprinidae (BF > 28) and the rate-constant model never outperformed any of the non-constant models tested (Table 2).

Finally, the overall evolutionary events that shaped the diversification of African Cyprinidae are summarized in Figure 3. This figure showed that the speciation rate (Figure 3A) was roughly constant to 0.3 species per million year over the first 40 my. However, within the last 10 my, the following rate variations were observed. A first and sudden rate decrease to ~ 0.05 species/my occurred around 10 million years ago (Ma), then this rate increased almost simultaneously to 0.15 where it remains constant until ~ 2 Ma before a sudden rate increase to 0.4 occurred followed by a punctual decrease to 0.1 around 1–0 Ma (Figure 3A). Nonetheless, 50 Ma, the extinction rate that was at 0.2, decreased to 0.1 around 45 Ma but increased steadily to 0.2 until ~ 37 Ma and remained constant to the present (Figure 3B). There was only one but not decisive mass extinction (Figures 3C, D) and 12 non-significant extinction shifts (Figure 3E). However, there was five speciation shifts, of which two are significant: the first at ~ 10 Ma (rate decrease) and ~ 2 Ma (rate increase; Figure 3F).

Table 1. Interpretation of Bayes factors following Jeffreys (1961). Abbreviations: M_0 Model 0; M_1 model 1, BF Bayes Factor.

Interpretations	BF(M_0, M_1)	ln(BF(M_0, M_1))	log10(BF(M_0, M_1))
Negative value is a support for model M_1	<1	<0	<0
Barely M_0 worth mentioning	1 to 3.2	0 to 1.16	0 to 0.5
Substantial support for model M_0	3.2 to 10	1.16 to 2.3	0.5 to 1
Strong support for model M_0	10 to 100	2.3 to 4.6	1 to 2
Decisive support for model M_0	>100	>4.6	>2

Table 2. Bayes Factor (BF) values calculated for each pair of birth-death models tested on the phylogeny of African Cyprinidae. Abbreviations: ConstBD = constant-rate birth-death model; DecrBD = continuously variable-rate birth-death model; EpisodicBD = episodically variable-rate birth-death model, and; MassExtinctionBD = explicit mass-extinction birth-death model. The interpretations of these values should be done in comparison with the reference values in Table 1.

Model ₀	Model ₁	BF
EpisodicBD	ConstBD	28.635868
DecrBD	ConstBD	20.886607
EpisodicBD	MassExtinctionBD	20.276659
DecrBD	MassExtinctionBD	12.527398
MassExtinctionBD	ConstBD	8.359210
EpisodicBD	DecrBD	7.749261
ConstBD	ConstBD	0.000000
DecrBD	DecrBD	0.000000
EpisodicBD	EpisodicBD	0.000000
MassExtinctionBD	MassExtinctionBD	0.000000
DecrBD	EpisodicBD	-7.749261
ConstBD	MassExtinctionBD	-8.359210
MassExtinctionBD	DecrBD	-12.527398
MassExtinctionBD	EpisodicBD	-20.276659
ConstBD	DecrBD	-20.886607
ConstBD	EpisodicBD	-28.635868

Discussion

The subfamily Labeoninae is embedded within the subfamily Cyprininae on the phylogenetic tree presented in Suppl. material 1 (see paper in review). The topology our tree puts in question early treatments of Labeoninae (Thai et al. 2007; Tang et al. 2009; Zheng et al. 2010) but supports the most recent treatment of Yang et al. (2015) who reported that the former Labeoninae is actually Cyprininae.

Using this phylogenetic tree, we found that the diversification rate of African Cyprinidae, even in the absence of extinction, is 0.11 species/ Myr, which is far lower than the rates reported for the Cichlids in various Lakes on the same continent. For example, in the Lake Malawi, McCune (1997) reported a rate between 3.00–5.99 species/Myr. In the Lake Victoria, an unusually high rate of 8.29–62.15 species/Myr was reported (Verheyen et al. 2003) whereas a latter study found that African Cichlids radiated in

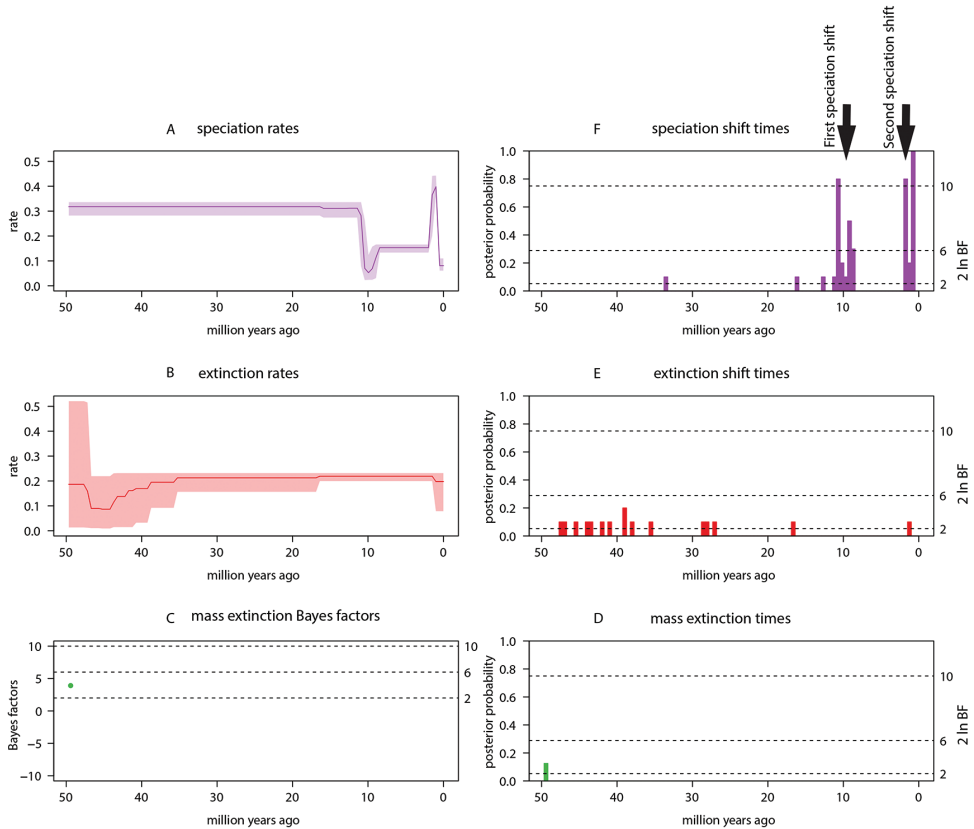


Figure 3. Summary of all evolutionary events (A–F) reported in this study. This summary was presented using the Compound Poisson Process (CPP) on Mass Extinction Time (CoMET) model. Diversification hyperpriors are specified *a priori* and empirically. Result reported are for priors set *a priori* as this does not differ from when empirical priors were set.

the Lake Tanganyika with a rate six time slower (1.67–2.71) than the rates in Lakes Malawi and Victoria (Day et al. 2008). The particularly lower radiation rate found in the present study suggests that the environment of African freshwaters is certainly less conducive for the radiation of Cyprinidae. For example, the rapid radiation of Cichlids and perhaps many other fish groups in African Lakes may have caused these groups to be the first to occupy much of the available ecological niches (Fryer and Iles 1972; Kornfield and Smith 2000), thus leading to strong competitions between these groups and Cyprinidae. Such competitive interactions may drive the low radiation of Cyprinidae as predicted in the density-dependent radiation model (McPeck 2008). However, even the rapid radiation of African Cichlids in the last 150,000 years (potentially promoted by hybridization; Meier et al. 2017; see also review in Seehausen 2015), could perhaps be an exception to the global Cichlids radiation, as a rate-constant radiation was instead reported for the South-American Cichlids (Hulsey et al. 2010). What is the temporal diversification pattern for African Cyprinidae?

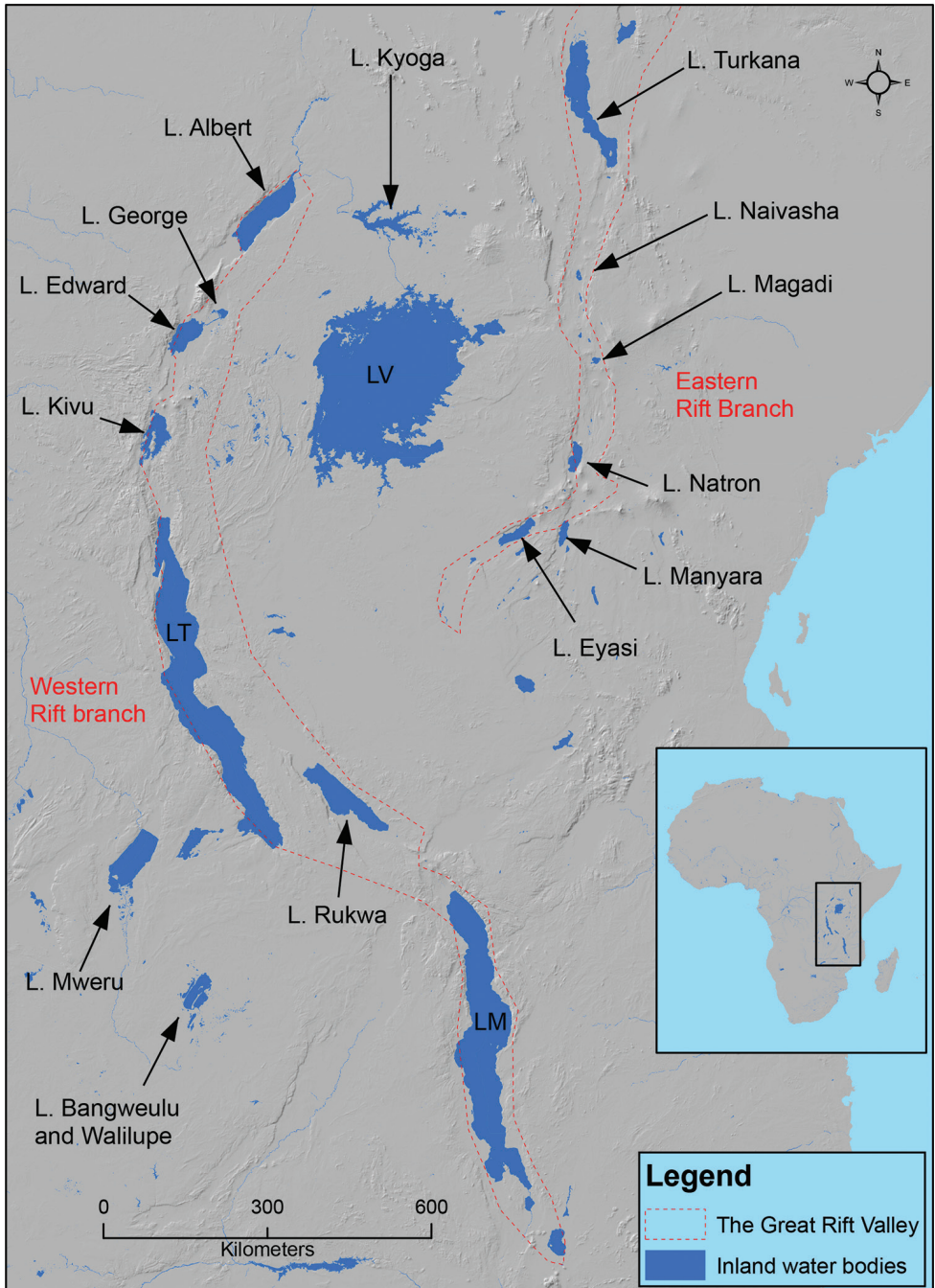


Figure 4. The Great Rift Valley used as a model river system to interpret the diversification of African Cyprinidae. Abbreviations: LV, Lake Victoria; LT, Lake Tanganyika, LM, Lake Malawi.

All analyses performed in this study pointed to a non-constant diversification for African Cyprinidae. Specifically, the episodically variable-rate birth-death model was the best model found for the diversification pattern of African Cyprinidae. This model suggests that some decisive rate shifts have occurred during the speciation and extinction events of African Cyprinidae but, between two consecutive rate shifts, the diversification rate was constant (Stadler 2011; Höhna 2015). Indeed, as showed in Figures 3A, F, two decisive rate shifts were observed in the last 10 million years (see also Bloom et al. 2013 for New World freshwater fishes), and these were interspersed by constant radiations. The first constant speciation was before the last 10 million years and the second constant radiation occurred between 10 and 2 million years ago. In addition, there was evidence for 12 extinction events (Figure 3E), confirming frequent extinction events reported in freshwaters; e.g., extinction rates in freshwaters are 60 times greater than in marine waters (Bloom et al. 2013). However, none of the 12 extinction events found for African Cyprinidae was statistically decisive (see Table 1 for interpretation of BF).

The observed rate shifts can only be understood if analysed within the African context of geological and paleo-climatic events (Danley et al. 2012). Geological events are well established as drivers of vicariant speciation especially in freshwaters (Burrige et al. 2006; Albert and Carvalho 2011). For example, vicariance-promoting diversifications were reported in freshwater fishes (including Cyprinidae) within the south-western Cape Floristic Region during the Miocene-Pliocene transition (Chakona et al. 2013).

We used the example of the Great Lakes (Figure 4) as a model system to interpret our results, as this is a major river system that has been very well studied on the continent. These geological events first drive the formation of some major freshwater ecosystems in Africa, e.g., the Great Lakes (Figure 4), known as key “cradles” and “museums” of fish diversity (Danley et al. 2012). These events include shift of tectonic plates and opening of rifts, e.g., the East Africa rift system (Figure 4). This system, in particular, is made of eastern and western rifts (Nyblade and Brazier 2002). The eastern rifting started 30–35 Ma (Roberts et al. 2012) and generated some stress that was later transported westward, resulting in the creation of the western branch of the rift ~ 12–10 Ma (Roberts et al. 2012), a period that coincided with the first sudden decrease in speciation rate of African Cyprinidae (Figure 3A, F). This suggests that the geological rifting and the inherent stress likely mediated the speciation rate decrease. Later, the Lakes Tanganyika and Malawi were created (Ebinger et al. 1989; Mortimer et al. 2007); both experienced rifting around 9–12 Ma and 8–12 Ma (Cohen et al. 1993), respectively, and this may have further contributed to the observed decrease of fish speciation. During the same period, the Lakes underwent an extension northward and southward (Talbot and Williams 2009), causing the opening of new ecological niches that may have triggered the rapid speciation observed immediately after the rate decrease (between 10 and 2 Ma; Figure 3F).

In addition, there has been an extension and uplift concurrently with the rifting causing a back-ponding between the eastern and the western rifts, creating the Lake Victoria (Johnson et al. 1996; Nicholson 1996) (Figure 4). This new Lake, the largest freshwater lake in the tropics and the second largest in the world, provided new ecological niches. The fact that this lake was formed around 1.6–0.40 Ma (Danley et al.

2012), a period that coincided with the significant speciation-rate increase of African Cyprinidae, may have triggered the speciation shift.

What's more, the dynamic of the African paleoclimate over the last 10 million years (Kingston et al. 2002) may have also mediated the diversification patterns. Around 8–10 Ma, a period that corresponds to the first significant speciation shift, African climate was humid (Cerling et al. 2011), and then became arid around 7–5 Ma (Cerling et al. 1997). Around 5–3 Ma, the climate became warmer and wetter across Africa (Raymo et al. 1996), and this wetter condition has driven the expansion of Lake Tanganyika (Meyer 1993), further opening new ecological niches that may have predisposed African Cyprinidae to the second speciation shift. The great depths of several African Lakes facilitated the persistence of fish lineages (most African Cyprinidae are benthic) during stressful environmental conditions (rifting, lake desiccation, mega-drought, etc.; Lipitsch 1997). In such conditions, species hybridized and the hybrid clades developed adaptive genetic (e.g., polyploidy) and ecological novelties. Indeed, Cyprinidae developed a wide range of polyploidy levels (Tsigenopoulos et al. 2002) that predispose for large ecological tolerance (Otto and Whitton 2000), a key evolutionary mechanism of speciation (Soltis and Soltis 1999). Additionally, several African *Labeobarbus* species have evolved unique anatomical features (Sibbing et al. 1998), piscivory (De Graaf et al. 2008) and lacustrine spawning (De Graaf et al. 2005) to survive harsh conditions. When the conditions became suitable (e.g., ~12–13 thousand years ago (ka)), lake levels filled to their current level (Stager and Johnson 2008), and the pre-adapted lineages may have shifted their speciation rate to fill new niches. However, around 2.0 Ma, Africa became drier (Trauth et al. 2005) and the extreme climatic variation in the last 500ka led to the desiccation of several African Lakes (Johnson et al. 1996), potentially leading to the sudden decrease of diversification of African Cyprinidae toward the present-day (Figure 3F).

Overall, the diversification rate of African Cyprinidae is much lower than that reported for African Cichlids. Most of diversification events of African Cyprinidae occurred in the last 10 million years following an episodic birth-death diversification model. This is in accord with what has been reported for Cyprinidae in the Asian freshwater (Yuan et al. 2010). Specifically, Yuan et al. (2010) reported that the speciation events of Cyprinidae in Chinese freshwaters likely occurred between 11.4 and 2.3 Mya, perhaps pointing to a simultaneous diversification at global scale.

In addition, 12 extinction events were observed during this diversification, supporting an earlier report that extinction event is frequent in freshwaters (Bloom et al. 2013). All these events could have been mediated through geological events and historical climate fluctuations on the continents (Danley et al. 2012; Chakona et al. 2013). As we should caution against interpreting evolution events based on a single analysis, we also tested our findings assessing their sensitivity to an automatic empirical hyperprior, and we found consistency for the findings reported in the present study. However, one potential caveat to this study is that it relies solely on a mitochondrial marker which could potentially show saturation and thus underestimate the branch lengths towards the origin of the phylogenetic tree (Revell et al. 2005). If this is true for the phylogeny of African Cyprinidae based on COI marker alone, we should expect

a burst of speciation at the base of the radiation because of underestimation of older branch lengths. Our results did not corroborate a burst of speciation towards the origin of diversification, thus undermining potential bias due to the use of COI alone.

Nonetheless, although we do not foresee any reason why the marker used may blur the diversification pattern, it is important to remind us that the present study is based on a single gene marker and that “type 2” species outnumber the “type 1”. The study should therefore be regarded as a basis for further investigation. We call for more studies that should use more markers to revisit the diversification patterns reported in this study.

Acknowledgement

The South Africa’s National Research Foundation (NRF) is acknowledged for funding (Grant No: 103944; 277583, 277581 and 112113) and the University of Johannesburg (Grant No: 073450).

References

- Adeoba MI, Kabongo R, Van der Bank H, Yessoufou K (2018) Re-evaluation of the discriminatory power of DNA barcoding on some specimens of African Cyprinidae (subfamilies Cyprininae and Danioninae). *ZooKeys* 746: 105–121. <https://doi.org/10.3897/zookeys.746.13502>
- Albert JS, Carvalho TP (2011) Neogene assembly of modern faunas. In: Albert JS, Reis RE (Eds) *Neotropical Freshwater Fishes*. University of California Press, Berkeley and Los Angeles, 119–136. <https://doi.org/10.1525/california/9780520268685.003.0007>
- Baele G, Lemey P, Vansteelandt S (2013) Make the most of your samples: Bayes factor estimators for high-dimensional models of sequence evolution. *BMC bioinformatics* 14: 85. <https://doi.org/10.1186/1471-2105-14-85>
- Baldwin BG, Sanderson MJ (1998) Age and rate of diversification of the Hawaiian silversword alliance (Compositae). *Proceedings of the National Academy of Sciences* 95: 9402–9406. <https://doi.org/10.1073/pnas.95.16.9402>
- Bininda-Emonds OR, Cardillo M, Jones KE, MacPhee RD, Beck RM, Grenyer R, Price SA, Vos RA, Gittleman JL, Purvis A (2007) The delayed rise of present-day mammals. *Nature* 446: 507. <https://doi.org/10.1038/nature05634>
- Bloom DD, Weir JT, Piller KR, Lovejoy NR (2013) Do freshwater fishes diversify faster than marine fishes? A test using state-dependent diversification analyses and molecular phylogenetics of New World silversides (Atherinopsidae). *Evolution* 67: 2040–2057. <https://doi.org/10.1111/evo.12074>
- Burridge CP, Craw D, Waters JM (2006) River capture, range expansion, and cladogenesis: the genetic signature of freshwater vicariance. *Evolution* 60: 1038–1049. <https://doi.org/10.1111/j.0014-3820.2006.tb01181.x>

- Cavender TM (1991) The fossil record of the Cyprinidae. In: Winfield IJ, Nelson JS (Eds) *Cyprinid Fishes: Systematics, Biology and Exploitation*. Chapman and Hall, London, 34–54. https://doi.org/10.1007/978-94-011-3092-9_2
- Cerling TE, Wynn JG, Andanje SA, Bird MI, Korir DK, Levin NE, Mace W, Macharia AN, Quade J, Remien CH (2011) Woody cover and hominin environments in the past 6 million years. *Nature* 476: 51–56. <https://doi.org/10.1038/nature10306>
- Cerling TE, Harris JM, MacFadden BJ, Leakey MG, Quade J, Eisenmann V, Ehleringer JR (1997) Global vegetation change through the Miocene/Pliocene boundary. *Nature* 389: 153–158. <https://doi.org/10.1038/38229>
- Chakona A, Swartz ER, Gouws G (2013) Evolutionary drivers of diversification and distribution of a southern temperate stream fish assemblage: Testing the role of historical isolation and spatial range expansion. *PLoS ONE* 8:e70953. <https://doi.org/10.1371/journal.pone.0070953>
- Cohen AS, Soreghan MJ, Scholz CA (1993) Estimating the age of formation of lakes: an example from Lake Tanganyika, East African Rift system. *Geology* 21: 511–514. [https://doi.org/10.1130/0091-7613\(1993\)021<0511:ETAOFO>2.3.CO;2](https://doi.org/10.1130/0091-7613(1993)021<0511:ETAOFO>2.3.CO;2)
- Crisp MD, Cook LG (2009) Explosive radiation or cryptic mass extinction? Interpreting signatures in molecular phylogenies. *Evolution* 63: 2557–2265. <https://doi.org/10.1111/j.1558-5646.2009.00728.x>
- Danley PD, Husemann M, Ding B, DiPietro LM, Beverly EJ, Peppe DJ (2012) The impact of the geologic history and paleoclimate on the diversification of East African cichlids. *International Journal of Evolutionary Biology* 2012: 1–20. <https://doi.org/10.1155/2012/574851>
- Day J, Cotton J, Barraclough T (2008) Tempo and mode of diversification of Lake Tanganyika cichlid fishes. *PLoS ONE* 3: e1730. <https://doi.org/10.1371/journal.pone.0001730>
- De Graaf M, Nentwich ED, Osse JWM, Sibbing FA (2005). Lacustrine spawning, a new reproductive strategy among ‘large’ African cyprinid fishes? *Journal of Fish Biology* 66: 1214–1236. <https://doi.org/10.1111/j.0022-1112.2005.00671.x>
- De Graaf M, Dejen E, Osse JWM, Sibbing FA (2008). Adaptive radiation of Lake Tana’s (Ethiopia) *Labeobarbus* species flock (Pisces, Cyprinidae). *Marine and Freshwater Research* 59: 391–407. <https://doi.org/10.1071/MF07123>
- Ebinger CJ, Deino AL, Drake RE, Tesha AL (1989) Chronology of volcanism and rift basin propagation- Rungwe volcanic province, East Africa. *Journal of Geophysical Research* 94: 15785–15803. <https://doi.org/10.1029/JB094iB11p15785>
- Froese R, Pauly D (2017) FishBase. <http://www.fishbase.org> [assessed March 2017]
- Fryer G, Iles TD (1972) *The Cichlid Fishes of The Great Lakes of Africa*. Oliver and Boyd, Edinburgh, 641 pp.
- García-Maroto F, Mañas-Fernández A, Garrido-Cárdenas JA, Alonso DL, Guil-Guerrero JL, Guzmán B, Vargas P (2009). $\Delta 6$ -Desaturase sequence evidence for explosive Pliocene radiations within the adaptive radiation of Macaronesian *Echium* (Boraginaceae). *Molecular Phylogenetics and Evolution* 52: 4563–4574. <https://doi.org/10.1016/j.ympev.2009.04.009>
- Harmon LJ, Weir JT, Brock CD, Glor RE, Challenger W (2007) GEIGER: investigating evolutionary radiations. *Bioinformatics* 24: 129–131. <https://doi.org/10.1093/bioinformatics/btm538>

- Harvey PH, May RM, Nee S (1994) Phylogenies without fossils. *Evolution* 48: 523–529. <https://doi.org/10.1111/j.1558-5646.1994.tb01341.x>
- He S, Mayden RL, Wang X, Wang W, Tang KL, Chen WJ (2008) Molecular phylogenetics of the family Cyprinidae (Actinopterygii: Cypriniformes) as evidenced by sequence variation in the first intron of S7 ribosomal protein-coding gene: Further evidence from a nuclear gene of the systematic chaos in the family. *Molecular Phylogenetics and Evolution* 46: 818–829. <http://dx.doi.org/10.1016/j.ympev.2007.06.001>
- Höhna S (2015) The time-dependent reconstructed evolutionary process with a key-role for mass-extinction events. *Journal of Theoretical Biology* 380: 321–331. <https://doi.org/10.1016/j.jtbi.2015.06.005>
- Höhna S, May MR, Moore BR (2015) TESS: an R package for efficiently simulating phylogenetic trees and performing Bayesian inference of lineage diversification rates. *Bioinformatics* 32: 789–791. <https://doi.org/10.1093/bioinformatics/btv651>
- Hughes C, Eastwood R (2006) Island radiation on a continental scale: exceptional rates of plant diversification after uplift of the Andes. *Proceedings of the National Academy of Sciences* 103: 10334–10339. <https://doi.org/10.1073/pnas.0601928103>
- Hulsey CD, Hollingsworth PR, Fordyce JA (2010) Temporal diversification of Central American cichlids. *BMC Evolutionary Biology* 10: 279.
- Jablonski D (1995) Extinctions in the fossil record. *Philosophical Transactions of the Royal Society B: Biological Sciences* 344: 11–17. <https://doi.org/10.1098/rstb.1994.0045>
- Jablonski D (2005) Mass extinctions and macroevolution. *Paleobiology* (S2): 192–210. [https://doi.org/10.1666/0094-8373\(2005\)031\[0192:MEAM\]2.0.CO;2](https://doi.org/10.1666/0094-8373(2005)031[0192:MEAM]2.0.CO;2)
- Jeffreys H (1961) *The Theory of Probability*. Oxford University Press.
- Jetz W, Thomas GH, Joy JB, Hartmann K, Mooers A (2012) The global diversity of birds in space and time. *Nature* 491: 444–448. <https://doi.org/10.1038/nature11631>
- Johnson TC, Scholz CA, Talbot, MR, Kelts K, Ricketts RD, Ngobi G, Beuning K, Ssemmanda I, McGill JW (1996) Late Pleistocene desiccation of Lake Victoria and rapid evolution of cichlid fishes. *Science* 273: 1091–1093. <https://doi.org/10.1126/science.273.5278.1091>
- Kadereit JW, Griebeler EM, Comes HP (2004) Quaternary diversification in European alpine plants: pattern and process. *Philosophical Transactions of the Royal Society B: Biological Sciences* 359: 265–274. <https://doi.org/10.1098/rstb.2003.1389>
- Kay KM, Reeves PA, Olmstead RG, Schemske DW (2005) Rapid speciation and the evolution of hummingbird pollination in neotropical *Costus* subgenus *Costus* (Costaceae): evidence from nrDNA ITS and ETS sequences. *American Journal of Botany* 92: 1899–1910. <https://doi.org/10.3732/ajb.92.11.1899>
- Kingston JD, Jacobs BF, Hill A, Deino A (2002) Stratigraphy, age and environments of the late Miocene Mpesida Beds, Tugen Hills, Kenya. *Journal of Human Evolution* 42: 95–116. <https://doi.org/10.1006/jhev.2001.0503>
- Klak C, Reeves G, Hedderson T (2004) Unmatched tempo of evolution in southern African semi-desert ice plants. *Nature* 427: 63–65. <https://doi.org/10.1038/nature02243>
- Kornfield I, Smith PF (2000) African cichlid fishes: model systems for evolutionary biology. *Annual Review of Ecology and Systematics* 31: 163–196. <https://doi.org/10.1146/annurev.ecolsys.31.1.163>

- Kozak KH, Weisrock DW, Larson A (2006) Rapid lineage accumulation in a non-adaptive radiation: phylogenetic analysis of diversification rates in eastern North American woodland salamanders (Plethodontidae: Plethodon). *Proceedings of the Royal Society of London B: Biological Sciences* 273: 539–546. <https://doi.org/10.1098/rspb.2005.3326>
- Kuhn TS, Mooers AØ, Thomas GH (2011) A simple polytomy resolver for dated phylogenies. *Methods in Ecology and Evolution* 2: 427–436. <https://doi.org/10.1111/j.2041-210X.2011.00103.x>
- Lippitsch E (1997). Phylogenetic investigations on the haplochromine Cichlidae of Lake Kivu (East Africa), based on lepidological characters. *Journal of Fish Biology* 51: 284–299.
- Machordom A, Macpherson E (2004) Rapid radiation and cryptic speciation in squat lobsters of the genus *Munida* (Crustacea, Decapoda) and related genera in the southwest Pacific: molecular and morphological evidence. *Molecular Phylogenetics and Evolution* 33: 259–279. <https://doi.org/10.1016/j.ympev.2004.06.001>
- Magallón S, Sanderson MJ (2001) Absolute diversification rates in angiosperm clades. *Evolution* 55: 1762–1780. <https://doi.org/10.1111/j.0014-3820.2001.tb00826.x>
- May MR, Höhna S, Moore BR (2016) A Bayesian Approach for Detecting Mass-Extinction Events When Rates of Lineage Diversification Vary. *Methods in Ecology and Evolution* 7: 947–959. <https://doi.org/10.1101/020149>
- May RM, Lawton JH, Stork NE (1995) Assessing extinction rates. In: Lawton JH, May RM (Eds) *Extinction rates*. Oxford Univ. Press, Oxford, 1–24.
- McCune A (1997) How fast is speciation? Molecular, geological and phylogenetic evidence from adaptive radiations of fishes. In: Givnish TJ, Sytsma KJ (Eds) *Molecular evolution and adaptive radiation*. Cambridge University Press, Cambridge, 585–610.
- McPeck, MA (2008) The ecological dynamics of clade diversification and community assembly. *American Naturalist* 172: E270–E284. <https://doi.org/10.1086/593137>
- Meier JL, Marques DA, Mwaiko S, Wagner CE, Excoffier L, Seehausen O (2017) Ancient hybridization fuels rapid cichlid fish adaptive radiations. *Nature communications* 8: 14363. <https://doi.org/10.1038/ncomms14363>
- Meyer A (1993) Phylogenetic relationships and evolutionary processes in East African cichlid fishes. *Trends in Ecology and Evolution* 8: 279–284. [https://doi.org/10.1016/0169-5347\(93\)90255-N](https://doi.org/10.1016/0169-5347(93)90255-N)
- Morrison CL, Rios R, Duffy JE (2004) Phylogenetic evidence for an ancient rapid radiation of Caribbean sponge-dwelling snapping shrimps (*Synalpheus*). *Molecular Phylogenetics and Evolution* 30: 563–581. [https://doi.org/10.1016/S1055-7903\(03\)00252-5](https://doi.org/10.1016/S1055-7903(03)00252-5)
- Mortimer E, Paton DA, Scholz CA, Strecker MR, Blisniuk P (2007) Orthogonal to oblique rifting: effect of rift basin orientation in the evolution of the North basin, Malawi Rift, East Africa. *Basin Research* 19: 393–407. <https://doi.org/10.1111/j.1365-2117.2007.00332.x>
- Moyle RG, Filardi CE, Smith CE, Diamond J (2009) Explosive Pleistocene diversification and hemispheric expansion of a “great speciator”. *Proceedings of the National Academy of Sciences* 106: 1863–1868. <https://doi.org/10.1073/pnas.0809861105>
- Nicholson SE (1996) A review of climate dynamics and climate variability in Eastern Africa. *The Limnology, Climatology and Paleoclimatology of The East African Lakes* 1: 25–56.

- Niklas KJ (1997) *The Evolutionary Biology of Plants*. Univ. of Chicago Press, Chicago, 470 pp
- Nyblade AA, Brazier RA (2002) Precambrian lithospheric controls on the development of the East African rift system. *Geology* 30: 755–758. [https://doi.org/10.1130/0091-7613\(2002\)030<0755:PLCOTD>2.0.CO;2](https://doi.org/10.1130/0091-7613(2002)030<0755:PLCOTD>2.0.CO;2)
- Nylander JAA (2004) Modeltest v2. Program Distributed by the Author. Evolutionary Biology Centre, Uppsala University, Sweden.
- Otto SP, Whitton J (2000) Polyploid incidence and evolution. *Ann Rev Genet* 34: 401–437. <https://doi.org/10.1146/annurev.genet.34.1.401>
- Peters SE, Foote M (2002) Determinants of extinction in the fossil record. *Nature* 416: 420–424. <https://doi.org/10.1038/416420a>
- Phillimore AB, Price TD (2008) Density-dependent cladogenesis in birds. *PLoS Biology* 6:e71. <https://doi.org/10.1371/journal.pbio.0060071>
- Pybus OG, Harvey PH (2000) Testing macro-evolutionary models using incomplete molecular phylogenies. *Proceedings of the Royal Society of London B: Biological Sciences* 267: 2267–2272. <https://doi.org/10.1098/rspb.2000.1278>
- Pyron RA, Burbrink FT, Wiens JJ (2013) A phylogeny and revised classification of squamata, including 4161 species of lizards and snakes. *BMC Evolutionary Biology* 13: 93. <https://doi.org/10.1186/1471-2148-13-93>
- R Development Core Team (2011) R: A language and environment for statistical computing. R Foundation for statistical computing, Vienna. <http://www.rproject.org/>
- Rabosky DL (2015) No substitute for real data: A cautionary note on the use of phylogenies from birth-death polytomy resolvers for downstream comparative analyses. *Evolution* 69: 3207–3216. <https://doi.org/10.1111/evo.12817>
- Rabosky DL, Santini F, Eastman J, Smith SA, Sidlauskas B, Chang J, Alfaro ME (2013) Rates of speciation and morphological evolution are correlated across the largest vertebrate radiation. *Nature communications* 4: 1958. <https://doi.org/10.1038/ncomms2958>
- Rabosky DL (2006) LASER: a maximum likelihood toolkit for detecting temporal shifts in diversification rates from molecular phylogenies. *Evolutionary Bioinformatics* 2. <https://doi.org/10.1177/117693430600200024>
- Rambaut A, Drummond AJ (2007) TreeAnnotator (version 1.5.4). <http://beast.bio.ed.ac.uk> [Accessed 13 Dec 2015]
- Raymo ME, Grant B, Horowitz M, Rau GH (1996) Mid-Pliocene warmth: stronger greenhouse and stronger conveyor. *Marine Micropaleontology* 27: 313–326. [https://doi.org/10.1016/0377-8398\(95\)00048-8](https://doi.org/10.1016/0377-8398(95)00048-8)
- Raup DM (1976) Species diversity in the Phanerozoic: an interpretation. *Paleobiology* 2: 289–297. <https://doi.org/10.1017/S0094837300004929>
- Revell LJ, Harmon LJ, Glor RE (2005) Under-parameterized model of sequence evolution leads to bias in the estimation of diversification rates from molecular phylogenies. *Systematic Biology* 54: 973–983.
- Richardson JE, Pennington RT, Pennington TD, Hollingsworth PM (2001) Rapid diversification of a species-rich genus of neotropical rain forest trees. *Science* 293: 2242–2245. <https://doi.org/10.1126/science.1061421>

- Roberts EM, Stevens NJ, O'connor PM, Dirks PH, Gottfried MD, Clyde WC, Armstrong RA, Kemp AI, Hemming S (2012) Initiation of the western branch of the East African Rift coeval with the eastern branch. *Nature Geoscience* 5: 289–294. <https://doi.org/10.1038/ngeo1432>
- Rokas A, Kruger D, Carroll SB (2005) Animal evolution and the molecular signature of radiations compressed in time. *Science* 310: 1933–1938. <https://doi.org/10.1126/science.1116759>
- Ronquist F, Huelsenbeck JP (2003) MRBAYES 3: Bayesian phylogenetic inference under mixed models. *Bioinformatics* 19: 1572–1574. <https://doi.org/10.1093/bioinformatics/btg180>
- Rüber L, Zardoya R (2005) Rapid cladogenesis in marine fishes revisited. *Evolution* 59: 1119–1127. <https://doi.org/10.1111/j.0014-3820.2005.tb01048.x>
- Seehausen O (2015) Process and pattern in cichlid radiations—inferences for understanding unusually high rates of evolutionary diversification. *New Phytologist* 207: 304–312. <https://doi.org/10.1111/nph.13450>
- Seehausen O, Terai Y, Magalhaes IS, Carleton KL, Mrosso HD, Miyagi R, van der Sluijs I, Schneider MV, Maan ME, Tachida H, Imai H (2008) Speciation through sensory drive in cichlid fish. *Nature* 455: 620. <https://doi.org/10.1038/nature07285>
- Shaw AJ, Cox CJ, Goffinet B, Buck WR, Boles SB (2003) Phylogenetic evidence of a rapid radiation of pleurocarpous mosses (Bryophyta). *Evolution* 57: 2226–2241. <https://doi.org/10.1111/j.0014-3820.2003.tb00235.x>
- Sibbing FA, Nagelkerke LAJ, Stet RJM, Osse JWM (1998) Speciation of endemic Lake Tana barbs (Cyprinidae, Ethiopia) driven by trophic resource partitioning; a molecular and ecomorphological approach. *Aquatic Ecology* 32: 217–227. <https://doi.org/10.1023/A:1009920522235>
- Skelton PH, Tweddle D, Jackson PBN (1991). Cyprinids in Africa. In: Winfield IJ, Nelson JS (Eds) *Cyprinid Fishes—Systematics, Biology and Exploitation*. Chapman & Hall, London, 211–239. https://doi.org/10.1007/978-94-011-3092-9_7
- Skelton PH (2016) Name changes and additions to the southern African freshwater fish fauna. *African Journal of Aquatic Science* 41: 345–351. <https://doi.org/10.2989/16085914.2016.1186004>
- Soltis DE, Soltis PS (1999) Polyploidy: recurrent formation and genome evolution. *Trends in Ecology Evolution* 14: 348–352. [https://doi.org/10.1016/S0169-5347\(99\)01638-9](https://doi.org/10.1016/S0169-5347(99)01638-9)
- Stadler T (2011) Mammalian phylogeny reveals recent diversification rate shifts. *Proceedings of the National Academy of Sciences* 108: 6187–6192. <https://doi.org/10.1073/pnas.1016876108>
- Stager JC, Johnson TC (2008) The late Pleistocene desiccation of Lake Victoria and the origin of its endemic biota. *Hydrobiologia* 596: 5–16
- Talbot MR, Williams MA (2009) Cenozoic evolution of the Nile Basin. In: *The Nile*. Springer, Netherlands, 37–60. https://doi.org/10.1007/978-1-4020-9726-3_3
- Tang KL, Agnew MK, Hirt MV, Sado T, Schneider LM, Freyhof J, Sulaiman Z, Swart E, Vidthavanon C, Miya M, Saitoh K, Soimios AM, Wood RM, Mayden RL (2010) Systematics of the subfamily Danioninae (Teleostei: Cypriniformes: Cyprinidae). *Molecular Phylogenetics and Evolution* 57: 189–214. <https://doi.org/10.1016/j.ympev.2010.05.021>
- Tang Q, Getahun A, Liu H (2009) Multiple in-to-Africa dispersals of Labeonin fishes (Teleostei: Cyprinidae) revealed by molecular phylogenetic analysis. *Hydrobiologia* 632: 261–271. <https://doi.org/10.1007/s10750-009-9848-z>

- Thomas GH, Hartmann K, Jetz W, Joy JB, Mimoto A, Mooers AO (2013) PASTIS: an R package to facilitate phylogenetic assembly with soft taxonomic inferences. *Methods in Ecology and Evolution* 4: 1011–1017. <https://doi.org/10.1111/2041-210X.12117>
- Trauth MH, Maslin MA, Deino A, Strecker MR (2005) Late cenozoic moisture history of East Africa. *Science* 309: 2051–2053. <https://doi.org/10.1126/science.1112964>
- Tsigenopoulos CS, Rab P, Naran D, Berrebi P (2002) Multiple origins of polyploidy in the phylogeny of southern African barbs (Cyprinidae) as inferred from mtDNA markers. *Heredity* 88: 466–473. <https://doi.org/10.1038/sj.hdy.6800080>
- Valente LM, Savolainen V, Vargas P (2010) Unparalleled rates of species diversification in Europe. *Proceedings of the Royal Society of London B: Biological Sciences* 277: 1489–1496. <https://doi.org/10.1098/rspb.2009.2163>
- Verboom GA, Linder HP, Stock WD (2003) Phylogenetics of the grass genus *Ehrharta*: evidence for radiation in the summer-arid zone of the South African Cape. *Evolution* 57: 1008–1021. <https://doi.org/10.1111/j.0014-3820.2003.tb00312.x>
- Verheyen E, Salzburger W, Snoeks J, Meyer A (2003) Origin of the superflock of cichlid fishes from Lake Victoria, East Africa. *Science* 300: 325–329. <https://doi.org/10.1126/science.1080699>
- Wang Z-C, Gan X, Li J, Mayden R, He S (2012) Cyprinid phylogeny based on Bayesian and maximum likelihood analyses of partitioned data: implications for Cyprinidae systematics. *Science China Life Sciences* 55: 761–773. <https://doi.org/10.1007/s11427-012-4366-z>
- Weir JT, Schluter D (2007) The latitudinal gradient in recent speciation and extinction rates of birds and mammals. *Science* 315: 1574–1576. <https://doi.org/10.1126/science.1135590>
- Weir J (2006) Divergent timing and patterns of species accumulation in lowland and highland Neotropical birds. *Evolution* 60: 842–855. <https://doi.org/10.1111/j.0014-3820.2006.tb01161.x>
- Williams ST, Reid DG (2004) Speciation and diversity on tropical rocky shores: a global phylogeny of snails of the genus *Echinolittorina*. *Evolution* 58: 2227–2251. <https://doi.org/10.1111/j.0014-3820.2004.tb01600.x>
- Xiang QY, Manchester SR, Thomas DT, Zhang W, Fan C (2005) Phylogeny, biogeography, and molecular dating of cornelian cherries (*Cornus*, Cornaceae): tracking Tertiary plant migration. *Evolution* 59: 1685–1700. <https://doi.org/10.1111/j.0014-3820.2005.tb01818.x>
- Yang L, Sado T, Hirt MV, Pasco-Viel E, Arunachalam M, Li J, Wang X, Freyhof J, Saitoh K, Simons AM, Miya M, He S, Mayden RL (2015) Phylogeny and polyploidy: Resolving the classification of cyprinine fishes (Teleostei: Cypriniformes). *Molecular Phylogenetics and Evolution* 85: 97–116. <https://doi.org/10.1016/j.ympev.2015.01.014>
- Yuan J, He Z, Yuan X, Jiang X, Sun X, Zou S (2010) Speciation of polyploid Cyprinidae fish of common carp, crucian carp, and silver crucian carp derived from duplicated Hox genes. *Journal of Experimental Zoology* 314B:445–456. <https://doi.org/10.1002/jez.b.21350>
- Zardoya R, Doadrio I (1999) Molecular evidence on the evolutionary and biogeographical patterns of European Cyprinids. *Journal of Molecular Evolution* 49: 227–237. <https://doi.org/10.1007/PL00006545>
- Zheng LP, Yang JX, Chen XY, Wang WY (2010) Phylogenetic relationships of the Chinese Labeoninae (Teleostei, Cypriniformes) derived from two nuclear and three mitochondrial genes. *Zoologica Scripta* 39: 559–571. <https://doi.org/10.1111/j.1463-6409.2010.00441.x>

Supplementary material 1

Phylogenetic tree used in the present analysis

Authors: Mariam I. Adeoba, Kowiyou Yessoufou

Data type: molecular data

Explanation note: Paper currently in review in which we have presented the phylogenetic tree of African Cyprinidae. We submit it here as supplementary Information because we do not want to publish the same phylogeny twice.

Copyright notice: This dataset is made available under the Open Database License (<http://opendatacommons.org/licenses/odbl/1.0/>). The Open Database License (ODbL) is a license agreement intended to allow users to freely share, modify, and use this Dataset while maintaining this same freedom for others, provided that the original source and author(s) are credited.

Link: <https://doi.org/10.3897/zookeys.806.25844.suppl1>

